ผลของแบคทีเรียในระบบทางเดินอาหารต่อพยาธิกำเนิดและภูมิคุ้มกันของ
กุ้งกุลาดำ *Penaeus monodon*

นางสาววิภาศิริ สุนทรชัย

วิทยานิพนธ์นี้เป็นส่วนหนึ่งของการศึกษาตามหลักสูตรปริญญาวิทยาศาสตรดุษฎีบัณฑิต
สาขาวิชาเทคโนโลยีชีวภาพ
คณะวิทยาศาสตร์ จุฬาลงกรณ์มหาวิทยาลัย
ปีการศึกษา 2558

EFFECTS OF BACTERIA IN DIGESTIVE SYSTEM ON PATHOGENESIS AND IMMUNITY OF BLACK TIGER SHRIMP *Penaeus monodon*

Miss Wipasiri Soonthornchai

A Dissertation Submitted in Partial Fulfillment of the Requirements
for the Degree of Doctor of Philosophy Program in Biotechnology
Faculty of Science
Chulalongkorn University
Academic Year 2015

Thesis Title	EFFECTS OF BACTERIA IN DIGESTIVE SYSTEM ON PATHOGENESIS AND IMMUNITY OF BLACK TIGER SHRIMP *Penaeus monodon*
By	Miss Wipasiri Soonthornchai
Field of Study	Biotechnology
Thesis Advisor	Professor Padermsak Jarayabhand, Ph.D.
Thesis Co-Advisor	Pikul Jiravanichpaisal, Ph.D.
	Professor Kenneth Söderhäll, Ph.D.

Accepted by the Faculty of Science, Chulalongkorn University in Partial Fulfillment of the Requirements for the Doctoral Degree

.....Dean of the Faculty of Science
(Associate Professor Polkit Sangvanich, Ph.D.)

THESIS COMMITTEE

.....Chairman
(Associate Professor Charoen Nitithamyong, Ph.D.)

.....Thesis Advisor
(Professor Padermsak Jarayabhand, Ph.D.)

.....Thesis Co-Advisor
(Pikul Jiravanichpaisal, Ph.D.)

.....Thesis Co-Advisor
(Professor Kenneth Söderhäll, Ph.D.)

.....Examiner
(Assistant Professor Sanit Piyapattanakorn, Ph.D.)

.....Examiner
(Assistant Professor Kittinan Komolpis, Ph.D.)

.....External Examiner
(Sirawut Klinbunga, Ph.D.)

.....External Examiner
(Puttharat Baoprasertkul, Ph.D.)

วิภาศิริ สุนทรชัย : ผลของแบคทีเรียในระบบทางเดินอาหารต่อพยาธิกำเนิดและภูมิคุ้มกันของกุ้งกุลาดำ *Penaeus monodon* (EFFECTS OF BACTERIA IN DIGESTIVE SYSTEM ON PATHOGENESIS AND IMMUNITY OF BLACK TIGER SHRIMP *Penaeus monodon*) อ.ที่ปรึกษาวิทยานิพนธ์หลัก: ศ. ดร. เผดิมศักดิ์ จารยะพันธุ์, อ.ที่ปรึกษาวิทยานิพนธ์ร่วม: ดร. พิกุล จิรวาณิชไพศาล, ศ. ดร. เคนเน็ท โซเดอร์ฮอลล์, 194 หน้า.

การแพร่ระบาดของโรคกุ้งเป็นสาเหตุให้กุ้งตายเป็นจำนวนมาก และส่งผลให้เกิดความเสียหายต่ออุตสาหกรรมการส่งออกกุ้งอย่างมาก ส่วนใหญ่แล้วลักษณะของการเกิดโรคจะปรากฏที่บริเวณทางเดินอาหารของกุ้ง ดังนั้นความเข้าใจเกี่ยวกับปฏิสัมพันธ์ระหว่างแบคทีเรียก่อโรคและระบบภูมิคุ้มกันของกุ้งกุลาดำในระบบทางเดินอาหาร จึงมีความสำคัญในการหาทางป้องกันการติดเชื้อในระบบทางเดินอาหารของกุ้ง การศึกษาโดยใช้กล้องจุลทรรศน์อิเล็กตรอนสามารถนำมาใช้ตรวจสอบปฏิสัมพันธ์ของแบคทีเรียไม่ก่อโรคและแบคทีเรียก่อโรคกับบริเวณภายในของทางเดินอาหารได้ การแสดงออกของยีนที่เกี่ยวข้องกับระบบภูมิคุ้มกันที่แตกต่างกันสามารถตรวจสอบโดยใช้วิธี suppression subtractive hybridization (SSH) และ RNA sequencing (RNA-seq) จากการศึกษาพบว่า *Vibrio harveyi* 1526 มีการเพิ่มจำนวนและพบโครงสร้างลักษณะคล้ายไบโอฟิล์ม (biofilm-like formations) ในบริเวณกระเพาะอาหาร และตอนบนถึงกลางของลำไส้ส่วนกลาง แต่ไม่พบลักษณะดังกล่าวในบริเวณตอนท้ายของลำไส้ส่วนกลางและลำไส้ส่วนปลาย และมีการสร้างไฟเบอร์เส้นเดี่ยว (single polar fibre) เพื่อยึดเกาะเนื้อเยื่อบุผิวของกระเพาะอาหารของกุ้ง ส่วน *Vibrio parahaemolyticus* มีการสร้างโครงสร้างลักษณะคล้ายเพอริทริคัสพิลี (peritrichous pili-like structures) เพื่อยึดเกาะพื้นผิวของกระเพาะอาหาร ในขณะที่แบคทีเรียไม่ก่อโรคในกลุ่ม *Vibrio* sp. และ *Micrococcus luteus* ไม่พบลักษณะการยึดเกาะพื้นผิวในบริเวณทางเดินอาหารของกุ้ง จากการหายีนในกระเพาะอาหารที่เกี่ยวกับการตอบสนองของกุ้งในภาวะติดเชื้อ *V. parahaemolyticus* 3HP โดยวิธี suppression subtractive hybridization โดยการสุ่มโคลน และหาลำดับนิวคลีโอไทด์จำนวน 612 โคลน พบว่ามียีนที่มีลำดับนิวคลีโอไทด์เหมือนกับยีนในฐานข้อมูลจำนวน 69 ยีน โดยพบยีนที่เกี่ยวข้องกับภูมิคุ้มกันมีการแสดงออกเพิ่มขึ้นในกระเพาะอาหารหลังการเหนี่ยวนำให้ติดเชื้อผ่านไป 6 ชั่วโมงเมื่อเทียบกับกลุ่มควบคุม ได้แก่ salivary alkaline phosphatase, pacifastin heavy chain precursor, ubiquitin-conjugating enzyme H5b, ferritin, astakine variant 1 และ dicer 2 พบยีนที่มีการแสดงออกแตกต่างกันจำนวน 1,514 ยีน (ยีนที่มีการแสดงออกเพิ่มขึ้นจำนวน 1,122 ยีน และยีนที่มีการแสดงออกลดลงจำนวน 392 ยีน) สามารถจำแนกเป็นยีนที่เกี่ยวข้องกับระบบภูมิคุ้มกันจำนวน 141 ยีน และสามารถจัดกลุ่มตามหน้าที่ได้ 10 หน้าที่ ได้แก่ เปปไทด์ต้านจุลชีพ วิถีการส่งต่อสัญญาณ ระบบโปรพีโอ (proPO system) สภาวะเครียดออกซิเดชัน (oxidative stress) เอนไซม์ย่อยโปรตีนหรือเอนไซม์ยับยั้งการย่อยโปรตีน (proteinases/proteinase inhibitors) โปรตีนที่เกี่ยวข้องกับอะพอพโทซิสทูเมอร์ (apoptosic tumor-related protein) ตัวรับที่จดจำสิ่งสิ่งแปลกปลอม (pathogen recognition receptors) ระบบการแข็งตัวของเลือด (blood clotting system) โปรตีนยึดเกาะ (adhesive protein) และฮีทช็อคโปรตีน (heat shock protein) และพบไอโซฟอร์มใหม่ของแอนตี้ไลโพพอลิแซคคาไรด์แฟคเตอร์ (ALF) ในกระเพาะอาหาร ที่มีนิวคลีโอไทด์ที่สามารถแปลรหัสได้จำนวน 369 คู่เบส จึงเรียกไอโซฟอร์มใหม่นี้ว่า *Pm*ALF7 และพบการแสดงออกเพิ่มขึ้นในกระเพาะอาหารหลังการเหนี่ยวนำให้ติดเชื้อผ่านไป 6 และ 12 ชั่วโมง เมื่อเทียบกับกลุ่มควบคุม นอกจากนี้การศึกษายีน C-type lectin ที่ได้จากห้องสมุดยีนเก่าของตับและตับอ่อนของกุ้งกุลาดำ ซึ่งเป็นยีนที่มีความสำคัญเกี่ยวกับภูมิคุ้มกันในตับและตับอ่อน พบ นิวคลีโอไทด์ที่สามารถแปรรหัสได้จำนวน 522 นิวคลีโอไทด์ และการแสดงออกลดลงในตับและตับอ่อนหลังการเหนี่ยวนำให้ติดเชื้อผ่านไป 6 ชั่วโมงเมื่อเทียบกับกลุ่มควบคุม การศึกษาครั้งนี้แสดงให้เห็นว่าแบคทีเรียมีการเข้ายึดครองพื้นที่ในทางเดินอาหารก่อน โดยเฉพาะอย่างยิ่งบริเวณกระเพาะอาหารที่มีไคติน หลังจากนั้นมีการปล่อยสาร และเอนไซม์ที่ก่อให้เกิดโรคเพื่อทำให้กุ้งมีการติดเชื้อ ขณะเดียวกันกุ้งจะมีการป้องกันตัวจากเชื้อ โดยกระบวนการทางกายภาพ และกลไกของภูมิคุ้มกัน โดยความรู้เพิ่มเติมเกี่ยวกับปฏิสัมพันธ์ของแบคทีเรียและทางเดินอาหารของกุ้งกุลาดำ สามารถนำไปใช้ในการควบคุมและจัดการการเกิดโรคในกุ้งได้

สาขาวิชา เทคโนโลยีชีวภาพ ลายมือชื่อนิสิต .....

ปีการศึกษา 2558 ลายมือชื่อ อ.ที่ปรึกษาหลัก .....

ลายมือชื่อ อ.ที่ปรึกษาร่วม .....

ลายมือชื่อ อ.ที่ปรึกษาร่วม .....

5373827423 : MAJOR BIOTECHNOLOGY
KEYWORDS: SHRIMP IMMUNE BACTERIA GASTROINTESTINAL TRACT

WIPASIRI SOONTHORNCHAI: EFFECTS OF BACTERIA IN DIGESTIVE SYSTEM ON PATHOGENESIS AND IMMUNITY OF BLACK TIGER SHRIMP *Penaeus monodon*. ADVISOR: PROF. PADERMSAK JARAYABHAND, Ph.D., CO-ADVISOR: PIKUL JIRAVANICHPAISAL, Ph.D., PROF. KENNETH SöDERHäLL, Ph.D., 194 pp.

The outbreak of shrimp diseases causes massive mortality, and a huge loss of income from the shrimp exporting industry. Since most of the symptoms appear in the gastrointestinal tract, understanding the interaction between pathogenic bacteria and shrimp immune system in the digestive system is crucial to possible find means to prevent the infection of the gut. Scanning electron microscopy (SEM) was used to investigate the interaction between bacteria, both pathogenic and non-pathogenic, and the inner surface of the gastrointestinal tract of *P. monodon*. The differential expression of immune-related genes during an infection was examined using suppression subtractive hybridization (SSH) as well as RNA sequencing (RNA-seq). Results showed that an infection by *Vibro harveyi* 1526 was initiated by a proliferation of the bacteria in the biofilm-like formations in the stomach, the upper and middle midgut, but neither in the posterior midgut nor the hindgut. SEM also revealed the induced production of peritrichous pili-like structures by the *Vibrio parahaemolyticus* attaching to the stomach lining, whilst only a single polar fibre was seen forming an apparent physical bridge between *V. harveyi* and the host's epithelium. In contrast, no adherences or linkages were seen when trials were conducted with non-pathogenic *Vibrio* sp. or with *Micrococcus luteus*, and no obvious resultant changes to the host's gut surface was observed. A total of 612 randomly recombinant clones from SSH was matched to 69 known transcripts. The expressions of known genes, *i.e.* salivary alkaline phosphatase, pacifastin heavy chain precursor, ubiquitin-conjugating enzyme H5b, ferritin, astakine variant 1 and dicer 2 homologues were significantly up-regulated in stomach at 6 hours post infection. A set of 1,514 DEGs (1,122 unique genes up-regulated and 392 unique genes down-regulated) in the stomach was reported during *V. parahaemolyticus* (3HP) infection. Among these significantly differentially expressed genes, 141 unique genes could be classified as immune-related genes, and their functions were categorized into 10 functions including antimicrobial peptides, signal transduction pathways, proPO system, oxidative stress, proteinases/proteinase inhibitors, apoptosic tumor-related proteins, pathogen recognition immune regulators, blood clotting system, adhesive proteins and heat shock proteins. A novel isoform of anti-lipopolysaccharides was significantly increased in the stomach at 6 and 12 hours post infection. After characterization, this novel isoform contains 369 bp of the open reading frame, and was named *Pm*ALF7. Additionally, a C-type lectin receptor from an older *P. monodon* library was identified in hepatopancreas, and it is likely an important gene in the immune response of the hepatopancreas. The C-type lectin receptor contains 522 bp of the open reading frame, and its expression was significantly decreased in the hepatopancreas at 6 hours post infection. The current dissertation suggests that pathogens of *P. monodon* must be able to colonize in the digestive tract, particularly the stomach, where chitin is present, and then they use an array of virulent factors and enzymes to establish an infection in their host and *P. monodon* responds to pathogenic bacteria through physical barriers and activation of immune processes. These studies about interaction between bacteria and gastrointestinal tract of *P. monodon* increase the knowledge of how the shrimp stomach responds to bacteria and might provide new strategies for controlling and managing shrimp diseases.

Field of Study: Biotechnology
Academic Year: 2015

Student's Signature .....
Advisor's Signature .....
Co-Advisor's Signature .....
Co-Advisor's Signature .....

ACKNOWLEDGEMENTS

I am sincerely grateful to my advisor, Professor Dr. Padermsak Jarayabhand, my co-advisors Dr. Pikul Jiravanichpaisal and Professor Dr. Kenneth Söderhäll, my special advisors Dr. Sirawut Klinbunga and Dr. Sage Chaiyapechara for their invaluable guidance and value suggestions including constant encourage throughout this study.

I am also grateful to my dissertation examination committee consisting of Associate Professor Dr. Charoen Nitithamyong, Assistant Professor Dr. Kittinan Komolpis, Assistant Professor Dr. Sanit Piyapattanakorn, Dr. Puttharat Baoprasertkul, who contributed their time to help bringing my work to perfection.

I am thankful to Dr. Sithichoke Tangphatsornruang, Dr. Narongsak Puanglarp and Dr. Bavornlak Khamnamtong for very useful comments and suggestion, Miss Thippawan Yoocha for helping in RNA sequencing, Miss Wilawan Thongda for transcriptome analysis using CLC workbench program, and Mr. Seri Donnuea for supporting and suggesting about cultured shrimp at the Center of Excellence for Marine and Biotechnology (CEMB).

I would like to extend my special thanks to everyone in AAMG and CEMB laboratory in the National Center for Genetic Engineering and Biotechnology (BIOTEC) and laboratory in Department of Comparative Physiology based on Professor Kenneth Söderhäll, Uppsala University for their help and friendly assistance.

I wish to acknowledge the contributions of the Institute for Promotion of Teaching Science and Technology (IPST), Thailand, via Development and Promotion of Science and Technology Talents Project (DPST) for my scholarship, the 90th Anniversary of Chulalongkorn University Fund (Ratchadaphiseksomphot Endowment Fund) for my research fund and the National Center for Genetic Engineering and Biotechnology (BIOTEC) for approving the use of the equipment at the Aquatic Molecular Genetics and Biotechnology Laboratory (AAMG) and the Center of Excellence for Marine and Biotechnology (CEMB).

Finally, indispensable person, my gratefulness are my family and my boyfriend for their guidance, understanding, encouragement, endless love and support along my study.

CONTENTS

Page

Page

Page

Page

LIST OF TABLES

Page

Page

LIST OF FIGURES

Page

Page

Page

Page

Page

ABBREVATIONS

bp	Base pair
ºC	Degree Celsius
CTAB	Cetyl trimethylammonium bromide
DEPC	Diethylpyrocarbonate
DNA	Deoxyribonucleic acid
dNTP	Deoxyribonucleotide triphosphate
EDTA	Ethylenediaminetetraacetic acid
IPTG	Isopropyl β-D-1-thiogalactopyranoside
Kb	Kilobase
kD	Kilo daltan
L	Liter
M	Molar
mg	Miligram
ml	Mililiter
mM	Milimolar
ng	Nanogram
PCR	Polymerase chain reaction
pI	Isoelectric point
RNA	Ribonucleic acid
RNase A	Ribonuclease A
rpm	Revolution per minute
SDS	Sodium dodecyl sulfate
Tris	Tris (hydroxyl methyl amino methane
µg	Microgram
µl	Microliter
µM	Micromolar
U	Unit
UV	Ultraviolet

CHAPTER I

INTRODUCTION

1.1 Rationales

Shrimp aquaculture is an important sea food industry in the world and a great potential to generate high export earnings in China, Thailand, Indonesia, Vietnam, Ecuador and India [1]. However, its development is seriously affected by the outbreak of viral and bacterial diseases.

In aquatic animals, gut microbes have been recognized to play a role in the development, nutrition, immune response and disease resistance of their hosts [2-5]. In shrimp, bacteria may also have several beneficial roles [4-6]. As with other animals, the gut of shrimp are exposed to the environment, *i.e.* pond bottom and water. This is an important port of entry for pathogens (bacteria and viruses), which they can establish and develop into an infection.

Vibrios are ubiquitous marine bacteria that are found in a wide range of aquatic habitats, and are frequently encountered in association with marine organisms. Some species of *Vibrio* such as *Vibrio parahaemolyticus* and *Vibrio cholera* are a concern in food safety as the pathogenic bacteria that can cause gastroenteritis in human. Both species of *Vibrio* can produce chitinolytic enzymes and utilize chitin; they are frequently associated with the exoskeletons of crustacean [7]. Chitin-binding proteins for the attachment of these *Vibrio* species to chitin have been reported in *Vibrio harveyi* [8,9] and *V. parahaemolyticus* (*i.e.* chitovibrin) [10]. In black tiger shrimp *Penaeus monodon*, vibriosis is a generic term for an infection caused by any number of *Vibrio* species including *V. harveyi, Vibrio vulnificus* and *V. parahaemolyticus,* any of which can result in mass mortality of stock in hatcheries and grow-out ponds [11,12]. Among these, *V. harveyi* and *V. parahaemolyticus* are the virulent and dominant pathogens of cultured penaeid shrimp [13-15].

A recently emerging disease in shrimp aquaculture is AHPND (Acute Hepatopancreatic Necrosis Disease)/EMS (Early Mortality Syndrome) that causes mass mortalities of black tiger shrimp *P. monodon* and white shrimp *Litopenaeus vannamei*

during the first 20 to 30 days after rearing in a pond [16,17]. The first outbreak was reported in South of China in 2010 [16-18]. In Thailand, it was widespread in the eastern coast of the Gulf of Thailand during late 2012 causing a large decrease in the production of shrimp aquaculture [18,19]. Food and Agriculture Organization of the United Nations (FAO) [20] reported that AHPND was a major problem for shrimp aquaculture in Thailand, resulting in 25% lower production in 2014 compared to 2013.

Histopathology studies showed that the effects appear to be limited to the hepatopancreas. More specially, the tubule epithelial cells of hepatopancreas sloughed into the tubule lumens [17,21]. Recently, the bacteria in stomachs of AHPND-positive shrimp were identified as *V. parahaemolyticus* [21]. The bacteria were also isolated from hepatopancreas of shrimp collected at a shrimp farm experiencing massive death in Thailand and were also identified as *V. parahaemolyticus*. Three strains of *V. parahaemolyticus* isolated from hepatopancreas showed the characteristics of AHPND in hepatopancreas. *V. parahaemolyticus* 3HP is highly virulent both if it is used for injection into the animal or oral infections [19]. Consequently, stomach and hepatopancreas are the organs of AHPND infection.

Host defense in invertebrates such as shrimp is believed to rest entirely on innate, non-adaptive immune responses [22]. A cDNA library of hepatopancreas *P. monodon* was already constructed and several genes in HP and their response to pathogenic bacteria have been studied [23-26]. But no studies in the literature of immune response to pathogenic bacteria in stomach exists, and only one study in stomach immune response to WSSV has been published [27].

A healthy gastrointestinal tract is vital for human well-being and the same is true for shrimp. Consequently, it is crucial to understand the interaction between gastrointestinal bacteria and shrimp immune response in both healthy and infected conditions. In order to study the effects of bacteria in the shrimp digestive system, scanning electron microscopic examination are important tools for investigating the interaction between pathogenic *Vibrio* and the inner surface of the digestive tract of *P. monodon*. To understand the immune response, the differentially expressed genes (DEGs) in the stomach of uninfected and infected *P. monodon* was compared by

suppression subtractive hybridization and Ion torrent sequencing. Additionally, C-type lectin genes from the *P. monodon* EST database [23] were identified and characterized.

1.2 Objectives

1. To examine the attachment and localization of bacteria in gastrointestinal tract *P. monodon* during non-pathogenic and pathogenic infection.

2. To identify DEGs in the stomach of uninfected and infected *P. monodon* and characterize candidate immune-related gene.

3. To identify and characterize pattern recognition receptor proteins (PRRP) in hepatopancreas from the *P. monodon* EST database.

CHAPTER II

LITERATURE REVIEWS

2.1 Shrimp Aquaculture in Thailand

Shrimp aquaculture has increased dramatically since the early 1970s [28], and Thailand has been a world leader in the export of cultured shrimp since 1992 [29]. *P. monodon* was the most important farmed shrimp because this species has a high export value and is able to grow quickly [30]. The rapid development of aquaculture also brought several problems for shrimp farming. From 2000 to 2002, the production of *P. monodon* decreased (Figure 2.1) because of retarded growth and outbreaks of shrimp diseases [31-34].

The retard growth is mainly caused by hepatopancreatic parvovirus (HPV) but it also can be caused by other virus or bacterial pathogens [34]. Additionally, *P. monodon* has a fairly low reproductive maturation in female broodstock when domesticated and has a low quality of sperms from captive male broodstock [35]. In order to avoid these problems in *P. monodon*, *L. vannamei* has been introduced in Thailand aquaculture since 2003. An advantage of *L. vannamei* is rapid growth rate, tolerance to high stock density, high survival rate during larval rearing, lower protein requirement, it resists to low salinity and temperature, and it has certain disease resistance especially if specific pathogen resistant stocks are used. However, *L. vannamei* has a disadvantage, *i.e. L. vannamei* is an alien species of Thailand and broodstock must be imported from the outside. Therefore, it might act as a carrier of various pathogens, *i.e.* Taura Syndrome Virus (TSV) [36] and acute hepatopancreatic necrosis disease (AHPND) [18].

In late 2012, EMS (Early Mortality Syndrome) was reported in Thailand [18], and it resulted in a significant decrease of *L. vannamei* production in 2013 (Figure 2.1). EMS is defined as causing massive mortality in shrimp within the first 35 days after rearing in ponds. The new disease called acute hepatopancreatic necrosis disease (AHPND), which might be caused by different *V. parahaemolyticus* isolates [19].

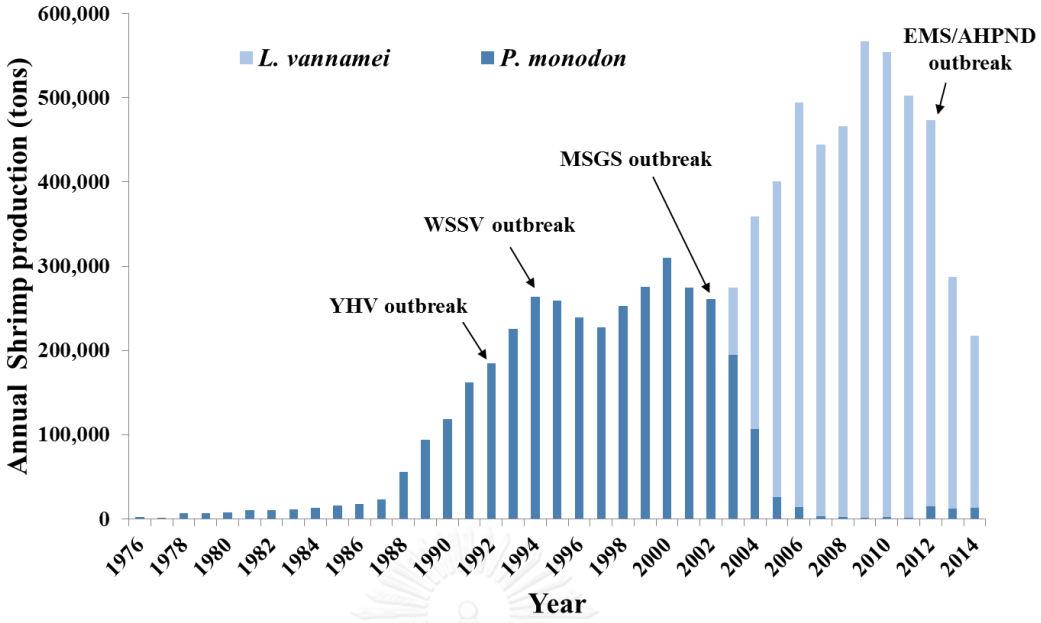

Figure 2.1 Production of *P. monodon* and *L. vannamei* in Thailand from 1976 to 2014 (Source: International Technical Seminar/Workshop "EMS/AHPND: Government, Scientist and Farmer Responses")

2.2 *P. monodon* Biology

2.2.1 Taxonomy of *P. monodon*

The common name of *P. monodon* is black tiger shrimp (English) and Kung klula-dam (Thailand). *P. monodon* is classified as detailed below.

Kingdom: Animalia

Phylum: Arthropoda

Class: Malacostraca

Order: Decapoda

Family: Penaeidae (Rafinesque, 1985)

Genus: *Penaeus* (Fabricius, 1798)

Species: *Penaeus monodon* (Fabricius, 1798)

2.2.2 Morphology

Cephalothorax and abdominal segments are main parts of the external anatomy of shrimp (Figure 2.2). The cephalothorax consists of a carapace, a rostrum, compound eyes and appendages. The carapace covers the whole cephalothorax to protect the internal organs and supports muscle regions. The rostrum curves down very slightly with 7-8 dorsal teeth and 3-4 ventral teeth. The appendages have several functions, *i.e.* an antennae and antennules forming sensory organ, mandibles and maxillaes forming jaw-like structures and maxillipeds are for food handing and walking legs (pereiopods).

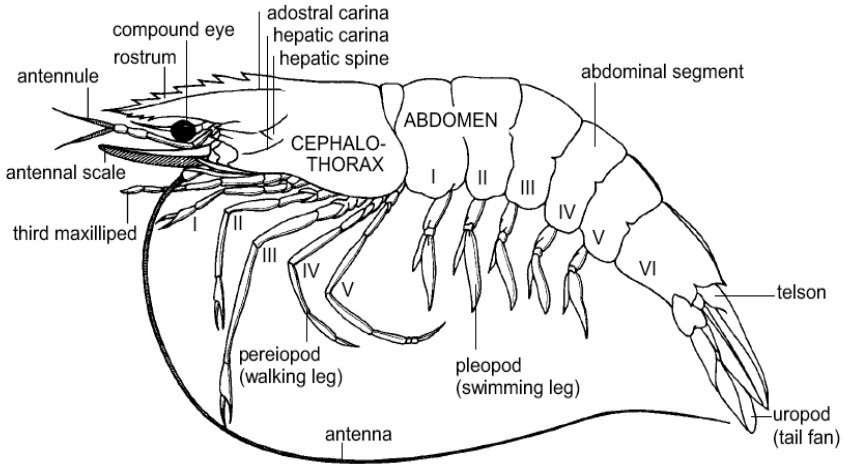

Figure 2.2 Lateral view of the external anatomy of a female penaeid shrimp (Source: Primavera, 1990) [37]

The basic internal organs of penaeid shrimp are divided into 4 systems including digestive system, circulatory system, nervous system and reproductive system. The digestive system consists of stomach, intestine, hindgut and hepatopancreas. The hepatopancreas is the main part of the cephalothorax. The stomach ends connecting with the anterior intestine and is inserted into the hepatopancreas and connects together with the primary duct. The anterior stomach is on the upper part of hepatopancreas. The intestine longitudinally lays on the abdominal segment and

connects to hindgut at the end of the abdominal segment. The open circulatory system of penaeid shrimps has a heart which is located on the hepatopancreas. One of the hemolymph vessels leaves the heart and ends in the lymphoid organ, where the hemolymph is filtered. This organ is located ventro-anteriorly to the hepatopancreas. The hematopoietic tissue which contains the stem cells of hemocytes is mainly located around the stomach and in the onset of the maxillipeds. The nervous system consists of a dorsal brain, a pair of ganglia and two ventral nerve cords. The reproductive system consists of ovary and testis. Both ovary and testis are located on the hepatopancreas and along the tail following intestine. Additionally, the body movement is controlled by several kinds of muscle, and the gills are the respiratory organ.

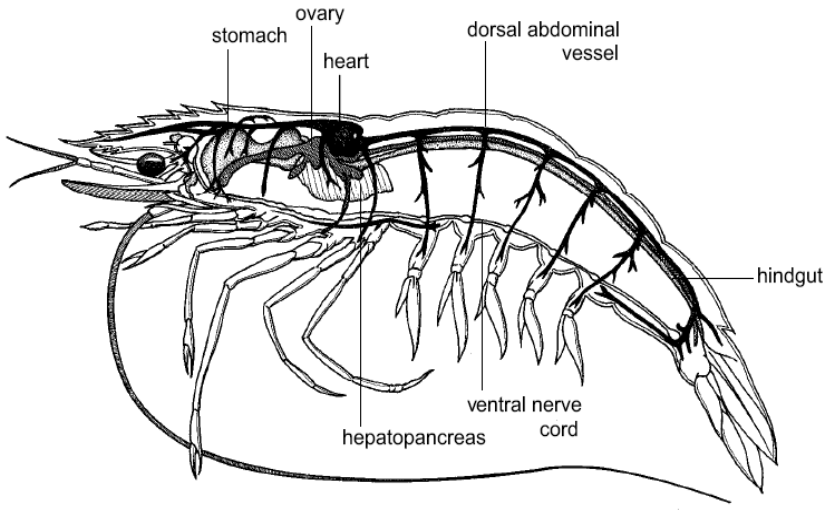

Figure 2.3 Lateral view of the internal anatomy of a female penaeid shrimp (Source: Primavera, 1990) [37]

2.2.3 Digestive system

The digestive system is divided into three parts: foregut, midgut and hindgut. Additionally, hepatopancreas is also included in the digestive system which helps to produce digestive enzyme. The foregut comprises oral, esophagus, and stomach. The midgut is composed of the intestine, anterior midgut caeca and posterior midgut caeca. Finally, the hindgut consists of rectum and anus.

The foregut comprises mouth, esophagus and stomach. The mouth is located between a pair of mandible, and is covered with cuticle. The mandibles are used to cut, smash and grind food. After that, there is a labrum to push the grinded food into the esophagus. Additionally, the mouth has a pair of paragnatha to protect the food from reversing. The esophagus is a short tube covered with epicuticle, exocuticle, endocuticle and a membranous layer. It receives the food from mouth and sends it to the stomach. The stomach is located at the middle hepatopancreas and consists of a cardiac stomach and pyloric stomach. The cardiac stomach is the anterior stomach lined with cuticle. The end of cardiac stomach has an upper and lower cardiac groove to receive enzyme from hepatopancreas, as well as gastric mill to grind food. The pyloric stomach is posterior stomach also lined with cuticle. The pyloric stomach is divided into dorsal and ventral subchamber. Teeth and ossicle are in the dorsal subchamber. They grind and send the food to the ventral subchamber. The ventral subchamber has gastric sieves to filter the ingested food. The gastric sieves consist of setae and longitudinal inter-setal groove to send ingested food to midgut.

The midgut is composed of intestine, anterior and posterior midgut caeca. The intestine is a hollow tubule extending from the pyloric stomach to hindgut. It is divided into mucosa layer and submucosa layer. The mucosa layer has microvilli covered with peritrophic matrix (PM). The anterior midgut caeca is inserted into the pyloric stomach, which secretes the PM. Additionally, the posterior midgut caeca is located at the end of intestine. The anterior and posterior midgut caeca have several tegmental glands. The hindgut connects from posterior caeca to anus, which is lined by cuticle. The folding of a simple epithelium forms a multi-chamber tube in hindgut. There are several tegmental glands in hindgut especially near posterior midgut caeca. The end of hindgut forms an ampulla [38].

2.3 The Major Shrimp Diseases in Thailand

2.3.1 Luminous disease

Luminous disease has been the major problem in shrimp farming since 1990s. *Vibrio harveyi* is the main bacterium which causes the luminous symptoms in

P. monodon larvae and juveniles [14,39,40]. *V. harveyi* is a rod shaped, Gram-negative bacterium with 0.5-0.8 µm width and 1.4-2.6 µm length. Presumptive diagnosis is based on clinical signs such as blood or hepatopancreas that is streaked on a *Vibrio*-selective or general marine agar plate. After incubation at room temperature overnight, colonies of *V. harveyi* grow and show strong luminescence in dim light. *Vibrio* species live in cultured water, in low oxygen environments such as in the gut of aquatic animals and sometimes are found in the bottoms of shrimp ponds. Consequently, this bacteria can enter shrimp via the cuticle or sub-cuticle that also give the name shell disease or black/brown spot disease, punctured wounds such as loss of limbs and into the gut or hepatopancreas and can cause general septicaemia [41].

The infected shrimp have a milky white body and appendages, are weak, have a disoriented swimming, lethargy and loss of appetite. The post larvae display cloudy hepatopancreas and brown gills [42,43]. Finally, it leads to death. Histopathology of infected shrimp organs are done using basophilic and histological techniques [14]. Hepatopancreatic and midgut epithelial cells in the gut lumen are commonly detached. The cuticular colonization is the reason of necrosis of the cuticular epithelium and the formation of melanised lesion. Septic hemocytic nodules are formed in the lymphoid organ, heart and connective tissues of the gills, hepatopancreas, antennal gland, nerve cord, telson and muscle [15,43].

2.3.2 AHPND/EMS

A newly emerging disease called early mortality syndrome (EMS) caused a mass mortality of shrimp in southern China in 2009 and spread over China in 2010. EMS was found in Vietnam in 2010 and was spread to the Mekong Delta (South Vietnam) in 2011. In addition, the disease was reported in Malaysia in 2011. In Thailand, it was recently spread in the eastern coast of the Gulf of Thailand during late 2012 [16,18,44].

Early mortality syndrome (EMS) is generally a term of unusually high mortality of shrimp postlarvae within 30 days after pond stocking due to the problem of pond management and pathogen related factors. White spot syndrome virus (WSSV), yellow head virus (YHV) and vibriosis have been linked to outbreaks of EMS [44]. Acute hepatopancreatic necrosis disease (AHPND) is the definition of the characteristic

histopathology of shrimp which also includes (1) acute progressive degeneration and dysfunction of the hepatopancreas, (2) necrosis and sloughing of tubule epithelial cells of hepatopancreas (3) hemocytic infiltration, necrotic and sloughed hepatopancreatic tubules. Additionally, the infected shrimp have a white hepatopancreas, an atrophy of hepatopancreas and soft shells and guts with no contents (Figure 2.4) [44].

Recently, the bacteria in stomach and hepatopancreas of AHPND-positive shrimp were identified as *V. parahaemolyticus* [19,21]. *V. parahaemolyticus* is a rod shaped Gram-negative bacterium with 0.5 - 0.8 μm in width and 1.4 - 2.6 μm in length [45]. The AHPND *V. parahaemolyticus* strains carries a 69-kb plasmid which contains the insecticidal *Photorhabdus* insect-related binary toxin PirAB [46,47].

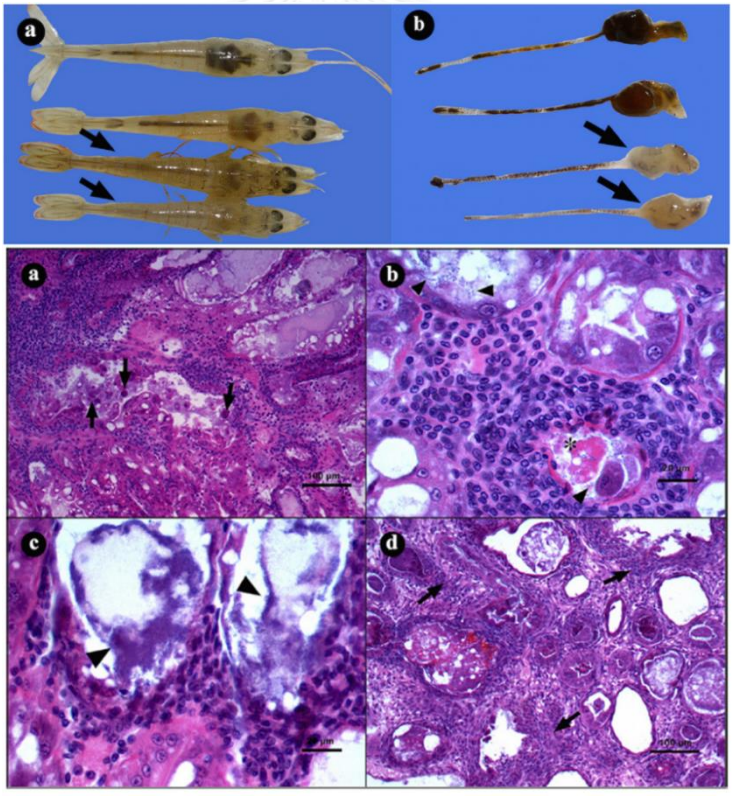

Figure 2.4 The hepatopancreas of white shrimp *L. vannamei* naturally infected by AHPND. (a and b) of blue background show infected white shrimp which showed atrophy and white color of hepatopancreas (arrow), and (a-d) show the terminal stage of AHPND infection in hepatopancreas. (Source: Soto-Rodriguez et al., 2015) [48]

2.3.3 White Spot Syndrome Virus (WSSV)

White Spot Syndrome Virus (WSSV) infections started in Taiwan since 1992 and then rapidly spread over Asia, Pacific Ocean, North, South and Central America. The disease causes up to 100% mortality within 10 days in shrimp [33,49-51]. WSSV is a tailed, rod shaped, double stranded DNA virus with a very large circular genome of about 300 kbp [52,53].

WSSV is infecting all life stages of shrimp. WSSV infected shrimp has white spots on the inner carapace. The white spot has a small dark spot at the center when observed under the light microscope. The infected shrimp displays a pale or reddish body color and has swollen or shrunken lymphoid organs [54]. The target tissue of WSSV infection is connective tissue, nervous tissue, muscle tissue and epithelium [55]. The pathogenicity shows an initial stage with a prominent eosinophilic response with an intranuclear inclusion with a clear zone around to a heavy stage with a large basophilic response with an intranuclear inclusion with variable multifocal necrosis [49,56].

2.4 Shrimp Immune Response

The immune system is generally classified into two types: namely innate and adaptive immunity. Host defense in invertebrates such as shrimp is believed to rest entirely on innate, non-adaptive immunity [22]. At present, there are several publications studying the shrimp immunity and their defense against pathogens. However, only a few publications have studied the immune response in the gastrointestinal tract and since there are a few studies of the intestine of fruit fly *Drosophila melanogaster* it has been used as a model to understand shrimp innate immune response in gastrointestinal tract. However recently some studies have been published on the shrimp immune system in intestine.

2.4.1 Antimicrobial peptide (AMP) production

Toll and Immune Deficiency (Imd) pathway regulate the synthesis of antimicrobial peptide in *Drosophila*. Those pathways are triggered by the pathogen-associated molecular patterns (PAMPs) to produce the antimicrobial peptides. In

shrimp, the Toll and IMD pathways have been studied since 2007 but until now the full details of the pathways are not known.

2.4.1.1 Toll pathway

The components of *D. melanogaster* Toll pathway consist of Spätzle, Toll, dMyD88, Tube, Pelle, TNF receptor associated factors 6 (dTRAF6), Dorsal, Dorsal-related immune (DIF) and Cactus. After an infection in *D. melanogaster* PAMPs from the pathogen trigger a pro-Spätzle processing enzyme to cleave pro-Spätzle to Spätzle which can bind to the ectodomain of the transmembrane receptor Toll. Then after, the intracellular TIR domains of the activated Tolls recruit dMyD88 to form a trimeric complex (dMyD88-Tube-Pelle). The trimeric complex triggers a cytoplasmic Dorsal/Cactus complex leading to phosphorylation and degradation of Cactus. Then, the Dorsal is released and translocated into the nucleus to activate immune-related genes, *i.e.* Drosomycin and other antimicrobial peptides [57-60].

In shrimp, Spätzle was found in Chinese shrimp *Fenneropenaeus chinensis* and white shrimp *L. vannamei*. The functions are possibly involved in the innate immune signal pathways to defend both a *Vibrio alginolyticus* and a WSSV infections [61,62].

Tolls and Toll-like receptors (TLR) have evolutionary conserved transmembrane glycoproteins which are characterized by an extracellular domain containing several numbers of leucine-rich repeat (LRR) motifs and an intracellular signaling domain homologous to Toll/IL-1 receptor (TIR) domain [63]. In shrimp, Toll-like receptors have been cloned in white shrimp *L. vannamei* (*Lv*Toll), black tiger shrimp *P. monodon* (*Pm*Toll), kuruma shrimp *Marsupenaeus japonicus* (*Mj*Toll) and Chinese shrimp *F. chinensis* (*Fc*Toll) [64-66]. They are likely to be involved in defense mechanism in shrimp. Recently, the silencing *Lv*Toll significantly decreased penaeidin 3; therefore, *Lv*Toll might be involved in regulation of the penaeidin production [67].

In *D. melanogaster*, dMyD88, Tube and Pelle formed a trimeric complex (dMyD88-Tube-Pelle) to trigger Dorsal/Cactus complex, which regulates the Toll-dependent gene expression, *i.e.* antimicrobial peptides and many other innate immune responsive genes [57,58]. The dMyD88 protein contains a death domain (DD)

in the N-terminus and a TIR domain in the C-terminus [68]. Tube contains the N-terminal DD and five evolutionarily conserved 8-amino acid repeats in the C-terminus [69]. Pelle contains the N-terminal DD and a catalytic kinase domain in the C-terminus [70]. In shrimp, MyD88s have been characterized in Chinese shrimp *F. chinensis*, black tiger shrimp *P. monodon* and white shrimp *L. vannamei* [71-73]. *Fc*MyD88 responded to bacterial and viral pathogen, and *Pm*MyD88 responded to WSSV infection [71,72]. Two isoforms of Tube (*Lv*Tube and *Lv*Tube-1) were isolated in white shrimp *L. vannamei*, and they showed different activities, different tissue distributions and different expression profiles during bacterial and viral stimulation. It might play different roles in the TLR pathway[73]. Two Pelles were cloned in white shrimp *L. vannamei*. They responded to pathogenic infection and are likely involved in Toll pathway [73,74].

TNF receptor associated factors 6 (TRAF6) and Pelle can form a receptor complex and this complex is downstream of the Toll pathway [75-77]. TRAF6 was identified in white shrimp *L. vannamei*. It could activate the promoters of antimicrobial peptide genes in *D. melanogaster* S2 cells, and it is likely to play an important role in host defense mechanism to bacterial and viral pathogen [78].

Cactus/Dorsal complex is triggered by the trimeric complex (dMyD88-Tube-Pelle) to phosphorylate and degrade the Cactus; therefore, the Dorsal is released and translocated into the nucleus to activate antimicrobial production [57-60]. Cactus was identified in Chinese shrimp *F. chinensis*, white shrimp *L. vannamei* and black tiger shrimp *P. monodon* [79-81]. Dorsal was identified in Chinese shrimp *F. chinensis* and white shrimp *L. vannamei* [82,83].

2.4.1.2 Immune Deficiency pathway

In *D. melanogaster*, IMD pathway is essentially activated by Gram-negative bacteria through the recognition of the diaminopimelic acid (DAP)-type peptidoglycan by specific PGRPs [84]. The components of *D. melanogaster* IMD pathway consist of the PGRP-LC receptor, Immune deficiency (IMD), TGF-β-activated kinase 1 (TAK1), TGF-β–activated kinase 1/MAP3K7 binding protein 2 (TAB2), *Drosophila* inhibitor of apoptosis protein (DIAP2), IκB kinase signalosome (IKK1, IKK2), *Drosophila* fas-associated death domain protein (dFADD) adaptor, death-

related ced-3/Nedd2-like protein (Dredd) and Relish [58]. Gram negative bacteria directly binds to PGRP-LC receptor which activates a cytoplasmic IMD [85,86]. Active IMD interacts with dFADD adaptor, and this adaptor binds to caspase DREDD [87] to cleave Relish/Rel. Then, the Rel is released and translocated into the nucleus to activate immune-related genes, *i.e.* Diptericin and other antimicrobial peptides [88,89]. Additionally, an activated IMD triggers the Tab2/Tak1 complex leading to activate the IKK complex [90-93]. The IKK complex phosphorylates and cleaves Relish/Rel [92], and then the Rel is released and translocated into the nucleus to activate immune-related genes.

IMD was characterized in white shrimp *L. vannamei* and Chinese shrimp *F. chinensis* [94,95]. In *L. vannamei*, *Lv*IMD transcript was expressed in most tissues and, it was induced in hepatopancreas and hemocytes after immune challenge with LPS (from *E. coli*) and Gram-negative *V. alginolyticus*, while not induced in gill after immune challenge. In addition, the localization study showed that *Lv*IMD was localized in the cytoplasm [94]. In *F. chinensis*, *Fc*IMD mRNA was expressed in gill and stomach. It was induced in hemocytes and gill after WSSV infection, but no change in gills after challenge with *V. anguillarum*. Additionally, *Fc*IMD localization shows that *Fc*IMD was localized in the cytoplasm of hemocytes [95].

TGF-β–activated kinase 1/MAP3K7 binding protein 2 (TAB2) was identified in white shrimp *L. vannamei*, and its transcript was expressed in most tissues. The expression level of TAB2 was induced in gill and hemocyte post infection with LPS, *V. parahaemolyticus* and WSSV. TAB2 silencing caused a down-regulation of anti-bacterial peptide, *i.e.* ALF and penaeidin. Moreover, TAB2 protein was located in cytoplasm of hemocyte [96].

Inhibitor of apoptosis protein (IAP) was characterized in black tiger shrimp *P. monodon* and white shrimp *L. vannamei* [97-99]. All IAPs were expressed in most tissues. *Pm*API could block Rpr's pro-apoptotic activity in insect cells [97]. *Lv*API1 might be involved in host defense to WSSV, while *Lv*API2 might be involved in host defense to bacteria [98].

IκB kinase signalosome (IKKs) were identified in white shrimp *L. vannamei* (*Lv*IKKβ and *Lv*IKKε), their transcripts were expressed in most tissues. The

expression level of *Lv*IKKβ was induced in gill, and *Lv*IKKε was slightly induced in gill, hemocyte and hepatopancreas post WSSV infection. Moreover, the *Lv*IKKβ and *Lv*IKKε transcripts were increased in gill, hepatopancreas and intestine post *V. alginolyticus* infection. The localization of IKKs showed that *Lv*IKKβ was localized in the cytoplasm and nucleus, while *Lv*IKKε was only localized in the cytoplasm of *Drosophila* S2 cells. The silencing of *Lv*IKKβ or *Lv*IKKε decreased the antimicrobial peptide of *L. vannamei*, *i.e.* penaeidin, lysozyme and crustins, but shrimp was more resistant to WSSV infection. Therefore, *Lv*IKKβ and *Lv*IKKε might participate in the regulation of shrimp antimicrobial peptides and that WSSV may subvert the *L. vannamei* IKK–NF-κB signaling pathway to facilitate viral gene expression [100].

Relish was found in Chinese shrimp *F. chinensis* and white shrimp *L. vannamei* [101,102]. The expression of *Fc*Relish was mainly in hemocytes as well as the lymphoid organ, and its transcription profile was induced after infection with *V. anguillarum*, *Micrococcus lysodeikticus* and WSSV [83,102]. Silencing of *Fc*Relish could significantly affect ALF, crustin, penaeidin 3 and penaeidin 5 production [102,103].

2.4.1.3 Antibacterial peptides

Antimicrobial peptides (AMPs) are one important parts of innate immunity. In all kingdoms, from bacteria to human, a wide variety of AMPs have been identified and characterized. Normally, AMPs contain less than 150-200 amino acid residues and have a wide variety and diversity in amino acid sequence, structure and range of activity. AMPs are active against a broad spectrum of microorganisms such as bacteria, filamentous fungi, virus and parasites [104,105] and also exhibit an anti-tumor property [106]. Depending on their tissue distribution, AMPs ensure either a systemic or local protection of the host against pathogen. The major AMPs in shrimp includes anti-lipopolysaccharide factors (ALFs), crustin and penaeidins.

ALFs are active against a broad spectrum of microorganism such as Gram-negative, Gram-positive bacteria, fungi and virus. ALF was initially isolated and characterized in hemocytes of the horseshoe crab *Limulus polyphenus* [107]. Additionally, several isoforms of ALF were reported in crustacean species, *i.e.* six isoforms from black tiger shrimp *P. monodon* [108,109], six isoforms from Chinese

shrimp *F. chinensis* [110], seven isoforms from swimming crab *Portunus trituberculatus* [111-114] and three isoforms from white shrimp *L. vannamei* [115]. Each isoform is similar in nucleotide sequence, and showed a conserved cysteine residues as the LPS-binding domain (LBD) [108,110,116]. In *P. monodon*, *Pm*ALF2 and *Pm*ALF3 were major expressed in hemocytes, and were significantly increased after *V. harveyi*-challenge [117].The localization of *Pm*ALF3 was studied and shown to be mainly in hemocytes and this ALF was increased after *V. harveyi* infection [118]. Additionally, ALF*Pm*6 was significantly increased at 6 hours post infection with *V. harveyi* and at 12, 24 and 48 hours post infection with WSSV [109].

Crustins are cationic cysteine-rich AMPs with single whey acidic protein (WAP) domain at the C-terminus, and are classified into three types including type I, II and III [119]. Crustins are active against Gram-negative, Gram-positive bacteria, fungi and virus. Crustin was initially isolated and characterized in the shore crab *Carcinus maenas* [120]. After that, crustin was identified and characterized in several crustacean species, *i.e*. black tiger shrimp *P. monodon* [121-126], white shrimp *L. vannamei* [127,128], Chinese shrimp *F. chinensis* [129-132] and kuruma shrimp *M. japonicus* [133-135]. In vitro study of the protein of Crus*Fc* and Crustin*Pm*1 had only activity against Gram-positive bacteria and had no inhibition on the growth of Gram-negative bacteria [130,136]. However, the expression profile of crustin-like antimicrobial peptide was decreased at 6 hours then after it was a significant increase in hemocyte at 24 hours post injection with *V. harveyi* in *P. monodon* [125]. Additionally, the transcript level of crustin was decreased at 4 hours post-injection and the decreased transcript levels returned to initial levels by 72 hours post-injection with LPS in *L. vannamei* [137].

Penaeidins contain a proline-rich N-terminus and a C-terminus containing six cysteine residues engaged in three disulfide bridges [138,139]. Penaeidins were classified into three subgroups based on amino acid sequence comparison and the position of specific amino acids [140,141]. They have a strong antimicrobial activity against Gram-positive bacteria, fungi and a modest activity against Gram-negative bacteria [138,142,143]. Penaeidin was initially isolated and characterized in hemocytes of *L. vannamei* [144]. Subsequently, the penaeidins were

detected in several shrimps, *i.e.* black tiger shrimp *P. monodon* [122,145-147], white shrimp *L. vannamei* [141,148] and Chinese shrimp *F. chinensis* [143,149]. The expression level of penaeidin was significantly decreased in *P. monodon* hemocytes at 3 hours post injection with *V. harveyi* [108]. Additionally, the transcript of penaeidin 2, penaeidin 3, penaeidin 4 were decreased in hemocytes at 4 hours post injection with LPS and returned to initial levels at 72 hours post injection in *L. vannamei* [137]. However, the expression levels of penaeidin 5 increased after 24 hours post injection with a bacterial mix of both *S. aureus* and *V. anguillarum* in all tissues especially in hemocyte, heart, gill, hepatopancreas, stomach and intestine of *F. chinensis* [143].

2.4.2 Melanization and the prophenoloxidase system

Melanization is an important component to defend the pathogen by producing the toxic intermediates and activated proteins which are involved in wound healing, encapsulation, elimination and killing of the microorganism [150-152]. Its reaction products provide both toxic quinone substances and other short-lived reaction intermediates to form melanin for the encapsulation process, to form sclerotisation for wound healing and to help phagocytosis during cellular defense [153]. Melanization requires the activation of phenoloxidase (PO) which catalyses the oxygenation of monophenols to o-diphenols and further oxidation of o-diphenols to o-quinones and eventually the synthesis of melanin [154].

The proPO system is an important innate immune defense in invertebrate and consists of several proteins involved in melanin production, cell adhesion, encapsulation and phagocytosis [152,153,155-157]. Additionally, the proPO system might fulfil some functions of a complement-like system in chordate animals, because the activation of this system producing cytotoxic and opsonic factors [157]. The proPO system is triggered by pathogen-associated molecular patterns (PAMPs), *i.e.* lipopolysaccharide from Gram negative bacteria, peptidoglycan from Gram positive bacteria and β-1,3-glucan from fungi [156,158,159]. The proPO activating system requires a serine proteinase cascade to activate the proPO activating enzyme (proPPAE) into active PPAE, then PPAE cleaves the proPO into active PO. The proPO activation is inhibited by serpin/pacifastin [153,154] (Figure 2.5).

The proPO activating enzymes (PPAE) is synthesized and maintained as a zymogenic protein (proPPAE) and is activated another serine proteinase [153,160]. The C-terminal half of the proPPAE is composed of a typical serine proteinase domain with a sequence similar to other invertebrate and vertebrate serine proteinase domain, the N-terminal half contains glycine-rich domain, a cationic proline-rich domain and a clip-domain, in which the disulfide-bonding pattern is likely to be identical to those of the horseshoe crab big defensin and mammalian β defensins [161]. In crustacean, the PPAE was initially identified in crayfish *Pacifastacus leniusculus* [162,163] and later in black tiger shrimp *P. monodon* [164,165] and white shrimp *L. vannamei* [166,167]. Additionally, several clip-domain serine protein proteinases were identified in black tiger shrimp *P. monodon* [168], Chinese shrimp *F. chinensis* [169], Indian white shrimp *Fenneropenaeus indicus* [170] and white shrimp *L. vannamei* [166]. The *Pm*PPAE1, *Pm*PPAE2, *Lv*PPAE1 and *Lv*PPAE2 [164-167] are only the clip domain containing protein involved in the proPO activating system.

Phenoloxidase (PO) is a major enzyme produced during proPO system activation, and it is necessary for the melanization. It is generally synthesized and maintained as an inactive form (proPO) activated by PPAE to active form (PO) [153,154]. It was first cloned and characterized in crayfish *P. leniusculus* [171] , later in black tiger shrimp *P. monodon* [25,172], brown shrimp *Penaeus californiensis* [173], white shrimp *L. vannamei* [174-176], giant freshwater prawn *M. rosenbergii* [177,178] and Chinese shrimp *F. chinensis* [179]. In shrimp, the expression of proPO was significantly constant expression after injection with LPS [137] and *V. alginolyticus* [176] in *L. vannamei* and feeding with β-1,3-glucan [180]. The expression of proPO was up-regulated post *V. anguillarum* infection in Chinese shrimp *F. chinensis* [179]. In contrast, the proPOI and proPOII expressions significantly decreased in white shrimp *L. vannamei* after injection with *V. alginolyticus* and WSSV [174,181]. Silencing of proPO demonstrated a decrease of the hemocyte count, an increase of the bacterial load and the shrimp mortality in Chinese shrimp *F. chinensis* [182], and also increased the mortality of white shrimp *L. vannamei* post infection with *V. harveyi* [166]. In addition, silencing of proPO component resulted in the decline of the PO activity in hemolymph and the increase of the shrimp mortality post infection with *V. harveyi* in black tiger

shrimp *P. monodon* [25,164,165]. All results suggest that proPO system is a vital system to defend against pathogenic infection in penaeid shrimp.

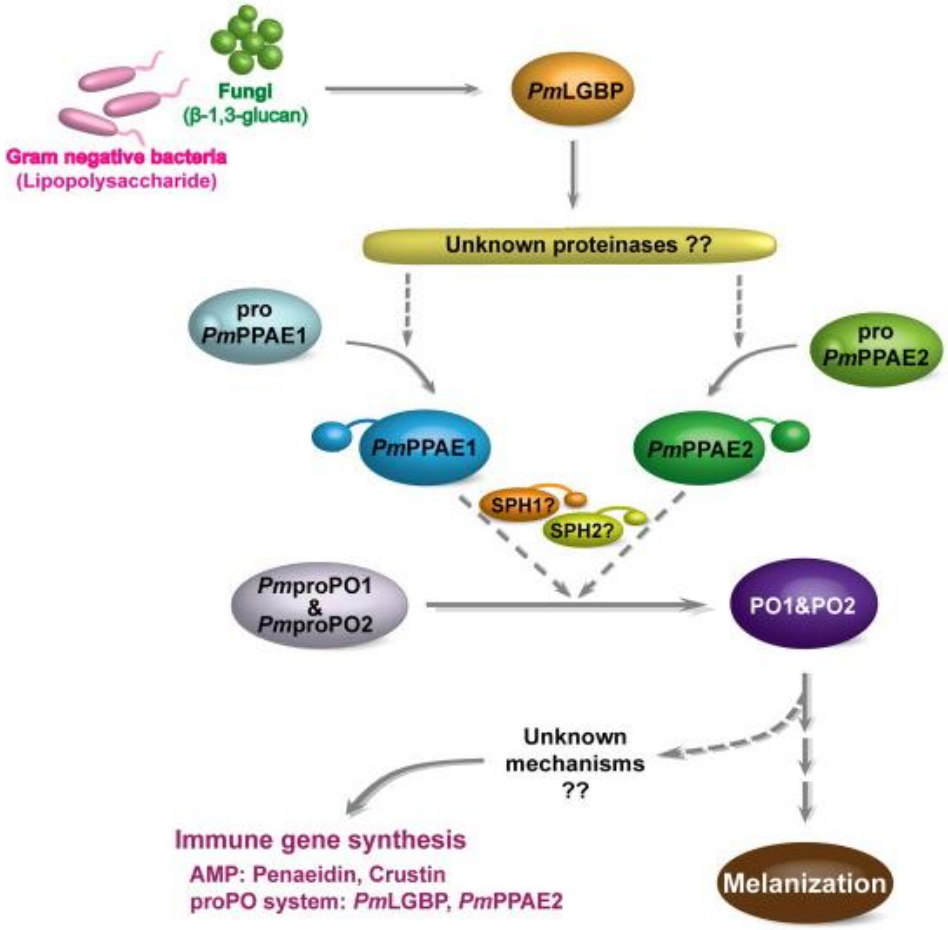

Figure 2. 5 The proPO cascade in the penaeid shrimp *P. monodon* (Source: Amparyup et al., 2013) [183]

Proteinase cascades such as that of the proPO system have to be cautiously regulated by some process to prevent excessive activation of endogenous cascades and damage to host tissue. PO can produce highly toxic intermediates; consequently, host cells can produce several proteinase inhibitors for preventing over-activation of ppA [162]. The proteinase inhibitors, *i.e.* pacifastin, serpin and melanization-inhibiting protein (MIP), are negative regulators of proPO activation or activity [153]. In crustacean, pacifastin is a protein inhibitor, which is specific to

PPAE1 in crayfish *P. leniusculus* [184]. In shrimp, several proteinase inhibitors were identified in black tiger shrimp *P. monodon* (*Pm*MIP, *Pm*SERPIN) [185-188], white shrimp *L. vannamei* [189-191], Chinese shrimp *F. chinensis* [192] and kuruma shrimp *M. japonicus* [193]. In black tiger shrimp *P. monodon*, *Pm*SERPIN3 is potentially regulation of the proPO activating system. The expression of *Pm*SERPIN3 was constantly expressed in hemocytes post infection with *V. harveyi*, WSSV and YHV. *In vitro* experiments showed that the recombinant *Pm*SERPIN3 could inhibit the proPO activating system. Additionally, *Pm*SERPIN3 reduced the *V. harveyi* clearance rate in hemolymph of shrimp [186]. Moreover, *Lv*SERPIN, *Lv*SERPIN3 and *Lv*SERPIN7 may play an important role to inhibit the proPO system and an involvement in innate immunity of *L. vannamei* [189-191]. Overall, the SERPINs of shrimp likely play a role as inhibitor proteins of the proteases of the proPO system.

2.4.3 Pattern recognition protein receptors

Innate immune processes are often activated by components of pathogens called pathogen-associated molecule pattern (PAMPs) such as lipopolysaccharides (LPSs), peptidoglycans (PDNs), lipoteichoic acids of bacteria, glycolipids of mycrobacteria, mannans of yeasts, β-1,3-glucan of fungi and double stranded RNA (dsRNA) of replicating viruses [152,194,195]. The PAMPs can bind to conserved structures called pattern recognition receptors (PRR) on host cells, *i.e*. peptidoglycan recognition proteins (PGRPs), Gram-negative binding proteins (GNBP) or lipopolysaccharide, β-1,3-glucan binding proteins (LGBPs), C-type lectins, galectins, thioester-containing proteins (TEPs), fibrinogen-related proteins (FREPs), scavenger receptors (SRs), Down syndrome cell adhesion molecules (DSCAMs) and Toll like receptors (TLRs) [196-198]. PRR is localized on the surface of cells and secreted into the hemolymph, ready to signal the presence of invading pathogen in every compartment.

β-1,3-glucans are structurally complex homopolymers of glucose and usually isolated from yeast and fungi. Differentially physicochemical parameters, such as solubility, primary structure, molecular weight, branching, and polymer charge, influence the biological activities of β-1,3-glucans. It is apparently monovalent and does not induce agglutination but activates degranulation and proPO system. Therefore,

these recognition proteins are capable of activating cellular activities only after reaction with microbial carbohydrates that are LPS, peptidoglycan or glucan [199]. β-1,3-glucan binding proteins were first characterized in crayfish *P. leniusculus* [200] and later in several crustaceans including, yellow leg shrimp *Penaeus californiensis* [195], white shrimp *L. vannamei* [199,201], *M. japonicus* [202] and *F. chinensis* [203].

C-type lectins or immulectins constitute a large family of PRRs found in almost all metazoans and their functions depend on the carbohydrate recognition domain [204,205]. C-type lectins are abundant in shrimp and have various functions in innate immunity, including phagocytosis, melanization, respiratory burst, agglutination, antibacterial and anti-viral responses [206]. Several shrimp C-type lectins are identified, *i.e. Pm*AV [207], *Pm*Lec [208], *Pm*LT [209] in black tiger shrimp *P. monodon*, *Fc*lectin [210], *Fc*-hsL [211], *Fc*Lec2-5 [212-215] in Chinese shrimp *F. chinensis* and *Lv*LT[216], *Lv*CTL1 [217], *Lv*Lec [218], *Lv*Lectin-1, *Lv*Lectin-2 [219] in white shrimp *L. vannamei*. Both *Pm*AV and *Pm*Lec were found in *P. monodon* and contain a single CRD domain and *Pm*AV contributed to virus resistance, while *Pm*Lec served as a PRR for Gram-negative bacteria. A two CRD domain is *Pm*LT which was detected only in the hepatopancreas and the transcript level decreased initially and then gradually increased after WSSV-challenge whereas its expression was not affected by bacteria.

Galectins are a family of proteins first identified as galactoside-binding lectins in vertebrates [220] This family is defined into two properties: a characteristic affinity for β-galactosides, and a conserved CRD [221]. The galectins were classified into three types: prototype containing one CRD, the tandem-repeat-type galectins containing two homologous CRDs in a single polypeptide chain and chimera type containing a C-terminal CRD and a N-terminal domain rich in proline and glycine [222]. Recently, Galectins were characterized in Chinese shrimp *F. chinensis* [223] and white shrimp *L. vannamei* [224,225]. *Mj*Gal was up-regulated in hemocytes and hepatopancreas post infection with *V. anguillarum.* The recombinant *Mj*Gal protein was bound to lipoteichoic acid (LTA) and lipopolysaccharide (LPS). Additionally, *Mj*Gal protein promoted phagocytosis activity towards microbial pathogens. Silencing *Mj*Gal

also promoted bacterial infection in hemolymph; therefore, *Mj*Gal may play a key role in the shrimp defense against bacterial infection [223].

The thioester-containing protein (TEP) family is present in a wide variety of species. These proteins play a central role in the innate immune responses of vertebrates as complement factors C3, C4, and C5 [226]. The TEP, a complement-like protein, TEP1 has been shown to specially bind to the surface of the ookinete stage of Plasmodium parasites in susceptible mosquitoes [227]. In *Drosophila*, Tep family was characterized including Tep1-Tep6. They are involved in innate immunity [228]. Recently, a *Pl*TEP was first reported in crayfish *P. leniusculus* [229]. It was found specifically expressed in gill and intestine, and was shown to have an important immune function in intestine since if the thioester motif was silenced, crayfish were more susceptible to bacterial infection. [229].

Fibrinogen-related proteins are identified by a highly conserved fibrinogen-like domain (FBG) found in vertebrates and invertebrates [230]. They play an important role in the innate immunity of crustaceans. For example, the tachylectins, which was identified in the horseshoe crab *Tachypleus tridentatus*, can agglutinate Gram-positive and Gram-negative bacteria and human erythrocytes in calcium-dependent manner [231]. In shrimp, a fibrinogen-related protein was isolated in kuruma shrimp *M. japonicus* (*Mj*FREP1). The expression of *Mj*FREP1 was mainly in the gill, and the expression profile was significantly increased post infection with *V. anguillarum*, *S. aureus* and WSSV. The recombinant *Mj*FREP1 protein could agglutinate Gram-positive bacteria *Bacillus subtilis*, *B. thuringiensis*, *B. megaterium*, and *S. aureus* in calcium-dependent manner. Moreover, the recombinant protein could bind peptidoglycans, LPS, Gram positive and negative bacteria and VP28 of WSSV [232].

Down syndrome cell adhesion molecule (DSCAM) consists of immunoglobulin (Ig) and fibronectin (FN) domains at the extracellular region, and it plays an essential role in neural circuit formation [233,234]. In invertebrates, DSCAM was initially identified in *D. melanogaster*, and its transcripts was expressed in the neural system, fat body cells and hemocytes. Silencing DSCAM could significantly reduce the phagocytic activity in hemocyte. Additionally, DSCAM could bind onto pathogen surfaces. Therefore, it is possibly in immunity in *Drosophila* [197]. In

shrimp, DSCAM was characterized in white shrimp *L. vannamei* [235] and black tiger shrimp *P. monodon* [235]. The *Lv*Dscam transcript was highly expressed in the lymphoid organ and heart [235], while the *Pm*Dscam was highly expressed in lymphoid organ, heart and nerve [235]. Both *Lv*Dscam and *Pm*Dscam are likely to play a crucial immune response to WSSV [235,236].

2.4.4 Blood clotting system

The clotting system is a vital process to limit hemolymph loss and to begin wound healing in all metazoans. It is a humoral immune response, which is the first line defense of the invertebrate immune system, and it is quickly forming a secondary barrier to infection and immobilizing bacteria. There are two different models to explain the clotting system one in crayfish and one in horse-shoe crab. In crayfish, the clotting system depends on a transglutaminase (TGase)-dependent clotting reaction [237,238]. The coagulation is formed by the polymerization of a clotting protein in plasma catalyzed by a calcium ion dependent TGase, which is released from the hemocytes under foreign particle stimulation or tissue damage [238]. Another model, the clotting system in horse-shoe crabs is regulated by a proteolytic cascade that is linked with the release of antimicrobial substances [239,240].

The clotting protein, a glycoprotein, has two physiological factions one is in crustacean coagulation and it is also involved in lipid transport [241]. The regulation and localization of clotting protein are in the outer layer of stromal matrix cells of lymphoid organ [242]. Crustacean clotting proteins were first cloned and characterized in the crayfish *P. leniusculus* [237,238] , and later in the sand crayfish *Ibacus ciliatus* [243], the black tiger shrimp *P. monodon* [244], the white shrimp *L. vannamei* [245] and the pink shrimp *Farnfantepanaeus paulensis* [246].

TGase, calcium ion dependent enzymes, catalyze calcium-dependent acyl-transfer reactions between glutamine residues and lysine residues in protein substrates in the presence of calcium ion to form a soft gel at the wounding site [163]. TGase gene was initially cloned and localized in crayfish *P. leniusculus* [247] and two TGase genes including STG I and STG II were characterized in black tiger shrimp *P. monodon* [248]. Another type of TGase was found to be involved in the coagulation of the black tiger

shrimp *P. monodon* [249]. Moreover, a biochemical study was utilized to investigate the involvement of TGase in coagulating the plasma clotting protein [247]

In shrimp, the silencing of TGase in kuruma shrimp *M. japonicus* significantly reduced the concentration of antimicrobial peptides, *i.e.* crustin and lysozyme [250], and therefore it is possible that the clotting system of shrimp might be linked to the antimicrobial peptide production. Therefore, the shrimp clotting system is similar to the horse-shoe crab clotting system and may have a function in AMP production. In addition, the silencing of TGase in kuruma shrimp *M. japonicus* significantly increased shrimp mortality post infection with *Vibrio penaecida* and WSSV [251]. In white shrimp *L. vannamei*, the TGase activity was reduced post infection with Taura Syndrome Virus (TSV) resulting in poor coagulation [252], while the expression of TGase was increased post infection with *V. harveyi* [253].

2.4.5 Epithelial immune response

The epithelial surface must be protected with efficient systems for microbial recognition and control because the barrier epithelia are in constant contact with large numbers of microorganisms. *Drosophila* lives on decaying matter and feeds on fermented medium. Both gut and trachea, two main routes of infection, are lined with a chitinous matrix. Moreover, the gut lumen is hostile to microbial colonization due to its physical and physiological properties and the secretion of lysozymes [254,255]. In addition, local production of reactive oxygen species (ROS) and AMPs (Figure 2.6) provide two complementary inducible defense mechanism in the gut [58]. In *Drosophila*, natural gut infection has been associated with the rapid synthesis of ROS and the dynamic cycle of ROS generation and elimination appears to be vital, because flies that lack ROS-removal capacity have an increased mortality [256]. The dual oxidase (Duox) proteins form a conserved family of molecules containing both the NADPH domain and N-terminal extracellular peroxidase domain (PHD) that can produce ROS in a regulated manner [257]. These proteins can transform H_2O_2 into the highly microbicidal hypohalic acid (HOCL). Excessive ROS production is prevented by immune responsive catalase (IRC) [258], so ROS can be detoxified by IRC. The IRC and Duox phenotype demonstrate that a fine redox balance is critical for control of microorganisms in the gut lumen. This ROS-dependent gut immunity is not affected by

the Imd pathway and provides an additional barrier against ingested microorganisms [259].

Local AMP production in the gut has been suggested to be a second line of defense after ROS production to fight pathogens. The use of GFP reporter transgenes has revealed that AMP genes are expressed in several surface epithelia that are in contact with the external environment [260]. This AMP synthesis is referred to as the local immune response as opposed to the systemic response. One can distinguish between constitutive and inducible AMP expression in epithelia. Firstly, the AMP gene is expressed constitutively in a defined tissue, and its transcription is not up-regulated during microbial infection such as Drosomycin in salivary glands and in the female spermatheca, and for Cecropin in the male ejaculatory duct [260]. This constitutive expression is regulated by various tissue specific transcription factors such as the homeobox-containing protein Caudal [261,262]. Secondly, there is the inducible local AMP gene expression. This response is triggered upon natural infection by Gram-negative bacteria and is mediated by the Imd pathway [260,263] such as Drosomycin and Diptericin induced in both trachea and gut via the Imd pathway in response to local infection by bacteria [264].

In shrimp, the role of ROS in innate immunity has been studied in systemic immune system. During infection, ROS production was produced such as O_2^-, the hydroxyl radical (OH^-), H_2O_2 and singlet oxygen ($^1O_2$). In white shrimp *L. vannamei*, the production of O_2^- was related to the concentration of bacteria in hemocytes during *E. coli* infection [265]. Moreover, the expression level of superoxide dismutase (SOD) was increased at early stage of 1 hour post WSSV infection revealing an early ROS detoxification response, while its transcript was decreased at later stage of 12 hours post infection indicating that it is an important mechanism to limit viral replication in white shrimp *L. vannamei* [266]. It has previously been reported that the O_2^- production is involved in Nox and phenoloxidase pathways in hemocytes of giant freshwater prawn *M. rosenbergii* [267]. Recently in kuruma shrimp *M. japonicus*, the *Mj*Nox, nitric oxide synthase *(Mj*NOS) and Dual oxidases (*Mj*Duox) were characterized. The nitric oxide (NO) was generated after LPS stimulation [268]. The transcript of *Mj*NOS was increased post *V. penaecida* injection in the gills [269]. The expression level of *Mj*Nox

was up-regulated post *V. penaeicida* or poly (I:C) challenge [270]. In addition, the *Mj*Duox transcript was up-regulated in the gills post WSSV infection [271]. All results show that the ROS productions are also important in innate immune response in shrimp.

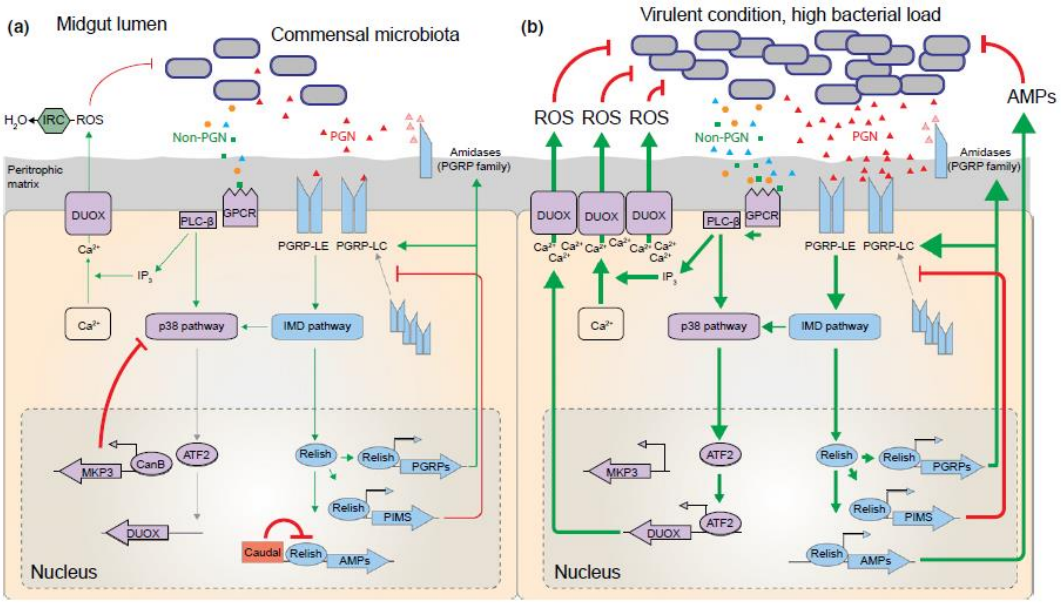

Figure 2.6 The midgut immune response in *Drosophila* (Source: Engel and Moran, 2013) [272]

2.4.6 Intestinal epithelium cell renewal

In *Drosophila*, a factor that the host is producing to survive from pathogenic infection is epithelium cell renewal [273]. The infection of pathogens causes a damage of the epithelium layer; therefore, the tissue proliferation and differentiation of intestinal stem cells (ISCs) to rebuild the epithelial intestine are of importance for host survival [274,275]. There are three signaling pathways in progenitor cells regulating cell proliferation and differentiation including the Wingless, JAK/STAT and Epidermal growth factor receptor (Egfr) pathway (Figure 2.7) [276-281]. Firstly, the JAK/STAT ligand Upd3 and the epidermal growth factor Keren are induced by JNK and Hippo signaling pathways. Secondly, the induction of the JAK/STAT pathway in progenitor cells increases their differentiation and promotes the synthesis of Upd3 and the epidermal growth factor Spitz. Additionally, the activation of JAK/STAT in the

surrounding visceral muscles promotes the synthesis of the epidermal growth factor ligand Vein. Thirdly, Upd3, Karen, Spitz and Vein factors induce the Egfr pathway in ISCs to increase the ISC proliferation rate. In contrast, the kinase Gcn2 is increased and the target of rapamycin (Tor) signaling decreasing lead to a lack of epithelial repair during pathogenic infection resulting to the death of the fly [282].

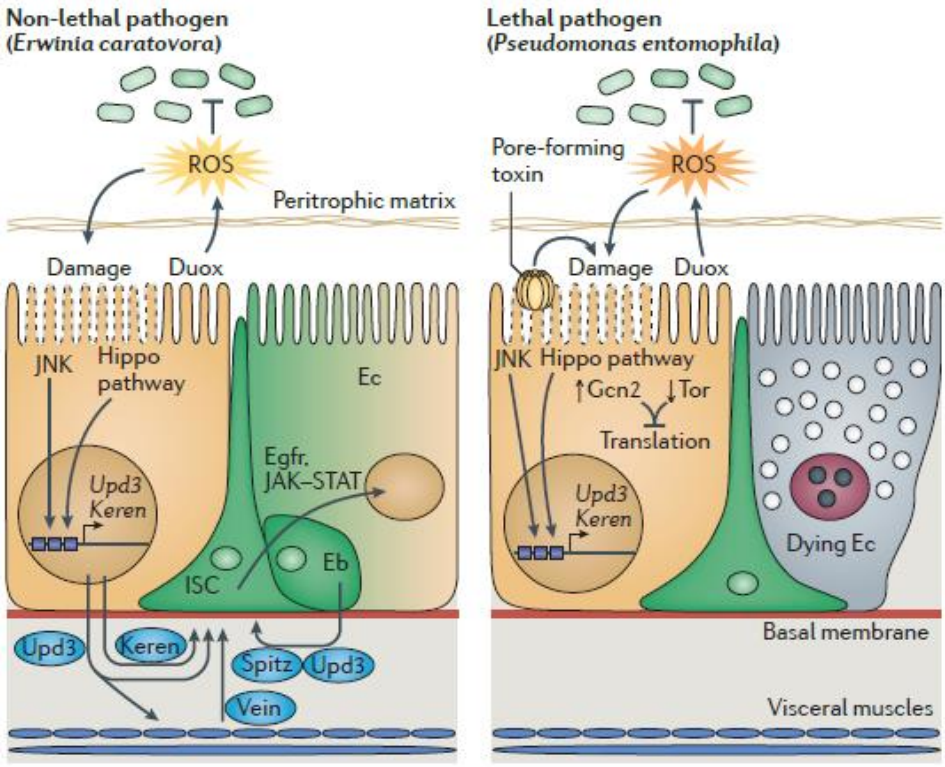

Figure 2. 7 Intestinal epithelium cell renewal in *Drosophila* (Source: Buchon et al., 2013) [282]

In crustaceans, the JAK/STAT pathway is only studied in shrimp. There are main cellular components in JAK/STAT pathway including the Janus Kinase (JAK) Hopscotch and the STAT transcription factor [283]. Stats were identified in black tiger shrimp *P. monodon* (*Pm*STAT) [284] and Chinese shrimp *F. chinensis* (*Fc*STAT) [285]. The transcript level of *Pm*STAT was down-regulated, but activated *Pm*STAT protein was increased in the cephalothorax after WSSV infection [284]. The transcript of *Fc*STAT was detected in all tissues, and the *Fc*STAT transcript was up-regulated in

hemocytes, hepatopancreas, and intestines at an early stage of infection with WSSV. Additionally, the *Fc*STAT transcript was up-regulated in hemocytes and hepatopancreas after *V. anguillarum* infection [285]. Although some component of the JAK/STAT pathway was studied, but the studies do not relate to the cell proliferation and differentiation. The studies are focused on WSSV infection.

CHAPTER III

METHODOLOGY

3.1 The Presence of Normal Flora in Un-infected *P. monodon*

3.1.1. Normal shrimp

One-month old shrimp were obtained from the Marine Technology Research Center, Faculty of Marine Technology, Burapha University Chanthaburi Campus, Thailand. The shrimp were raised in a 20 × 20 m plastic-lined pond (10-11 parts per thousand (ppt) salinity) and fed four times daily with a commercial feed (Starfeeds® containing 40% protein). Once the shrimp arrived in the laboratory, apparently healthy individuals were selected for the study. The entire gastrointestinal (GI) tract including the stomach, midgut and hindgut from several shrimp were prepared for SEM to study the presence and attachment of normal flora in the GI tract of *P. monodon*.

3.1.2 Scanning electron microscopy (SEM)

The GI tract from each *P. monodon* was dissected and then fixed in 3% glutaraldehyde in 0.1M phosphate buffer (19 ml of 0.2 M $NaH_2PO_4.2H_2O$ and 81 ml of 0.2 M $Na_2HPO_4.2H_2O$) pH 7.4. The samples were stored in the dark overnight at 4 °C and then rinsed twice with 0.1 M phosphate buffer for 10 minutes followed by one rinse of distilled water for 10 minutes. Thereafter they were dehydrated through graded ethanol series, *i.e.* 10 minutes each in 30, 50, 70 and 95% ethanol, and followed by 10 minutes each in three changes of absolute ethanol. The samples were subsequently critical-point dried using carbon dioxide as the transitional fluid and mounted on stubs. During mounting, samples of the foregut, midgut and hindgut were split longitudinally to expose the gut contents and the inner lining of the gut. After sputter coating the samples with gold using a Blazers model SCD 040, the specimens were examined in a JEOL model JSM-5410LV scanning electron microscope. All process were performed at Science and Technological Research Equipment Centre, Chulalongkorn University.

3.2 The Interaction of Pathogenic and Non-pathogenic Bacteria with the Epithelial Surface of the Gastointestinal Tract of *P. monodon*

3.2.1 Bacteria and experiment animal

Vibrio harveyi 1526 [286] and *V. parahaemolyticus*, previously isolated from wounded *P. monodon*, were chosen as representatives of shrimp pathogens, whilst *Micrococcus luteus* Ml 11 [287] and *Vibrio* B4-24, closely related to *V. sagamiensis* based on 16S rDNA and isolated from intestines of broodstock shrimp, served as two non-pathogenic species for the assessment.

One month old shrimp (average 2-3 g body weight) were obtained from a commercial shrimp farm in Pathumthani province and transported to Chulalongkorn University where they were maintained in tank with running, aerated 5 ppt water at ambient temperature (28 ± 2 °C).

Adult *Artemia* were purchased from Sunday Market at Chatuchak, Thailand. They were maintained in a plastic tank with artificially aerated seawater at 30 ppt salinity overnight before the experiment was performed.

3.2.2 Bacterial preparation

Bacterial colony was inoculated in tryptic soy broth (TSB) (Oxoid, Basingstoke, UK) with either no supplement (*M. luteus*) or with 2% NaCl (marine bacteria) with constant agitation and optimal temperature. Bacterial cells were harvested from stationary phase, washed twice with 2% NaCl for marine bacteria or 0.85% NaCl for freshwater bacteria, and resuspended in the same solution. Bacterial cells were diluted to the optical density (OD) values at 600 nm [19,21] of 1.0 (approximately 1.0×10^8 CFUs). *Artemia* were allowed to filter feed on each bacterial suspension for 30 minutes before they were presented to the shrimp.

3.2.3 Oral route of infection with the delivery of bacteria via an *Artemia* diet

Individual shrimp was placed in 5 L plastic boxes each containing 1.5 L of 5 ppt salinity seawater. Each shrimp was fed once with 60 *Artemia* (control, *V. harveyi*, *V. parahaemolyticus*, *M. luteus* Ml 11 and *V. sagamiensis*) and feeding was monitored for 60 minutes to ensure that the shrimp consumed all 60 *Artemia*. Three shrimp from

each treatment group were collected at 1.5, 6 and 24 hours post infection and then processed for SEM. The bacterial concentrations of the pre-soaked *Artemia* were determined on TCBS agar (Oxoid). One *Artemia* was subsequently found to contain approximately 10^7 CFU of bacteria, and hence each shrimp received approximately 6×10^8 CFUs of bacteria/shrimp.

3.2.4 SEM

SEM was performed as mentioned in section 3.1.2.

3.3 The Appearance of the Pathogenic Bacteria in Gastointestinal Tract

3.3.1 Shrimp collection

To confirm the presence of *V. harveyi* and *V. parahaemolyticus* in the GI tract, the experiment design was as mentioned in session 3.2.1-3.2.3 and shrimp were collected at 24 hours to confirm shrimp infection by fluorescence in situ hybridization (FISH) assay, PCR-denaturing gradient gel electrophoresis (DGGE) and quantitative real-time PCR.

3.3.2 Fluorescence in situ hybridization (FISH) assay

FISH was used to identify and detect localization of bacterial cell in GI tract. Two sectioning methods consisting of parafin section and cryosectioning were used. All method were modified form Seidman [288].

3.3.2.1 Parafin section

Hepatopancrease, stomach and intestine were dissected and fixed for 24 hours in 4% paraformaldehyde prepared in 0.1 M phosphate buffer pH 7.4. After fixation, all samples were washed 3 times with 0.1 M phosphate buffer pH 7.4 and 50% ethanol, respectively. All samples was kept in 70% ethanol at 4 °C until next process.

Hepatopancreas, stomach, midgut and hindgut were dissected by a single edge razor blade and placed into embedding cassettes. The cassette containing the tissue were twice dehydrated in the following solutions: ethanol series (70%, 85%, 95% and 100% absolute ethanol) and Bioclear (Bio Optica, Milan, Italy) for 50 minutes. The parafin was allowed to infiltrate into the dehydrated tissue for 1.5 hours at 56 ºC.

The parafin infiltrated tissues were placed in embedding molds, and the embedding molds was filled with melted parafin. The molds were placed on a cold trays for about 20 minute. Lastly, the infiltrated tissues were separated from embedding molds to obtain the succesfully infiltrated tissue blocks for sectioning. The tissue blocks were kept in -20 °C until used.

For sectioning, the sample blocks were carefully face-trimmed untill part of tissue could be seen and the kept at -20 ºC. A new disposable microtome blade was used, and a microtome was set the thick section at 6 µm. Each samples were cut as a series ribbon and floated on water bath at 42 ºC to expand and separate the ribbon. The sample was collected in the water bath using a glass slide and then excess water was removed. The dry slides were placed on slide warmer at 45 ºC overnight to fix. All slides were allowed to be cool at room temperature and kept in in -20 °C until used.

For fluorescence *in situ* hybridization (FISH), the sample slides were dewaxed in toluene for 3 minute twice, then slides were redehydrated for 3 minutes per each in the following solutions: 100, 95, 70, 50% ethanol and sterile water. The slides were incubated with 2 mg/ml lysozyme in 100 mM Tris-HCl, pH 7.2 at 37 ºC to partially digest the bacterial cell membrane. After incubation, the slides were washed with 100 mM Tris-HCl, pH 7.2 for 10 minutes. A 20 µl of hybridization buffer (30% formamide, 0.9 M NaCl, 0.01% SDS in 20mM Tris-HCl, pH 7.2) was mixed with a 10 µl of 1.5 µg/ml probe (Table 3.1) per slide and allowed to hybridize with the samples incubatein a dark moist chamber at 50 °C for 1-3 hours. After incubation, slides were wash with hybidization buffer without formamide for 20 minutes. Finally, the slide samples were mounted with Antifade Mounting Medium (Vectashield, CA, USA) and observed using Olympus microscope BX51 fluorescence (Olympus, Tokyo, Japan).

Table 3.1 Fluorescence bacterial probes

Name	Specificity	Sequence (5′ to 3′)	Label	References
UNIV1390	Universal bacteria	GACGGGCGGTGTGTACAA	5′ CY3	[289]
VIB572a	*Vibrio* spp.	ACCACCTGCATGCGCTTT	5′ FAM	[290]
LGC354b	Gram positive bacteria	CGGAAGATTCCCTACTGC	5′ CY3	[291]
SP_VP1253	*Vibrio parahaemolyticus*	CACTTTCGCAAGTTGGCTGCCC	5′ HEX	[292]
SP_VH	*Vibrio harveyi* (can not use)	CCGCATAATACCTACGGGTCAA AGAGGG	5′ FAM	[293]

3.3.2.2 Cryosectioning

Bacteria were prepared as mentioned in section 3.2.2. and a 10 µl resuspended bacteria were dropped onto a coated glass slide. The slides were dried at room temperatureand heat-fixed by quickly passing through the flame from an alcohol lantern. Additonally, the fixed slides were refixed with ethanol/formaline (9:1) at room temperature for 20 minutes.

The intestine and stomach were first disected and immersed into Jung Tissue Freezing Medium (Leica, Nussloch, Germany) at -20 ºC in Leica CM1950 cyostate (Leica), then the samples were placed at -20 ºC until freezing medium became a solid. The samples were sectioned at 7 µM thickness and the warm slide was collected the sample. The sample slides were fixed with 4% paraformaldehyde for 6-10 minutes.

To stop the fixation reaction, all slides were washed with 3X PBS, pH 7.2 (390 mM NaCl/30 mM Na_2HPO_4 and 390 mM NaCl/30 mM Na_2PO_4) for 2 minutes followed by rinsing twice with 1X PBS for 2 minutes each. After that, slides were dehydrated with ethanol series (50%, 70% and 95%) for 5 minutes each and then 3 times with 100% ethanol for 5 minutes to completely dehydrate. Sample slides were air-dried at room temperature until they were completely dried, kept in slide box and stored at -80 ºC. FISH was performed as mentioned above.

3.3.3 PCR-denaturing gradient gel electrophoresis (DGGE) analysis

3.3.3.1 DNA extraction

Total genomic DNA from shrimp stomach and intestine was extracted by CTAB and chloroform-isoamylalcohol extraction method modified from Zhou et al. [294]. Briefly, tissue were thoroughly ground in 250 µl of 2% NaCl, and 750 µl of 2% NaCl was added to homogenized samples to make 1 ml volume. The homogenate of each sample was centrifuged at 10,000 rpm for 1 minute at room temperature, and then the supernatant was discarded. The pellet was resuspended with 600 µl of extraction buffer (final concentration 100 mM Tris-HCl pH 8.0, 100 mM sodium EDTA pH 8.0, 100 mM sodium phosphate, 1.5 M NaCl, 1% CTAB) and 10 µl proteinase K (10 mg m/ml), and then mixed by vortex. The mixture was incubated at 65 °C for 2 hours and gently mixed by inversion every 15 minutes. At the end of the incubation period, 75 µl 20% sodium dodecyl sulfate (20% SDS) was added. The mixture was further incubated for 1 hour at 65 °C and gently mixed by inversion every 15 minutes during the incubation. After incubation, the sample was centrifuged at 8,000 rpm for 10 minutes. The supernatant was collected in a new microcentrifuge tube and the pellet was re-extracted with extraction buffer and SDS for 15 min using the same procedure. The supernatant was mixed twice with equal volume of chloroform: isoamylalcohol (24:1) and centrifuged at 8,000 rpm for 2 minutes at room temperature to separate the phase. The aqueous phase was carefully transferred into a new collection tube to precipitate with 0.6X volume of isopropanol for 1 hour at room temperature. The DNA pellet was recovered by centrifugation at 12,000 rpm for 10 minutes at room temperature and washed with 1 ml of 70% ethanol. The DNA pellet was completely air dried at room temperature and resuspended in 100 µl of TE buffer (10 mM Tris-HCl pH 8.0 and 0.1 mM EDTA). The DNA solution was stored at -20 ºC until analysis. A total DNA quality and concentration were measured by gel electrophoresis and spectrophotometer.

3.3.3.2 Measuring of DNA concentration using NanoDrop 2000c UV-Vis spectrophotometers

Total genomic DNA quality and concentration were measured by NanoDrop 2000c UV-Vis spectrophotometers (Thermo Fisher Scientific, DE, USA).

One µl of total genomic DNA was pipetted onto lower measurement pedestal, and then upper measurement pedestal was closed. The operating solfware calculated the optical density at 260 nanometre (OD_{260}). Additionally, the quality of total DNA can be assessed from a ratio of OD_{260}/OD_{280}, which the ratio of 1.8 and 2.0 is considered good quality.

3.3.3.3 PCR amplification

First, a PCR amplification of near-complete 16S rDNA fragments from the isolates was conducted using primer 8fm and primer 1492R (Table 3.2) as described by Lane [295]. Briefly, PCR amplification was performed in 25 µl consisting of 1X Mg-free PCR buffer, 3.0 mM $MgCl_2$, 0.2 mM dNTPs, 200 nM of each primer, 0.4 U DyNAzyme II DNA Polymerase (Thermo Fisher Scientific, Vilnius, Lithunia) and approximately 20-100 ng template. A BSA solution (10 mg/mL) was added into the PCR reaction to increase yield in PCR amplification. The PCR cycle parameters were 4 minutes initial denaturation at 95 °C, 35 cycles of 1 minute at 95 °C, 30 seconds at 55 °C, 2 minutes at 72 °C, and 7 minutes final extension at 72 °C on DNA Thermal Cycler PTC-200 (MJ Research Inc., MA, USA). The presence of a 1,500-bp fragment was confirmed on a 1 % agarose gel electrophoresis and visualized with a UV transilluminator Gel Doc^{TM} XR imaging system (Bio-Rad, Milan, Italy) after ethidium bromide staining. PCR-DGGE was performed following standard methods but with some modifications [296]. Briefly, the 1:10 diluted product from the first PCR reactions were used as a template for the nested PCR using 338f with GC clamps attached to the 5′ end and 517r primers (Table 3.2). The PCR conditions for the nested DGGE were as follows: an initial denaturation of 4 minutes at 95°C, followed by 25 cycles of 30 seconds at 95°C, 30 seconds at 60°C, 30 seconds at 72°C, and then a 7 minutes final extension at 72°C. The presence of a 200-bp fragment was confirmed on a 1.5% agarose gel electrophoresis.

3.3.3.4 DGGE

A 10 µl aliquot of each PCR-DGGE product was loaded directly onto an 8% acrylamide gel with a 20% to 55% denaturant vertical gradient. Samples were loaded with in-house DGGE clone ladders (two per gel) and reference DGGE products (a mix of DGGE products from two samples; four per gel) to assist in the alignment

and comparison between different gels [297]. The electrophoresis was performed at 200 V at 60 °C for 5 hours using a DGGE Electrophoresis System (CBS Scientific, Union City, CA). After electrophoresis, the gels were stained using SYBR gold (Invitrogen, Carlsbad, CA) and visualized using a Pharos FX™ Molecular Imager (Bio Rad Laboratories Inc., Hercules, CA).

3.3.3.5 DGGE analysis

All gel analyses were performed using InfoQuest™ Software (Bio-Rad Laboratories Inc). Individual DGGE profiles were subjected to normalization among different gels using clone ladders and reference samples [297].

Table 3.2 List of 16S rDNA universal PCR primers used in this study

Primer name	Sequence (5′ to 3′)	Product size (bp)	Ta (°C)	Reference
8fm	AGAGTTTGAT(AC)MTGGCTCAG	1500	55	[295]
1492r	G(CT)TACCTTGTTACGACTT			
338f-GC[a]	(GC)-ACTCCTACGGGAGGCA	200	60	[296]
517r	ATTACCGCGGCTGCTGG			

[a]This primer has the following GC clamp at its 5'end:
5' CGCCCGCCGCGCGCGGCGGGCGGGGCGGGGGCACGGGGG- 3' [296]

3.3.4 Quantitative real-time PCR

3.3.4.1 Primer

Specific bacterial species primer were obtained form previous publications that revealed specific for *V. harveyi* and *V. paraheamolyticus*. *V. harveyi*-specific primers targeting to the gyrase B gene (gyr B) [298], and *V. paraheamolyticus* specific primers targeting 2 genes: gyr B [299] and thermolabile hemolysin (tlh) [300] were listed on Table 3.3.

Table 3.3 List of real-time PCR primers to detect the stomach and midgut bacteria

Target organism	Primer name	Sequence (5′ to 3′)	Product Size (bp)	Ta (°C)	Reference
All bacteria	Eub338	ACTCCTACGGGAGGCAGCAG	181	55	[301]
	Eub518	ATTACCGCGGCTGCTGG			
V. harveyi	A2	TCTAACTATCCACCGCGG	362	64	[298]
	B3	AGCAATGCCATCTTCACGTTC			
V. parahaemolyticus	VP-1	CGGCGTGGGTGT TTCGGTAGT	385	58	[299]
	VP-2r	TCCGCTTCGCGCTCATCAATA			
	tlh-f	ACTCAACACAAGAAGAGATCGACAA	207	60	[300]
	tlh-R	GATGAGCGGTTGATGTCCAA			

3.3.4.2 DNA extraction

Total gDNA were extracted using QIAamp DNA blood mini kit (Qiagen, Hildn, Germany) according to the instruction of the manufacturer. The GI was infected with *Vibrio* species which is gram negative species, thus the purification of total DNA from animal tissue protocol was applied to extract total gDNA in this study. Briefly, the stomach and intestine of each shrimp were separately ground into the sterile microcentrifuge tube with 180 µl ATL buffer, and then a 20 µl proteinase K was added into the ground tissue. The sample was thoroughly mixed by votexing, and incubated at 56 °C overnight to completely lysed. After incubation, the sample was mixed by votexing for 15 seconds then a 200 µl Al buffer was added into the sample and mixed thoroughly by votexing. To remove unlysed tissue, the mixture was centrifuged at 10,000 rpm for 1 minute and the supernatant was transferd to the new microcentrifuge tube. A 200 µl ethanol was added into the sample then mixed as above. The mixture was pipeted onto the DNeasy mini spin column placed in a 2 ml collection tube, and centrifuged at 13,000 rpm for 1 minute. Washing step, the column was washed by centrifugation at 13,000 rpm for 1 minute with 500 µl of AW1 and AW2 buffer, respectively. To completely dry column, the colume placed in a new 2 ml collection

tube was continuely centrifuged at 13,000 rpm for 3 minutes. The elution step, the column was placed onto the 1.5 ml sterile microcentrifuge tube, and 50 µl AE bufer was directly pipated onto the DNeasy membrane then incubated for 2 minutes. The column was centrifuged at 13,000 rpm for 2 minutes. Additionaly, the step of elution was repeated to completely elution. The total gDNA solution was measured by NanoDrop 2000c UV-Vis spectrophotometers as mentioned in section 3.3.3.2, after that stored at -20 °C

3.3.4.3 PCR amplification for external standard curve preparation

A total gDNA was amplified using specific primer for gyr B gene of *V. harveyi* and for gyrB and tlh genes of *V. parahaemolyticus*. The PCR amplification was performed in 25 µl consisting of 1X Mg-free PCR buffer, 3.0 mM $MgCl_2$, 0.2 mM dNTPs, 200 nM of each primer (Table 3.3), 0.4 U Taq DNA polymerase and 100 ng gDNA of *V. harveyi* or *V. parahaemolyticus*. The PCR cycle parameters were 4 minutes initial denaturation at 95 °C, 35 cycles of 1 minute at 95 °C, 30 seconds at 60 °C, 30 minutes at 72 °C, and 7 minutes final extension at 72 °C. The presence of a PCR product fragment was confirmed on a 1.5 % agarose gel electrophoresis.

3.3.4.4 PCR product purification

The PCR products were purified using illustra GFX PCR DNA and gel band purification kit (GE Healthcare, Buckinghamshire, UK) according to the instruction of kit. Briefly, a 500 µl capture buffer type 3 was added to the PCR product and mixed. The mixture was transferred to GFX column and then re-centrifuged at 13,000 rpm for 30 seconds. The column was washed with 500 µl wash buffer type I by centrifugation at 13,000 rpm for 30 seconds. The column was again centrifuged at 13,000 rpm for 2 minutes to dry the colume. PCR product purification was eluted from the column by elution buffer type 4 and stored at -20 °C.

3.3.4.5 PCR product ligation

The ligation reaction was perfomed in 10 µl of total volume containing 1X ligation buffer, 5% polyethylene glycol (PEG), 25 ng pGEM®-T Easy vector, 3 weiss units T4 DNA ligase (Promega, WI, USA), and 6.25 µl purified product.

The ligation reactions were incubated overnight at 4 °C to increase the efficiency of ligation reaction.

3.3.4.6 Competent *E. coli* cells preparation

A *E. coli* JM109 was inoculated in Lysogeny Broth (LB) (1% Bactotryptone, 0.5% Bactoyeast extract and 0.5% NaCl, pH 7.0) with 250 rpm agitation at 37 °C overnight used as a starter. A 1 ml of starter bacteria was inoculated into 50 ml of LB broth and continually cultured until an OD_{600} reached to 0.4-0.6. The cultured cells were transferred to 50 ml centrifuge tube and also chilled on ice for 30 minutes. To collected bacterial cells, 50 ml centrifuge tubes were centrifuged at 3,000 rpm for 15 minute at 4 °C. The bacterial pellets were resuspended in 30 ml of ice-cold $MgCl_2/CaCl_2$ solution (80 mM $MgCl_2$ and 20 mM $CaCl_2$) and then incubated on ice for 45 minutes. The cold resuspended bacterial cells were centrifuged as above to collect the bacterial pellets. The bacterial pellets were resuspended in 2 ml of ice-cold 0.1 M $CaCl_2$ containing 15% glyceral and a 100 μl of resuspended cells was pipetted to cold microcentrifuge tube. These competent cells were immediately used or stored at -80 °C for subsequently used.

3.3.4.7 Transformation of ligation product to *E. coli* host cells

E. coli JM109 competent cells were placed in an ice for 5 minutes. The ligation product was added, gently mixed by pipetting and incubated in an ice for 30 minutes. After incubation, the mixture was heat-shocked in 42 °C water bath for exactly 45 seconds and immediately placed in an ice for 5 minutes. The mixture was transferred into 1 ml of SOC (2% tryptone, 0.5% yeast extract, 10 mM NaCl, 2.5 mM KCl, 10 mM MgCl2, 10 mM MgSO4 and 20 mM glucose) and cultured at 37 °C with 250 rpm agitation for 1.5 hours. The transformation cells were collected by centrifuged at 10,000 rpm for 1 minute. A 900 μl of supernatant was discarded thus 100 μl of supernatant were resuspended the bacterial pellet to spread onto a selective LB agar plate containing 50 μg/ml of ampicillin, 25 μg/ml of IPTG and 20 μg/ml of X-gal. The transformation plates were incubated at 37 °C overnight.

3.3.4.8 Colony PCR selection

Due to lacZ′ system, the white bacterial colonies contained inserted DNA recombinant clones, whereas the blue bacterial colonies did not contain the inserted DNA. A single colony was picked up to streak to new selective LB agar plate and also put into the mixed PCR reaction. The PCR reaction was carried out in a 25 µl reaction mixture, containing 1X Mg-free PCR buffer, 4 mM $MgCl_2$, 100 µM dNTPs (1 mM), 100 µM of each primer (pUC1: 5′-TTCGGCTCGTATGTTGTGT GGA-3′ and pUC2: 5′-GTGGTGCAAGGCGATTAAGTTGG-3′) and 1 U Taq DNA polymerase. The PCR cycle parameters were 3 minutes initial denaturation at 94 °C, 35 cycles of 30 seconds at 94 °C, 1 minute at 50 °C, 30-180 seconds depended on the length of inserted DNA (1 minute for 1 Kbp) at 72 °C, and 7 minutes final extension at 72 °C on a thermal cycler. The colony PCR products were analyzed through 1.5% agarose gel.

3.3.4.9 Recombinant plasmid DNA extraction

Plasmid DNA was extracted using illustra plasmidPrep mini spin kit (GE Healthcare, Buckinghamshire, UK) according to the instruction of kit. Briefly, a selected clone was inoculated into 3 ml LB broth containing 50 µg/ml of antibiotic ampicillin and cultured at 37 °C overnight with 250 rpm agitation. The culture was twice transferred to 1.5 ml microcentrifuge tube and centrifuged at 14,000 rpm for 1 minute. After harvesting of bacterial cells, the bacterial pellet was thoroughly resuspended in a 175 µl Lysis buffer type 7 and also in a 175 µl Lysis buffer type 8. The mixture was immediately mixed by gentle inversion until solution became clear and viscous and then 350 µl Lysis buffer type 9 was added to the mixture, and also mixed immediately. The mixture was centrifuged at 14,000 rpm for 10 minutes. After centrifugation, the cleared supernatant was transferred onto the illustra plasmid mini column and centrifuged at 14,000 rpm for 1 minute. To wash the column, a 400 µl wash buffer type 1 was added to the column and centrifuged at 14,000 rpm for 1 minute. The column was re-centrifuged at 14,000 rpm for 2 minute until it is completely dry. To elute the plasmid, the column was placed on the 1.5 ml sterile microcentrifuge tube. A 30 µl elution buffer type 4 was added onto the center of the column, and the column was incubated at room temperature for 2 minutes before centrifuged at 14,000 rpm for

2 minutes. The plasmid concentration was measured by NanoDrop 2000c UV-Vis spectrophotometers as mentioned in section 3.3.3.2, after that stored at -20 °C.

3.3.4.10 Standerd curve amplification

Plasmid DNA of each gene was used as the template to calculate the copy number of each gene following equation [302].

$$\text{DNA copy (copies/µl)} = \frac{6.02\times10^{23}\ \text{(copy/mol)}\times\text{DNA amount (g)}}{\text{DNA lenght (bp)}\times660\ \text{(g/mol/bp)}}$$

A 10-fold serial dilution of a known copy number was prepared corresponding to 10^3-10^8 copy number/µl for standard curve amplification. All real-time PCR reactions were carried out in a 96 well plate and each sample was amplified in duplicate using a LightCycler® 480 II system (Roche diagnostic Ltd., Rotkreuz, Switzerland). LightCycler® 480 SYBR Green I Master (Roche, Mannheim, Germany) and 0.2 µM primer concentration were used for real-time PCR amplification. The thermal profile for real-time PCR was 95 °C for 10 minutes followed by 40 cycles of 95 °C for 15 seconds, 55-64 °C (Table 3.3) for 30 seconds and 72 °C for 30 seconds. The correlation efficiency of 0.995-1.000 was considered acceptable for use as a standerd curve.

3.3.4.11 Quantitative real-time PCR amplification

Total gDNA of stomach and intestine from each shrimp fed with *Artemia* (control), *Artemia-V. harveyi* were diluted to 50 ng/µl and 5 ng/µl for PCR detection of *V. harveyi* and all bacteria, respectively. Additionally, the gDNA of *Artemia* (control), *Artemia-V. parahaemolyticus* were also diluted to 200 ng/µl and 5 ng/µl for PCR detection of *V. parahaemolyticus* and all bacteria, respectively. Each diluted gDNA was used as a template in quantitative real-time PCR amplification. The reactions were performed following the condition of each standard curve, and the cycles of amplification were 50 cycles.

3.3.4.12 Data analysis

The ratio of each gene and 16s rDNA was calculated to express the relative numbers of *V. harveyi* or *V. parahaemolyticus* to all bacteria in the stomach and intestine of shrimp. The difference between treatments was analyzed using

independent sample *t*-test ($P<0.05$) with SPSS 13.0 software for windows. Since there can be multiple copies of 16S rDNA per genome of bacteria (1-13 copies in all bacteria) [303], we assumed for calculation purpose that the average copy number of 16S rDNA was 10.25, based on the average 16S rDNA copy number of *V. parahaemolyticus* and *V. harveyi* (11 for *V. parahaemolyticus* and 8-11 for *V. harveyi*) [304,305].

3.4 Histopathology of AHPNS/EMS Infected Shrimp

3.4.1 Bacteria and experimental animal

V. parahaemolyticus 3HP used in this study was isolated and identified by Centex Shrimp, Faculty of Science, Mahidol University [19]. This bacterium was isolated from hepatopancreas (HP) of shrimp that were collected from a shrimp farm that had experienced a massive mortality. Additionally, this stain showed a positive PCR result with AP2 primer set [19].

Adult *Artemia* were purchased from Sunday Market at Chatuchak, Thailand. They were maintained in a plastic tank with artificially aerated seawater at 30 ppt salinity overnight before performed experiment.

Juvenile shrimp (15-20 grams) were obtained from Shrimp Genetic Improvement Center (BIOTEC), Surat Thani province. They were acclimated for 2 weeks at the Center of Excellence for Marine and Biotechnology (CEMB), Chulalongkorn University in tanks with running aerated water at 28±2 ºC, 16 ppt salinity before performed experiment.

3.4.2 Bacterial preparation

Bacteria from glycerol stock was steaked onto TSA containing 2% NaCl and incubated at 28 ºC. A single bacterial colony was inoculated in TSB (Oxoid) supplemented with 2% NaCl at 28 ºC for 15 hours. Bacterial cells were harvested and washed twice with 2% NaCl then the bacterial pellets were resuspended in the 2% NaCl. The suspended bacteria were diluted to the optical density (OD) of 1 at 600 nm (approximately 1.0×10^8 CFUs). *Artemia* were allowed to filter feed on each bacterial suspension for 30 minutes before they were presented to the shrimp. To monitor the

number of bacteria fed shrimp, ten *Artemia* immersion was ground in 1 ml of 2% NaCl and diluted for plate count.

3.4.3 Orally challenged test for AHPNS/EMS pathogenesis

Individual shrimp was placed in 5 L plastic boxe each containing 1.5 L of 16 ppt salinity seawater. Each shrimp was fed once with 20 *Artemia* (control, Vp_{3HP}) and feeding was monitored for 60 minutes to ensure that the shrimp consumed all 20 *Artemia*. The bacterial concentrations of the pre-soaked *Artemia* were determined on TCBS agar. Average concentration of bacteria for one *Artemia* was found to contain approximately 2×10^6 CFUs of bacteria, and hence each shrimp received approximately 4×10^7 CFUs of bacteria/shrimp. Three shrimp from each treatment group were collected at 3, 6, 12 and 24 hours post infection and then fixed with Davidson's fixative [306]. The fixative was injected into the body of shrimp at the third of segment and into the hepatopancreas of shrimp to better fixation. The sample was fixed for 48 hours and then changed to 70% alcohol for long-term preservation.

3.4.4 Paraffin embedding

The fixed shrimp were divided into 2 parts: head and body. The body of each shrimp was disected for intestine, whereas the head of each shrimp was further divided longitudinally into two parts: stomach and hepatopancreas. Separate histological embedding cassette was used for each sample. Paraffin embedding were performed as mentioned in section 3.3.2.1.

3.4.5 Sectioning

Sectioning of sample was performed as mentioned in section 3.3.2.1 with some modification. The thickness of each sample was 5 μm and all samples were kept in slide boxes at room temperature until use.

3.4.6 Staining

The staining method was modified from Bell and Lightner [306] using hematoxylin and eosin dry [307]. Staining methodology is shown as Figure 3.1.

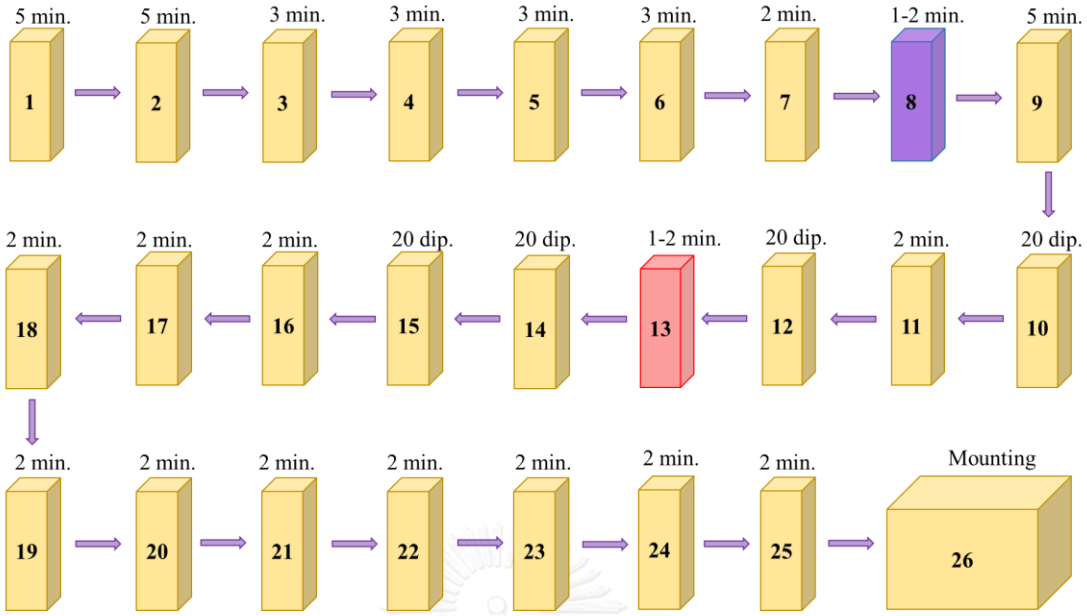

Figure 3.1 The diagram of staining using hematoxylin and eosin dry. 1. toluene I, 2. toluene II, 3. absolute ethanol I, 4. absolute ethanol II, 5. 95% ethanol, 6. 70% ethanol, 7. slowly dripping tap water, 8. PATH.1 modified hematoxylin solution (C.V. Laboratories co., ltd., Bangkok, Thailand), 9. slowly dripping tap water, 10. Bluing solution (C.V. Laboratories co., ltd.), 11. slowly dripping tap water, 12. 95% ethanol, 13. PATH.2 eiosin solution (C.V. Laboratories co., ltd.), 14. 95% ethanol I, 15. 95% ethanol II, 16. absolute ethanol I, 17. absolute ethanol II, 18. absolute ethanol:toluene (1:1), 19. toluene I, 20. toluene II, 21. histosove I, 22. histosove II, 23. tuluene I, 24. tuluene II, 25. tuluene III and 26. Mounting media

3.5 Differentially Expressed Genes (DEGs) Libraries of Control and Challenge Stomach

In this study, differential gene expression libraries was constructed with 2 techniqes: suppressive subtractive hybridization (SSH) and ion torrent sequencing.

3.5.1 Construction of suppressive subtractive hybridization (SSH) stomach cDNA libraries

Base on the histopathology of AHPND/EMS results, the experiment was performed as mentioned in section 3.4.3 and shrimp were collected at 6 hours. Two groups of shrimp in this experiment control and challenged were assigned as driver and

tester for SSH, respectively. Seven shrimp from each group were collected to carry out each SSH stomach cDNA libraries. SSH cDNA libraries were performed using the PCR-select cDNA subtraction kit (Clontech, Heidelberg, Germany) according to the manufacturer's instruction.

3.5.1.1 Total RNA extraction

Total RNA were extracted using TriPure isolation reagent (Roche, IN, USA) according to the instruction of the manufacturer with some modification. Breifly, the frozen stomach was immediately placed in mortar containing liquid nitrogen and ground to a fine powder. The fine tissue was homogenized in 1 ml TriPure isolation reagent for 5 minutes at room temperature to dissociate nucleoprotein complexes, then the homogenized solution was centrifuged at 12,000xg for 10 minutes at 4 ºC. The supernatant was transferred to a new microcentrifuge tube and 200 µl chloroform were added then vigorously mixed by votexing for at least 15 seconds and incubated at room temperature for 15 minutes. After incubation, the mixture was centrifuged at 12,000xg for 15 minutes at 4 ºC. The mixture was separated into the red lower phenol-chloroform phase, the interphase, and the colorless upper aqueous phase. The colorless aqueous phase containing total RNA was carefully transferred to a new microcentrifuge tube and precipitated by an addition of 0.5 ml of isopropanol. The solution was thoroughly mixed and incubated at -20 ºC for at least 30 minutes. After incubation, the sample was centrifuged at 12,000xg for 10 minutes at 4 ºC, the pellet was washed with 1 ml of 75% ethanol. The RNA pellet was air-dried and dissolved with an appropriate amount of diethyl pyrocarbonate (DEPC)-treated H_2O for being immediately used. Alternatively, the RNA pellet was kept in absolute ethanol at -80 ºC until used.

3.5.1.2 Poly(A)$^+$ RNA purification

Poly(A)$^+$ RNA was purified using a QuickPrep micro mRNA Purification Kit (GE Healthcare, Buckinghamshire, UK)) according to the manufacturer's instruction with some modification. Breifly, a 500 µg/25 µl of total stomach RNA was thoroughly mixed with 200 µl extraction buffer, and then 400 µl elution buffer were added. At the same time, 500 µl elution buffer were incubated at 65 ºC for elution step, and 1 ml oligo(dT)-cellulose solution was pipeted into the

microcentrifuge tube. To collect the oligo(dT)-cellulose pellet, the solution was centrifuged at 16,000xg for 1 minute then the supernatant was removed. The homogenized RNA was transferred into the microcentrifuge tube containing the oligo(dT)-cellulose pellet, gently mixed by inversion and incubated at room temperature for 3 minutes. The mixture was centrifuged at 16,000xg for 10 seconds at room temperature and the supernatant was carefully removed. The pellet was washed five times with 1 ml high salt buffer by centrifugation at 16,000xg for 10 seconds at room temperature followed by washing twice with 1 ml low salt buffer by centrifugation at 16,000xg for 10 seconds at room temperature. Eventually, a 300 µl low salt buffer was added to the oligo(dT)-cellulose pellet and thoroughly mixed by pipetting. The slurry was transferred into a Micro Spin Column placed in a microcentrifuge tube, centrifuged at 16,000xg for 5 seconds then the flow-though solution was discarded. A 500 µl low salt buffer was washed the MicroSpin Column twice by centrifugation at 16,000xg for 5 seconds then the column was centrifuged at 16,000xg for 10 seconds at room temperature to dry. A 200 µl prewarmed elution buffer (65 °C) was pipetted to the top of column and centrifuged at 16,000xg for 5 seconds and the elution step was repeated to elute poly(A)$^+$ RNA. A 400 µl poly(A)$^+$ RNA solution was precipitated by an addition of 10 µl glycogen solution, 40 µl potassium acetate solution and 1 ml absolute alcohol then the solution was incubated at -80 °C for 30 minutes. To collect the poly(A)$^+$ RNA precipitation, the incubated solution was centrifuged at 12,000xg for 10 minutes at 4 ºC, and the pellet was washed with 1 ml of 75% ethanol. The poly(A)$^+$ RNA pellet was air-dried and dissolved with an appropriate amount of diethyl pyrocarbonate (DEPC)-treated H_2O for being immediately used. Alternatively, the pellet was kept in absolute ethanol at -80 ºC until used.

3.5.1.3 First strand cDNA synthesis

A 2 µg poly(A)$^+$ RNA from was synthesized to the first-stand cDNA with 1 µl of 10 µM cDNA synthesis primer (oligo primer) and then incubated at 70 ºC for 2 minutes. The reaction was immediately chilled on ice for 2 minutes and briefly spun. After that, the composition of the first strand cDNA synthesis (Table 3.4) was added, gently mixed and briefly spun. The mixture was incubated at 42 ºC for 1.5 hours.

After incubation, the reaction was stopped by placing on ice, then the second strand was processed immediately.

Table 3.4 The reagent of the first strand cDNA synthesis

Reaction component	**per rxn**
Sterile H_2O	1.0 µl
5X first-strand Buffer	2.0 µl
dNTPs mix (10 mM each)	1.0 µl
DTT (20 mM)	1.0 µl
SMARTScribe reverse transcriptase (100 U/µl)	1.0 µl
Total volume	**6.0 µl**

3.5.1.4 Second strand cDNA synthesis

After the first strand cDNA synthesis, the second strand component (Table 3.5) was immediately added into the completed first strand cDNA tubes. The reaction was gently mixed and briefly spun and further incubated at 16 ºC for 2 hours in a thermal cycler. After incubation, a 2 µl (6 U) of T4 DNA Polymerase was carefully added, gently mixed and briefly spun. The mixture was continually incubated at 16°C for 30 minutes. To terminate second-strand synthesis, a 4 µl of 20X EDTA/Glycogen and a 100 µl of phenol:chloroform:isoamyl alcohol (25:24:1) were added, and then thoroughly mixed by votexing. The mixture was centrifuged at 14,000 rpm for 10 minutes at room temperature. The supernatant was carefully transferred to the new microcentrifuge tube. This step was repeated with 100 µl of chloroform:isoamyl alcohol (24:1). The double strand (ds) cDNA was precepitated with 40 µl of 4 M NH_4OAc and 300 µl of 100% ethanol. The cDNA pellete was collected by centrifugation at 14,000 rpm for 10 minutes and washed with 70% ethanol. The supernatant was carefully removed and the cDNA pellet was dried at room temperature for 10 minutes. The pellet was dissoved in 50 µl of sterile H_2O and a 6 µl of cDNA solution was collected to check the quality of ds cDNA products by agarose gel electrophoresis. A 44 µl of ds cDNA solution was continually digested in next step.

Table 3.5 The reagent of the second strand cDNA synthesis

Reaction component	**per rxn**
Sterile H_2O	48.4 µl
5X second-strand buffer	16.0 µl
dNTPs mix (10 mM each)	1.6 µl
20X second-strand enzyme cocktail	4.0 µl
Total volume	**70.0 µl**

3.5.1.5 *Rsa* I Digestion

The ds cDNA tester and driver were digested with *Rsa* I restiction enzyme to geneate shorter, blunt-ended ds cDNA fragments which are optimal for subtraction and required for adaptor ligation. The reaction consisted of 43.5 µl ds cDNA, 1X *Rsa* I restriction buffer and 15 U *Rsa* I, then thoroughly mixed by votexing and briefly spun. The mixture was incubated at 37 ºC for 1.5 hour, and then the reaction was terminated with 2.5 µl of 20X EDTA/Glycogen. *Rsa* I-digested cDNA was isolated and precipitated as described above. The pellet was dissoved in 5.5 µl of sterile H_2O and stored at -20 ºC. This *Rsa* I-digested cDNA was served as the experimental driver cDNA of each libraries, while *Rsa* I-digested cDNA was continually ligated with adapters to create the experimental tester cDNA. A 1 µl of *Rsa* I-digested cDNA and a 2.5 µl of undigested cDNA were determined by 1% agarose gel electrophoresis.

3.5.1.6 Experimental tester cDNA preparation

A 1 µl of each *Rsa* I-digested cDNA (challenge and control) was diluted into a 5 µl of sterile H_2O. To ligate each adaptor, the master mix was prepared including 1X ligation buffer, 400 U of T4 DNA ligase, and then each reaction was prepared following Table 3.6 in the new microcentrifuge tube, a 2 µl of tester 1-1 and tester 1-2, and a 2 µl of tester 2-1 and tester 2-2 were mixed to generate unsubtracted tester control 1-c and 2-c, respectively. All reactions were incubated at 16 ºC overnight, added 1 µl of the EDTA/glycogen and heated at 72°C for 5 minutes to inactivate the

ligase activity. The ligation efficeincy was determined by PCR using PCR primer 1, elongation factor 1α (EF1α) forward and reverse primer (Table 3.7).

Table 3.6 Ligation reactions of the tester cDNA of forward (tester 1-1 and 1-2) and reverse (tester 2-1 and 2-2) subtraction libraries

Component	**cDNA for forward library**		**cDNA for reverse library**	
	Tube 1	**Tube 2**	**Tube 3**	**Tube 4**
	Tester 1-1	**Tester 1–2**	**Tester 2–1**	**Tester 2–2**
	(μl)	**(μl)**	**(μl)**	**(μl)**
Diluted *Rsa* I-digested cDNA	2.0	2.0	2.0	2.0
Adaptor 1 (10 μM)	2.0	-	2.0	-
Adaptor 2R (10 μM)	-	2.0	-	2.0
Master Mix	6.0	6.0	6.0	6.0
Final volume	**10.0**	**10.0**	**10.0**	**10.0**

Table 3.7 Sequences of the PCR select cDNA synthesis primer, adaptors and PCR primers and control primers

Primer/Adaptor	**Sequence**
cDNA synthesis primer	5′- TTTTGTACAAGCTT$_{30}$N$_1$N -3′
Adaptor 1	5′- CTAATACGACTCACTATAGGGCTCGAGCGGCCGCCCGGGCAGGT -3′
	3′- GGCCCGTCCA -5′
Adaptor 2R	5′-CTAATACGACTCACTATAGGGCAGCGTGGTCGCGGCCGAGGT-3′
	3′-GCCGGCTCCA-5′
PCR primer 1	5′- CTAATACGA CTCCATATAGGGC -3′
Nested PCR primer 1	5′- TCGAGCGGCCGCCCGGGCAGGT -3′
Nested PCR primer 2R	5′- AGCGTGGTCGCGGCCGAGGT -3′
EF1αF	5′- ATGGTTGTCAACTTTGCCCC -3′
EF1αR	5′- TTGACCTCCTTGATCACACC -3′

3.5.1.7 First Hybridization

For first hybridization, each of experimental subtraction was prepared following Table 3.8 in the PCR tube. The reactions were mixed thoroughly and spun briefly, and then the reactions were initially incubated at 98 °C for 1.5 minutes following by 68 °C for 10 hours in a thermal cycler. After finished first hybridization, the second hybridization was proceed immediately.

Table 3.8 Compositions of the first hybridization reaction of each subtraction

Component	**cDNA for a forward library**		**cDNA for a reverse library**	
	Tube 1	**Tube 2**	**Tube 3**	**Tube 4**
	Tester 1-1*	**Tester 1-2***	**Tester 2-1***	**Tester 2-2***
	(µl)	**(µl)**	**(µl)**	**(µl)**
Rsa I-digested Driver cDNA	1.5	1.5	1.5	1.5
Adaptor 1-ligated Tester 1-1	1.5	-	-	-
Adaptor 2R- ligated Tester 1-2	-	1.5	-	-
Adaptor 1- ligated Tester 2-1	-	-	1.5	-
Adaptor 2R- ligated Tester 2-2	-	-	-	1.5
4x Hybridization Buffer	1.0	1.0	1.0	1.0
Final volume	**4.0**	**4.0**	**4.0**	**4.0**

3.5.1.8 Second Hybridization

For second hybridization, the driver cDNA was separately prepared. A 1 µl *Rsa* I -digested diver cDNA was mixed with 1 µl of 4X hybridization buffer and 2 µl of sterile H_2O, and then the mixture was incubated at 98 °C for 1.5 minute. The two samples from the first hybridization of each library and the fresh denatured driver cDNA were carefully mixed and briefly spun, then the reactions were incubated at 68 °C overnight. Finally, a 200 µl dilution buffer was added to successefully subtracted cDNA and mixed by pipetting. The reaction was continually incubated at 68°C for

7 minutes in a thermal cycler. The diluted subtracted cDNA was stored at -20 °C or continued to amplify by PCR.

3.5.1.9 Primary and secondary PCR amplification

A 1 µl of each diluted subtracted cDNA samples or unsubtracted cDNA control was amplified as template for the primary PCR amplification. The reaction was performed in 25 µl consisting of 1X Advantage® 2 PCR buffer (40 mM Tricine-KOH, 15 mM KOAc, 3.5 mM $Mg(OAc)_2$, 3.75 µg/ml BSA, 0.005 % Tween 20, and 0.005% Nonidet-P40), 0.2 mM dNTPs, 400 nM PCR primer I, 1X advantage® 2 polymerase mix (Clontech), and cDNA template. The PCR cycle parameters were 25 seconds initial denaturation at 94 °C, 35 cycles of 10 seconds at 94 °C, 30 seconds at 66 °C, 1.5 minutes at 72 °C on a thermal cycler. A 5 µl of each primary PCR product was analyzed by agarose gel electrophorisis, and then 3 µl of each primary PCR product were diluted with 27 µl of sterile H_2O to amplify the secondary PCR amplification.

The secondary PCR amplification was performed in 25 µl consisting of 1X Advantage® 2 PCR buffer, 0.2 mM dNTPs, 200 nM nested PCR primer I, 200 nM nested PCR primer 2R, 1X advantage® 2 polymerase mix, and 1 µl diluted primary PCR product. The PCR cycle parameters were 15 cycles of 10 seconds at 94 °C, 30 seconds at 68 °C, 1.5 minutes at 72 °C on a thermal cycler. A 5 µl of each primary PCR product was analyzed by agarose gel electrophorisis. The secondary PCR products were stored at -20 °C for further analysis.

3.5.1.10 PCR cloning

The PCR cloning was performed as mentioned in section 3.3.4.4-3.3.4.9 with some modification. Briefly, the secondary PCR products were purified using illustra GFX PCR DNA and gel band purification kit, and then the purified products were ligated to pGEM®-T Easy vector in total volume 20 µl. The ligation products were transformed to *E. coli* JM109. The white colonies were amplified to seclect the positive clone.

3.5.1.11 Colony PCR digestion

The PCR products of colony PCR were digested with *Bsu* RI (*Hea* III) restriction enzyme to select out the repeated clone. The reaction was performed in

10 µl consisting of 1X buffer R (1 mM Tris-HCl, pH8.5, 1 mM $MgCl_2$, 10 mM KCl, 0.01mg/ml BSA), 1 U *Bsu*RI restriction enzyme (Fermentas), and 5 µl colony PCR product. The mixtures were incubated at 37 °C overnight, then the digested products were analyzed by 1.5 % agarose gel electrophorisis. The patterns of each digestion were shown the diferrent or similar product. All different and 2-3 similar products of clones were selected to culture for plasmid DNA extraction.

3.5.1.12 Recombinant plasmid DNA extraction

The recombinant plasmid DNA extraction was performed as mentioned in section 3.3.4.9 Additionally, the recombinant plasmid DNA was digested with *Eco*RI (Promega) to confirm size selection. The reaction were performed in 12 µl consisting of 1X buffer H (90 mM Tris-HCl, pH 7.5, 10 mM $MgCl_2$, 50 mM NaCl), 0.1 mg/ml BSA, 1 U *Eco*RI restriction enzyme (Promega), and 1 µl recombinant plasmid DNA. The reactions were thorouhly mixed and incubated at 37 °C overnight. The digested products were analyzed by 1.5 % agarose gel electrophoresis.

3.5.1.13 Sequencing and data analysis

The recombinant plasmids were diluted to 100 ng/µl in total volume 20 µl and were submitted for sequencing at Macrogen (Korea). Vector and adaptor sequence were removed from raw sequences. The sequences, which were less than 100 bp. in length were discarded from analysis. All sequences were assembled by CAP3, a DNA sequence assembly program [308]. The contig and singleton were searched in the GenBank database using BlastX in National Center for Biotechnology Information (NCBI) and the Uniprot Knowledgebase (UniProtKB) for functional information. Similarity with known transcripts was considered significant when the probability (E) value is $<10^{-3}$. Blast2Go program was used to identify Gene Ontology (GO) and KEGG enzymatic pathway. GO annotation was determined using the default parameters. Additionally, InterProScan and Annex were also considered functional annotation to improve the annotation result. The function was classified into 3 terms including: biological process, molecular function, and cellular component at level 2^{nd}.

3.5.1.14 The PCR primer for validation of SSH stomach cDNA libralies

Quantitative real-time PCR primers were designed from 9 genes of each library and housekeeping gene (EF1α) was used as an internal control (Table 3.9). The primer premier 5 program and primer 3 online program [309,310] were used to design primer. The appropiated primer was choosen based on following parameter: 1) GC content about 50-60%, 2) the length of primer: 18-22 bp., 3) melting temperature around 58-62 °C, 4) max 3' self complementary: 1, 5) max poly-x: 3 6) the length of product:100-250 bp. Each pair of forward and reverse primers had closely similar Tm values and they were checked for minimal hairpin self-dimer and hetero-dimer formation.

Table 3.9 List of quantitative real-time PCR primers for validating SSH libralies

Gene description	**Primer sequence (5'-3')**	**PCR product size (bp)**
Foreward library		
Cuticle protein AMP1B	F: CTCCGAGGGTCAGAGCAACA R: GAGGAAGGCTGGTAACCGAAC	108
Clottable protein	F: GAAAGGTAGCGTGGCTCTCG R: ACTTCGCAGGGATAGTTGGTCT	270
Salivary alkaline phosphatase	F: CACAGGAGAAAGAAGCCGATTA R: GCCCACCGTGATACCCAGT	137
Ig-like and fibronectin type-III domain-containing protein (predicted protein)	F: TACGCCGACAATGGCTACG R: TCTCCACCACACGAGTGAAGG	168
DD9A	F: TGCCTTTGCCTTCCCTCAG R: GTCGGTAACCTGCTTCGTCG	239
Pacifastin heavy chain precursor	F: CCGCCTTCTGAGTGAGGTCTA R: GTCTTCCCGATGCCTGTGTG	147
Cathepsin B	F: CAGCAAGGGCAAGAGCAACT R: CGAGCCTCCTGATACAATACCA	142
C-type lectin	F: CGCCGCTAACAGTTATTGCTC R: ACCCGTTGCCTCCAGTGTG	212
Spz1	F: ATGGTAAGCAAGGAGCAGGA R: CAGCCTCTGGGAACAGACA	244
Reverse library		
GPx isotype 2	F: AACCAGTTCGGGAAGCAAGA R: CTCGTCCACCCCATTCACAT	135

Table 3.9 Cont.

Gene description	Primer sequence (5'-3')	PCR product size (bp)
Reverse library **(cont.)**		
Ubiquitin-conjugating enzyme H5b	F: GACGACCTCTTTCACTGGCAA R: GCTGGACTCCATTGGGTTCTAA	206
Fibronectin type-III domain-containing protein (predicted protein)	F: GGACCCTGAGTCTGACTTGAC R: GGATGTAGCTGCTGGAGAGG	217
I-connectin	F: AGCACATCTGTTGTCCCTCA R: TGGTGCTTTGAGTTATTTCCA	154
Chondroitin proteoglycan2	F: TGATGCTGACTGCCAGATTCC R: GGTTGAACACAAGCCCTTCG	182
Peroxiredoxin	F: GATCCCTCTTCTGGCTGACAA R: TCTACATCACGCCCAACTGG	159
Ferritin	F: TGGAGAAGCAGGTCAATCAG R: AGCACGCTTCAGCTTGGTAA	158
Astakine variant1	F: CAGAATGTTGTCAGTGGCTTGC R: CATTCCGTGGTAAGAGTCCGT	250
Dicer 2	F: GGACTCGATCAAACCAGTGA R: GGTCAGAGGGTATGCCATAAAG	110
EF1α [311]	F: TCCGTCTTCCCCTTCAGGACGTC R:CTTTACAGACACGTTCTTCACGTTG	218

3.5.1.15 Sample collection

The experiment was performed as mention in section 3.4.3 and the stomach of three shrimp were collected at 6 hours. All samples were stored at -80 ºC until use.

3.5.1.16 Total RNA extraction

Total RNA was extracted as mentioned in session 3.5.1.1.

3.5.1.17 The elimination of DNA from total RNA

DNA contamination in total RNA samples was removed by treating 15 µg of total RNA with 7.5 U of RQ1 RNase-free DNase (Promega) in total volune 50 µl at 37 ºC for 30 minutes. After incubration, a 50 µl DEPC and 100 µl TriPure was added, thoroughly mixed by votexing, and incubated at room temperature for 5 minutes. Next step was the same as a total RNA extraction, but 0.1 volume of 3 M sodium acetate ($Na_2C_2H_3O_2$) was added to complete precipitation.

3.5.1.18 First strand synthesis

The first strand cDNA was synthesized from 1.5 µg of DNA-free RNA using an ImPromII^{TM} Reverse Transcription System Kit (Promega) according to the manufacturer's instruction. DNA-free RNA was combined with 0.5 µg of oligo (dT_{15}) and DEPC-treated H_2O in a final volume of 5 µl. The reaction was incubated at 70 ºC for 5 minutes and immediately chilled on an ice, and then the reverse transcription reaction mixture (1X reaction buffer, 2 mM $MgCl_2$, 0.8 mM dNTP Mix, 20 U Recombinant RNasin® Ribonuclease Inhibitor and 1 µl of ImProm-II™ Reverse Transcriptase) was added and gently mixed. The reaction was incubated at 25 ºC for 5 minutes and 42 ºC for 90 minutes. The transcriptase activity was terminated by incubating at 70 ºC for 15 minutes. The first strand cDNA was stored at -20 ºC untill used.

3.5.1.19 External standard curve preparation and amplification

The external standard curves were prepared as mentioned in session 3.3.4.3 and 3.3.4.4. The cDNA template concentration, primer concentration and annealing temperature of each gene were shown in Table 3.10.

Table 3.10 The conditions of real-time PCR reaction for validating SSH libralies

Gene homology	cDNA template concentration (ng)	Primer concentration (µM)	Ta (ºC)
Cuticle protein AMP1B	100	0.1	58
Clottable protein	100	0.3	58
Salivary alkaline phosphatase	500	0.3	56
Ig-like and fibronectin type-III domain-containing protein (predicted protein)	500	0.1	58
DD9A	100	0.2	60
Pacifastin heavy chain precursor	500	0.2	58
Cathepsin B	100	0.3	60
MBP	500	0.2	62
Spz1	500	0.1	62
GPx isotype 2	400	0.3	56
Ubiquitin-conjugating enzyme H5b	400	0.3	58
Fibronectin type-III domain-containing protein	400	0.3	58
I-connectin	400	0.3	60

Table 3.10 Cont.

Gene homology	cDNA template concentration (ng)	Primer concentration (µM)	Ta (°C)
Chondroitin proteoglycan2	100	0.2	60
Peroxiredoxin	200	0.3	61
Ferritin	100	0.3	60
Astakine variant1	500	0.3	61
Dicer 2	500	0.3	61
EF1α	1.25	0.3	58

3.5.1.20 Data analysis

Statistical analysis was performed using independent sample *t*-test (two-tail) with SPSS 13.0 software for windows. Differential expression was examined statistically significant at *P*-value<0.05. Data were expressed as mean±SEM.

3.5.2 Construction of transcriptome of differentally expressed genes of stomach cDNA libraries by ion torrent sequencing

3.5.2.1 Total RNA extraction

Total RNA extraction was performed as mentioned in section 3.5.1.1.

3.5.2.2 DNase treatment and Ion torrent sequencing

Total RNA were deliveried to Genomic Research Laboratory, National Center for Genetic Engineering and Biotechnology to treat DNase, purify mRNA, construct cDNA and sequence. Firstly, total RNA were treated with Dnase to remove genomic DNA using the Ambion® DNA-free™ DNase Treatment and Removal Reagents (Life Tecnologies™). Secondly, mRNA were purified from DNA-free RNA using Absolutely mRNA Purification Kit (Agilent Technologies), and then cDNA libaries were constructed using Ion Total RNA-Seq Kit v.2 (Ion Torrent by Life Tecnologies™). Finally, cDNA libraries were sequenced using Ion Proton™ Semiconductor Sequencer (Ion Torrent by Lift Technologies™).

3.5.2.3 *De novo* assembly and functional annotation

To assembly sequencing reads, CLC Genomics Workbench software (version 4.8.1) was used following the user manaul. The raw reads with quality score limited to 0.05 and maximum number of ambiguities greater at 2 were trimmed. The adaptor sequences (primer A: CCATCTCATCCCTGCGTGTCTCCGACTCAG and primer P1: CCTCTCTATGGGCAGTCGGTGAT) were then cut from raw sequences. Finally, the raw reads length shorter than 30 bp were discarded.

The clearn reads were assembled by *de novo* assembly. This assembly was performed by various de Brujin graph assemblers to obtain the best assembly results.

3.5.2.4 Identification of different gene expression

All contigs from *de novo* assembly were analyzed for differential expression using Gene Expression Analysis modules of the CLC Genomics Workbench pakage (version 4.8.1). Transformation, normalization and statistical analysis had been performed. For analysis level, all parameters including *t*-test between control and challenge (original values), baggerley's test between control and challenge (original and normalized values), difference, fold change, test statistic, *p*-value, bonferroni, FDR-*p*-value correction, weighted proportion differrence and weighted proportion fold change were set. The proportion-based test was used to identify the differential expressed genes between control and challenged shrimp with p-value < 0.05. In addition, the fold change values of transcripts were larger than 1.5 that express as differentially expressed genes.

3.5.2.5 The PCR primer for validation of stomach cDNA libraly

Relative real-time PCR primer pairs were designed as mentioned in section 3.5.1.14 The primer pairs of each gene were shown in Table 3.11.

Table 3.11 List of quantitative real-time PCR primers for validating transcriptome

Gene description	**Primer sequence (5'-3')**	**PCR product size (bp)**
Antilipopolysaccharide factor isoform 3	F: GCGACGAGGCTAACAGGATT R: ACCACTCCCGACCTGCTTC	179
Crustin 3	F: TGGAGTGGCGTGAGGAGTT R: TCTTCCCAGTACACTGCCAG	238
Calnexin	F: CTGTTGTCACGGAAGAGCAA R: AGCAGGTTCTACTGCCCAAA	212
Prophenoloxidase-activating enzyme 2a	F: TCTTCCTGTCTCCCAACGCA R: TCAAGTTAGAGGTCTGTCCGCA	204
Masquerade-like serine proteinase-like protein 3	F: AGTCAACGTCACCACAACCA R: AACTCGCCGAACTGACTCTC	156
Serine proteinase inhibitor 6	F: TTCACTCGGAGGTGGATAGG R: CTCTGGGAAGGTGTTGGAAG	209
Single whey acidic protein domain-containing protein isoform 1	F: ATCTTCTCCATCTGCGTCGTG R: AACCACAGCCAGGCACTCA	108
Alpha2 macroglobulin isoform 2	F: TGAGAATCTTGGCTCCCTTG R: TCATCATGGCGATAGCGTAG	189
Defender against apoptotic death	F: CCTTCAACTCCTTCCTGTCTGG R: GATGAAATCAGCAAAGCCTCG	140
Fibrinogen C domain-containing protein 1-B	F: GAGGGCGTGGAGGTATGGT R: GCTGGATGACTGTAGGCGACT	249
Clottable protein	F: TGTCAGCAGCAATGTCAAGGA R: TCCAGGTGGCAGTGATGTGA	131
Peroxinectin	F: CAAGCTCTCGAAGGATCAGG R: GGAGGATACGCTGAACTGGA	194
Protein toll	F: CCATCACCCTCATCGTCTTC R: GTCACGAACACCTCGTCCTT	160
Cactus protein	F: TCGGGTTTCCTGTCTGGTTC R: CGTTTTCGGGCGTATCTGA	250
IMD	F: CAGCAGCTGGAAGAGTCTGG R: GAGTCTGGCCACAGTAGCATC	154
Relish	F: AGCTACAGCAGCAGCAACAA R: AAGCAGCTAGGCAGGTCAAA	226
Cytokine receptor	F: AGCTTGAGTGGCTTGTGGTT R: TTGGGTCAGTTTCCTGTGTG	195
Mitogen-activated protein-binding protein-interacting protein	F: CCACGGACCCTTACCCAGA R: CCTTCCTCGCATTCCATCAG	227
Lipoprotein receptor	F: TTCCCAGCAACTTGACCTTC R: TGCTTGAATGATGTGGCTGT	164

Table 3.11 Cont.

Gene description	Primer sequence (5'-3')	PCR product size (bp)
Galectin	F: TCTGAACAAGGCCCTGGGT R: CATGATGGAAGCCTTTGTGC	149
Single VWC domain protein 3	F: TACCCTGGAAGGTGCTTTGT R: GCAACTATCAGACGGGATGG	161
EF1α	F: TCCGTCTTCCCCTTCAGGACGTC R:CTTTACAGACACGTTCTTCACGTTG	218

3.5.2.6 Sample collection

The experiment was performed as mentioned in section 3.4.3 and the stomach of five shrimp of control and challanged group were collected at 6 hours. All samples were stored at -80 ºC until use.

3.5.2.7 cDNA preparation

Total RNA was extracted as mentioned in section 3.5.1.1. Next, the contaminated genomic DNA was eliminated as mentioned in section 3.5.1.17. Finally, cDNA was synthesized as mentioned in section 3.5.1.18.

3.5.2.8 Relative real-time PCR

All real-time PCR reactions were carried out in a 96 well plate and each sample was amplified in duplicate using a LightCycler® 480 II system (Roche). LightCycler® 480 SYBR Green I Master (Roche), 0.1-0.3 µM primer concentration (Table 3.12) and 250 ng/µl of each cDNA were used for real-time PCR amplification. The thermal profile for real-time PCR was 95 °C for 10 minutes followed by 40 cycles of 95 °C for 15 seconds, 58-62 °C (Table 3.12) for 30 seconds and 72 °C for 30 seconds. Aditionally, the melting-curve was produced by increasing the temperature from 65 to 98 °C. Finally, all reactions were cooled down at 40 °C for 30 seconds. A no template was run on all genes.

Table 3.12 The conditions of real-time PCR reaction for validating transcriptome

Gene description	**Primer concentration (µM)**	**Ta (ºC)**
Antilipopolysaccharide factor isoform 3	0.1	62
Crustin 3	0.3	60
Calnexin	0.2	62
Prophenoloxidase-activating enzyme 2a	0.3	62
Masquerade-like serine proteinase-like protein 3	0.3	62
Serine proteinase inhibitor 6	0.1	62
Single whey acidic protein domain-containing protein isoform 1	0.2	62
Alpha2 macroglobulin isoform 2	0.3	60
Defender against apoptotic death	0.1	58
Fibrinogen C domain-containing protein 1-B	0.1	62
Clottable protein	0.1	60
Peroxinectin	0.1	62
Protein toll	0.3	62
Cactus protein	0.3	62
IMD	0.1	60
Relish	0.1	58
Cytokine receptor	0.3	60
Mitogen-activated protein-binding protein-interacting protein	0.3	60
Lipoprotein receptor	0.3	60
Laminin receptor	0.3	60
Galectin	0.1	62
Single VWC domain protein 3	0.1	62
EF1α	0.3	60

3.5.2.9 Data analysis

The relative quantification and the mathematical model described by Livak and Schmittgen [312] was used to determine the relative expression. The change in gene expression was measured based on a calibrator which is the EF1α gene. Both target gene and calibrator are amplified in separate tubes so C_T values were averaged before performing the ΔC_T calculetion. The data were analyzed using this equation (The C_P data from LightCycler® 480 II system are the same as C_T data from this equation). Data were expressed as mean±SEM.

$$\text{Amount of target} = 2^{-\Delta\Delta C_{\mathrm{T}}}$$

Where $\Delta\Delta C_{\mathrm{T}} = (C_{\mathrm{T,Target}} - C_{\mathrm{T,Cal.}})_{\mathrm{Time}\ x} - (C_{\mathrm{T,Target}} - C_{\mathrm{T,Cal.}})_{\mathrm{Time}\ 0}$

Time *x* is any time point

Time 0 is the 1x expression

$C_{\mathrm{T,Target}}$ is C_{T} value of target gene

$C_{\mathrm{T,Cal.}}$ is C_{T} value of caribator

3.6 Characterization of the Full Length cDNA of C-type Lectin

A partial cDNA sequence of C-type lectin was received from *P. monodon* EST database (Contig no. SG7730). The full length cDNA of C-type lectin was sucessfully constructed using a SMART™ RACE cDNA Amplification Kit (Clontech).

3.6.1 3' and 5'-RACE-ready cDNA preparation

To generate 3' and 5'-RACE-ready cDNA for rapid amplification of cDNA ends (RACE) PCR, total RNA were extracted from hepatopancreas of juvenile *P. monodon* using TriPure isolation reagent (Roche) as mentioned in section 3.5.1.1, after that poly(A)$^+$ RNA was purified using a QuickPrep micro mRNA Purification Kit (GE Healthcare) as mentioned in section 3.5.1.2. A 1 µg of poly(A)$^+$ RNA was combined with 3'-CDS primer A for 3' RACE-ready cDNA, while with 5'-CDS primer and BD SMART II A oligo (Table 3.13) for 5'-RACE-ready cDNA in a final volume of 5 µl, mixed thoroughly, and spun briefly. The mixture was incubated at 70°C for 2 minutes, immediately cooled on ice for 2 minutes and spun briefly. After incubration, a 5 µl synthezyed reaction mixture consisting of 1X first-strand buffer, 2 mM DTT, 1 mM dNTP mix and PowerScript™ Reverse Transcriptase were added, gently mixed by pipetting, and spun briefly. The reactions were incubated at 42°C for 1.5 hours in a thermal cycler then dilutted with 125 µl of TE buffer. The reactions were finally incubated at 72°C for 7 minutes. The 3' and 5'-RACE-ready cDNA was stored at -20°C.

3.6.2 Primer design

Gene-specific primer (GSP) was designed using primer premier 5 program from a partial cDNA sequence of C-type lectin. The appropiated primer was choosen based on following parameter: 1) GC content about 50-70%, 2) the length of primer: 23-28 bp., 3) melting temperature around 65-75 °C. The sense primer (RACECrF1:5'-TTGATTCCTCGGAGCAGTTGGCAGC-3') for 3'-RACE PCR and anti-sense (RACECrR1:5'-GCCAACTGCTCCGAGGAATCAAAGAC-3') for 5'-RACE PCR were combined in RACE PCR reaction.

Table 3.13 Primer sequences for the first strand cDNA synthesis for RACE-PCR

Primer	Sequence
BD SMART II™ A Oligonucleotide (12 µM)	5'- AAGCAGTGGTATCAACGCAGAGTACGCGGG -3'
3'-RACE CDS Primer A (3'-CDS; 12 µM)	5'- AAGCAGTGGTATCAACGCAGAGTAC$(T)_{30}$V N -3' (N = A, C, G or T; V = A, G or C)
5'-RACE CDS Primer (5'-CDS; 12 µM)	5'- $(T)_{25}$V N -3' (N = A, C, G or T; V = A, G or C)
10X Universal Primer A Mix (UPM)	Long : 5'- CTAATACGACTCACTATAGGGCAA GCAGTGGTATCAACGCAGAGT -3' Short : 5'- CTAATACGACTCACTATAGGGC -3'
Nested Universal Primer A (NUP; 12 µM))	5'- AAGCAGTGGTATCAACGCAGAGT -3'

3.6.3 Rapid amplification of cDNA ends (RACE) PCR

RACE-PCR was carried out in total volume 25 µl consisting of 1X advantage® 2 PCR buffer, 1X universal primer A mix (UPM), 200 µM GSPs, 200 µM dNTP, 1X advantage® 2 polymerase mix and 1.25 µl cDNA templates. The PCR cycle parameters were firstly 5 cycles of 30 seconds at 94 °C and 1 minute at 72 °C, secondly 5 cycles of 30 seconds at 94 °C, 30 seconds at 70 °C and 1 minute at 72 °C, finally 25 cycles of 30 seconds at 94 °C, 30 seconds at 68 °C and 1 minute at 72 °C and final extension at 72 °C for 7 minutes a thermal cycler. The presence of a PCR product fragment was analyzed on a 1.5 % agarose gel electrophoresis

3.6.4 PCR cloning

The PCR cloning was performed as mentioned in section 3.3.4.4-3.3.4.9.

3.6.5 Sequencing and data analysis

Nucleotide sequence was searched in the GenBank database using BlastX in National Center for Biotechnology Information (NCBI) to check the corrected gene and assembled with the partial sequence to generate the completed full length cDNA of C-type lectin. The full length cDNA was tranlated to protein sequence by ExPASy tranlate tool (http://web.expasy.org/translate/) and the protein sequence was analyzed by SMART (http://smart.embl-heidelberg.de/) and Protparam (http://www.expasy.org /tools/protparam.html) to predict protein domain, signal peptide, internal repeat, P*I* and molecular weight.

3.6.6 Phylogenetic analysis

The amino acid of C-type lectin (*P. monodon*) was compared to the C-type lectin of other shrimps that were retrieved from the GenBank database. Thirty-five amino acid sequences were selected to study the evolutionary relationships of C-type lectin. Sequence alignment and phylogenetic and molecular evolutionary analyses were conducted using MEGA6 [313]. The molecular evolution was inferred using the Neighbor-Joining method [314]. The percentage of replicate trees in which the associated taxa clustered together in the bootstrap test (1,000 replicates) are shown next to the branches [315]. In addition, the evolutionary distances were computed using the Poisson correction method [316].

3.6.7 The expression of C-type lectin transcript

3.6.7.1 Sample collection for tissue distribution

Three juvenile shrimp were dissected to collect the tissue including hemocyte, hepatopancreas, midgut, hindgut, stomach, muscle, lymphoid organ, pleopod, gill and heart. All samples were stored at -80 ºC until use.

3.6.7.2 Sample collection for EMS/AHPNS challenge

The experiment was performed as mention in section 3.4.3 and the hepatopancreas of three shrimp were collected at 3, 6 and 12 hours. All samples were stored at -80 ºC until use.

3.6.7.3 Total RNA preparation and first strand synthesis

Total RNA extraction, elimination of DNA from total RNA and first strand synthesis were performed as mentioned in section 3.5.1.1, 3.5.1.17 and 3.5.1.18, respectively.

3.6.7.4 Specific primer design of C-type lectin

Specific primer of C-type lectin (qPmCrF:5'-TTTGATTCCTCG GAGCAGTTG-3'; qPmCrR:5'-ATAGACGCCCGTATCGTAAGC-3') were designed from full length cDNA using the primer premier 5 program. The appropriated primer was choosen based on following parameter: 1) GC content about 50-60%, 2) the length of primer: 18-22 bp., 3) melting temperature around 58-62 °C, 4) no hairpin self-dimer and hetero-dimer formation.

3.6.7.5 Real-time PCR

The external standard curves were prepared as mentioned in section 3.3.4.3-3.3.4.10. The cDNA of each sample were diluted to 50 ng/µl and 0.625 ng/µl for C-type lectin and EF1α, respectively. Quantitative real-time PCR reaction was performed in 10 µl reaction containing 2 µl of diluted cDNA, 0.3 µl of 10 µM foreward and reverse primer and 5 µl of LightCycler® 480 SYBR Green I Master. The cycles of amplification were 40 cycles.

3.6.8 *In vitro* expression of the full length cDNA of C-type lectin using bacteria system

3.6.8.1 Primer design

To produce C-type lectin recombinant protein, the nucleotide coding to signal peptide site of gene was cut off. Therefore, the primer pair was designed after signal peptide and contained *Nde*I site (underline) for forward primer (5' CATATGATAGAATGCCCTACA GG 3') , whereas reverse primer (5' CCGGGATC CTCAATGATGATGATGATGATGCTTCGCCCGGCACATGTA 3') was designed at nucleotides before stop codon, six histidine residues encoded nucleotides and stop codon containing *Bam*HI site (underline).

3.6.8.2 Construction of recombinant plasmid in cloning and expression vector

The full length cDNA without signal peptide of C-type lectin was amplified in total volume 25 µl consisting of 1X reaction buffer with $MgSO_4$ (200 mM Tris-HCl pH 8.8, 100 mM KCl, 100 mM $(NH_4)_2SO_2$, 20 mM $MgSO_4$, 1 mg/ml nucease-free BSA, 1% Triton® X-100), 200 µM each primer, 200 µM dNTP, 0.5 U *Pfu* DNA polymerase (Promega) and 100 ng cDNA from hepatopancreas. The PCR cycle parameters were predenaturation at 95 °C for 2 minutes followed by 30 cycles of denaturation at 95 °C for 30 seconds, annealing at 60 °C for 30 seconds, extension at 72 °C for 45 seconds and final extension at 72 °C for 7 minutes. The presence of a PCR product fragment was analyzed on a 1.5 % agarose gel electrophoresis. The PCR was purified as mentioned in section 3.3.4.4. After PCR purification, the purified PCR and pET15 that is expression vector were double digested with *Nde*I and *Bam*HI restriction enzyme in total volume 30 µl consisting 1X buffer 3 (100 mM NaCl, 50 mM Tris-HCl, 10 mM $MgCl_2$, 100 µg/ml BSA, pH 7.9) and 20 U of each restriction enzyme. The digested products were analyzed with on a 1.5 % agarose gel electrophoresis and the specific band was cut from the gel and pirified as mention in session 3.3.4.4. The sticky-end product and vector were ligated with T4 DNA ligase and transformed into *E. coli* JM109 to generate a massive product. The plasmid containing C-type lectin gene and pET15 was transformed into *E. coli* BL21-CodonPlus (DE3). Two positive clones were selected to protein expression.

3.6.8.3 Expression of recombinant protein

A single colony of positive clone of C-type lectin was cultured in 3 ml of LB medium containing 50 µg/ml ampicillin and 50 µg/ml chloramphinical at 37°C. A 0.5% of bacterial culture was transferred to 30 ml of LB medium containing 50 µg/ml ampicillin and 50 µg/ml chloramphenical, and further incubated to an OD_{600} of 0.45-0.55. The culture was induced with 1.0 mM IPTG final concentration, and then collected at 0, 1, 2, 3, 4, 5, 6 hours at 37°C. The culture was centrifuged at 12,000xg for 1 minute. The pellet was resuspended in 1X PBS buffer and examined by 15% SDS-PAGE.

Additionally, a 50 ml of the IPTG induced-cultured cells at 37°C for 1 hour was harvested by centrifugation 5000 rpm for 15 minutes and resuspended in the lysis buffer (0.05 M Tris-HCl; pH 7.5, 0.5 M Urea, 0.05 M NaCl, 0.05 M EDTA pH 8.0 and 1 mg/ml lysozyme). The bacterial cell wall was broken using Digital Sonifier® sonicator Model 250 (Branson Ultrasonics Corporation, Connecticut, USA). The suspended bacteria were sonicated 2-3 times at 10% amplitude, pulsed on for 5 seconds and pulsed off for 5 seconds in a period off 5 minutes. Soluble and insoluble portions were separated by centrifuged at 14,000 rpm for 30 minutes. The protein concentration of both portions was measured using Quick Start™ Bradford Protein Assay (Bio-Rad, CA, USA). Expression of the recombinant protein was electrophoretically analyzed by 15% SDS-PAGE.

3.6.8.4 Detection of recombinant protein by western blot analysis

The recombinant protein was analyzed in 15% SDS-PAGE and transferred to a PVDF membrane (GE Healthcare) using Protein Blotting Equipment (Bio-Rad). Then, the membrane was washed with 1X Tris-buffer saline tween-20 (TBST; 25 mM Tris-HCl, 137 mM NaCl, 2.7 mM KCl and 0.05% tween-20) for 5 minutes and blocked with 15 ml of a blocking buffer (5% BSA in 1X TBST) on shaker at room temperature overnight. The membrane was washed 3 times in 1X TBST, and incubated with diluted Mouse Anti-His antibody IgG_2a (GE Healthcare; 1:3,000) in the 1X TSB buffer for 1 hour. The membrane was washed 3 times with 1X TBST buffer for 15 minutes, and then incubated with diluted goat anti-mouse IgG (H+L) conjugated with alkaline phosphatase (Promega, U.S.A.; 1:7,500) in the 1X TSB buffer for 1 hour. Next, the mambrane was re-washed 3 times with 1X TBST buffer for 15 minutes. To detect the immunoreactional signals, the membrane was incubated in NBT/BCIP (Roche, IN, USA) until the signal was appeared. Finally, the reaction was stop in water.

3.6.8.5 Purification of recombinant protein

Recombinant protein was purified using a His GraviTrap kit (GE Healthcare). First, a single colony of bacterial clone was cultured in 5 ml of LB medium, containing 50 µg/ml ampicillin and 50 µg/ml chloramphenical at 37°C. A 0.5% of bacterial culture was transferred to 500 ml of LB medium containing 50 µg/ml ampicillin and 50 µg/ml chloramphenical and further incubated to an OD_{600} of 0.45-

0.55. And then, the culture was induced with 1.0 mM IPTG final concentration and continually cultured for 3 hours. The cultured cells were transferred to 50 ml centrifuge tube, and the tube was centrifuged at 5,000 rpm for 15 minutes. The pellet cells were resuspended in 20 ml binding buffer containing 20 mM imidazole (20 mM sodium phosphate, 500 mM NaCl, 20 mM imidazole, pH 7.4), and sonicated until all bacterial cells were broken. After sonication, the solution was centrifuged at 3,000 rpm for 10 minutes, then the solution was transfered to the Nalgene™ Oak Ridge High-Speed centrifuge tube. The solution was centrifuged at 13,000 rpm for 30 minutes to separate the soluble and insoluble fraction. The pelllet was collected to continue process because C-type lectin protein was expressed in the inclusion body. The pellet was resuspended with 10 ml binding buffer containing 20 mM imidazole and 8 M urea and centrifuged at 8,000 rpm to discard the pellet. The solution was collected and loaded into the His GraviTrap column for 5-10 times, washed with 10 ml binding buffer containing 20 mM imidazole, followed by 5 ml binding buffer containing 40 mM imidazole and 80 mM imidazole. To collect the recombinant protein, a 8 ml elution buffer containing 500 mM imidazole was loaded into the column. Each fraction of the washing and eluting step was analyzed by SDS-PAGE and the purified proteins were stored -20 ^{o}C.

3.6.8.6 Polyclonal antibody production in rabbit

The purified *Pm*Cr protein was concentrated and loaded into 15% SDS-PAGE. The specific size of protein on gel was cut to colect the specific protein and this gel was continued to purify using Model 422 Electro-Eluter (Bio-Rad). The purified protein was sent to Faculty of Associated Medical Sciences, Changmai University to produce the polyclonal antibody in the rabit. Western blot analysis was carried out to examine specificity and sensitivity of the antibody.

3.6.9 Tissue distribution of C-type lectin protein

3.6.9.1 Sample collection

Juvenile shrimp were dissected to collect the plasma and tissue including hemocyte, hepatopancreas, midgut, hindgut, stomach, gill, and heart. All samples were stored at -20 ^{o}C until analysis. All samples excepting plasma were ground into 1X PBS and centrifuged at 14,000 rpm for 30 minutes at 4 ^{o}C. The solution was

collected and measured the concentration. All samples were anlyzed by 15% SDS-PAGE and wastern blot analysis using polygonal anti-body rabbit anti-C-type lectin.

3.6.9.2 Detection of C-type lectin protein

All samples in section 3.6.9.1 were loaded into 15% SDS-PAGE and transferred to a PVDF membrane. Western blot analysis was perform as mentioned in section 3.6.8.4, but the first antibody was changed to rabbit anti-C-type lectin (1:500) to detect the C-type lectin protein.

3.6.9.3 Polyclonal antibody purification

Because of the non-specificity of C-type lectin, polyclonal antibody was purified using protein A IgG purification kit (Thermoscientific, IL, USA) according to the manufacturer's instruction. Briefly, a 5 ml binding buffer was loaded into the column to equilibrate the column. Next, a 5 ml polyclonal antibody was flowed through the column, then the column was washed with 15 ml of binding buffer. Finally, the antibody was eluted from the column using the IgG elution buffer. The antibody was stored at -20 ^{o}C. Additionally, the specific of antibody was analyzed by wastern blot analysis.

3.6.10 Functional analysis of C-type lectin protein

3.6.10.1 Expression of recombinant protein

The expression of recombinant protein was prepared as mention in section 3.6.8.3.

3.6.10.2 Recombinant protein refolding

The recombinant protein pellet was resuspended with 30 ml lysis buffer (50 mM Tris-HCl pH 7.5, 100 mM NaCl, 5mM EDTA, 0.5% Triton-X 100) immediately adding 0.1 mM PMSF and 1mM DTT. The cell suspension was sonicated using Digital Sonifier® sonicator Model 250 until bacterial cell wall broken completely. And then, $MgSO_4$ and DNase were added at final concentration 10 mM and 0.001 mg/ml, respectively. The solution was incubated at room temperature for 20 minutes and centrifuged at 3,000 rpm for 15 minutes at 4 ^{o}C. Next, the solution was transferred into Nalgene™ Oak Ridge High-Speed centrifuge tube and centtrifuged at 13,000 rpm

for 30 minutes at 4 ºC. The supernatant was transferred to new tube and stored at -20 ºC, while the pellet was washed with 30 ml washing buffer (1 M urea, 50 mM Tris-HCl pH 7.5) and centrifuged at 3,000 rpm for 15 minutes at 4 ºC. The pellet was dissolved with refolding buffer (8 M urea, 20 mM DTT, Tris-HCl pH 7.5) and incubated at room temperature for 60 minutes. The refolding recombinant protein solution was centrifuged at 7,000 rpm for 15 minutes at 4 ºC, then transferred the solution into the new tube for dialysis process. The solution protein was measured the protein concentration and diluted to 1 mg/ml for dialysis.

3.6.10.3 Dialysis

The dialysis menbrane 6-8 kD (Spectra/Por®) was used for dialysis. The protein solution was packed into the dialysis membrane and placed into the 1,000 ml beaker containing 800 ml dialysis buffer (4 M urea, 20 mM DTT, Tris-HCl pH 7.5). The beaker was placed and stired at 4 ºC for 3 hours. After 3 hours of the first dialysis, buffer with half of the urea concentration (2 M urea) was changed and continually stired for 3 hours. New buffer with lower urea concentration was changed every 3 hours until the concentration was reduced to 0.25 M urea. Finally, the dialysis buffer without urea was replaced and stirred at 4 ºC for 3 hours. The recombinant protein was purified using a His GraviTrap kit (GE Healthcare) as described in section 3.6.8.5. Each fraction of the washing and eluting steps were analyzed by 15% SDS-PAGE and the purified proteins were stored -20 ºC.

3.6.10.4 Bacterial binding

A single colony of *M. luteus* and *S. aureus* was inoculated in tryptic soy broth, while a single colony *V. harveyi* and *V. parahaemolyticus* was inoculated in tryptic soy broth supplemented with 2% NaCl. All samples were cultured with constant agitation and optimal temperature overnight. Bacterial cells were harvested, washed 3 times with 0.85% NaCl for *M. luteus* and *S. aureus* and 2% NaCl for *V. harveyi* and *V. parahaemolyticus*. Bacterial pellet was weighed around 30-40 mg and resuspended 200 µl 0.85% or 2% NaCl. A 5 µg of C-type lectin recombinant protein and 5 mM $CaCl_2$ were added into suspended bacteria and incubated at room temperature for 1 hour. All samples were centrifuged at 3,500 rpm for 10 minutes at 4 ºC and the suppernatant (no binding) was collected. The pellet was washed 3 times with 1 ml 0.85% or 2% NaCl by

centrifugation at 3,500 rpm for 10 minutes at 4 ºC. The protein binding to bacteria was eluted with final concentration 0.8 M urea in Tris-HCl pH 7.5 and incubated for 15 minutes at room temperature. The protein solution was collected by centrifugation at 3,500 rpm for 10 minutes at 4 ºC and precipitated with 2 volume of aceton at -20 ºC for 2 hours. After incubation, the solution was centrifuged at 12,000 rpm for 30 minutes at 4 ºC, then the supernatant was discarded and the pellet was dried at room temperature. The pellet was resuspended with 4 M urea in 10 mM Tris-HCl pH 7.5. The supernatant (no binding) and protein binding to bacteria were analyzed by 15% SDS-PAGE and wastern blot analysis using C-type lectin antibody.

CHAPTER IV

RESULT

4.1 Characterization of Pathogenic and Non-pathogenic Bacteria

Four species of bacteria including *V. harveyi* 1526 [286], *V. parahaemolyticus* isolated from wounded *P. monodon*, *Vibrio* B4-24, closely related to *V. sagamiensis* based on 16S rDNA and isolated from intestines of broodstock shrimp, and *M. luteus* Ml 11 [287] were tested for their pathogenicity to shrimp. The result could be divided into 2 groups. Firstly, non-pathogenic isolates including B4-24 and *M. luteus* showed the shrimps did not die within one week. Another group is pathogenic isolates, which includes *V. harveyi* and *V. parahaemolyticus* to show the shrimps were died within three days.

4.2 Study of the Morphological Digestive Tract of Infected and Uninfected Shrimp (*P. monodon*)

4.2.1 General features of shrimp gastrointestinal tract

The GI tract of *P. monodon* consists of three main segments: a foregut, a midgut and, a hindgut. The midgut is the longest segment of the GI tract running from the posterior end of the pyloric stomach to the hindgut, and then to the anus. It is also connected to the hepatopancreas, the anterior-dorsal digestive caecum and the posterior-dorsal digestive caecum. The foregut and the hindgut originate from stomodeal and protodeal ectoderm, respectively, while the midgut is derived from endoderm. The inner surfaces throughout the foregut and hindgut are lined by cuticle (Figure 4.1A-D, K, L), but the inner surface of the midgut is not (Figure 4.1F-J).

4.2.2 Presence of a normal flora in the gastrointestinal tract of pond-cultured *P. monodon*

SEM observations (n = 4 shrimp) showed that the inner surface of the stomach is devoid of bacterial cells (Figure 4.1A-D), and that in the stomach bacterial cells were only found in association with ingested feed (Figure 4.1E). Bacterial cells

were found singly scattered on the peritrophic matrix (PM) of the midgut (Figure 4.1F-G), and large bacterial clusters were seen embedded in the PM within the posterior segment of the GI tract (Figure 4.1J). No bacteria were attached to the brush border of the midgut lumen or were seen in the ectoperitrophic space (between the PM and the midgut epithelium). A cluster of granules inside the cytoplasm of the epithelial cell were seen protruding through the microvilli into the lumen of the midgut (Figure 4.1H-I). The hindgut was observed to have a thick folded epithelium and a thin immature PM (Figure 4.1L). The posterior part of the hindgut or the rectum was also lined with cuticle with backward projecting spines (Figure 4.1K-L). A few bacterial cells were seen within the hindgut; these were principally short-rod shaped bacteria attaching to the inner surface or in small pits scattered on the inner surface of the hindgut (Figure 4.1K-L).

Of particular interest is one shrimp specimen that had patches of unique rod-shaped bacterial population firmly attached to the fibre setae (Figure 4.2A) or to the stomach lining (Figure 4.2B). The attached bacteria exhibited peritrichous pili-like structures or fimbria (Figure 4.2C), and a few fibres were seen linked to the PM (Figure 4.2D). In addition, these bacteria had the ability to degrade the PM, as evident by the presence of numerous holes in the PM and the exposure of cytoplasmic granules of the epithelial cells under the PM (Figure 4.2E). In addition to these, another group of irregular-shaped bacteria were found attached to the PM (Figure 4.2F). In the hindgut of the same shrimp, a cluster of short-rod shaped bacteria with polar flagella and irregular-shaped and non-identifiable particles were observed adhering to the wall of the hindgut (Figure 4.2G-I).

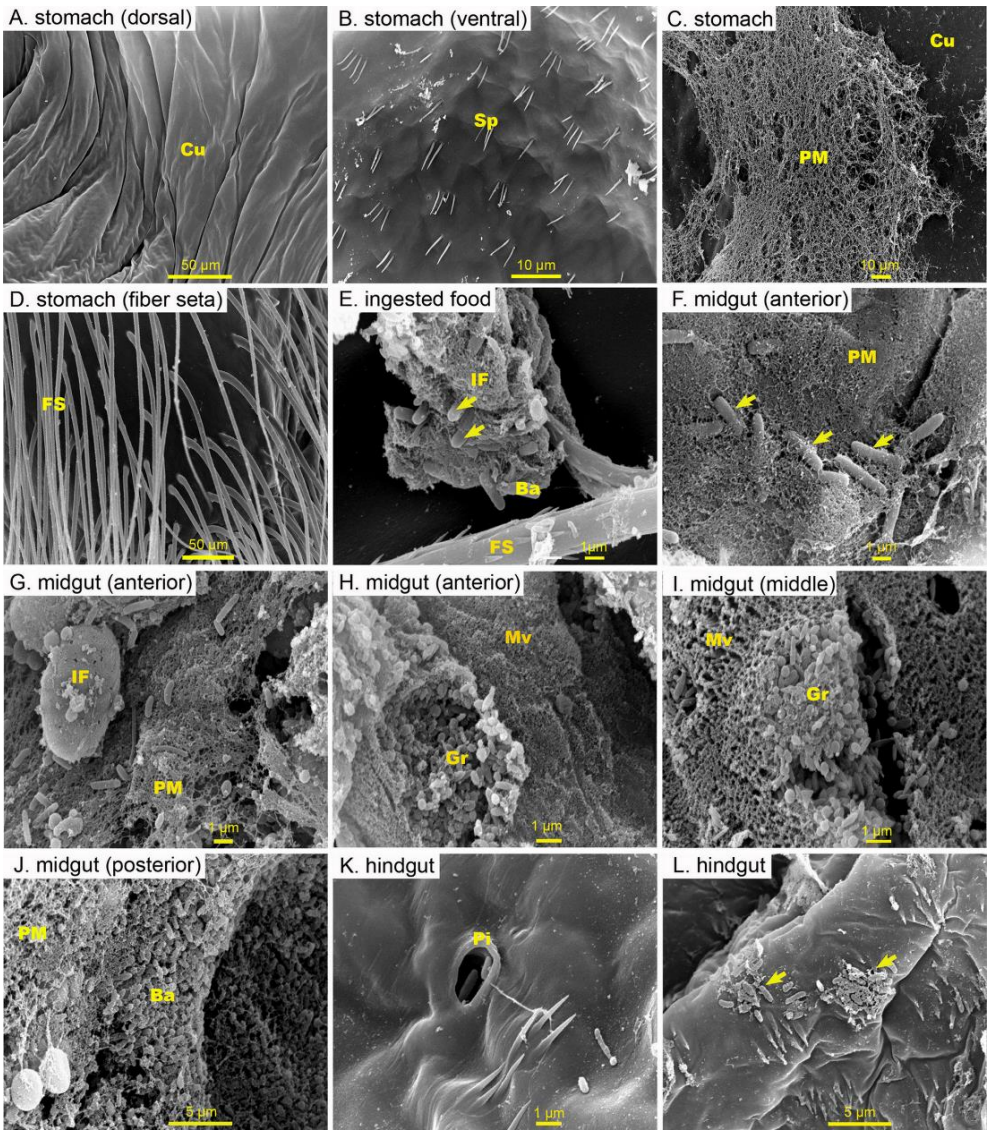

Figure 4.1 Representative scanning electron microscopy (SEM) micrographs of the inner surface of the digestive of farmed *P. monodon*. Inner surface of (A) the dorsal, (B) ventral, (C) peritrophic matrix, and (D) fiber seta of the stomach were devoid of bacteria. (E) Bacterial cells were seen in association with food inside the stomach. (F, G, H, I, J) Healthy midgut have intact microvilli, and a large number of bacteria were observed attached to the peritrophic matrix and food particle in the midgut. (F, I) Massive granules among the epithelial cells can be seen. (K, L) Only a few bacteria were seen attached to the cuticle lining of the hindgut. Abbreviation: cuticle (cu), spines (Sp), peritrophic matrix (PM), fiber seta (FS), ingested food (IF), bacteria (Ba), microvilli (Mv), granule (Gr), pit (Pi)

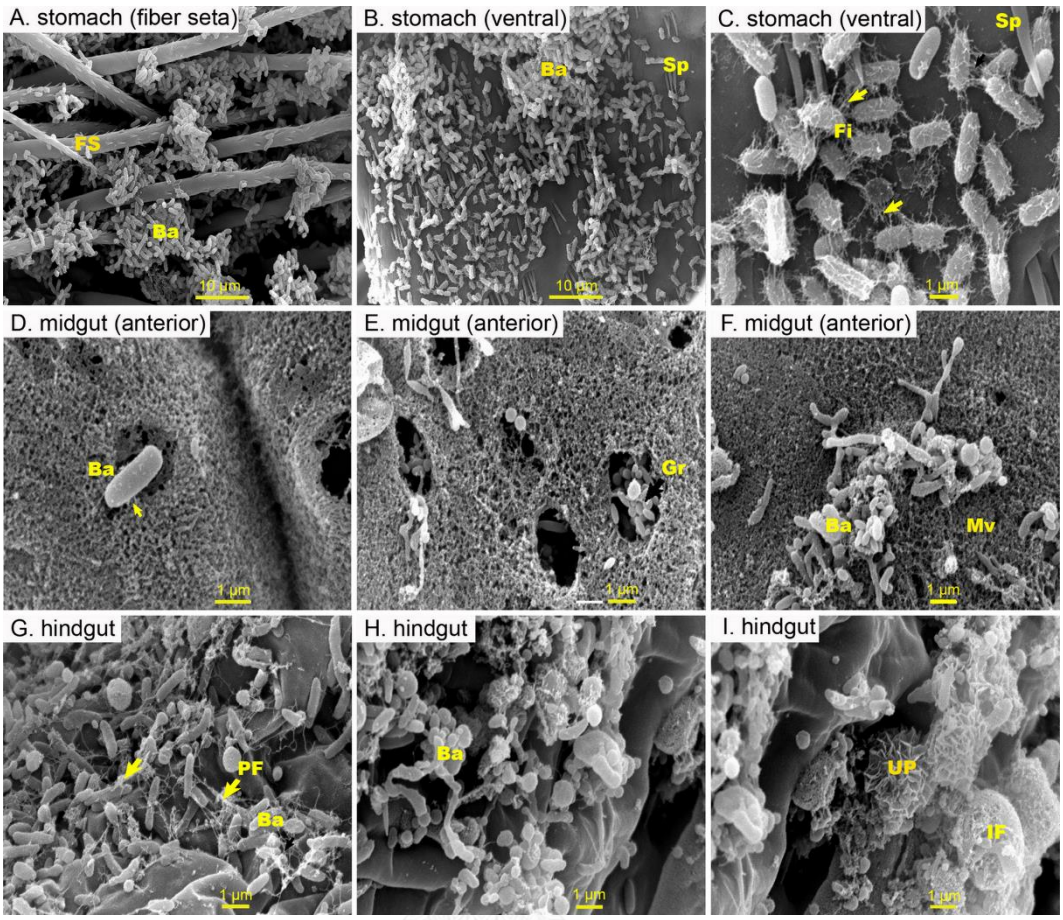

Figure 4.2 Representative SEM micrographs of the inner surface of the digestive tract of a suspected diseased *P. monodon* from a shrimp farm. A cluster of unique rod-shaped bacteria attached to (A) fibre setae or (B) to the lining of the stomach. (C) Higher magnification image of the attached bacteria in the stomach exhibiting peritrichous pili-like structures or fimbria, where (D) a few fibres linked to the peritrophic matrix (PM) can be seen (arrowhead). (E) Many holes were created in the PM and a few granules were seen inside the holes. (F) A group of irregular-shaped bacteria were found attached to the PM. (G) A cluster of short-rod shaped bacteria with polar flagella, (h) irregular-shaped, and (I) unidentified particles were seen attached to the hindgut wall. Abbreviation : fiber seta (FS), bacteria (Ba), spines (Sp), fimbria (Fi) granule (Gr), microvilli (Mv), polar flagella (PF), unknown particles (UP), ingested food (IF)

4.2.3 Colonization of pathogenic *Vibrio* and the pathological induced shrimp intestine

The progression of *Vh*- or *Vp*-induced pathological changes in the luminal surface tissues of the stomach, midgut and hindgut in infected shrimp at 1.5, 6 and 24 hours post-infection (PI) were visualized by SEM and compared. At 1.5 hours PI with *V. harveyi*, no bacteria were seen adhering to the surface of the stomach (Figure 4.3A), but numerous bacterial cells mixed with ingested food were found loosely attached to the lining of the stomach lumen (Figure 4.3B). At 6 hours PI, numerous rod-shaped bacteria of a single morphotype were found firmly attached to the stomach surface in places (Figure 4.3C) and to the upper and middle regions of the midgut (Figure 4.3D-E). The epithelial layers with colonizing bacteria exhibited signs of destruction in both the stomach and the upper midgut, whereas the areas further down the midgut to the hindgut without bacterial colonization were still intact (Figure 4.3G). Bacterial replication continued between 6 and 24 hours PI, indicating that the bacterial populations were growing *in situ*. At 24 hours PI, bacterial numbers dramatically increased within the stomach (Figure 4.3J) and persisted in the posterior part of the midgut (Figure 4.3K). Extensive, severe destruction of the epithelium in the upper midgut at 24 h PI was observed under the colonized bacterial mat as indicated by the disappearance of the epithelial layer and the exposure of the underlying basement membrane (Figure 4.3F-I). At this time point, however, most of the epithelium of the posterior midgut and hindgut remained intact (Figure 4.3H-I). The posterior part of the midgut was free of PM with some bacterial cells seen attached to the microvilli (Figure 4.3H), whilst the area between the hindgut and the midgut was covered by a very thick PM (Figure 4.3G). Scattered clusters of rod-shaped bacteria were also seen within the hindgut (Figure 4.3I), but it appears as if they were not detrimental to the host.

In shrimp fed *V. parahaemolyticus*, numerous straight-shaped bacteria (~1.8-2.2 μm in length) were seen attached to the fibre seta, to the short spines and to the inner surface of the stomach at 24 hours PI (Figure 4.4A-C). No severely damaged tissues were seen except some broken and detached spines from the stomach lining (Figure 4.4C). Attached bacteria within the stomach also produced peritrichous pili-like structures (Figure 4.4D). The posterior part of the midgut and the hindgut, however,

were extensively colonized by rod-shaped bacteria which differed morphologically from the attached bacteria within the stomach as no peritrichous pili-like fibres were observed (Figure 4.4E-F).

In the GI tract of *P. monodon* fed non-pathogenic bacteria, *i.e. M. luteus* and *Vibrio* B4-24, the bacteria were seen only on the hindgut lining (Figure 4.5D-E) and not on the stomach surface (Figure 4.5A, D) nor on the epithelium of the midgut (Figure 4.5E). In nearly all the shrimp that were examined, a high number of pits, measuring 2-5.5 µm in diameter, were found across the surface of the midgut (Figure 4.5F-G). Inside each pit, a massive number of cocci- and spindle-shaped granules, which normally reside in the cytoplasm of the epithelial cells, were observed in the anterior midgut (Figure 4.5H). Similar granules of larger size were observed further along the digestive tract in the posterior midgut (Figure 4.5I). Notably, the pit number varied among individual shrimp but was not correlated with the degree of infection. Among all examined shrimp, the hindgut bacteria were mostly varied in the number of bacteria observed, while the morphotypes were similar. Most of the hindgut tissues were intact (Figure 4.1H-I, 4.2G-L, 4.3I, 4.4F and 4.5D-E).

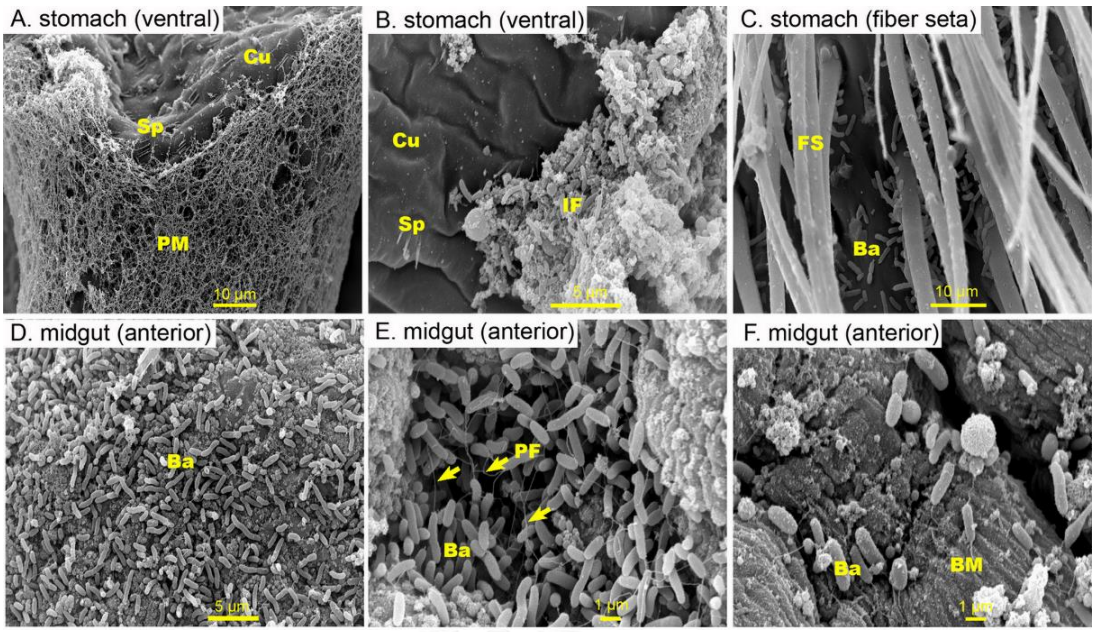

Figure 4.3 Representative SEM micrographs of the inner surface of *P. monodon* infected with *V. harveyi*. (A) At 1.5 h post-infection (PI), no bacteria adhering to the surface of the stomach linings were seen, but (B) numerous bacterial cells mixed with ingested food attaching the stomach surface were seen. (C) Numerous rod-shaped bacteria firmly attached to the stomach lining. (D) At 6 h PI, colonizing bacteria cover the epithelium of the anterior midgut. (E, yellow arrow) A higher magnification of the bacteria seen at 6 h show that they possess polar flagella that are linked with each other, and (F) heavy destruction of the epithelial layers by bacteria exposed of the basement membrane underneath.

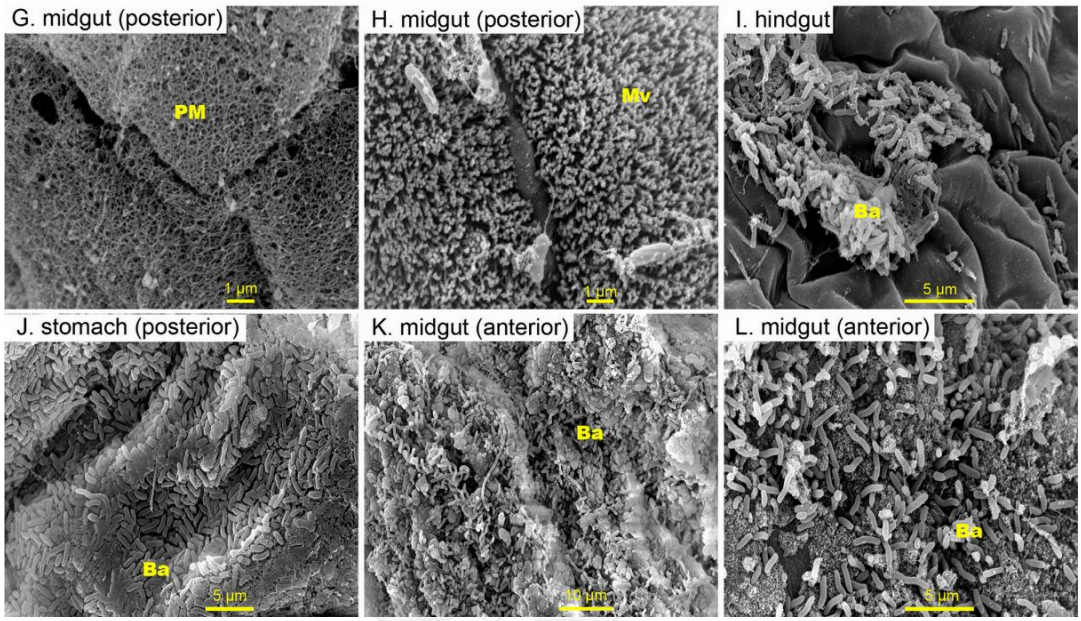

Figure 4.3 Cont. (G) The posterior portion of the midgut showing intact tissue with a thick peritrophic matrix or (H) with a few bacterial cells attached to the microvilli. (I) Scattered clusters of rod-shaped bacteria adhering to the lining of the hindgut. (J-L) At 24 h PI, the numbers of bacteria within the stomach of infected shrimp increased dramatically. Densely packed-bacteria were found covering the epithelium of the anterior midgut. Abbreviation: cuticle (Cu), spines (Sp), peritrophic matrix (PM), ingested food (IF), fiber seta (FS), polar flagella (PF), bacteria (Ba), basement membrane (BM), microvilli (Mv)

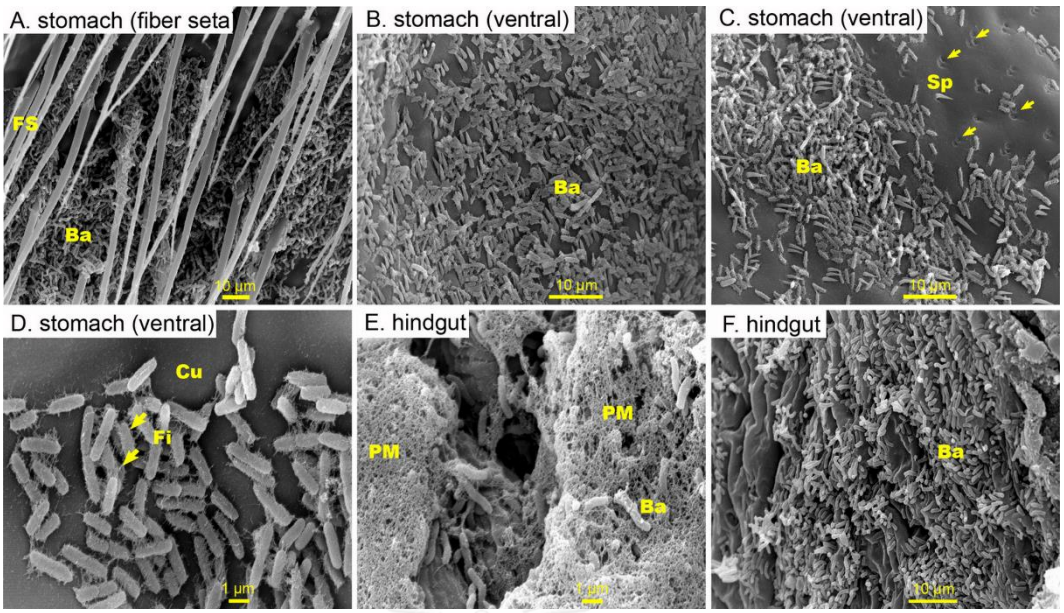

Figure 4.4 Representative SEM micrographs of the inner surface of the digestive tract of *P. monodon* infected with *V. parahaemolyticus*. (A) At 24 post-infection, numerous straight-shaped bacteria adhering to the fibre seta, to (B) short spines and (C) to the inner surface of the stomach. Some of the spines were broken and had detached from the stomach lining (arrowheads). (D-F) Attached bacteria producing peritrichous pili-like structures. Abbreviation: fiber seta (FS), spines (Sp), cuticle (Cu), fimbria (Fi), peritrophic matrix (PM)

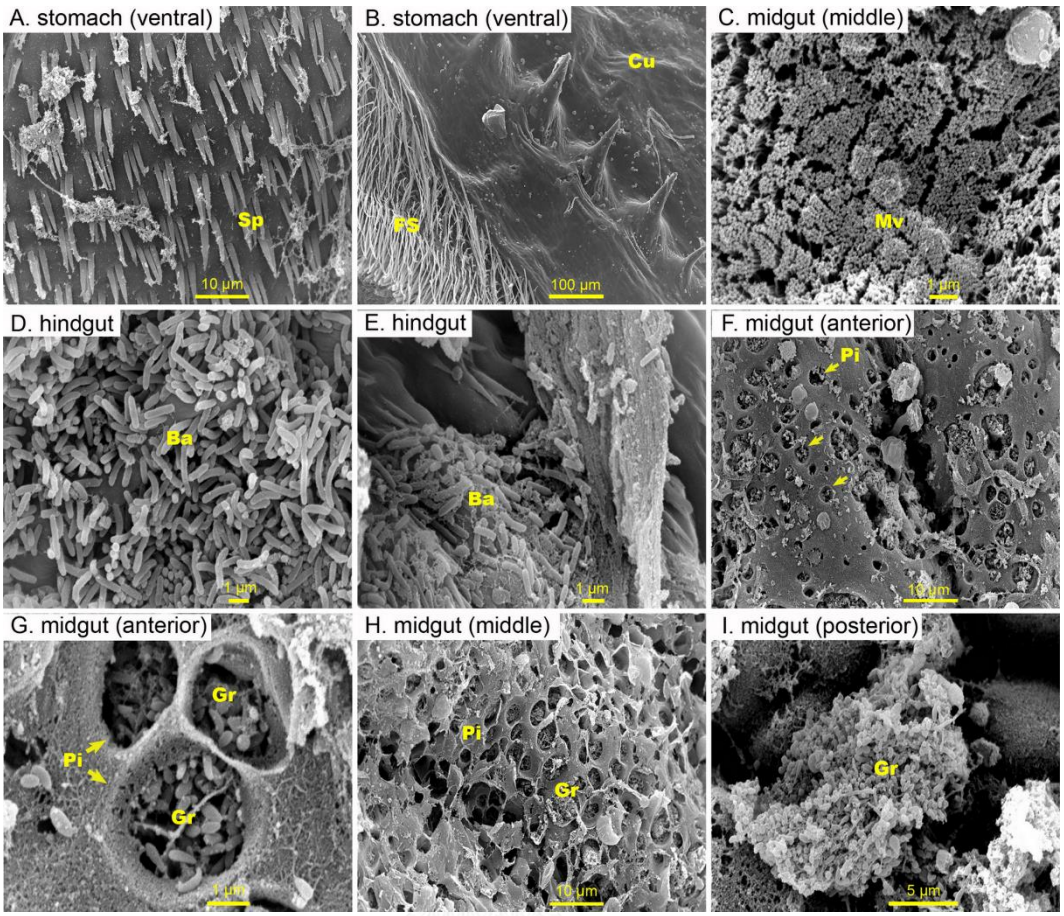

Figure 4.5 Representative SEM micrographs of the inner surface of the digestive tract from *P. monodon* receiving non-pathogenic bacteria (*M. luteus* and non-pathogenic *Vibrio* B4-24). No observed attachment of bacteria to the stomach (A - *M. luteus*, B- *Vibrio B4-24*) or to the midgut (C- *Vibrio* B4-24). The bacteria found in the hindgut were variable in number where most of the hindgut tissues were intact (D - *M. luteus*, E- *Vibrio* B4-24). A high number of pits were found across the surface of the midgut (G, H- *Vibrio* B4-24), where a large number of cocci- and spindle-shaped granules which resided in the epithelial cells were seen (I- *Vibrio* B4-24). Abbreviation: spines (Sp), fiber seta (FS), cuticle (Cu), microvilli (Mv), bacteria (Ba), pit (Pi), granule (Gr)

4.3 The Apperance of the Pathogenic Bacteria in Gastrointestinal Tract

4.3.1 Fluorescence *in situ* hybridization assay

The specificity of bacterial probe was examined. Nine bacteria (Gram positive: *Lactobacillus* sp. isolated from Betagen milk, *Streptococcus equi*, *Staphylococcus aureus* and *M. luteus*; Gram negative: *Pseudomonas aeruginosa*, *Aeromonas hydrophila*, *Escherichia coli*, *V. parahaemolyticus* and *V. harveyi*) from the collection in laboratory were cultured and investigated by FISH using UNIV1390, VIB572a, LGC354b, SP_VP1253 and SP_VH probes [289-293]. All probes except SP_VH could be hybridized to the specific bacteria (Figure 4.6A-E), while SP_VH did not hybridize to any bacteria (Figure 4.6F). The SP_VP1253 probe could be hybridized with *V. parahaemolyticus*, but the signal was too low to detect likely due to low quality of 5′ HEX fluorophore.

Universal Gram positive and *Vibrio* bacterial probes were examined the ability of probe to hybridize in paraffin-embedded tissue. The probes could hybridize with bacteria, but the signal was not clear because of high auto-fluorescence (Figure 4.7A-D).

Therefore, cryostat process was performed. This process could reduce the auto-fluorescence in Gram positive and *Vibrio* probes (Figure 4.8C-F), but not in universal bacterial probe (Figure 4.8A-B). The bacteria could not be seen in the tissue using the universal probe (Figure 4.8A-B), but the bacteria could be seen using Gram positive and *Vibrio* probes (Figure 4.8C-F). Gram positive bacteria were seen in the lumen of the intestine (Figure4.8C-D). The signal of *Vibrio* probe could be seen in the intestine tissue, but it was not clear if it is *Vibrio* bacteria or auto-fluorescence (Figure 4.8E-F). Additionally, the structure of the tissue from cryostat process was destroyed and dried during the process.

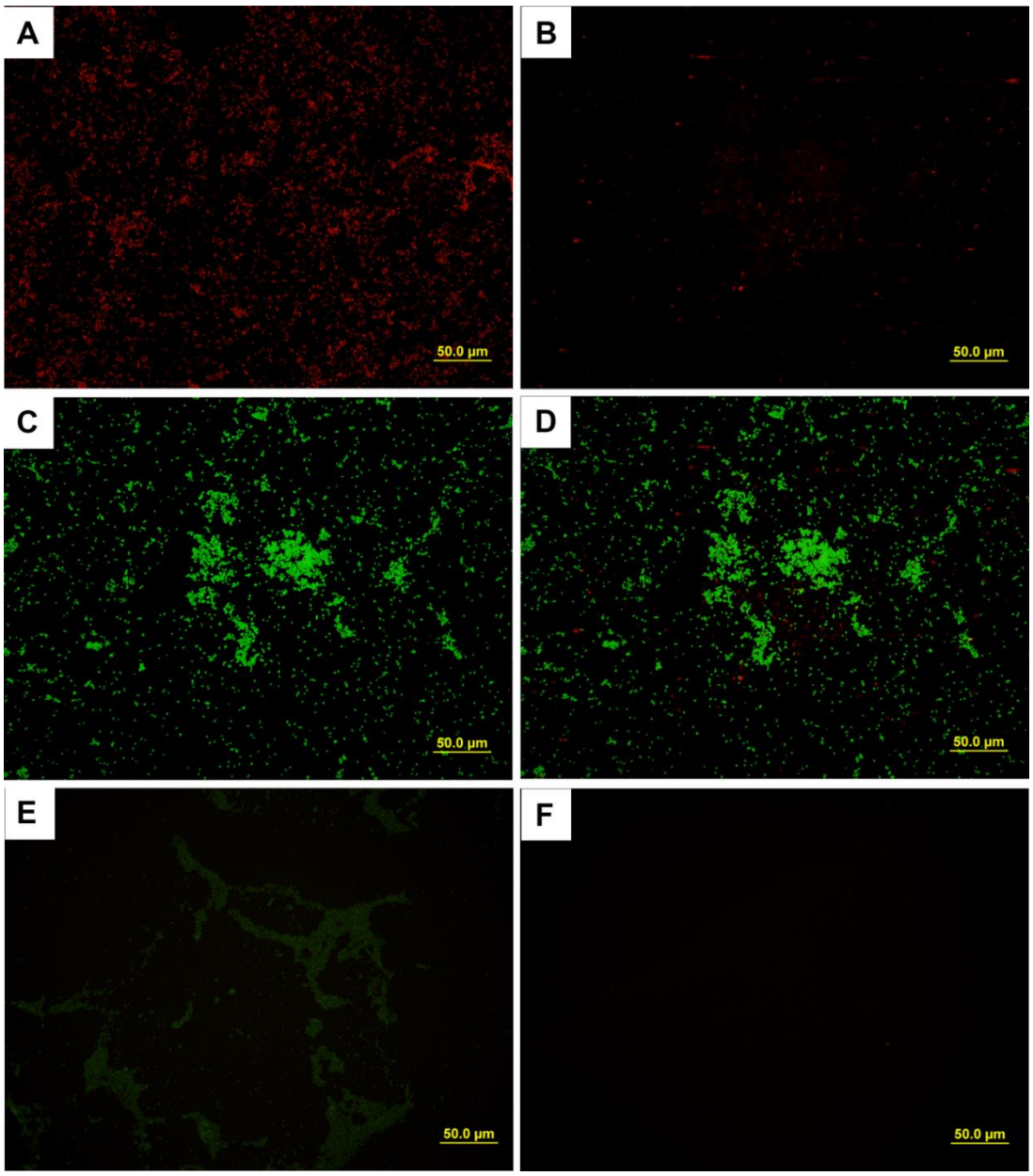

Figure 4.6 Representative fluorescent microscopy of nine bacteria using (A) UNIV1390 probe (red), (B) gram positive bacteria using LGC354b (red), (C) *Vibrio* spp. using VIB572a probe (green), (D) gram positive (red) and *Vibrio* spp. (green), (E) *V. parahaemolyticus* using SP_VP1253 probe (green) and (F) *V. harveyi* using SP_VH probe (no signal).

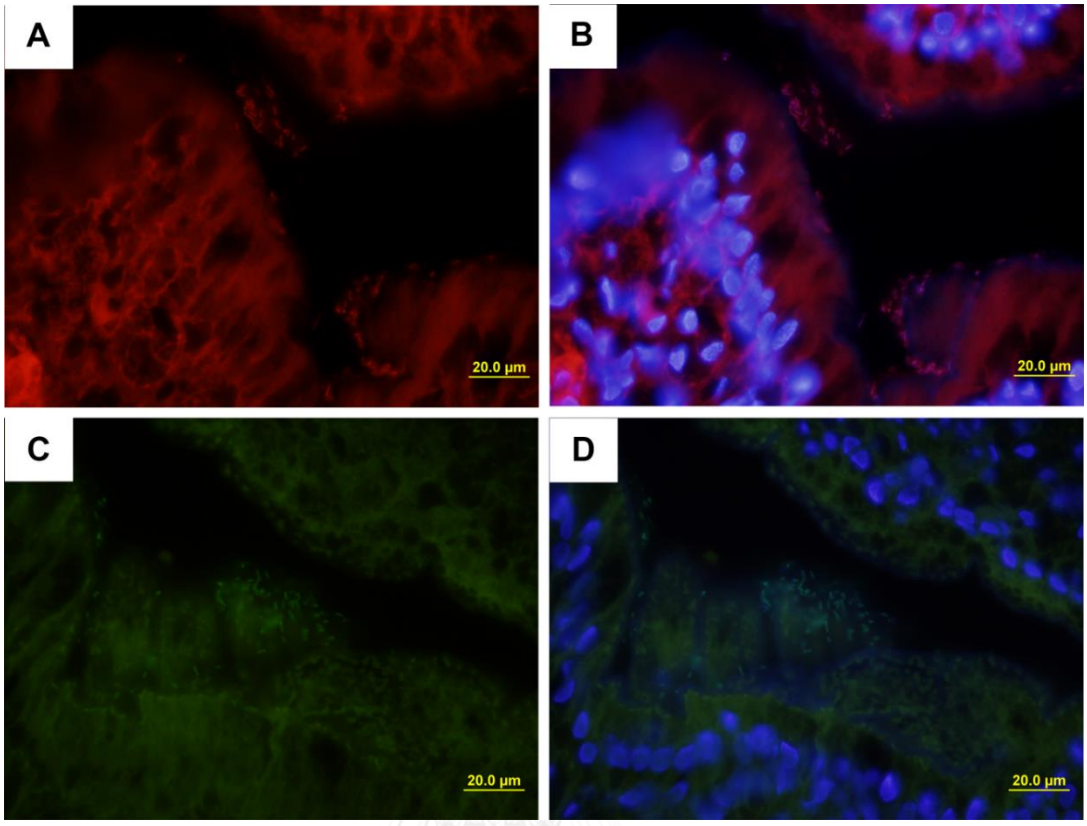

Figure 4.7 Representative the paraffin-embedded tissue hybridized with (A) gram-positive (red) and (C) *Vibrio* probes (green). (B, D) Counterstaining tissue with DAPI (blue)

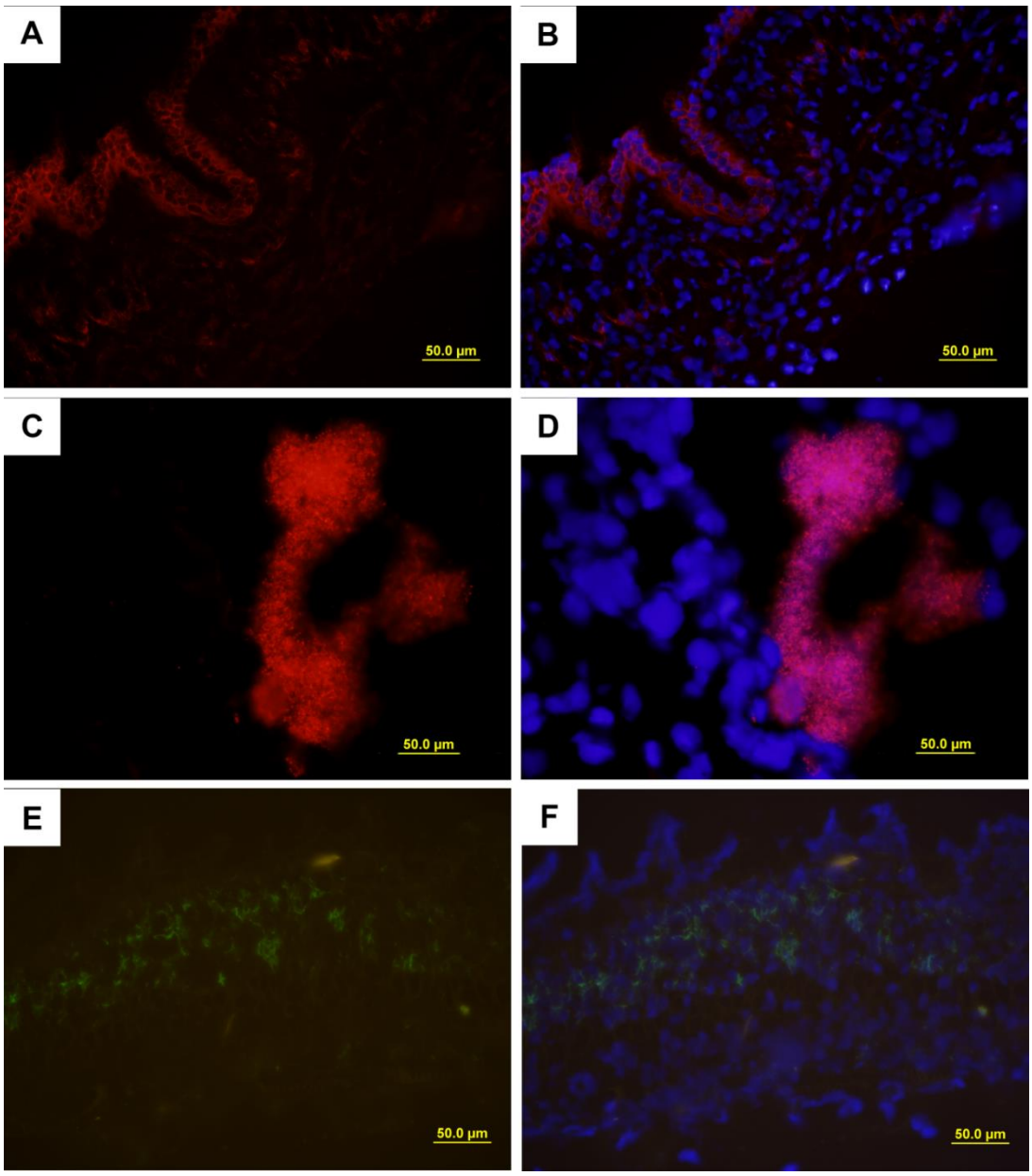

Figure 4.8 Representative the tissue from cryostat process hybridized with (A-B) universal (red), (C-D) gram positive (red) and (E-F) *Vibrio* bacterial probes (green). (B, D, F) Counterstaining tissue with DAPI (blue)

4.3.2 PCR-DGGE analysis

Although a single morphotype of proliferating bacteria was found in the shrimp fed either *V. parahaemolyticus* or *V. harveyi*, the DGGE profiles obtained from each shrimp were used to verify the bacterial community associated with each

treatment. By comparing the intestinal bacterial communities in the shrimp fed either *V. harveyi* via *Artemia*, fed an *Artemia* diet or a commercial feed diet as a control, two clusters could be seen. One discrete cluster consisted of the DGGE profile from the shrimp fed the *Artemia* diet only. The first cluster consisted of the profiles from the control and the *V. harveyi* challenged groups (2 of each). This cluster could be differentiated from the other by the presence of a strong DGGE band associated with a pure cultured *V. harveyi* isolate (Figure 4.9A).

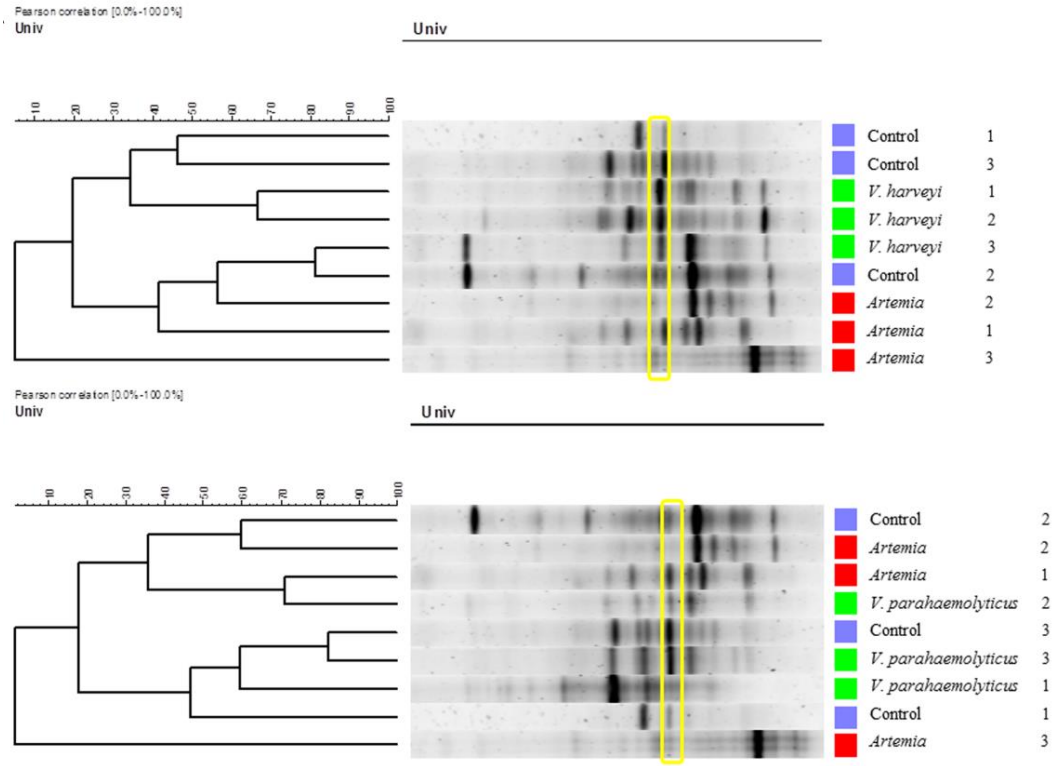

Figure 4.9 Cluster analysis of 16S rDNA PCR-DGGE profiles of individual shrimp from shrimp fed on commercial feed (blue), fed on *Artemia* (red) and fed on *V. harveyi* or *V. parahaemolyticus* containing *Artemia* (green).

4.3.3 Quantitative real-time PCR

Real-time PCR was used to confirm and quantify the presence of *V. harveyi* and *V. parahaemolyticus* specific genes (relative to 16S rRNA gene) in the stomach and the midgut at 24 hours post challenge (Figure 4.10 and 4.11). The ratio of *Vh*_gyrB to total bacteria in both stomach and midgut of the challenged shrimp (1437 x 10^{-6} and 303.5 x 10^{-6}, respectively) were significantly higher than that of the control group (P<0.05) (2.6 x 10^{-6} and 3.8 x 10^{-6}, respectively) (Figure 4.10). The ratio of *Vp*_gyrB to total bacteria in the stomach and the midgut of challenged shrimp (2.9 x 10^{-6} and 2.5 x 10^{-6}, respectively) was higher than that of the control shrimp (1.1 x 10^{-6} and 1.1 x 10^{-6}, respectively). Similarly, the ratio of *Vp*_tlh to total bacteria significantly increased in the stomach of challenged shrimp (9.6 x 10^{-6}) compared to that of the control unchallenged shrimp (P<0.05) (2.7 x 10^{-6}). The midgut of challenged shrimp also showed higher ratio of *Vp*_tlh to total bacteria (6.0 x 10^{-6}) than that of the unchallenged ones (3.7 x 10^{-6}), but the difference was not significant (Figure 4.11).

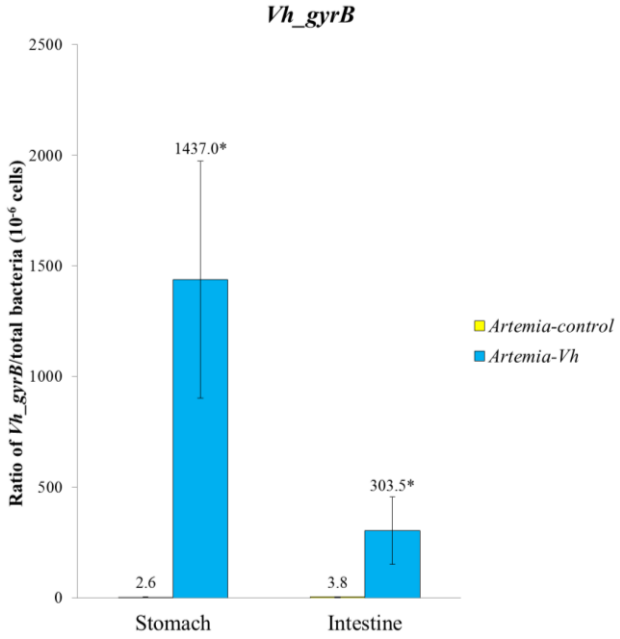

Figure 4.10 Real-time PCR presented of the ratio of the gyrB gene of *V. harveyi* and 16S rDNA bacteria in the GI tract of *P. monodon*. Error bars were expressed as ±SEM. Asterisk indicates significant differences between the control and challenged group (P<0.05).

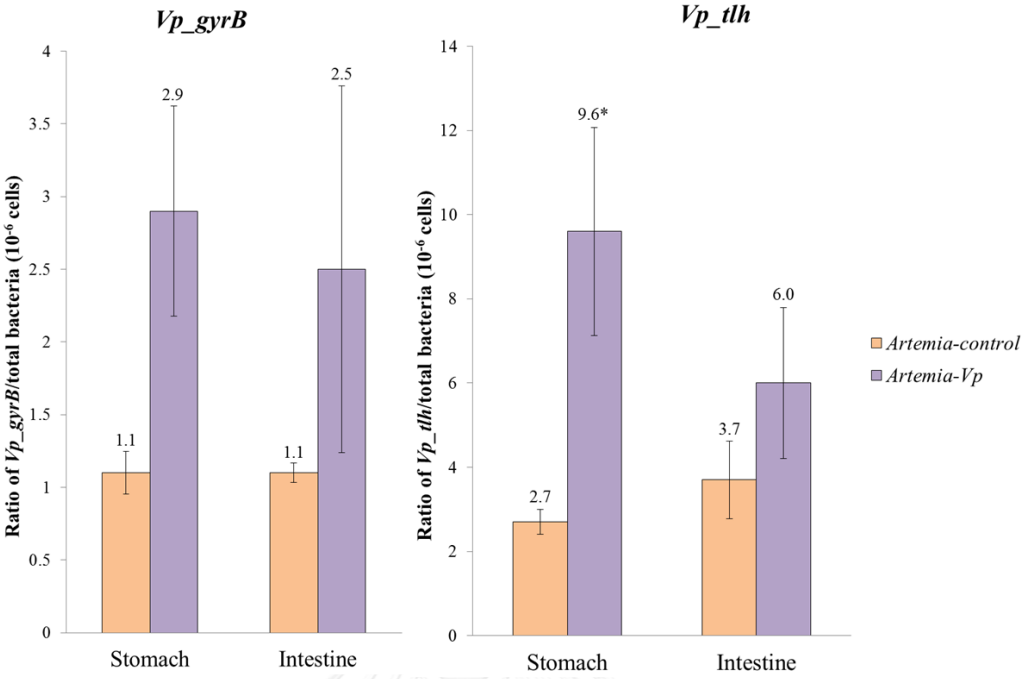

Figure 4.11 Real-time PCR presented of the ratio of the gyrB and tlh gene of *V. parahaemolyticus* and 16S rDNA bacteria in the GI tract of *P. monodon*. Error bars were expressed as ±SEM. Asterisk indicates significant differences between the control and challenged group ($P<0.05$).

4.4 Histopathology of Uninfected and Infected Shrimp by AHPNS/EMS Bacteria (*V. parahaemolyticu* 3HP)

The stomach of healthy shrimp is lined by endocuticle (Enc), exocuticle (Exc) and epicuticle (Epc) with brushes, spines, bristle and folds. The cuticle structure covers soft tissues including columnar cuticle epithelium and spongy connective tissue. The ingested food is found in the stomach lumen and the bacterial cells were not observed onto the spiny cuticle (Figure 4.12A-B). In addition, the hepatopancreas of shrimp consists of large compact ducts and blind ending tubes. Each tube contains a simple cylindrical epithelial layer surround by basal lamina and myoepithelial cells. The large vacuole and nucleus are observed in the hepatopancreas (Figure 4.12C-D).

The histopathology of infected shrimp by AHPNS/EMS bacteria was examined at 3, 6, 12 and 24 hours post infection. Two shrimp died during the experiment around 12-24 hours post infection. The degree of stomach infection was observed during an early stage at 3 hours to a later stage at 24 hours (Figure 4.13A-B, 4.14A-C, 4.15A-B and 4.16A-B). The attachment of bacteria were observed on the stomach cuticle at 3 hours (Figure 4.13-A-B) and more bacterial load were seen at 6 hours (Figure 4.14 A-C) and at 12 hours post infection (Figure 4.15A-B). Heavy stomach infection was observed at 12-24 hours post infection, and massive bacteria colonized and formed a biofilm so that they were permanently attached stomach cuticle (Figure 4.15A-B, 4.16A-B). Some stomach surface was destroyed, and the bacteria colonized the columnar cuticular epithelial layer (Figure 4.15 B, 4.16A-B). Additionally, the cuticle was lost and the columnar cuticular epithelial layer was infiltrated with large number of hemocyte cells (4.16A-B)

The initial stage of the hepatopancreas was found the hepatopancreatic tissue appeared normal at 3 hours post infection (Figure 4.13C-D). The hepatopancreatic tubular epithelial cells were sloughed into the hepatopancreatic lumens, and the hemocytes were infiltrated in the intertubular space between the hepatopancreatic tubes (Figure 4.14D-F and Figure 4.15C-D). In the terminal stage, massive lesions were observed and numerous bacteria colonized the hepatopancreatic lumens. Hemocytes formed capsules around the bacterial infected tissue (Figure 14.6C-D).

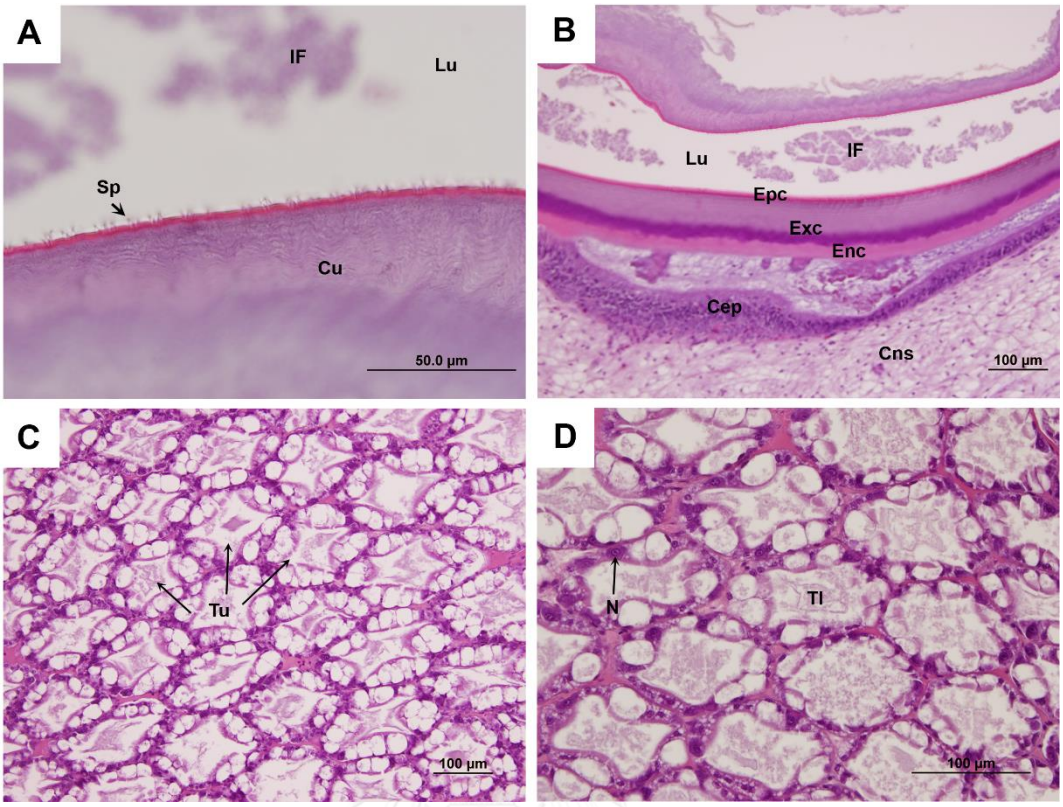

Figure 4.12 Representative light micrograph of the normal histology of stomach (A-B) and hepatopancreas (C-D) of control shrimp (*Artemia*-fed) at 24 hours post infection. Stained with H&E. Abbreviation: ingested food (IF), lumen (Lu), spine (Sp), cuticle (cu), epicuticle (Epc), exocuticle (Exc), endocuticle (Enc), columnar cuticular epithelium (Cep), spongy connective tissue (Cns), hepatopancreas tubules (Tu), tubule lumen (Tl), and nucleus (N)

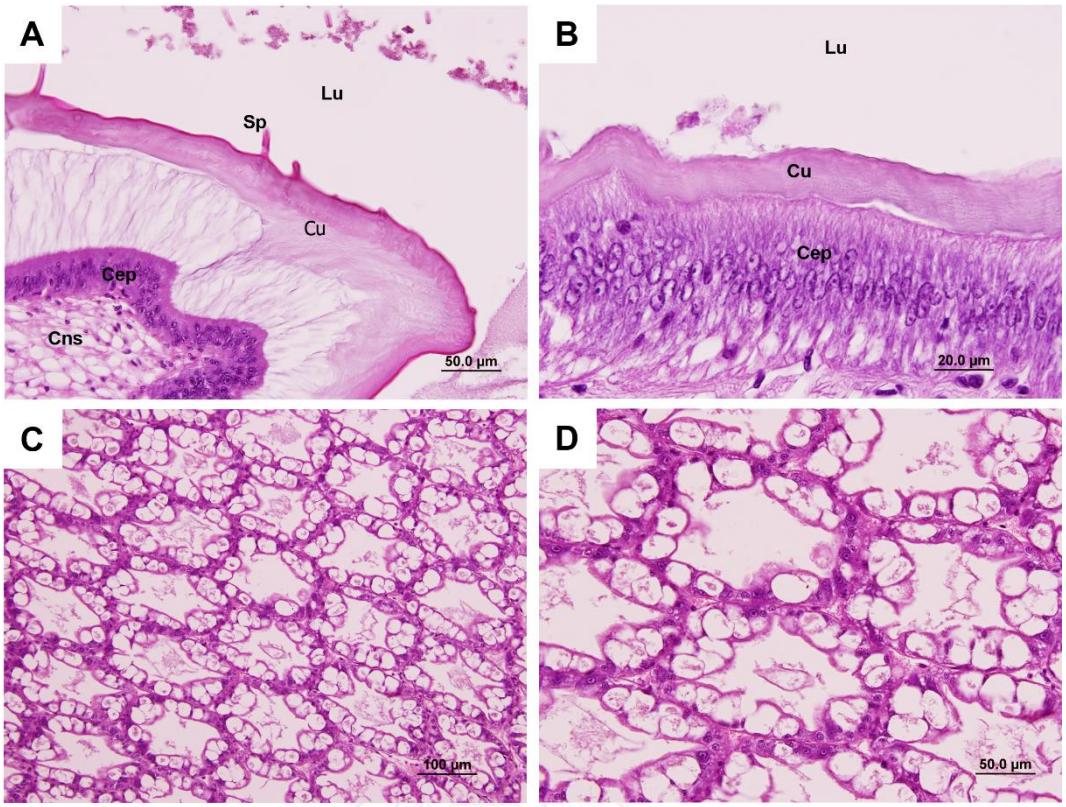

Figure 4.13 Representative light micrograph of the histopathology of stomach (A-B) and hepatopancreas (C-D) of shrimp fed *Artemia-Vp*$_{3HP}$ at 3 hours post infection. Stained with H&E. Abbreviation: lumen (Lu), spine (Sp), cuticle (Cu), columnar cuticular epithelium (Cep) and spongy connective tissue (Cns)

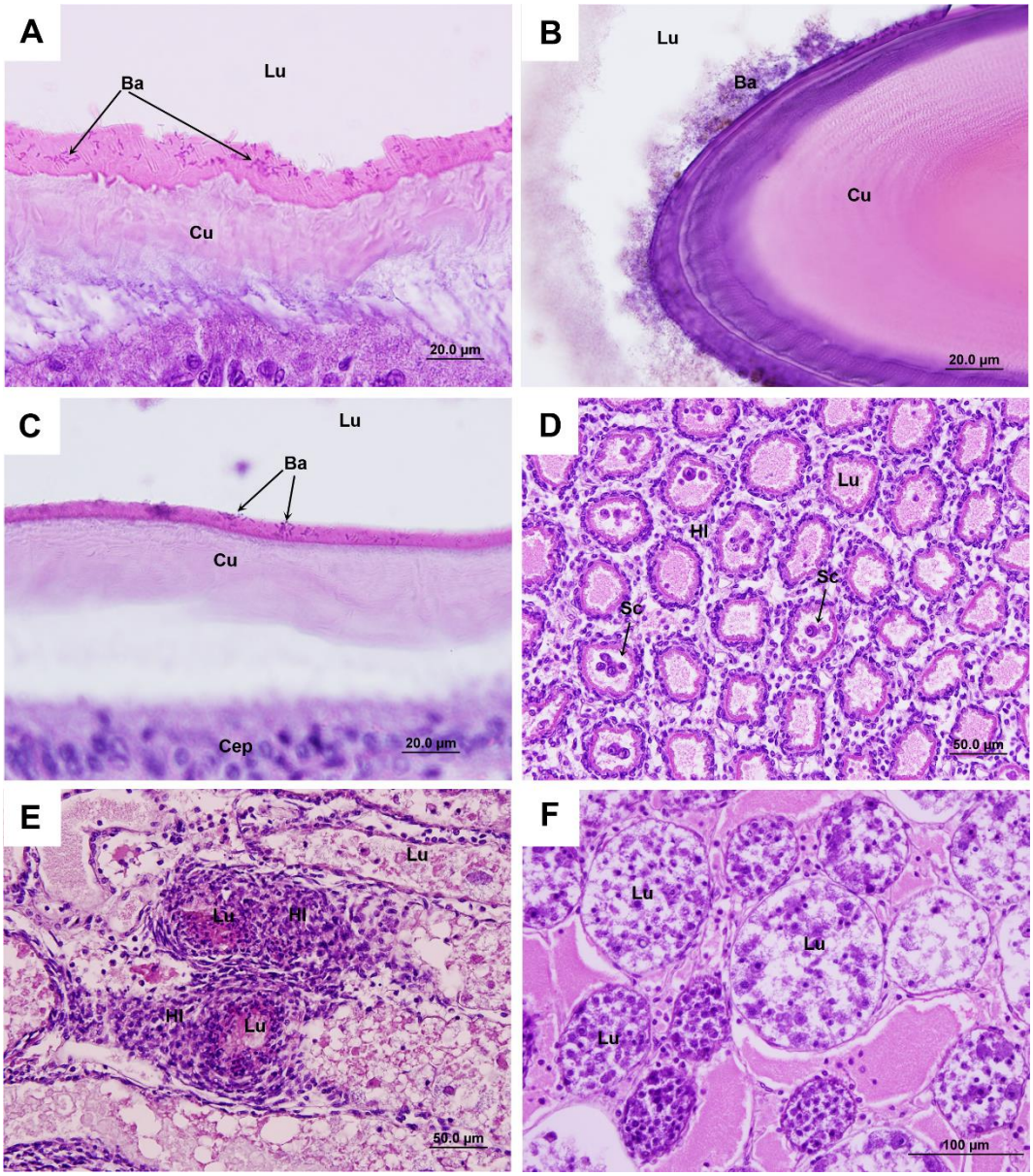

Figure 4.14 Representative light micrograph of the histopathology of stomach (A-C) and hepatopancreas (D-F) of shrimp fed *Artemia*-Vp_{3HP} at 6 hours post infection. The stomach cuticle were covered with bacteria (A-C), hemocyte infiltrated in the intertubular space between hepatopancreas tubes and sloughing of hepatopancreas tubular epithelial cells. Stained with H&E. Abbreviation: lumen (Lu), bacteria (Ba), cuticle (Cu), hemocyte infiltration (HI), columnar cuticular epithelium (Cep) and sloughing of hepatopancreas tubular epithelial cells (Sc)

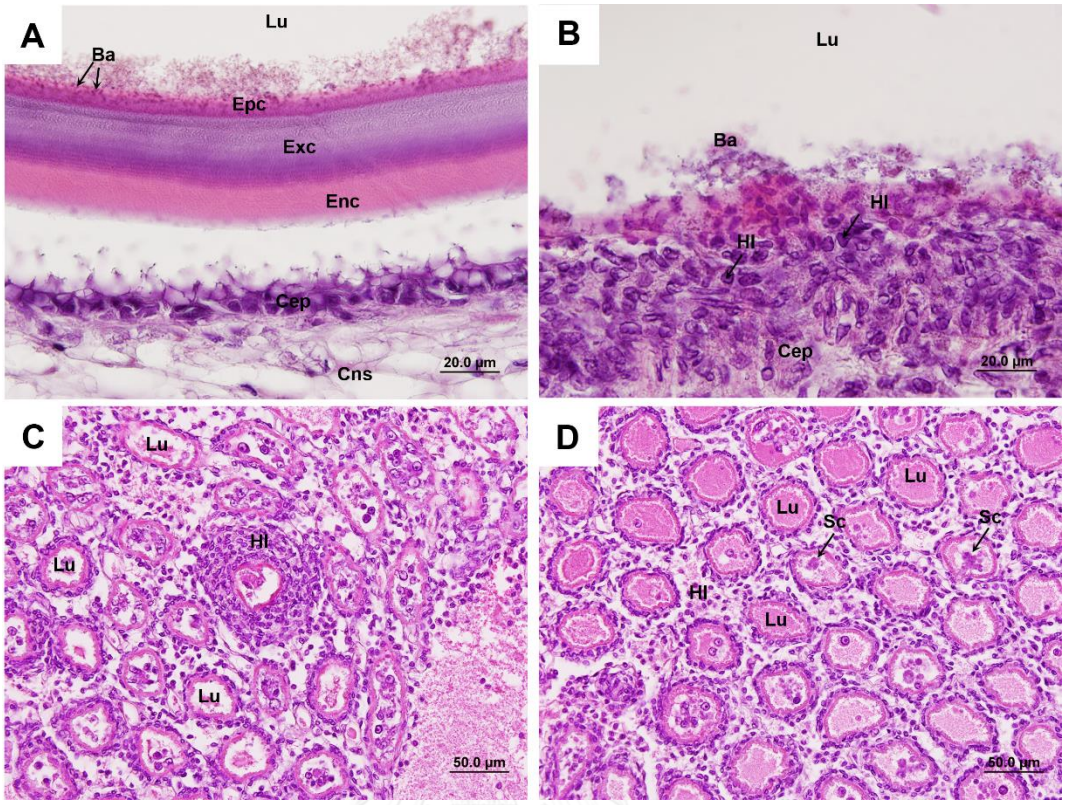

Figure 4.15 Representative light micrograph of the histopathology of stomach (A-B) and hepatopancreas (C-D) of shrimp fed *Artemia*-Vp_{3HP} at 12 hours post infection. The stomach cuticle were covered with bacteria and the epithelial membrane was separated from basal cells (A) and the bacteria destroyed the cuticle to invade the basal cells of stomach (B), hemocyte infiltrated in the intertubular space between hepatopancreas tubes and sloughing of hepatopancreas tubular epithelial cells (C-D). Stained with H&E. Abbreviation: lumen (Lu), bacteria (Ba), epicuticle (Epc), exocuticle (Exc), endocuticle (Enc), columnar cuticular epithelium (Cep), spongy connective tissue (Cns), hemocyte infiltration (HI) and sloughing of hepatopancreas tubular epithelial cells (Sc)

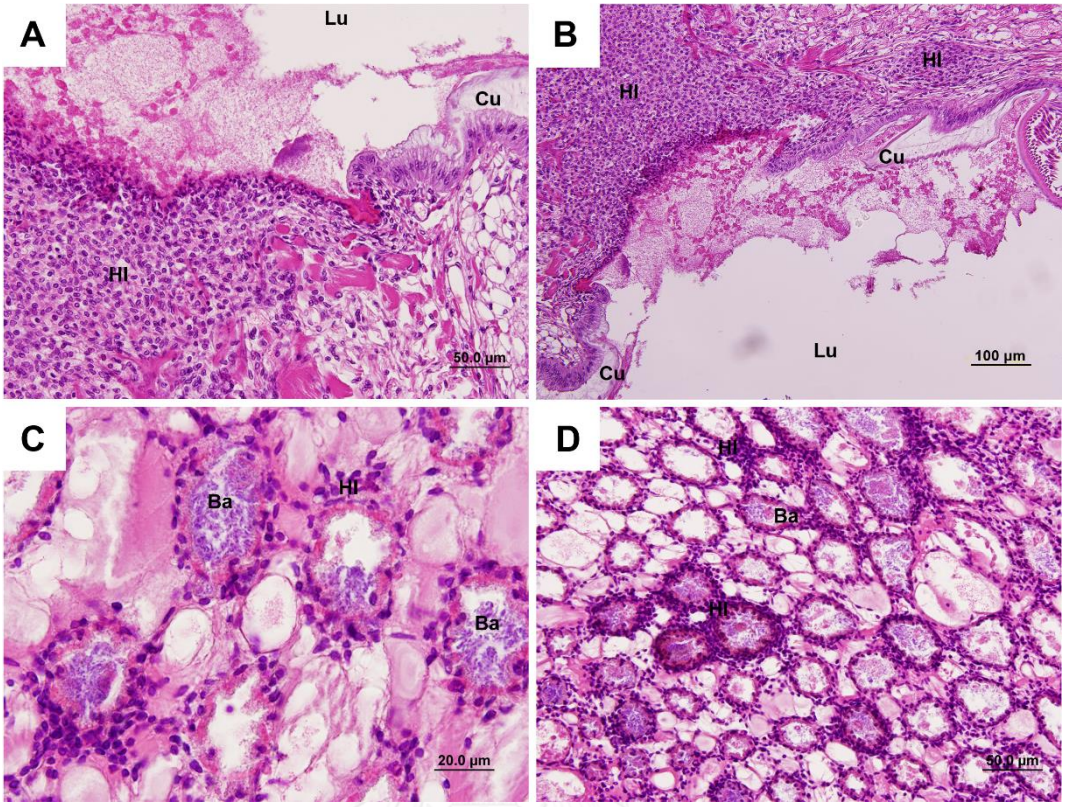

Figure 4.16 Representative light micrograph of the histopathology of stomach (A-B) and hepatopancreas (C-D) of shrimp fed *Artemia*-Vp_{3HP} at 24 hours post-infection. The massive infection in stomach resulted in that the cuticle was destroyed and hemocytes infiltrated into columnar cuticular epithelium (A-B), sloughing of hepatopancreas tubular epithelial cells are present in the hepatopancreas lumen and bacteria colonized to the hepatopancreas lumen. Stained with H&E. Abbreviation: lumen (Lu), cuticle (Cu), hemocyte infiltration (HI) and bacteria (Ba)

4.5 Identification of Differential Gene Expression Profiles in Stomach of Uninfected and Infected Shrimp (*P. monodon*) by AHPNS/EMS Bacteria

4.5.1 Suppressive subtractive hybridization (SSH) stomach cDNA libraries

A total of 306 clones of the forward SSH library was analyzed by manual NCBI blastX search, and the low- quality sequences were discarded from analysis. A total of 301 of clean sequence was classified into 127 clones of known transcripts (*E*-value $<10^{-3}$), 14 clones of hypothetical protein, 7 clones of unknown genes, and 153 clones of low or no homology (E-value $>10^{-3}$) identifying as novel genes (Table 4.1).

All sequences were assembled with CAP3 software [308]. There were 26 contigs from 213 clones and 93 singletons. All known transcripts are shown in Table 4.2.

Table 4.1 The percentage and number of clones found in the forward SSH stomach cDNA library of *P. monodon*

Transcripts	**Number**		
	%	**Contigs**	**Clones**
Known transcripts	41.50	12 (106 clones)	21
Hypothetical protein	4.58	2 (8 clones)	6
Novel genes	50.00	12 (99 clones)	54
Unknown genes (predicted protein)	2.29	-	7
Low-quality sequences	1.63	-	5
Total	**100**	**26 (213 clones)**	**93**

The relationship between the number of sequenced clones and the number of newly identified unique sequences showed that the discovery of new transcripts after 306 recombinant clones still did not reach a plateau of saturation. The discovery rate after 306 clones was at 30.21% (Figure 4.17). Therefore, new transcripts could be continually identified by further sequencing or by other technics. Highly discovered sequences revealed that the established library was highly diverse and more transcripts of genes responded to the *V. parahaemolyticus* 3HP infection.

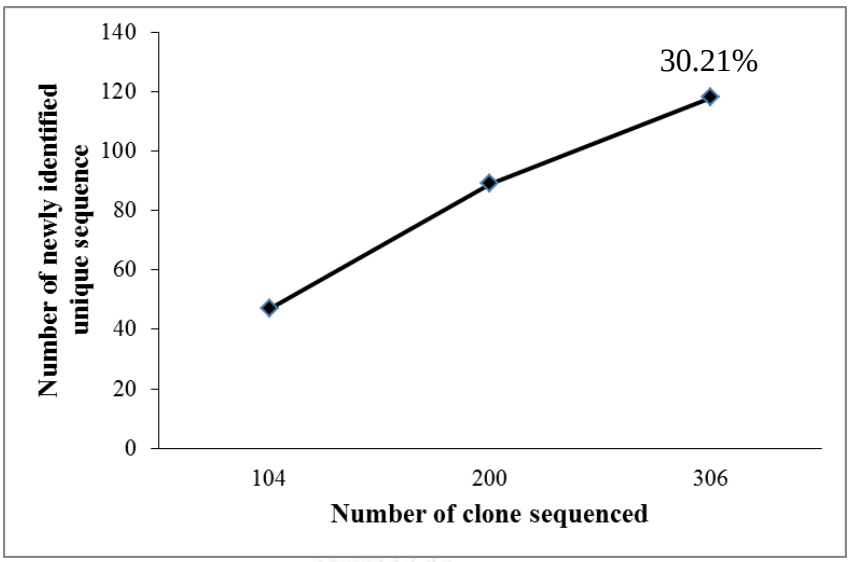

Figure 4.17 The relative number of clones sequenced and newly identified unique sequences from the forward SSH stomach cDNA library of *P. monodon*

All contigs and singletons of the forward SSH library were analyzed in accordance with Gene Ontology by Blast2GO program to define gene function. Blast2GO annotated the sequence according to three terms of gene ontology: biological process, cellular component, and molecular function.

Biological processes at level 2 were divided into 13 terms including cellular process (18%), single-organism process (16%), metabolic process (16%), biological regulation (9%), localization (9%), multicellular organismal process (7%), response to stimulus (7%), developmental process (7%), cellular component organization or biogenesis (4%), signaling (3%), immune system process (2%), growth (1%), and multi-organism process (1%) (Figure 4.18A).

Cellular components at level 2 were divided into 7 terms including cell (36%), organelle (26%), macromolecular complex (17%), membrane (12%), extracellular region (5%), membrane-enclosed lumen (2%), and cellular junction (2%) (Figure 4.18B).

Molecular functions at level 2 were divided into 5 terms including catalytic activity (36%), binding (31%), structural molecule activity (24%), transporter activity (7%) and receptor activity (2%) (Figure 4.18C).

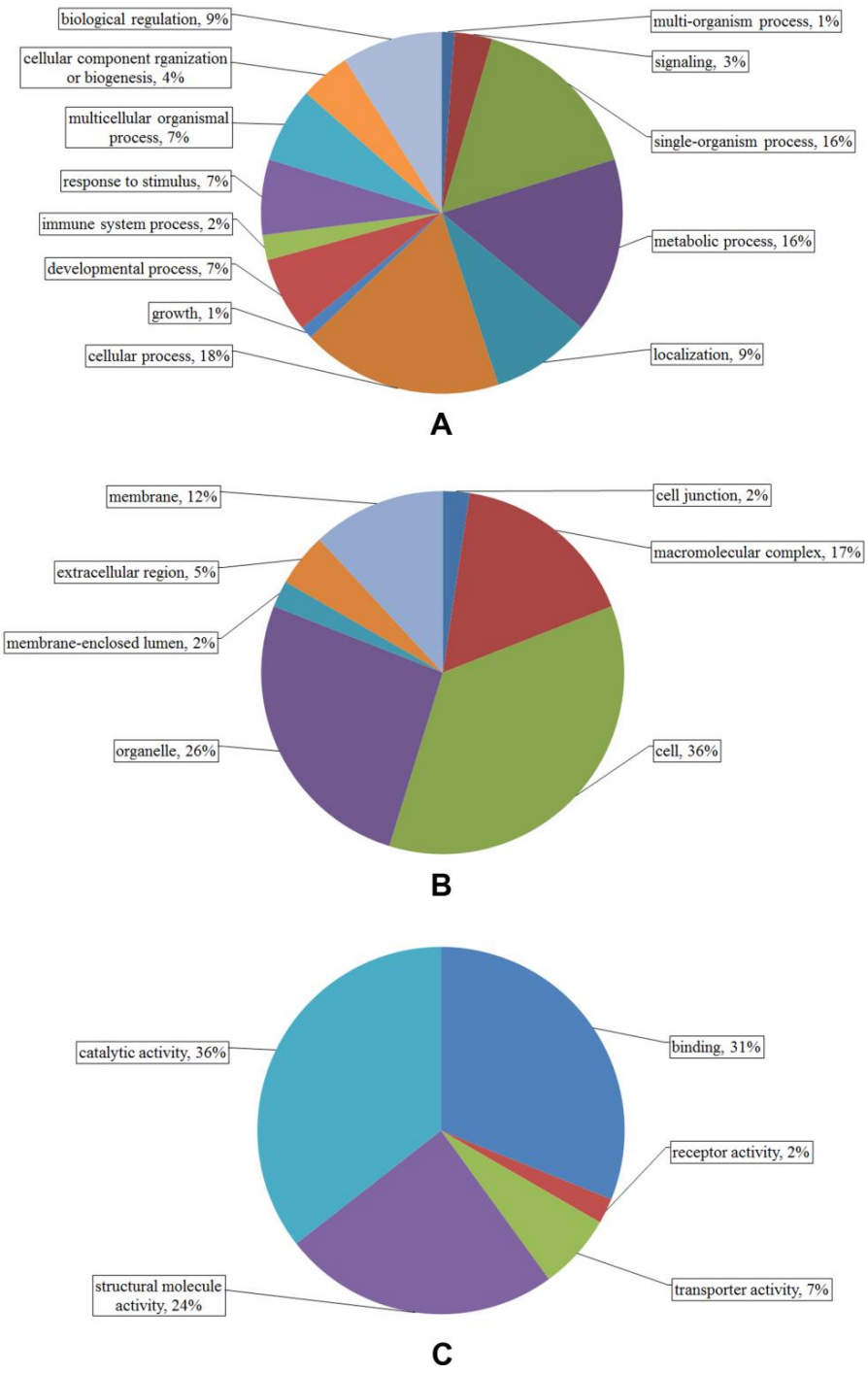

Figure 4.18 The percentage of three terms of gene ontology at level 2 in forward SSH stomach cDNA library. A-C are biological process, cellular component, and molecular function. A total 306 sequences were cut off at E-value $<10^3$ by blastX and sequences without annotation and InterPro are not included in this analysis.

Table 4.2 Identification of genes from forward SSH stomach cDNA library of *P. monodon* during EMS/AHPND pathogen infection.

Accession number	Length (bp)	Gene homology	Species homology	E-value	Similarity (%)	Function
EF213113	328	Cathepsin B	*Penaeus monodon*	4.00E-38	100	Regulation of catalytic activity
	321	Allergen Pen m 2	*Fenneropenaeus chinensis*	1.00E-19	100	Kinase activity
	624	Spz1	*Litopenaeus vannamei*	4.00E-112	99	NF-κB pathway
	382	Mitochondrial cytochrome c oxidase subunit VIb	*Litopenaeus vannamei*	3.00E-30	98	Cytochrome-c oxidase activity
	193	Ribosomal protein S9	*Procambarus clarkii*	7.00E-33	97	Translation
	939	Putative myosin regulatory light chain 2 smooth muscle	*Scylla paramamosain*	3.00E-08	97	Calcium ion binding
	394	Beta actin	*Scylla serrata*	1.00E-86	96	ATP binding
	177	Paxillin, putative	*Pediculus humanus corporis*	5.00E-30	84	Zinc ion binding
	1106	Spectrin beta chain	*Zootermopsis nevadensis*	9.00E-117	83	Phospholipid binding
	657	Glutamyl-prolyl-tRNA synthetase	*Oryzias latipes*	3.00E-80	81	Prolyl-tRNA aminoacylation
	260	DD5	*Marsupenaeus japonicus*	5.00E-13	79	Structural constituent of cuticle
	551	Kinesin-like protein unc-104	*Harpegnathos saltator*	6.00E-68	78	Microtubule-based movement
	415	DD9B	*Marsupenaeus japonicus*	2.00E-43	78	Structural constituent of cuticle
	340	Cuticle protein AMP1B	*Homarus americanus*	5.00E-29	75	Structural constituent of cuticle
	722	Cytoplasmic dynein 1 light intermediate chain 2	*Zootermopsis nevadensis*	2.00E-120	74	Microtubule motor activity
	426	Pacifastin heavy chain precursor	*Pacifastacus leniusculus*	2.00E-63	73	Iron ion transport
	323	Cuticle protein AMP1A	*Homarus americanus*	2.00E-26	73	Structural constituent of cuticle
	499	Pacifastin heavy chain	*Macrobrachium rosenbergii*	2.00E-44	70	Iron ion transport
	207	Calcified cuticle protein CP14.1	*Callinectes sapidus*	2.00E-13	70	Structural constituent of cuticle
	578	DD9A	*Marsupenaeus japonicus*	2.00E-44	67	Structural constituent of cuticle
	537	Ig-like and fibronectin type-III domain-containing protein C25G4.10	*Zootermopsis nevadensis*	1.00E-67	66	Cytokines and cytokine regulation

Table 4.2 Cont.

Accession number	Length (bp)	Gene homology	Species homology	E-value	Similarity (%)	Function
	435	BCS-1	*Amphibalanus amphitrite*	6.00E-15	62	Structural constituent of cuticle
	834	Clottable protein	*Marsupenaeus japonicus*	2.00E-100	59	Lipid transporter activity
	558	Chitin binding peritrophin-A domain-containing protein	*Artemia franciscana*	7.00E-10	59	Chitin metabolic process
	644	Salivary alkaline phosphatase	*Daphnia pulex*	2.00E-52	56	Alkaline phosphatase activity
	305	Cuticle protein 19.8	*Lepeophtheirus salmonis*	7.00E-19	56	Structural constituent of cuticle
	997	Paramyosin, long form	*Harpegnathos saltator*	1.00E-71	55	Motor activity
	210	Cuticular protein RR-2 family member 23 precursor	*Nasonia vitripennis*	5.00E-16	54	Structural constituent of cuticle
	541	C-type lectin	*Marsupenaeus japonicus*	3.00E-32	53	Carbohydrate binding
	1610	Pacifastin heavy chain	*Macrobrachium rosenbergii*	4.00E-98	50	Iron ion transport
	1156	Cuticle protein AM1159	*Cancer pagurus*	2.00E-11	50	Structural constituent of cuticle
	205	Histone H1	*Xenoturbella bocki*	8.00E-10	43	Nucleosome assembly
	250	Cuticle protein 16.8, partial	*Stegodyphus mimosarum*	4.00E-05	37	Structural constituent of cuticle

A total of 306 clones of the reverse SSH library was analyzed by manual NCBI blastX search and the low- quality sequences were discarded from analysis. A total of 297 clean sequences was identified into 135 clones of known transcripts (*E*-value $<10^{-3}$), 56 clones of hypothetical protein, 26 clones of unknown genes, and 80 clones of low or no homology (*E*-value $>10^{-3}$) identifying novel genes (Table 4.3). All sequences were assembled with CAP3 software. There were 41 contigs from 238 clones and 62 singletons. All known transcripts are shown in Table 4.4.

Table 4. 3 The percentage and number of clones found in the reverse SSH stomach cDNA library of *P. monodon*

Transcripts	**Number**		
	%	**Contigs**	**Clones**
Known transcripts	44.12	13 (112 clones)	23
Hypothetical protein	18.30	8 (53 clones)	3
Novel genes	26.15	16 (54clones)	26
Unknown genes (predicted protein)	8.49	4 (20 clones)	6
Low-quality sequences	2.94	-	9
Total		**41 (239 clones)**	**67**

The relationship between the number of sequenced clones and the number of newly identified unique sequence indicated that the discovery of new transcripts after 306 recombinant clones still did not reach of saturation. The discovery rate was at 16.98% (Figure 4.19). Therefore, the new transcripts could be identified by further sequencing or by other technics. The highly discovered sequences revealed that the established library is highly diverse and more transcripts of genes respond to *V. parahaemolyticus* 3HP infection.

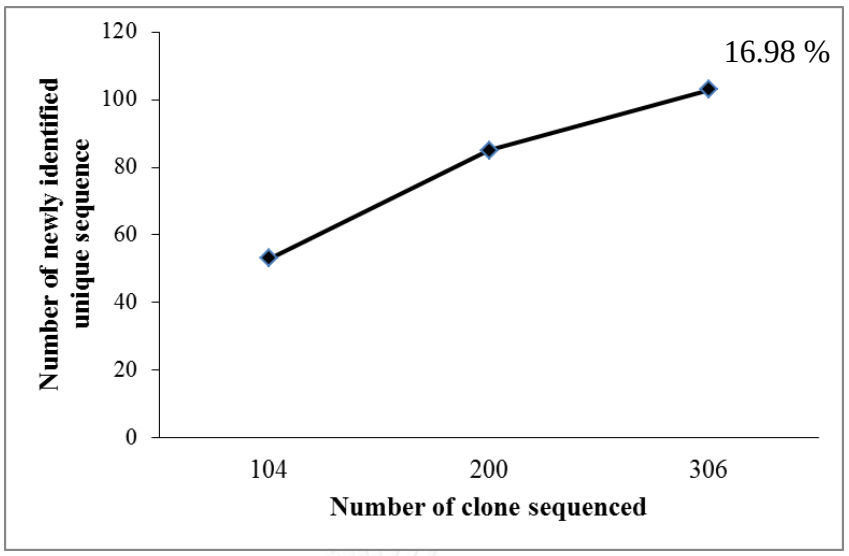

Figure 4.19 The relative number of clones sequenced and newly identified unique sequence from the reverse SSH stomach cDNA library of *P. monodon*

All contigs and singletons of the reverse SSH library were analyzed in accordance with Gene Ontology by Blast2GO program to define gene function.

Biological processes at level 2 were divided into 16 terms including metabolic process (29%), cellular process (18%), single-organism process (13%), biological adhesion (7%), biological regulation (6%), localization (5%), response to stimulus (5%), multicellular organismal process (3%), developmental process (3%), signaling (3%), cellular component organization or biogenesis (2%), locomotion (2%), immune system process (2%), multi-organism process (2%), reproduction (1%), and growth (1%) (Figure 4.20A).

Cellular components at level 2 were divided into 6 terms including extracellular region (33%), cell (24%), organelle (18%), macromolecular complex (11%), membrane (9%), and membrane-enclosed lumen (5%) (Figure 4.20B).

Molecular functions at level 2 were divided into 5 terms including binding (57%), catalytic activity (33%), structural molecule activity (24%), antioxidant activity (4%), and transporter activity (2%) (Figure 4.20C).

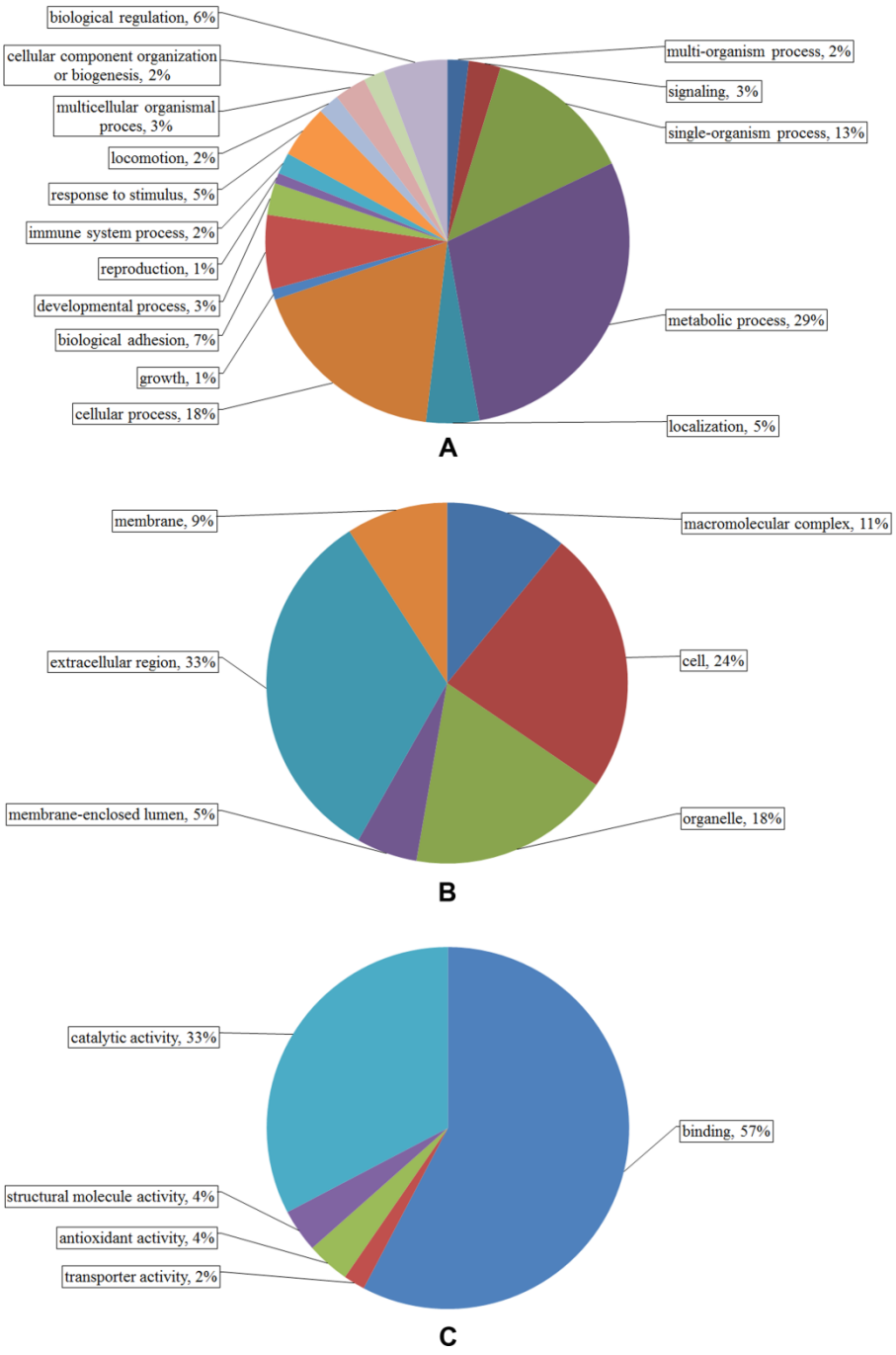

Figure 4.20 The percentage of three terms of gene ontology at level 2 in reverse SSH stomach cDNA library. A-C are biological process, cellular component, and molecular function. A total 306 sequences were cut off at E-value $<10^{3}$ by blastX and sequences without annotation and InterPro are not included in this analysis.

Table 4.4 Identification of genes from reverse SSH stomach cDNA library of *P. monodon* during EMS/AHPND pathogen infection.

Accession number	Length	Gene homology	Species homology	E-value	Similarity (%)	Function
	361	Activated protein kinase C receptor	*Litopenaeus vannamei*	1.00E-79	100	Kinase activity
	419	Ubiquitin-conjugating enzyme H5b	*Litopenaeus vannamei*	1.00E-87	100	Ligase activity
	185	Peroxiredoxin	*Fenneropenaeus indicus*	2.00E-34	100	Peroxiredoxin activity
	282	Ferritin	*Litopenaeus vannamei*	3.00E-59	100	Iron ion transport
	248	Astakine variant 1	*Penaeus monodon*	8.00E-16	100	Cytokine directly involved in hematopoiesis
JX624789	100	Dicer 2	*Penaeus monodon*	5.00E-12	100	RNA processing
FJ746694	726	Polehole-like protein (475-715)	*Penaeus monodon*	5.00E-145	100	Other
FJ746694	209	Polehole-like protein (928-996)	*Penaeus monodon*	2.00E-39	100	Other
AF510331	451	Ovarian peritrophin 1 precursor	*Penaeus monodon*	8.00E-94	99	Chitin metabolic process
AY144581	1004	Thrombospondin	*Penaeus monodon*	1.00E-168	98	Calcium ion binding
EU707329	884	Cyclin A	*Penaeus monodon*	1.00E-79	98	Cell division
	592	Myosin light chain	*Marsupenaeus japonicus*	2.00E-88	97	Calcium ion binding
	364	Beta-actin	*Scylla paramamosain*	2.00E-74	96	ATP binding
JX413010	672	Thrombospondin II	*Penaeus monodon*	8.00E-144	93	Calcium ion binding
	297	Ribosomal protein S10	*Palaemon varians*	4.00E-42	93	Ribosomal protein
JX413010	811	Thrombospondin II	*Penaeus monodon*	7.00E-127	92	Calcium ion binding
GU451715	910	Thrombospondin protein	*Penaeus monodon*	5.00E-97	88	Calcium ion binding
	445	40S ribosomal protein S13	*Danio rerio*	3.00E-78	86	Translation
AY144582	387	Thrombospondin	*Penaeus monodon*	1.00E-27	84	Calcium ion binding
	294	Cytochrome oxidase subunit II	*Lepidopa californica*	3.00E-41	82	Copper ion binding
	258	Peritrophin 3 precursor	*Penaeus monodon*	8.00E-41	76	Chitin metabolic process

Table 4.4 Cont.

Accession number	Length	Gene homology	Species homology	E-value	Similarity (%)	Function
	282	Peritrophin	*Fenneropenaeus chinensis*	3.00E-40	71	Chitin metabolic process
	293	Ovarian peritrophin 2 precursor	*Penaeus monodon*	3.00E-41	71	Chitin metabolic process
GU566728	454	Saposin isoform 1	*Penaeus monodon*	2.00E-57	69	Sphingolipid metabolic process
	741	I-connectin	*Procambarus clarkii*	3.00E-83	67	Hydrolase activity
	493	Cell division control protein 42 homolog	*Oncorhynchus mykiss*	4.00E-14	66	Cell division
	707	AAEL012429-PA	*Aedes aegypti*	2.00E-57	63	Negative regulation of vasodilation
	225	GPx isotype 2	*Perinereis nuntia*	2.00E-24	62	Peroxidase activity
	712	Lethal 35Di	*Anopheles darlingi*	2.00E-35	59	Other
	351	GJ21623	*Drosophila virilis*	7.00E-22	50	Carbohydrate metabolic process
	587	Chondroitin proteoglycan 2	*Stegodyphus mimosarum*	5.00E-23	49	Chitin metabolic process
	398	Reverse transcriptase/ribonuclease H	*Nuttalliella namaqua*	2.00E-27	47	RNA-directed DNA polymerase activity
	692	Polehole-like protein	*Penaeus monodon*	2.00E-46	46	Other
	1044	Chondroitin proteoglycan 2	*Stegodyphus mimosarum*	3.00E-20	41	Chitin metabolic process
	543	Methionine adenosyltransferase	*Ptychodera flava*	1.00E-19	38	Catalytic activity
	849	GJ13907	*Drosophila virilis*	1.00E-07	35	Chitin metabolic process

4.5.2 Validation of stomach cDNA libraries from suppression subtractive hybridization (SSH)

Real-time PCR was performed on 18 selected genes from the forward and reverse libraries, which based on the difference of gene ontology term, immunity or some unknown genes. Gene expressions of infected stomachs of shrimp at 3, 6, 12 hours post infection form the forward library were compared with uninfected shrimp (control). Salivary alkaline phosphatase and pacifastin heavy chain precursor were also significantly increased at 6 hours post infection (Figure 4.21A, B). The expression levels of 7 genes from the forward library consisted of cuticle protein AMP1B, clottable protein, Ig-like and fibronectin type-III domain-containing protein (predicted protein), DD9A, cathepsin B, C-type lectin and Spz1 were increased in infected stomach (Figure 4.21C-I). In addition, the expression patterns at each time point were examined. At 3 hours post infection, the expression of cuticle protein AMP1B, salivary alkaline phosphatase, Ig-like and fibronectin type-III domain-containing protein and pacifastin heavy chain precursor were down-regulated slightly, while clottable protein and cathepsin B were up-regulated slightly. At 12 hours post infection, salivary alkaline phosphatase was down-regulated significantly, while the expression of cuticle protein AMP1B, clottable protein, Spz1, pacifastin heavy chain precursor and cathepsin B were continuously up-regulated (Figure 4.21).

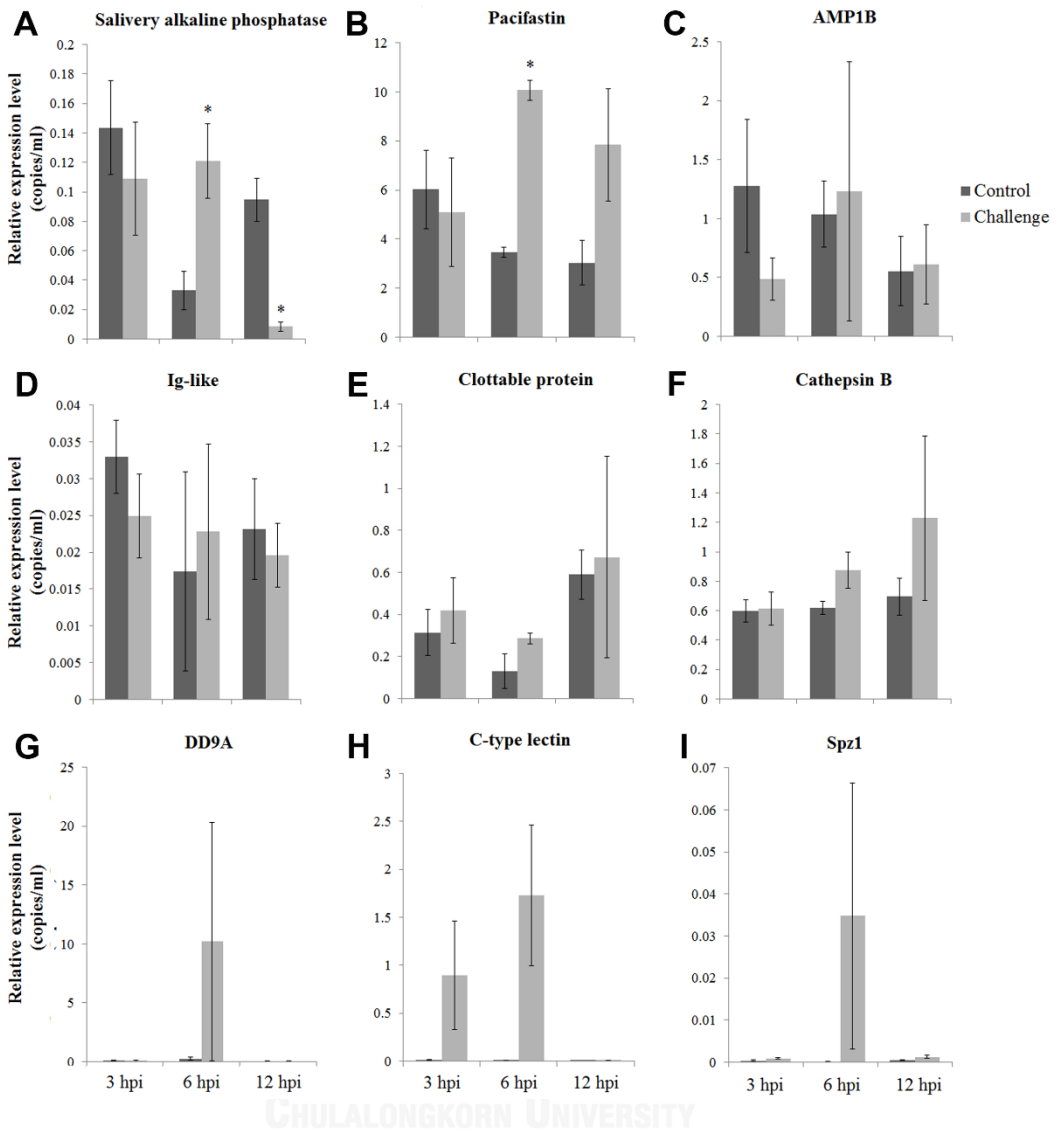

Figure 4.21 Quantitative real-time PCR of selected transcripts from the forward SSH stomach cDNA library of the *P. monodon*. Triplicate samples of each control and challenged group. Elongation 1-α factor was used as internal control. Error bars were express as ±SEM (n=3). (A) Salivary alkaline phosphatase, (B) Pacifastin heavy chain precursor, (C) AMP1B, (D) Ig-like and fibronectin type-III domain-containing protein (predicted protein), (E) Clottable protein, (F) Cathepsin B, (G) DD9A, (H) C-type lectin and (I) Spz1

From the reverse library GPx isotype 2, ubiquitin-conjugating enzyme H5b, I-connectin, fibronectin type-III domain-containing protein (predicted protein), chondroitin proteoglycan 2, peroxiredoxin, ferritin, astakine variant 1 and dicer 2 were examined. The expression of ubiquitin-conjugating enzyme H5b, ferritin, astakine variant 1 and dicer 2 were increased significantly (Figure 4.22A-D), while GPx isotype 2, I-connectin, chondriotin pepteoglycan 2 and peroxiredoxin were down-regulated (Figure 4.28E-H). Fibronectin type-III domain-containing protein was gradually reduced in expression at 6 hours post infection (Figure 4.22I). At 3 hours post infection, the expression of chondriotin proteoglycan 2 was up-regulated significantly. Additionally, the expression of ubiquitin-conjugating enzyme H5b, I-connectin, ferritin, astakine variant 1 and dicer 2 were moderately up-regulated, while GPx isotype 2, fibronectin type-III domain-containing protein and peroxiredoxin were down-regulated slightly. At 12 hours post infection, ubiquitin-conjugating enzyme H5b and dicer 2 transcription were significantly increased in expression. Moreover, fibronectin type-III domain-containing protein, ferritin and astakine variant 1 were increased, while GPx isotype 2, chondriotin pepteoglycan 2 and peroxiredoxin were reduced in expression (Figure 4.22).

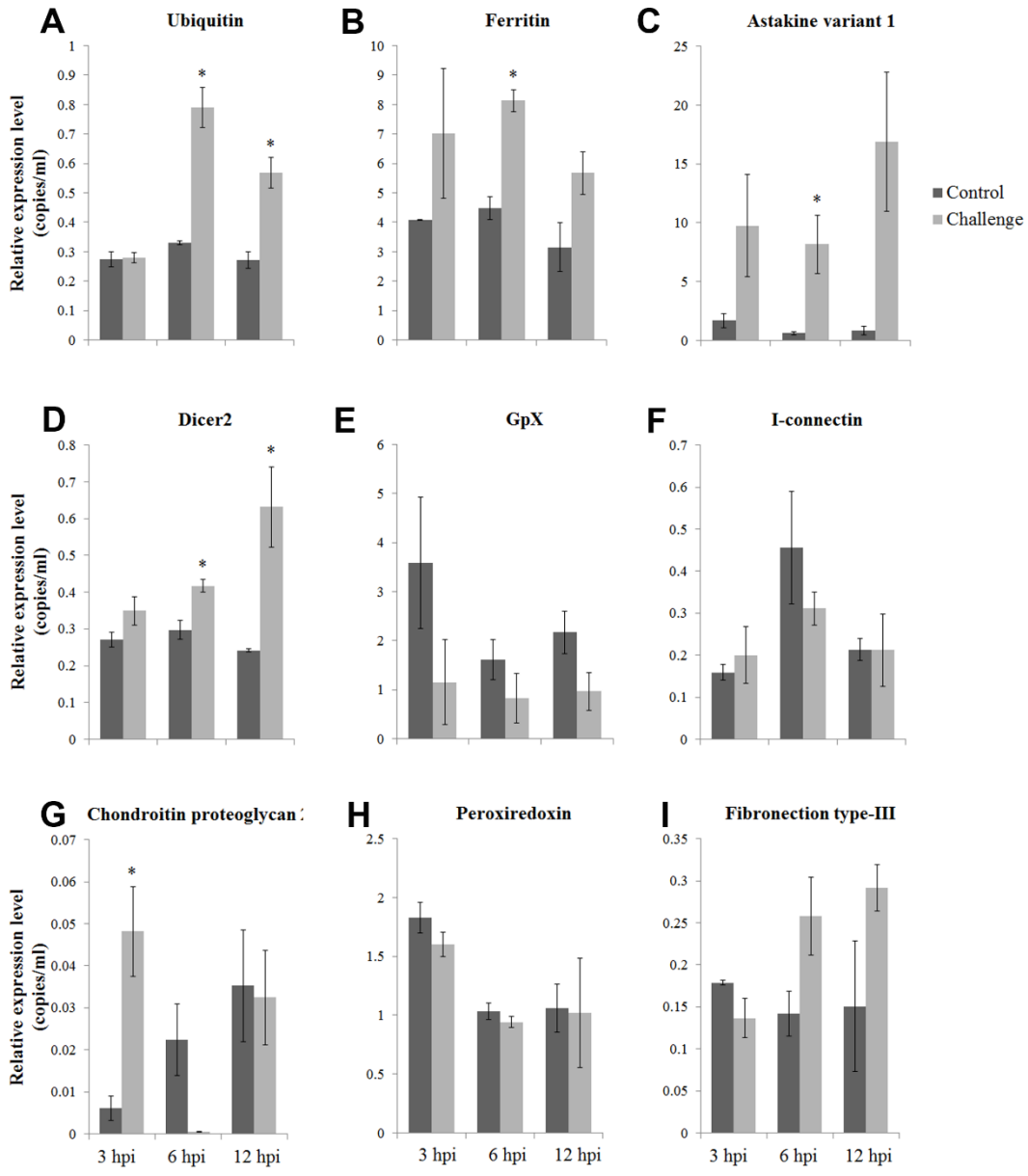

Figure 4.22 Quantitative real-time PCR of selected transcripts from the reverse SSH stomach cDNA library of the *P. monodon*. Triplicate samples of each control and challenged group. Elongation 1-α factor was used as internal control. Error bars were express as ±SEM (n=3). (A) Ubiquitin-conjugating enzyme H5b, (B) Ferritin (C) Astakine variant 1, (D) Dicer 2, (E) GPx isotype 2, (F) I-connectin (G) Chondroitin proteoglycan 2, (H) Peroxiredoxin and (I) Fibronectin type-III domain-containing protein (predicted protein)

4.5.3 A transcriptome of differentally expressed genes (DEGs) of stomach cDNA libraries by ion torrent sequencing

Four transcriptomes of stomach cDNA library were prepared from four groups ; two control and two challenged groups of *P. monodon*. Initially, the total RNA was pooled from 5 stomachs of each group. The mRNA was purified (Figure 4.23), cDNA was synthesized and sequenced using Ion Proton™ Semiconductor Sequencer.

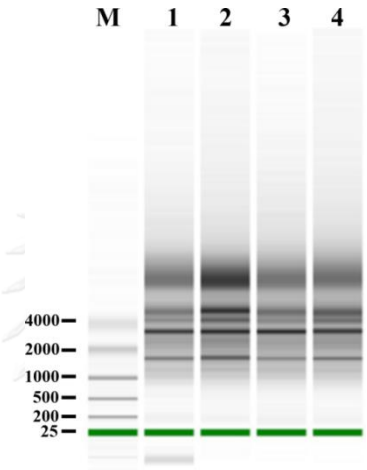

Figure 4.23 The quality of mRNA purified from 4 pooled stomach samples of *P. monodon* control (lane 1-2) and challenged (lane 3-4) groups, respectively. Lane M: DNA marker.

A total of 19,222,349 raw reads was obtained from the control 1 (8,409,850) and control 2 (10,812,499) groups, and 43,224,807 reads from the challenged 1 (23,306,782) and challenged 2 (19,918,025) groups. The average read length of control 1, control 2, challenge 1 and challenge 2 were 122.5, 117.3, 107.0 and 113.2 bp, respectively. The raw reads were further filtered to remove adaptor sequences, ambiguous reads and low quality reads, and as a result of this generating 7,589,049 (90.24%), 9,606,154 (88.84%), 21,651,269 (92.90%) and 18,419,290 (92.48%) of control 1, control 2, challenged 1 and challenged 2, respectively. The average read length after trimming was 129.0, 124.8, 110.5 and 117.3 bp of control 1, control 2, challenged 1 and challenged 2, respectively (Table 4.5).

Table 4.5 Summary of control and challenged transcriptome sequencing

Description	Samples				
	Control1	**Control2**	**Treatment1**	**Treatment2**	**Total**
Raw read (base)	1,029,950,375	1,268,165,451	2,492,811,657	2,255,706,674	7,046,634,157
Raw read (reads)	8,409,850	10,812,499	23,306,782	19,918,025	62,447,156
Average reads length (base)	122.5	117.3	107	113.2	
Number of reads after trimming	7,589,049	9,606,154	21,651,269	18,419,290	57,265,762
Average reads length after trimming (base)	129	124.8	110.5	117.3	-
Percentage of trimmed reads	90.24%	88.84%	92.90%	92.48%	-
Total of contigs	37,094	39,235	42,733	42,188	42,998
blastX hit	15,005	16,053	16,387	16,269	16,457
blastX no hit	22,089	23,182	26,346	25,919	26,541

All the clean reads were assembled using CLC Genomics Workbench solfware to generat *de novo* transcriptomes. The assembly of total reads produced 42,998 contigs (with N_{50} of 740 bp and mean of length 657 bp), and the length of contigs ranged from 113 to 13,364 bp. There were 34,417 shared contigs in both control and challenged group. Thirty-three contigs were found in control groups but were not found in the challenged groups, and 1,418 contigs were found in the challenged groups but were not found in the control groups (Figure 4.24).

High-quality reads were used to analyze of the DEGs using CLC Genomics Workbench solfware. A total of 4,648 from 42,998 assembled contigs (10.81%) demonstrated significantly DEGs between control (*Artemia*-fed) and challenged (*Artemia* with *V. parahemolyticus*-fed) shrimp. Additionally, all contigs were searched against the GeneBank database using the Blast2GO program. Finally, contigs from differentially expressed analysis and blastX were merged. A total of 1,585 from 42,998 assembled contigs (3.69%) were significantly DEGs matching known transcription (*E*-value $<10^{-5}$). Of the 1,585 contigs that exhibited differential expression profiles, 278 contigs (271 unique genes) of known transcripts, 91 contigs (91 unique genes) of hypothetical proteins, 26 contigs (24 unique genes) of predicted proteins and 4 contigs (4 unique genes) of unknown proteins were down-regulated, and 843 contigs (738

unique genes) of known transcripts, 276 contigs (272 unique genes) of hypothetical proteins, 63 contigs (63 unique genes) of predicted proteins and 4 contigs (4 unique genes) of unknown protein were up-regulated in the challenged shrimp, as compared with the expression profiles in the control group (Table 4.6).

Table 4.6 Significantly differentially expressed contigs of the stomach cDNA transcriptome between shrimp *Artemia*-fed and *Artemia* with *V. parahemolyticus*-fed

Transcripts	**Down-regulated at 6 hours post infection**		**Up-regulated at 6 hours post infection**	
	Contigs	**Unique genes**	**Contigs**	**Unique genes**
Known transcripts	278	271	843	783
Hypothetical protein	91	91	276	272
Predicted protein	26	26	63	63
Unknown protein	4	4	4	4
Total	**399**	**392**	**1,186**	**1,122**

The species distribution of the best match result from the database using Blast2GO program for each sequence is shown in Figure 4.25. A top blast species is damp-wood termite *Zootermopsis nevadensis* (15.53%) followed by water flea *Daphnia pulex* (8.94%), red flour beetle *Tribolium castaneum* (4.25%), black tiger shrimp *P. monodon* (3.00%) and head louse *Pediculus humanus* (2.87%).

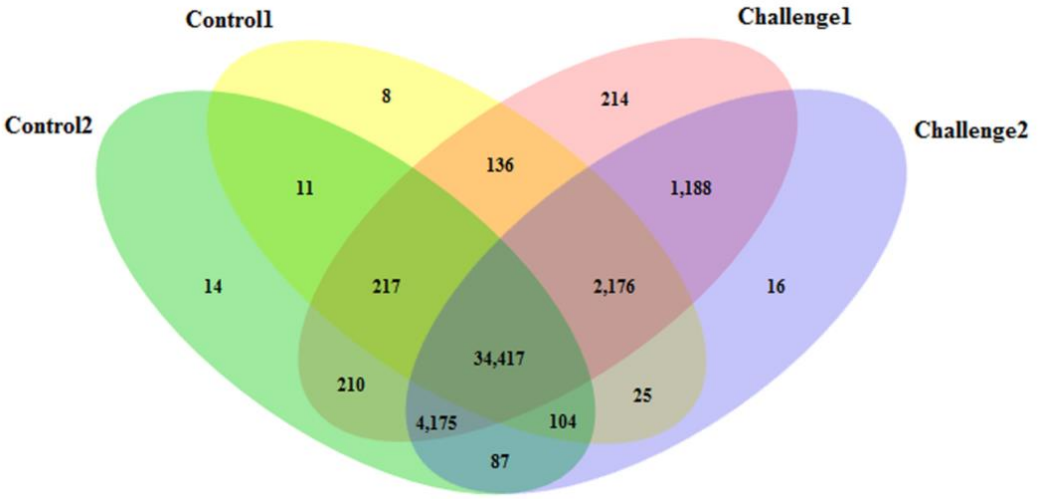

Figure 4.24 The Overlap of contigs expressed in each transcriptome.

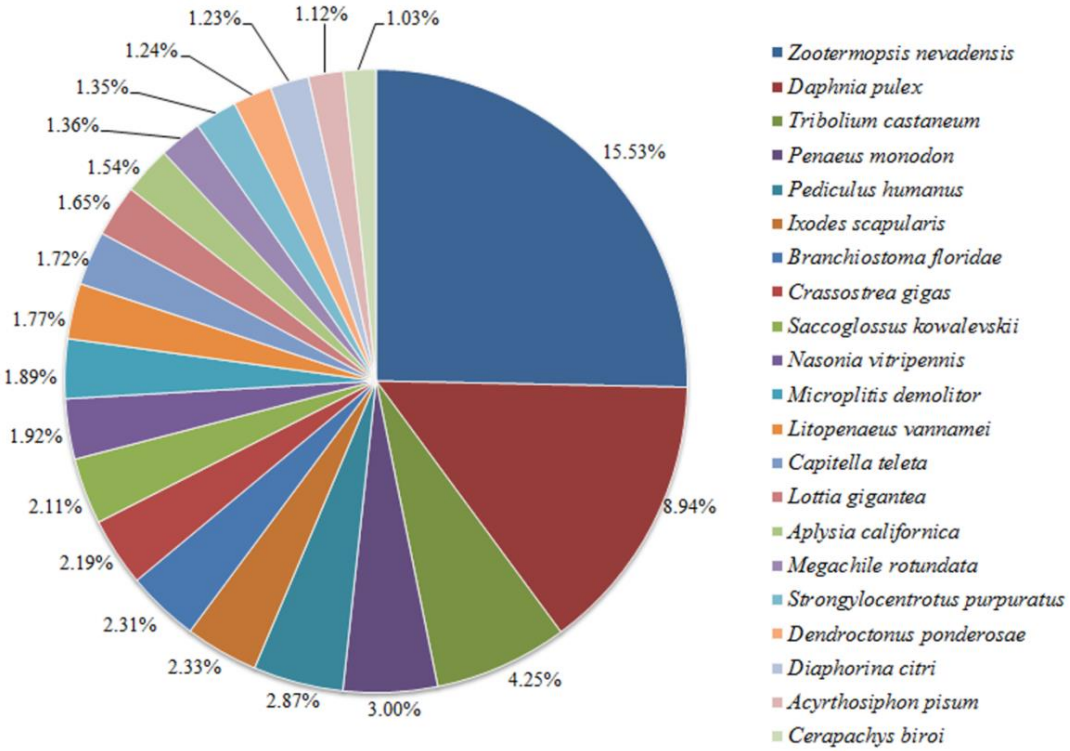

Figure 4.25 The species distribution of blastX result. Different colors represent each species. The percentage of each species more than 1% contigs are shown.

A total of 1,585 contigs of significantly DEGs and known transcription was analyzed in accordance with Gene Ontology by Blast2GO program to define gene function. The biological processes at level 2 was divided into 12 terms including metabolic process (23.79%), cellular process (23.66%), single-organism process (16.34%), localization (9.41%), cellular component organization or biogenesis (6.80%), response to stimulus (6.14%), biological regulation (5.10%), signaling (4.18%), biological adhesion (1.96%), immune system process (1.70%), developmental process (0.78%) and locomotion (0.13%).

The cellular components at level 2 were divided into 6 terms including cell (40.66%), organelle (26.26%), macromolecular complex (20.62%), extracellular region (7.98%), membrane (2.72%) and membrane-enclosed lumen (1.75%).

The molecular functions at level 2 were divided into 9 terms including binding (42.94%), catalytic activity (38.55%), transporter activity (7.63%), structural molecule activity (4.20%), molecular transducer activity (2.86%), nucleic acid binding transcription factor activity (1.91%), molecular function regulator (1.72%) and transcription factor activity, protein binding (0.19%) (Figure 4.26).

The DEGs was mapped to the referential canonical pathway in Kyoto Encyclopedia of Genes and Genomes (KEGG) database using Blast2Go program. From KEEG pathway analysis, forty-five pathways were presented in significant differentially expressed contigs. A top pathway is purine metabolism (22.41%) followed by thiamine metabolism (16.81%), biosynthesis of antibiotics (6.90%), amino benzoate degradation (4.31%), oxidative phosphorylation (4.31%) and T cell receptor signaling pathway (3.45%) (Figure 4.27).

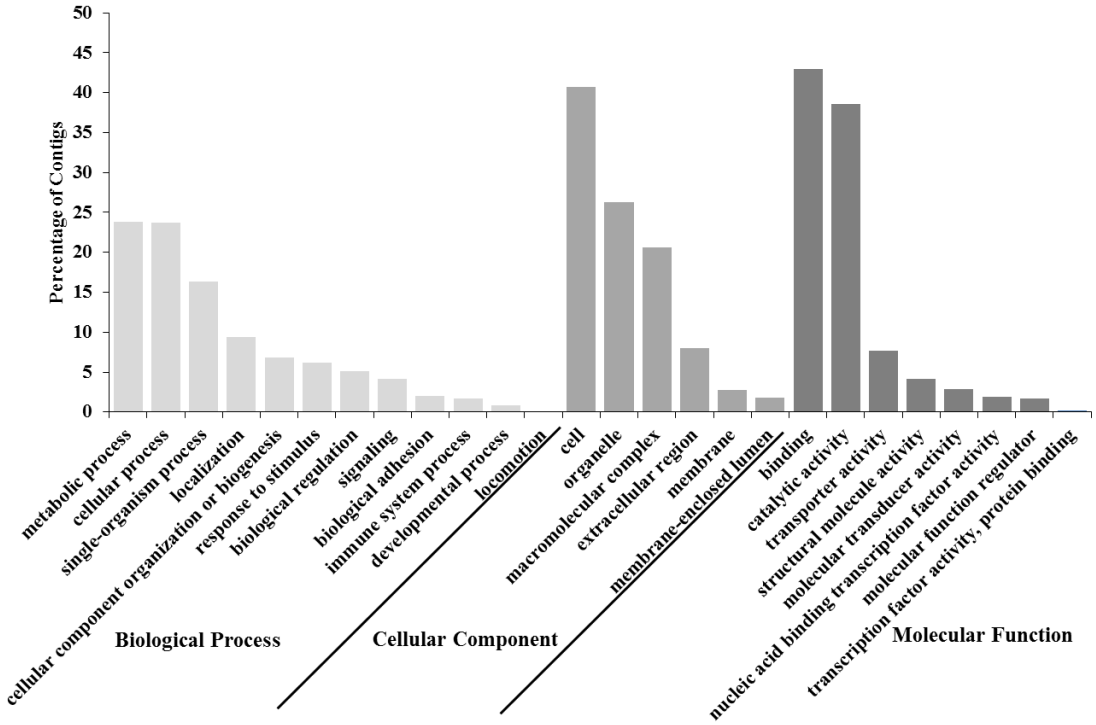

Figure 4.26 The percentage of three terms of gene ontology at level 2 in significant differentially expressed and known transcript contigs of stomach cDNA transcriptome. Total 1,585 contigs were cut off at E-value $<10^5$ by blastX and sequences without annotation are not included in this analysis.

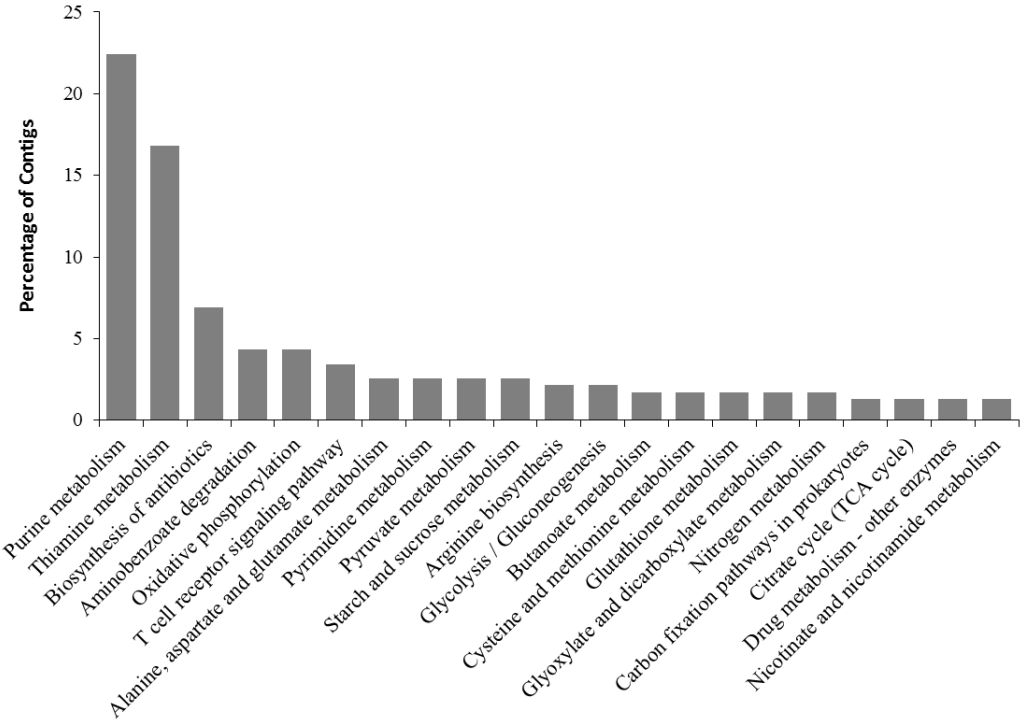

Figure 4.27 The percentage of KEGG pathway analysis of significant differentially expressed and known transcript contigs of stomach cDNA transcriptome. A total of 1,585 contigs were cut off at E-value $<10^5$ by blastX and sequences without annotation are not included in this analysis. The pecentage of each species more than 1% was shown.

DEGs were manually clustered to the immune-gene system. These immune genes were divided into 11 functions including antibacterial peptides, proPO system, oxidative stress, proteinases/proteinase inhibitors, apoptosis tumor-related protein, pathogen recognition immune regulators, blood clotting system, adhesive proteins, heat shock proteins, signal transduction pathways (Toll pathway, IMD pathway, JAK/STAT pathway, MAPK pathway, other signal pathway) and other immune genes (Table 4.7).

Table 4.7 Differentially expressed immune-related genes from stomach cDNA transcriptome of *P. monodon* during EMS/AHPND pathogen infection.

No.	Accession NO.	Gene homology	Species homology	Size (bp)	*E*-value	Similarity (%)	Fold Change
Antimicrobial peptide							
Contig11603	AER45468	Anti-lipopolysaccharide factor isoform 6	*Penaeus monodon*	630	7.51E-62	95	3.83
Contig6243	ACD11038	Crustin 3	*Fenneropenaeus chinensis*	529	7.88E-75	90	-2.27
Contig2269	ACZ63472	I-type lysozyme-like protein 2	*Penaeus monodon*	1295	4.50E-65	84	1.68
Contig27627	AFU61126	Antilipopolysaccharide factor isoform 3	*Fenneropenaeus chinensis*	561	1.85E-38	78	3.17
Contig6231	ABV25094	Crustin-like antimicrobial peptide	*Penaeus monodon*	314	1.69E-10	40	-2.69
proPO system							
Contig6001	ABI78947	Serine protease-like protein isoform 1	*Penaeus monodon*	503	1.29E-32	100	4.19
Contig13245	ACP19561	Clip domain serine proteinase 2	*Penaeus monodon*	1155	5.92E-143	99	10.35
Contig218	AIE45536	Prophenoloxidase 2-like protein	*Penaeus monodon*	1543	0.00E+00	99	-2.21
Contig14774	ADC42876	Serine proteinase inhibitor 6	*Penaeus monodon*	1438	1.04E-121	98	5.58
Contig13303	BAN20620	Serine/threonine-protein kinase tricorner	*Riptortus pedestris*	1212	2.92E-180	96	2.11
Contig3187	KDR14763	Serine/threonine-protein kinase mig-15	*Zootermopsis nevadensis*	1388	6.75E-179	94	1.60
Contig4996	ADR74382	Prophenoloxidase-activating enzyme 2a	*Penaeus monodon*	2940	3.25E-116	93	2.48
Contig1966	ADC42877	Serine proteinase inhibitor B3	*Penaeus monodon*	2256	1.69E-114	92	2.26
Contig18189	ADC42879	Serine proteinase inhibitor 8	*Penaeus monodon*	704	9.69E-57	87	3.21
Contig2139	ACP19563	Masquerade-like serine proteinase-like protein 3	*Penaeus monodon*	2505	3.04E-152	86	-2.18
Contig40356	AFA42361	Clip domain serine proteinase 3	*Portunus trituberculatus*	382	9.94E-19	76	22.32
Contig5116	AFH40332	Prophenoloxidase activating factor	*Litopenaeus vannamei*	334	1.60E-16	76	6.17
Contig12360	AFC61248	Serine proteinase 1	*Portunus trituberculatus*	1398	9.57E-40	75	2.18

Table 4.7 Cont. (1)

No.	Accession NO.	Gene homology	Species homology	Size (bp)	*E*-value	Similarity (%)	Fold Change
proPO system (cont.)							
Contig32137	EZA57507	Serine/threonine-protein kinase 17B	*Cerapachys biroi*	742	3.49E-55	74	2.81
Contig2544	AGL39540	Serine proteinase inhibitor	*Litopenaeus vannamei*	1791	4.29E-46	70	9.86
Contig7691	EGZ26432	Kazal-like serine protease inhibitor domain-containing protein	*Phytophthora sojae*	389	1.80E-07	68	2.97
Contig678	EFN63998	Serine proteinase stubble	*Camponotus floridanus*	2083	3.06E-38	58	-2.87
Contig17737	CAA57964	Putative serine proteinase inhibitor	*Pacifastacus leniusculus*	323	8.87E-12	53	2.74
Contig7496	KDQ97270	Serine/threonine-protein kinase unc-51	*Zootermopsis nevadensis*	910	1.31E-13	42	1.71
Oxidative stress							
Contig1507	ABZ80828	Peroxiredoxin	*Penaeus monodon*	1374	6.07E-140	99	-1.98
Contig520	NP_006692	Thioredoxin-like protein 4A	*Homo sapiens*	570	2.32E-76	97	2.81
Contig12171	KDR14020	Kelch-like protein 26	*Zootermopsis nevadensis*	418	1.28E-53	94	2.18
Contig9708	ACY66462	Thioredoxin-like protein-like protein	*Scylla paramamosain*	261	3.20E-25	92	-2.27
Contig2090	KDR09657	Putative oxidoreductase GLYR1-like protein, partial	*Zootermopsis nevadensis*	396	9.72E-46	85	2.53
Contig988	KDR21878	TAR DNA-binding protein 43	*Zootermopsis nevadensis*	4470	5.05E-111	83	1.99
Contig19859	KDR11784	Kelch-like ECH-associated protein 1	*Zootermopsis nevadensis*	518	5.49E-44	82	5.16
Contig17998	ACO12647	Thioredoxin domain-containing protein 9	*Lepeophtheirus salmonis*	929	2.81E-59	74	3.59
Contig4520	EZA58046	Glutathione S-transferase theta-1	*Cerapachys biroi*	1121	1.21E-52	73	-1.60
Contig4572	ADO00931	Calnexin	*Penaeus monodon*	3048	2.55E-172	85	1.61
Proteinases/proteinase inhibitors							
Contig30939	ACF28464	Single whey acidic protein domain-containing protein isoform 1	*Penaeus monodon*	409	1.49E-25	100	-2.29
Contig10257	ACU31810	Alpha2 macroglobulin isoform 2	*Fenneropenaeus chinensis*	899	8.32E-162	98	2.98

Table 4.7 Cont. (2)

No.	Accession NO.	Gene homology	Species homology	Size (bp)	*E*-value	Similarity (%)	Fold Change
Proteinases/proteinase inhibitors (cont.)							
Contig5228	AFW04307	Alkaline phosphatase, partial	*Macrobrachium rosenbergii*	1296	2.16E-59	87	1.67
Contig1452	KDR16648	Hemocyte protein-glutamine gamma-glutamyltransferase, partial	*Zootermopsis nevadensis*	1812	1.81E-76	79	1.54
Contig7041	AEC50080	Alpha-2-macroglobulin	*Pacifastacus leniusculus*	334	6.28E-29	76	-1.70
Contig16328	EFX85107	Salivary alkaline phosphatase	*Daphnia pulex*	960	1.95E-34	71	1.97
Contig10724	AGL61584	Caspase 4	*Litopenaeus vannamei*	315	3.76E-10	69	3.28
Contig4726	ACU31809	Alpha2 macroglobulin isoform 3	*Fenneropenaeus chinensis*	1889	1.79E-90	67	3.24
Contig515	ABP97431	Alpha 2 macroglobulin	*Fenneropenaeus chinensis*	1731	7.44E-80	66	-2.69
Contig11083	P04069	Carboxypeptidase B	*Astacus astacus*	1455	4.39E-35	60	1.91
Contig3358	XP_002905060	Protease inhibitor Epi11	*Phytophthora infestans*	1286	1.95E-36	51	-2.62
Contig16910	ADM45311	Caspase	*Eriocheir sinensis*	1911	1.79E-21	48	2.43
Apoptosic tumor-related protein							
Contig1767	ABU54835	Defender against apoptotic death	*Penaeus monodon*	593	4.24E-58	100	-1.91
Contig65	ABO38431	Inhibitor of apoptosis protein	*Penaeus monodon*	2865	0.00E+00	95	2.60
Contig35863	AAO61938	Translationally controlled tumor protein	*Penaeus monodon*	455	7.30E-09	87	7.00
Contig13614	AET34917	Apoptosis inhibitor	*Macrobrachium rosenbergii*	573	1.22E-72	87	-2.62
Contig2827	CCI71879	Gelsolin	*Homarus americanus*	1113	1.62E-134	77	-1.50
Contig14638	XP_002424620	Huntingtin-interacting protein, putative	*Pediculus humanus corporis*	1192	1.24E-34	74	4.45
Contig12200	KDR10981	Histone deacetylase complex subunit SAP130	*Zootermopsis nevadensis*	923	2.37E-34	70	2.38
Contig13595	EKC33017	BRCA1-associated protein	*Crassostrea gigas*	513	1.04E-42	68	2.39
Contig6080	EZA51743	Bcl-2-like protein	*Cerapachys biroi*	733	1.11E-21	58	3.63
Contig19079	XP_002413818	Programmed cell death protein, putative	*Ixodes scapularis*	1246	7.25E-65	58	2.94

Table 4.7 Cont. (3)

No.	Accession NO.	Gene homology	Species homology	Size (bp)	*E*-value	Similarity (%)	Fold Change
Apoptosic tumor-related protein (cont.)							
Contig2937	KDR14988	Autophagy-related protein 9A	*Zootermopsis nevadensis*	338	3.56E-08	51	-2.26
Pathogen recognition immune regulator							
Contig9538	ACJ06432	C-type lectin 4	*Fenneropenaeus chinensis*	1048	4.98E-74	99	5.55
Contig9040	AFJ59950	L-type lectin	*Marsupenaeus japonicus*	1157	3.24E-165	95	1.69
Contig8026	NP_001165397	C-type lectin 4 precursor	*Bombyx mori*	694	1.04E-15	89	-1.58
Contig2082	AAM73796	Hemolectin-like protein	*Penaeus monodon*	590	3.64E-62	84	1.54
Contig21561	AHA83583	C-type lectin 2	*Marsupenaeus japonicus*	405	5.11E-47	78	1.91
Contig2081	ABG75717	Hemolectin	*Callinectes sapidus*	286	9.75E-27	72	1.97
Contig9634	AFJ59945	C-type lectin 1	*Marsupenaeus japonicus*	374	1.07E-20	63	3.57
Contig1315	KDR23192	Hemocytin, partial	*Zootermopsis nevadensis*	311	6.20E-21	58	2.04
Contig14941	AFJ59948	Galectin	*Marsupenaeus japonicus*	281	5.05E-07	57	3.47
Contig9291	NP_001088141	Fibrinogen C domain-containing protein 1-B	*Xenopus laevis*	1125	1.35E-19	50	2.42
Blood clotting system							
Contig34408	Q9U572	Clottable protein	*Penaeus monodon*	482	9.53E-12	100	73.24
Contig2364	ABW77320	Clottable protein 2	*Penaeus monodon*	1352	3.27E-13	100	6.31
Contig66	Q9U572	Clottable protein	*Penaeus monodon*	370	3.55E-40	82	-2.10
Contig192	ABK59925	Clottable protein	*Marsupenaeus japonicus*	737	4.63E-76	80	-1.79
Contig14294	ABI95361	Hemolymph clottable protein	*Litopenaeus vannamei*	1992	3.21E-21	63	-2.22
Adhesive protein							
Contig15413	XP_001655514	Integrin-linked protein kinase 2 (ilk-2)	*Aedes aegypti*	659	4.71E-20	96	2.06
Contig1032	ABB55269	Peroxinectin	*Fenneropenaeus chinensis*	2530	0.00E+00	95	2.56
Contig747	ACY82398	Integrin	*Litopenaeus vannamei*	2734	0.00E+00	88	1.81

Table 4.7 Cont. (4)

No.	Accession NO.	Gene homology	Species homology	Size (bp)	*E*-value	Similarity (%)	Fold Change
Adhesive protein (cont.)							
Contig31694	KDR07128	Nischarin	*Zootermopsis nevadensis*	420	1.93E-09	62	4.04
Heat shock protein							
Contig40849	AFX84616	Heat shock protein 70 cognate	*Frankliniella occidentalis*	350	9.91E-11	97	14.00
Contig4288	CAL68989	Heat shock protein 70 kda	*Cyanagraea praedator*	1523	0.00E+00	94	2.07
Contig1716	ADA79523	Heat shock protein 70	*Moina mongolica*	1588	2.76E-86	93	2.15
Contig37792	EZA51720	Hsp90 co-chaperone Cdc37	*Cerapachys biroi*	343	2.70E-40	86	7.27
Contig8219	XP_002430975	Protein tumorous imaginal discs, putative	*Pediculus humanus corporis*	883	3.03E-52	78	1.83
Contig14014	EFX90405	Copper transporting patpase, ATP7a-like protein	*Daphnia pulex*	893	1.88E-73	74	2.63
Contig26178	EDL82295	Similar to dnaj (Hsp40) homolog, subfamily B, member 14 isoform 1, isoform CRA_a	*Rattus norvegicus*	269	7.11E-09	68	3.08
Contig20060	AET34915	Heat shock protein 21	*Macrobrachium rosenbergii*	1675	2.10E-23	44	38.17
Signal transduction pathway							
Toll pathway							
Contig5162	AGO81723	Flightless-I	*Litopenaeus vannamei*	1097	6.51E-96	89	-1.70
Contig12249	AGK40936	Toll-7	*Nilaparvata lugens*	744	6.23E-44	80	-3.64
Contig12355	AFO38331	Cactus protein	*Litopenaeus vannamei*	788	5.94E-59	67	3.42
Contig7118	KDR21043	Protein toll	*Zootermopsis nevadensis*	913	1.49E-49	66	-3.01
IMD pathway							
Contig29295	ACL37048	IMD	*Litopenaeus vannamei*	388	5.77E-30	100	-2.70
Contig9049	AFH66691	Relish	*Penaeus monodon*	3096	0.00E+00	85	2.39

Table 4.7 Cont. (5)

No.	Accession NO.	Gene homology	Species homology	Size (bp)	*E*-value	Similarity (%)	Fold Change
Signal transduction pathway (cont.)							
JAK/STAT pathway							
Contig2094	ADQ43367	HMGBb	*Litopenaeus vannamei*	1664	4.72E-84	100	1.85
Contig22409	KDR08064	HMG box transcription factor BBX	*Zootermopsis nevadensis*	449	5.59E-33	87	3.50
Contig1934	AAA39332	IFN-response element binding factor 2, partial	*Mus musculus*	1211	5.22E-12	42	-1.79
Contig2730	AHH29324	Cytokine receptor	*Scylla paramamosain*	1998	1.92E-74	60	2.69
Contig5943	AEI83865	Kruppel-like factor	*Penaeus monodon*	1332	0.00E+00	100	3.04
Contig14190	KDR21282	Ankyrin repeat family A protein 2	*Zootermopsis nevadensis*	864	6.48E-52	70	-2.94
Contig3739	KDR22205	Ankyrin repeat and KH domain-containing protein 1	*Zootermopsis nevadensis*	682	6.90E-41	64	-2.37
MAPK signal pathway							
Contig1964	ACY66411	Map kinase-interacting serine/threonine	*Scylla paramamosain*	1879	1.13E-161	97	1.69
Contig6457	AHA93093	Mitogen-activated protein kinase kinase	*Scylla paramamosain*	1208	1.09E-118	93	1.90
Contig6817	KDR19052	Mitogen-activated protein-binding protein-interacting protein	*Zootermopsis nevadensis*	820	6.48E-43	81	3.18
Contig36524	KDR08718	Mitogen-activated protein kinase kinase kinase 7-interacting protein 1	*Zootermopsis nevadensis*	459	1.72E-29	66	7.08
Contig1455	KDR21261	Mitogen-activated protein kinase kinase kinase 1	*Zootermopsis nevadensis*	986	9.08E-59	58	-2.55
Other signal pathway							
Contig1366	AFV09848	RAS-like protein, partial	*Procambarus clarkii*	1194	7.46E-80	100	2.79
Contig4989	KDR09308	Ras-related protein Rab-2A	*Zootermopsis nevadensis*	733	3.73E-102	98	1.72
Contig2135	ADV76255	Ras homolog enriched in brain	*Homarus americanus*	1345	3.61E-89	95	1.93
Contig1295	EKC27215	Ras GTPase-activating protein-binding protein 2	*Crassostrea gigas*	1029	6.59E-39	87	1.96
Contig32364	KDR21730	Ras-related protein Rab-21	*Zootermopsis nevadensis*	371	1.77E-07	74	5.12

Table 4.7 Cont. (6)

No.	Accession NO.	Gene homology	Species homology	Size (bp)	*E*-value	Similarity (%)	Fold Change
Signal transduction pathway (cont.)							
Other signal pathway							
Contig9223	EFN84867	Casein kinase II subunit alpha	*Harpegnathos saltator*	1276	3.17E-172	91	1.76
Contig15151	AEN25586	prdm1	*Petromyzon marinus*	1744	4.78E-10	73	2.03
Contig22323	KDR18212	Zinc finger CCHC domain-containing protein 9	*Zootermopsis nevadensis*	333	1.55E-27	71	3.36
Contig14237	EFN80830	Zinc finger CCCH domain-containing protein 10	*Harpegnathos saltator*	506	1.29E-08	68	2.82
Contig13525	KDR14709	Zinc finger CCCH domain-containing protein 11A	*Zootermopsis nevadensis*	1093	1.74E-16	54	2.92
Contig32403	XP_001843776	Zinc finger protein 58	*Culex quinquefasciatus*	272	6.64E-07	52	3.02
Contig34610	EKC42560	Dual serine/threonine and tyrosine protein kinase	*Crassostrea gigas*	449	6.63E-18	67	-1.83
Other immune genes							
Contig736	AGV55412	Arginine kinase	*Penaeus monodon*	443	1.47E-57	100	-2.48
Contig528	ABH10628	Laminin receptor	*Litopenaeus vannamei*	373	4.60E-56	100	-3.17
Contig5650	ABI98679	Ubiquitin-conjugating enzyme H5b	*Litopenaeus vannamei*	1117	1.45E-82	100	2.22
Contig3862	ADK63101	Thrombospondin protein	*Penaeus monodon*	1272	4.77E-11	100	10.35
Contig3826	AEC48730	Ubiquitin-conjugating enzyme E2 b	*Eriocheir sinensis*	1109	2.07E-81	100	2.04
Contig10673	AGI56293	Thrombospondin II	*Penaeus monodon*	828	1.03E-11	100	3.46
Contig13409	AGG20312	Peritrophin	*Palaemon carinicauda*	530	8.44E-61	97	-1.98
Contig3972	AGL08684	Dicer 2	*Penaeus monodon*	1822	0.00E+00	97	2.30
Contig2124	ACY66506	Ubiquitin associated protein 2-like protein	*Scylla paramamosain*	952	3.28E-18	92	-1.73
Contig23087	ACV32380	Thrombospondin	*Fenneropenaeus merguiensis*	489	8.01E-11	91	4.60
Contig10277	ADG22164	Chitinase 2	*Penaeus monodon*	564	5.88E-32	91	-2.05
Contig21333	AAZ66371	Peritrophin	*Fenneropenaeus chinensis*	547	1.46E-18	88	-2.33

Table 4.7 Cont. (7)

No.	Accession NO.	Gene homology	Species homology	Size (bp)	*E*-value	Similarity (%)	Fold Change
Signal transduction pathway (cont.)							
Other signal pathway (cont.)							
contig19798	KDR20136	Ubiquitin carboxyl-terminal hydrolase 2	*Zootermopsis nevadensis*	617	4.67E-61	84	3.36
contig8009	AEB54793	single VWC domain protein 3	*Litopenaeus vannamei*	353	2.78E-16	83	-6.52
contig10735	KDR15871	Laminin subunit beta-1	*Zootermopsis nevadensis*	559	2.81E-15	80	-3.57
contig193	ABL86146	peritrophin 3 precursor	*Penaeus monodon*	570	3.51E-32	79	-3.18
contig4688	KDR15871	Laminin subunit beta-1	*Zootermopsis nevadensis*	1494	0.00E+00	79	2.13
contig3339	AAF34332	peritrophin-like protein 2	*Penaeus semisulcatus*	508	1.47E-36	77	-3.04
contig4474	KDR14054	Protein ELYS	*Zootermopsis nevadensis*	1924	4.91E-27	75	2.44
contig15204	EKC32341	Ubiquitin carboxyl-terminal hydrolase 32	*Crassostrea gigas*	452	5.58E-25	71	3.45
contig1745	ABL86146	peritrophin 3 precursor	*Penaeus monodon*	1447	9.45E-06	64	-2.26
contig21399	EFN65888	Ubiquitin conjugation factor E4 A	*Camponotus floridanus*	733	1.26E-41	57	3.14
contig12284	XP_001270082	histone H3 variant, putative	*Aspergillus clavatus*	532	6.78E-10	57	-2.36
contig7208	XP_646792	histone H3	*Dictyostelium discoideum*	511	7.07E-07	57	-3.04

4.5.4 Validation of stomach cDNA libraries from transcriptome

To validate DEGs, a relative qPCR analysis on 22 randomly selected genes from DEGs was performed using the same RNA sample prepared for RNA-seq (a type of technical validation), and using RNA from new samples (a type of biological validation), which were collected at 6 hours post infection. The qPCR results (20 from 22 genes) from both technical and biological validation were significantly correlated with the RNA-seq result with correlation coefficients of 0.83 and 0.71 (p-value<0.001), respectively (Figure 4.28). Each product was shown as a sigle peak of melting curve and also as a single product on agarose gel.

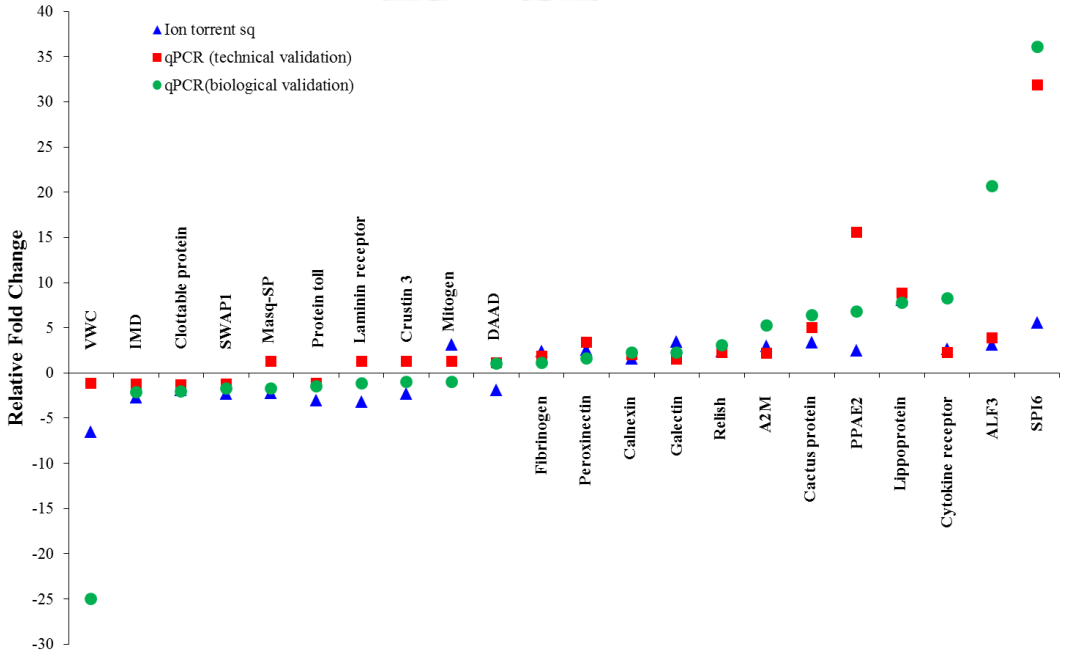

Figure 4.28 Comparison of relative fold change of selected genes from ion torrent sequencing and relative real-time PCR. VWC= single VWC domain protein 3, SWAP1= single whey acidic protein domain-containing protein isoform 1, Masq-SP= masquerade-like serine proteinase-like protein 3, DAAD= defender against apoptotic death, Mitogen= mitogen-activated protein-binding protein-interacting protein, Fibrinogen= fibrinogen C domain-containing protein 1-B, A2M= alpha2 macroglobulin isoform 2, Lipoprotein= lipoprotein receptor, PPAE2= prophenoloxidase-activating enzyme 2a, ALF3= antilipopolysaccharide factor isoform 3 (PmALF7) and SPI6= serine proteinase inhibitor 6

4.5.5 Identification of anti-lipopolysaccharide factor isoform 7 (*Pm*ALF7) of stomach cDNA libraries from transcriptome.

In this study, the novel ALF was discovered. It was searched against the GenBank database using BlastX showed that it is similar to ALF3 from Chinese shrimp *F. chinensis* (Table 4.7); therefore, it was called *Pm*ALF7 because ALFs of *P. monodon* have been reported for 6 isoforms until now. The full length cDNA of *Pm*ALF7 was obtained from the stomach transcriptome. It was significantly up-regulated in expression at 6 hours post infection form both ion torrent sequencing and relative real-time PCR (Table 4.7 and Figure 4.34). The confirmed full length cDNA of *Pm*ALF7 was 575 bp. The predicted open reading frame (ORF) is 369 bp from 60 to 428 bp corresponding to a polypeptide of 122 amino acids. The signal peptide sequence is from 1-24 bp, and the amino acids from 54 to 75 corresponded to the putative LPS-binding domain (Figure 4.29).

```
1     GCGGGAATTCATACCACTAACCTCTAGCACCAGGACAGTAAGAGTGTAATTTCCAAACGA
61    TGAGAGTGTCTGTGCTGACGATGGCGCTGACGGTGGCGCTGGCGGTCGCTCTTCCTTCGC
1     M  R  V  S  V  L  T  M  A  L  T  V  A  L  A  V  A  L  P  S

121   AGTGCAGCGCCGCGGGCTGGGGAGCGTTCATGCCCTCCATCGCGACGAGGCTAACAGGAT
21    Q  C  S  A  A  G  W  G  A  F  M  P  S  I  A  T  R  L  T  G

181   TGTGGGAGACGGGAGAGCTGGAGTTGCTGGGACGCTACTGCACCTACAGTGTGAAGCCAA
41    L  W  E  T  G  E  L  E  L  L  G  R  Y  C  T  Y  S  V  K  P

241   CGTTCCAGCAGTGGCAGTTGTACTTCATCGGCAGCATGTGGTGTCCCGGATGGACACCCA
61    T  F  Q  Q  W  Q  L  Y  F  I  G  S  M  W  C  P  G  W  T  P

301   TTAGGGGCGTAGCCGAAACACGAAGCAGGTCGGGAGTGGTTGGGAAAATGACACAAGATT
81    I  R  G  V  A  E  T  R  S  R  S  G  V  V  G  K  M  T  Q  D

361   TCGTCCGGAAAGCTTTGAGAGCAGATCTCCTGTCTAAAGAAGAGGCCGAAACCTGGCTCA
101   F  V  R  K  A  L  R  A  D  L  L  S  K  E  E  A  E  T  W  L

421   GTCATTGACAAGCTGTTGATGAATAAGAGTCAAGCGAATTTTACATCATAAATTATTGAC
121   S  H  *

481   TTTATCTGTACATATCTTAATCAAACCATTTCTGTAAAAGAAGTATTTTGAATTACATAA
541   ACTTAACGTACTGCAAAAAAAAAAAAAAAAAAAAA
```

Figure 4.29 The full length nucleotide (above) and predicted amino (below) sequence of *Pm*ALF cDNA from *P. monodon*. There are 575 bp of nucleotide sequence and deduced 122 amino acids of peptide. The predicted ORF is from 60 to 428 bp (the start and stop codon are shown in bold). The signal peptide sequence is indicated by a solid underline, the putative LPS-binding domain is shaded in yellow, polyadenylation signal is underlined and italicized.

A phylogenetic tree was constructed using the neighbour-joining method. The crustacean ALF could be categorized into three large groups. *Pm*ALF7 was most similar to *Fc*ALF3 from *F.* chinensis, *Mj*ALF1 from *M. japonicus*, *Pm*ALF6 from *P. monodon* and FcALF2 from *F.* chinensis, and they are in the group 1. Other PmALF isoforms are in the group 2 (Figure 4.30).

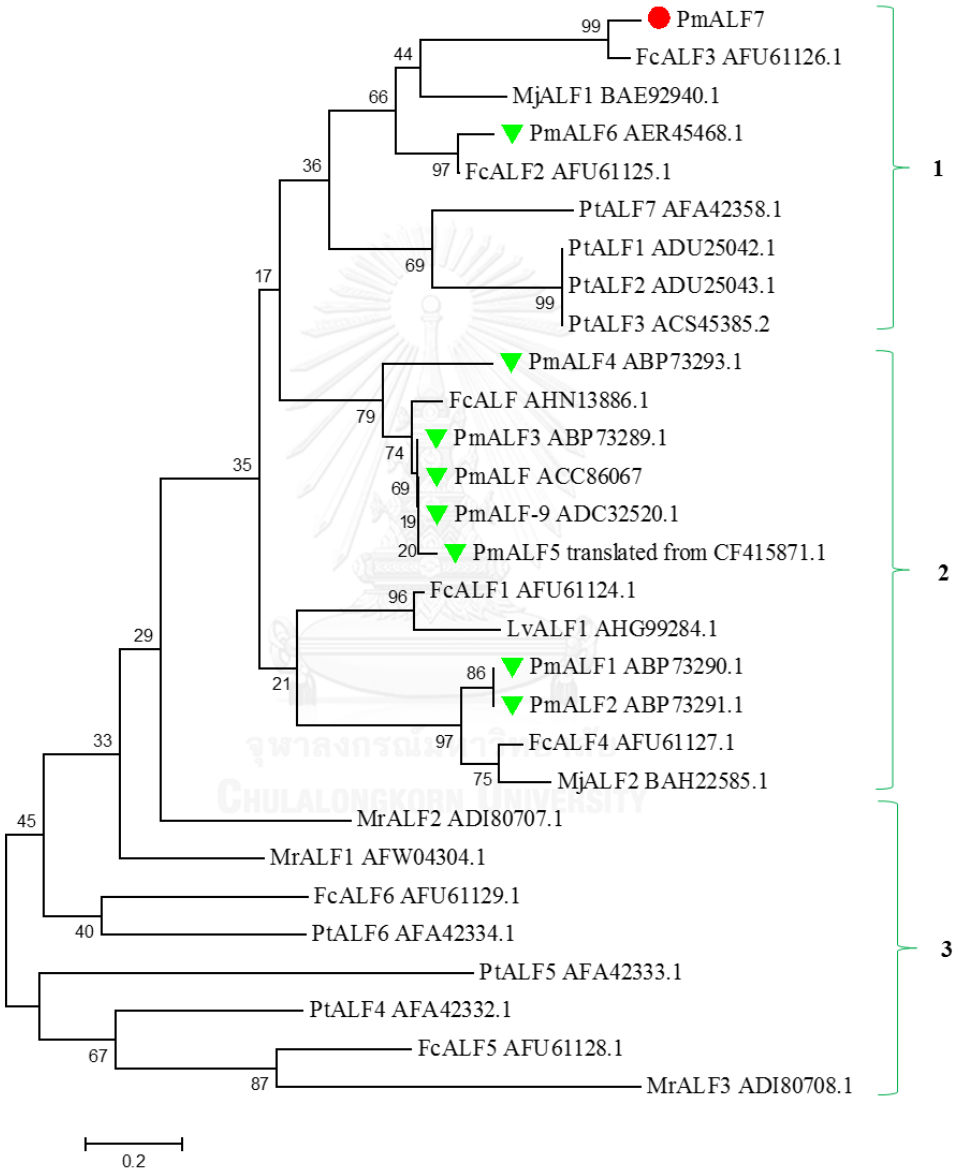

Figure 4.30 Phylogenetic analysis of crustacaen ALF based on the amino acid sequence. P. monodon ALF▼ and a noval ALF●. Fc= *F. chiensis*, Mj= *M. japonicus*, Pt= *Portunus trituberculatus*, Lv= *L. vannamei*, Mr= *M. rosenbergii*.

To design the specific primer for *Pm*ALF7, the nucleotide sequence of *Pm*ALF 7 was compared with other *Pm*ALF. The position of the forward primer was selected from 140 to 158, and the position of the reverse primer was from 316 to 334 based on the dissimilarity of the first base of 3' region of the primers. In addition, sequence comparison revealed conserved nucleotide sequence of all *Pm*ALF (Figure 4.31).

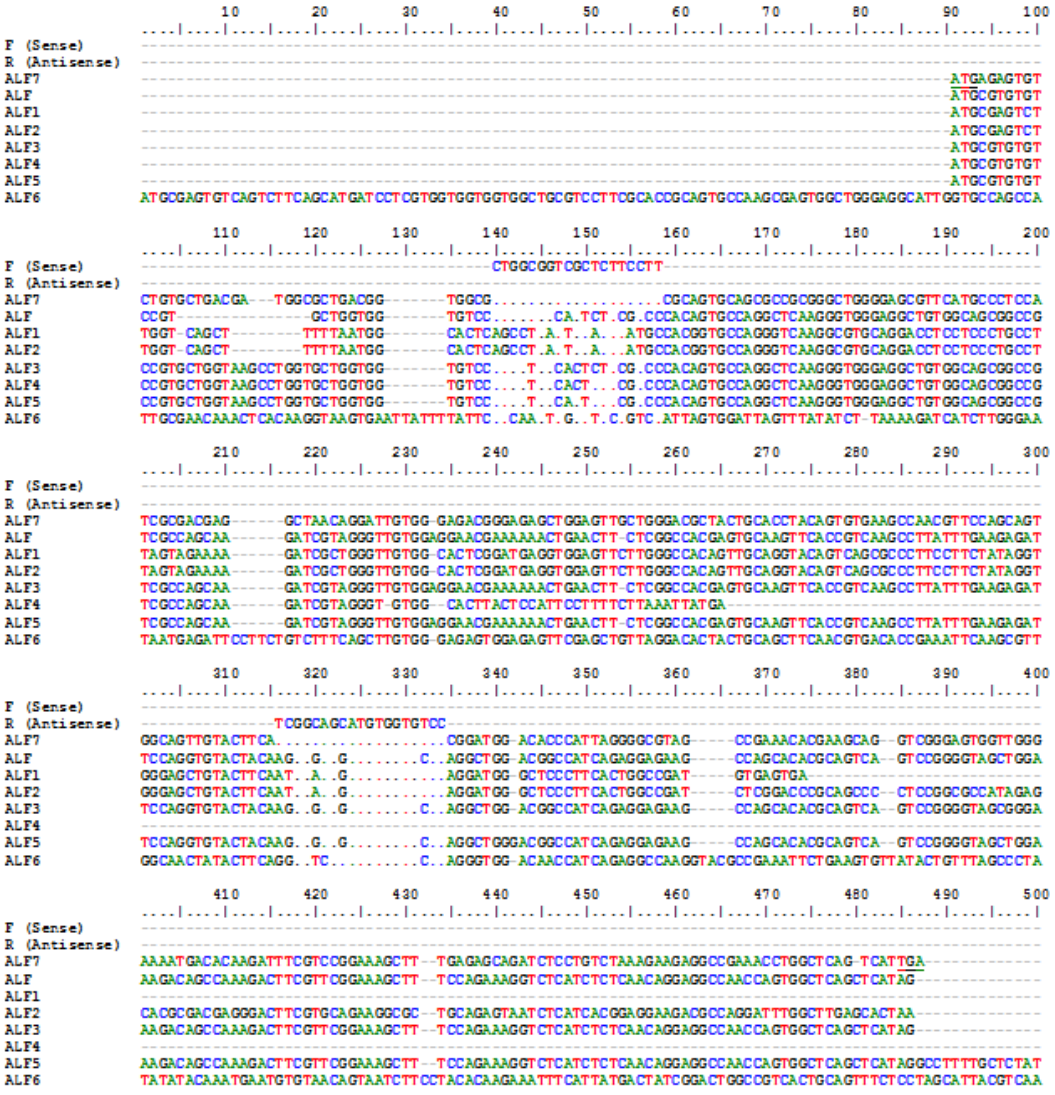

Figure 4.31 Multiple alignment of cDNA *Pm*ALF, seven sequences of other ALF and *Pm*ALF7 primer. The different nucleotides were shown as the different color.

The relative real time PCR was performed to investigate tissue distribution of *Pm*ALF7 in healthy shrimp. *Pm*ALF7 trascript was highly expressed in stomach and lymphoid organ, moderately in muscle, hemocyte, hepatopancreas and low in hindgut, heart, pleopod, midgut and gill (Figure 4.32).

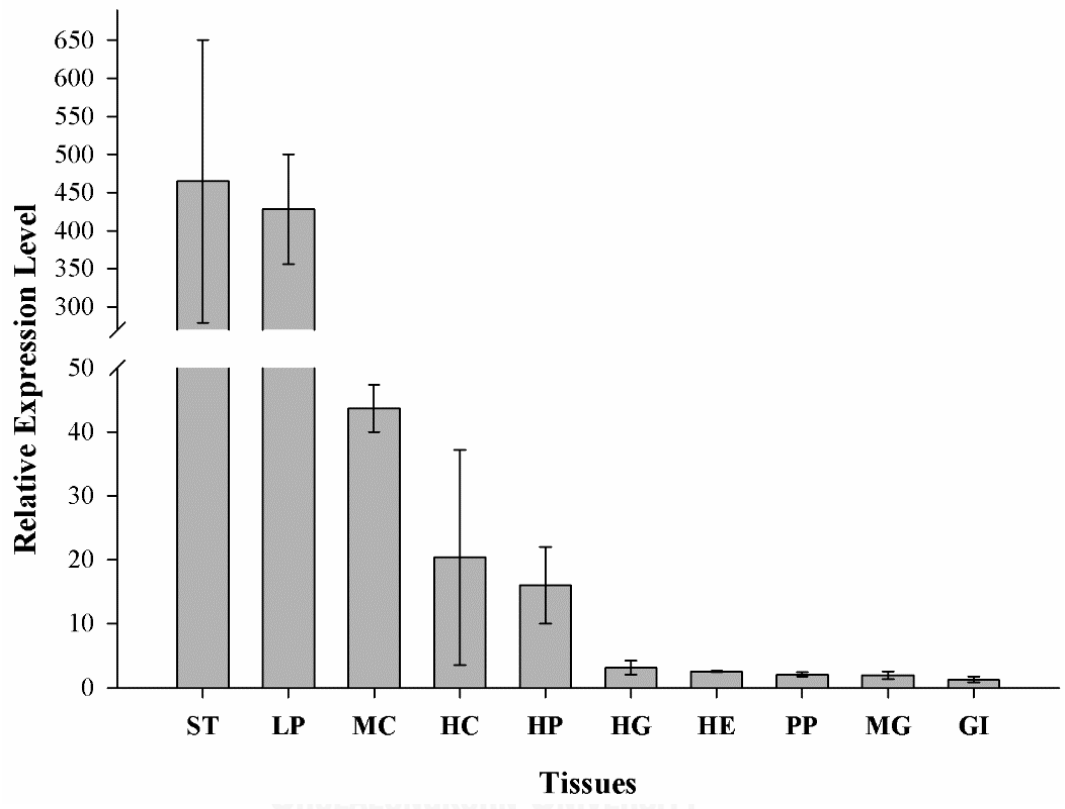

Figure 4.32 The tissue distribution of *Pm*ALF7 transcripts. ST=stomach, LP= lymphoid organ, MC=muscle, HC=hemocyte, HP= hepatopancreas, HG=hindgut, HE=heart, PP= pleopod, MG=midgut, GI=gill. Error bars were expressed as ±SEM.

The expression level of *Pm*ALF7 was slightly increased to a 1.8 fold induction at 3 hours post infection in stomach. The statistically significant increase of 26.8 and 52.8 fold of *Pm*ALF7 transcript was observed at 6 and 12 hours post infection compared to those at 3 hours post infection (Figure 4.33).

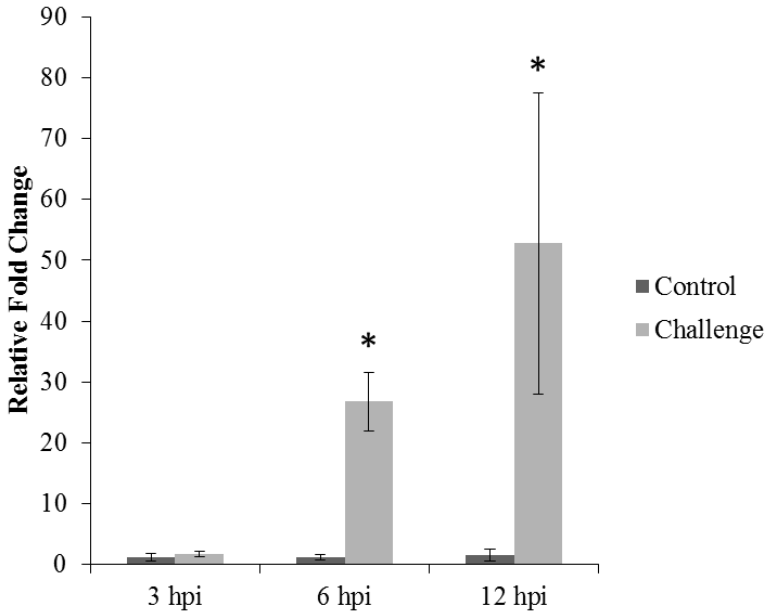

Figure 4.33 Relative fold change of *Pm*ALF7 transcripts in stomach between control (*Artemia*-fed) and challenge (*Artemia* with *V. parahaemolyticus*-fed) at each time point. Error bars were expressed as ±SEM (n=3). Asterisk indicates significant differences between the control and challenged group ($P<0.05$).

4.6 Examination of the Full Length cDNA of C-type Lectin

4.6.1 Characterization of the full length cDNA of C-type lectin

The full length cDNA of *Pm*Cr was obtained from hepatopancras. *Pm*Cr cDNA was 693 bp long with an open reading frame of 522 bp encoding a 173 amino acid containing protein. The deduced protein sequence consists of a putative 11 amino acid signal peptide and a single carbohydrate recognition domain (residues 23-171) (Figure 4.34). The mature *Pm*Cr protein has a theoretical molecular mass of 17.4 kDa and an isoelectic point of 4.68.

```
1     ACGCGGGGCTTGTTCAGCTGAACGTAGTTGAGATGGGGTTCAGTGGCCGTGTTCTAGCGT
1                                      M  G  F  S  G  R  V  L  A

61    GCGTTTTGGCCTTGGCTTCGGCTGGTCTCGCTATAGAATGCCCTACAGGATTCTTCGAGG
10    C  V  L  A  L  A  S  A  G  L  A  I  E  C  P  T  G  F  F  E

121   CAGGGGTCGGGTGCTTCGTAGTCCACAGCCAGCCTAGCACTGGCCAGACCAACTTGGACT
30    A  G  V  G  C  F  V  V  H  S  Q  P  S  T  G  Q  T  N  L  D

181   GGGAGGGAGCAAGGATTCTCTGCCAAAGCCTCTCGGATTCCAGCTGGACTGTTGACTTGG
50    W  E  G  A  R  I  L  C  Q  S  L  S  D  S  S  W  T  V  D  L

241   CTGTCTTTGATTCCTCGGAGCAGTTGGCAGCGATTTCGGAGGCGTGGGCTACGATCGGCG
70    X  V  F  D  S  S  E  Q  L  A  A  I  S  E  A  W  A  T  I  G

301   CCACCTACCCCTACCCCTACCCGTACATGTGGATCGGCGTGGAGCGACAGGGCGAGACGT
90    A  T  Y  P  Y  P  Y  P  Y  M  W  I  G  V  E  R  Q  G  E  T

361   GGACGTGGCTCGATGGAAGGCCCTTGTCTCGCTTCTCGAACATGTGGCGCGTAGACTATC
110   W  T  W  L  D  G  R  P  L  S  R  F  S  N  M  W  R  V  D  Y

421   CTGACGAAGCTTACGATACGGGCGTCTATCTCGAGGATTACAAGCTGTCCAACGGCGCCA
130   P  D  E  A  Y  D  T  G  V  Y  L  E  D  Y  K  L  S  N  G  A

481   ACGTCTTCGGGAGGCTGTACGTCGGGAATTCCGGACACCAGTGGCTGCGTCGTTACATGT
150   N  V  F  G  R  L  Y  V  G  N  S  G  H  Q  W  L  R  R  Y  M

541   GCCGGGCGAAGTAGGCGAGCGAGGTGGCTGACGGAGGATGGAGCTTCGTCTTGTGGGAGT
170   C  R  A  K  *

601   GTGTTGTGTTATAAACGAAAAAACACATGTTGGAAGTAACCAAAAAAAAAAAAAAAAAAA
661   AAAAAAAAA
```

Figure 4.34 The full length nucleotide (above) and predicted amino (below) sequence of *Pm*Cr cDNA from *P. monodon*. There are 693 bp of sequence and deduced 173 amino acids of peptide. The predicted ORF is from 57 to 578 bp (the start and stop codons are shown in bold). The signal peptide sequence is indicated by a solid underline, conserved cysteine residues that define the C-type lectin domain (23-171) are marked with ▲ and C-type lectin domain is shaded in yellow.

A phylogenetic tree was constructed using neighbour-joining method. The crustacean *Pm*Cr could be categorized into 3 large groups, and *Pm*Cr is in the group 2. The *Pm*Cr is closely related to C-type lectin receptor of swim crab *Portunus pelagicus* and C-type lectin-like domain (CTLD)-containing proteins of Chinese mitten crab *Eriocheir sinensis* (Figure 4.35).

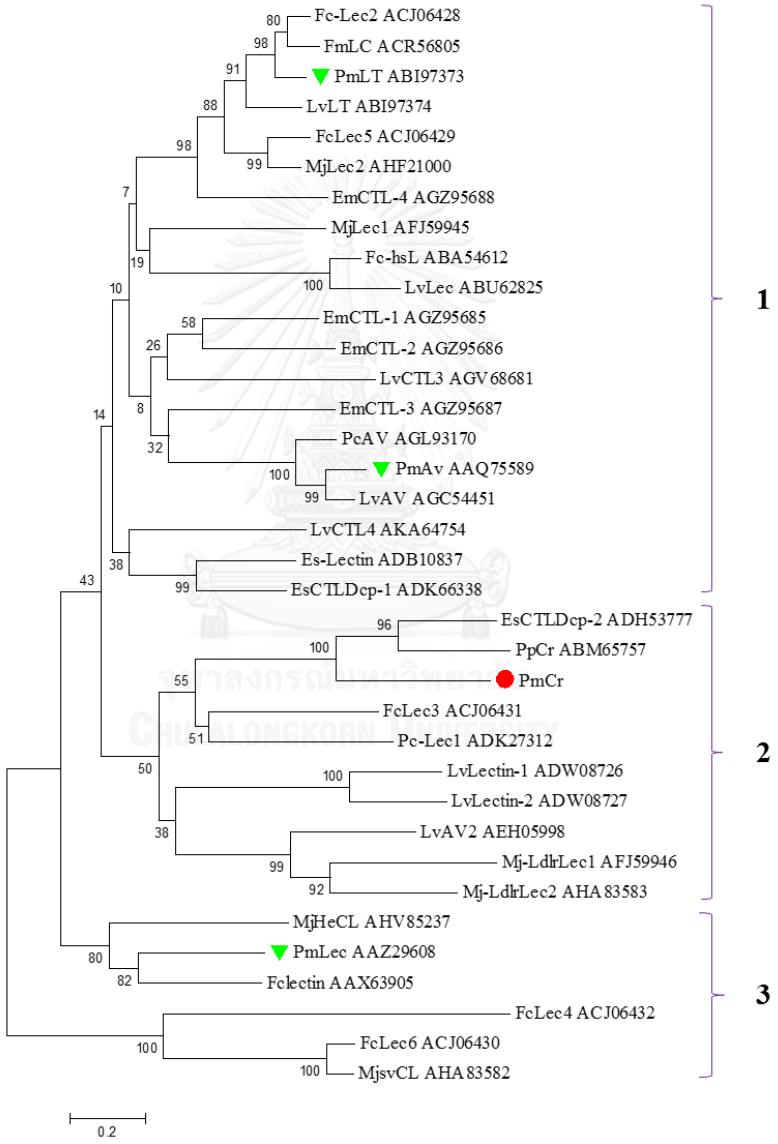

Figure 4.35 Phylogenetic analysis of crustacaen C-type lectin based on the amino acid sequence. Old C-type lectins ▼ and new C-type lectin ● of *P. monodon*; Fc= *F. chinensis*, Mj= *M. japonicus*, Lv= *L. vannamei*, Pp= *P. pelagicus*, Es= *Eriocheir sinensis*

4.6.2 Transcript expression of the C-type lectin

The relative real time PCR was performed to investigate tissue distribution of *Pm*Cr. The *Pm*Cr transcript was highly expressed in hepatopancreas and lowly expessed in other organs of *P. monodon* (Figure 4.36). In addtion, the expression level of *Pm*Cr was examined in hepatopancreas at 3, 6, 12 hours post infection. *Pm*Cr expression profile showed small up-regulation at 3 hours post infection of the challenged group (0.39±0.07) compared to the control group (0.36±0.07). There was a significant down-regulation at 6 hours post infection of the challenged group (0.42±0.04) compared to the control group (0.27±0.01). A 12 hours post infection, the *Pm*Cr expreesion of challenged group (0.25±0.06) was lower than the control group (0.28±0.03) (Figure 4.37).

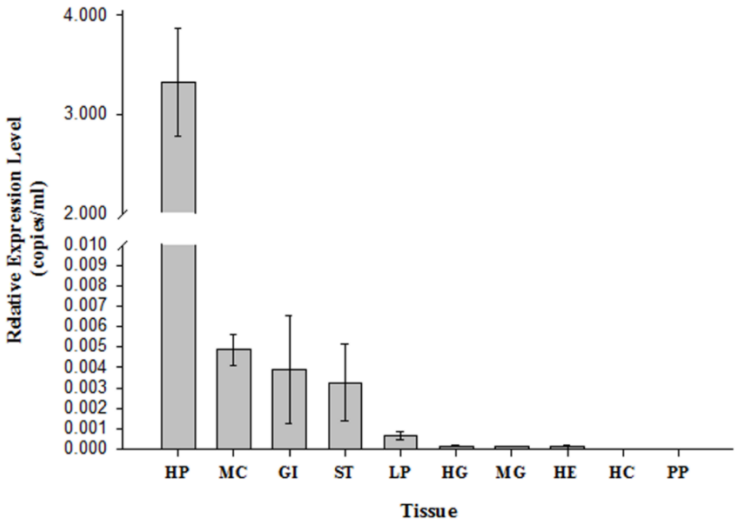

Figure 4.36 The tissue distribution of *Pm*Cr transcripts. HP= hepatopancreas, MC=muscle, GI=gill, ST=stomach, LP= lymphoid organ, HG=hindgut, MG=midgut, HE=heart, HC=hemocyte and PP= pleopod. Error bars were expressed as ±SEM (n=3).

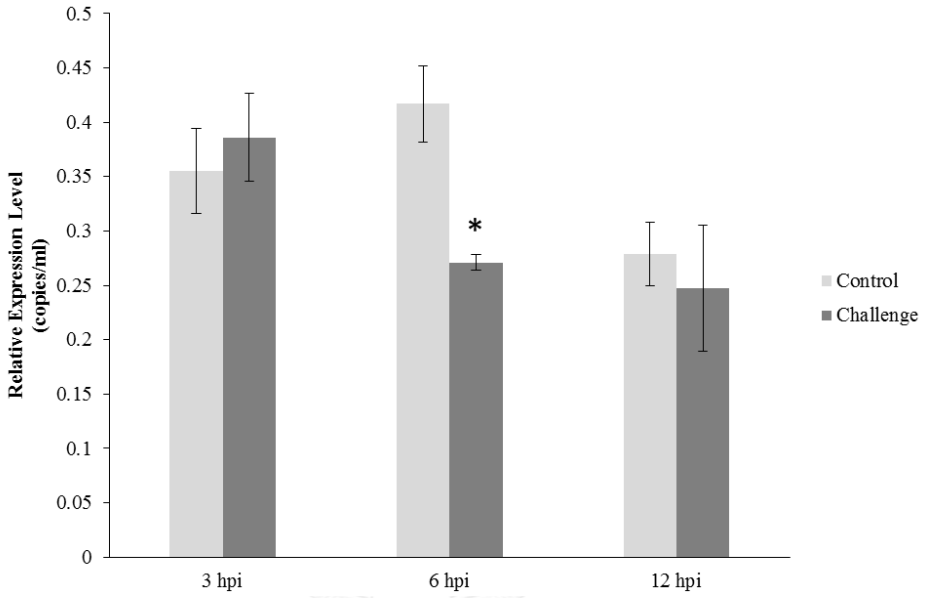

Figure 4.37 Relative expression level of *Pm*Cr transcripts in hepatopancreas between control (*Artemia*-fed) and challenged (*Artemia* with *V. parahaemolyticus*-fed) at each time point. Error bars were expressed as ±SEM (n=3). Asterisk indicates significant differences between the control and challenged group ($P<0.05$).

4.6.3 *In vitro* expression of full length cDNA of the C-type lectin protein

A recombinant clone of *Pm*Cr protein was examined for protein expression pattern at 0, 1, 2, 3, 4, 6 and 14 hours post IPTG induction. A coomassie-stained gel (Figure 4.38A) and western blot analysis (Figure 4.38B) showed that the recombinant *Pm*Cr was overexpressed at 1 hour post IPTG induction and that it was continually expressed until 14 hours after IPTG induction. The expected size is 17.4 kDa.

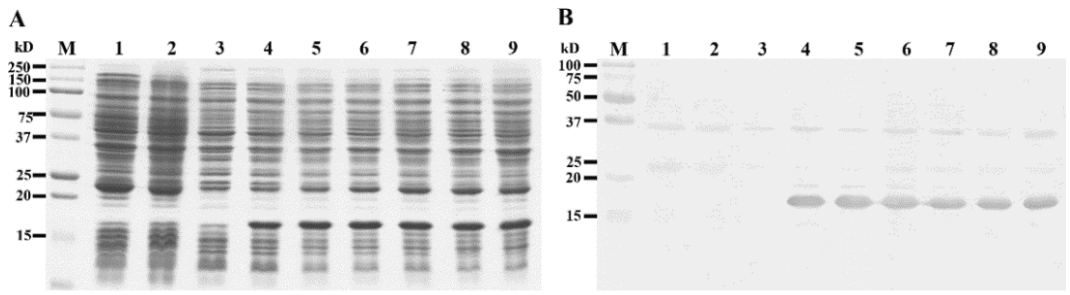

Figure 4.38 A coomassie-stained gel (A) and western blot analysis (B) of *in vitro* expression of *Pm*Cr at 0, 1, 2, 3, 4, 6 and 14 hours after induction with 1 mM IPTG (lanes 3-9; A and B), *E. coli* BL21-CodonPlus (DE3)-RIPL (lanes 1; A and B) and a pET-15b vector in *E. coli* BL21-CodonPlus (DE3)-RIPL (lanes 2; A and B) were included as the control.

The recombinant *Pm*Cr protein was overexpressed at 3 hours post induction with 0.4 mM, 0.8 mM and 1mM IPTG cultured at 37 °C. A coomassie-stained gel showed that the recombinant *Pm*Cr protein was an inclusion body for 1mM IPTG induction and was slightly expressed after induction with 0.4 mM, 0.8 mM IPTG at 37 °C (Figure 4.39).

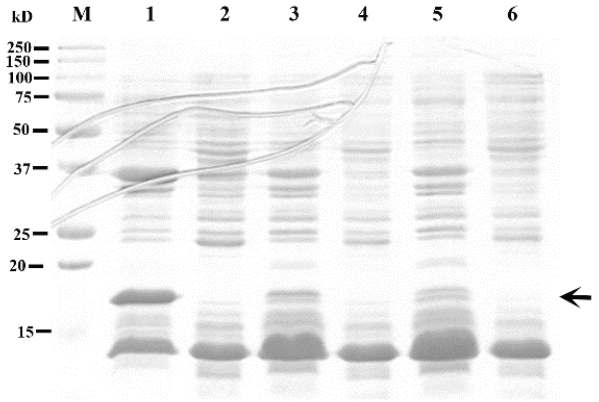

Figure 4.39 A coomassie-stained gel showing an insoluble protein fraction (lane 1, 3 and 5) and a soluble protein fraction (lane 2, 4 and 6) of recombinant *Pm*Cr protein (arrow) cultured at 37 °C for 3 hours post 1 mM (lane 1 and 2), 0.8 mM (lane 3 and 4) and 0.4 mM (lane 5 and 6) IPTG induction.

The inclusion body of *Pm*Cr was refolded by 8 M urea and purified. The washing and elution were detemined by a coomassie-stained gel which showed that the recombinant *Pm*Cr protein was in the first washing solution and disappeared in other washing solutions (Figure 4.40A). The recombinant *Pm*Cr protein was in the second and third elution (Figure 4.40B). Therefore, the second and third elution of the recombinant *Pm*Cr protein were collected and concentrated, and then run in a 15% SDS PAGE. The specific band of recombinant *Pm*Cr protein was cut and purified using electro-eluter. The recombinant *Pm*Cr protein from upper, intermidiate and lower fraction was detemined by 15% SDS PAGE and this showed the specific bands of recombinant *Pm*Cr protein (Figure 4.41).

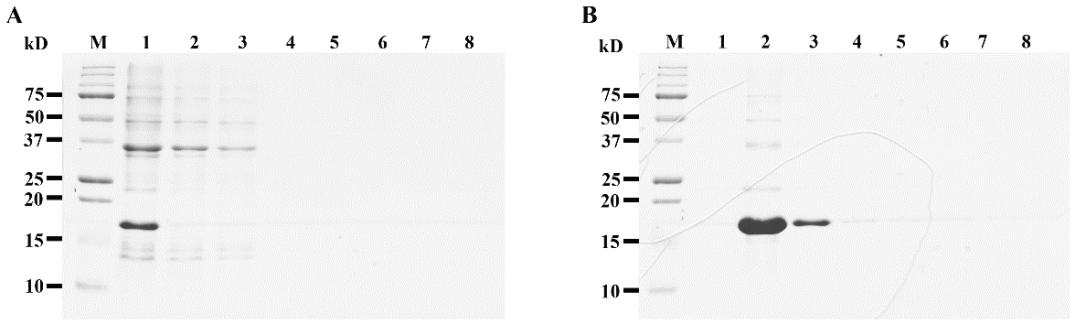

Figure 4.40 A coomassie-stained gel showing purification of recombinant *Pm*Cr cultured for 3 hours after 1mM IPTG induction. Washing fraction (A) and elution fraction (B)

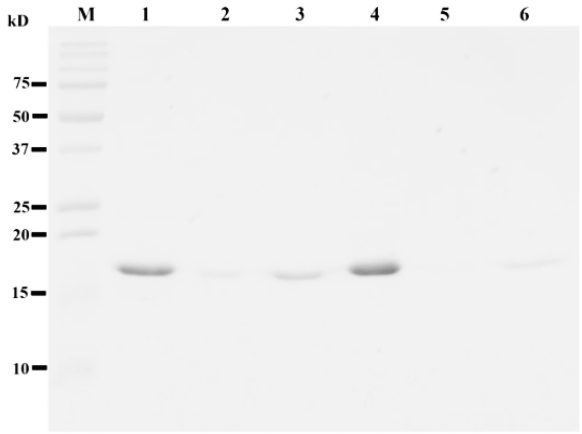

Figure 4.41 A coomassie-stained gel showing purification of recombinant *Pm*Cr from Model 422 Electro-Eluter. Lane 1-3: lower, upper and intermediate fraction of column 1, lane 4-6: lower, upper and intermediate fraction of column 2, respectively

4.6.4 Tissue distribution of the C-type lectin protein

The tissue distribution of this C-type lectin protein in plasma, hemocyte, gill, heart, midgut, hindgut, stomach and hepatopancreas was determined. The western blot analysis showed that the C-type lectin protein was detected in midgut, hindgut, stomach and hepatopancreas, but not in plasma, hemocyte, gill and heart (Figure 4.42).

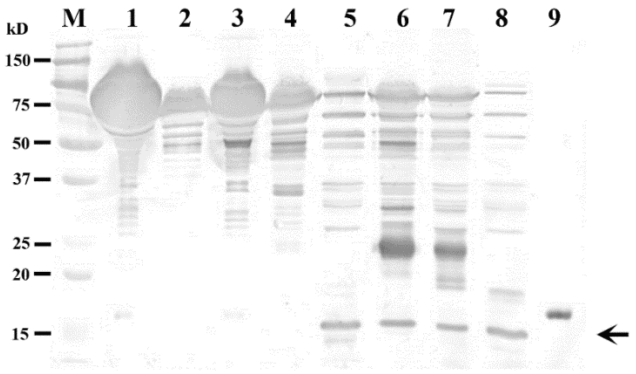

Figure 4.42 Western blot analysis of the distribution of *Pm*Cr protein (arrow) in normal shrimp using anti-*Pm*Cr (dilution 1:500). Lane M: marker, lane 1: plasma, lane 2: hemocyte, lane 3: gill, lane 4: heart, lane 5: midgut, lane 6: hindgut, lane 7: stomach, lane 8: hepatopancreas and lane 9: a recombinant protein *Pm*Cr

4.6.5 Bacterial binding

The binding activity of the refolded recombinant *Pm*Cr protein to bacteria (*M. luteus*, *S. aureus*, *V. harveyi* and *V. parahaemolyticus*) was determined. The western blot analysis showed that the refolding recombinant *Pm*Cr protein could bind to *M. luteus* the most followed by *V. harveyi*, *S. aureus* and *V. parahaemolyticus* in decreasing order (Figure 4.43).

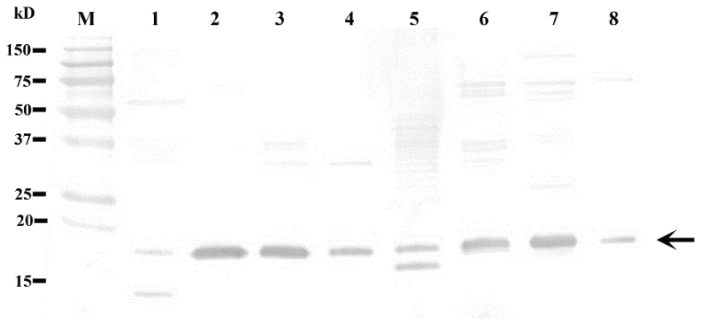

Figure 4.43 Western blot analysis of the binding of recombinant *Pm*Cr (arrow) to *M. luteus* (land 1-2), *S. aureus* (lane 3-4), *V. harveyi* (lane 5-6) and *V. parahaemolyticus* (lane 6-7). Lane 1, 3, 5, 7 are remaining protein and lane 2, 4, 6, 8 are binding protein.

CHAPTER V

DISCUSSION

5.1 The Morphological Digestive Tract of Uninfected and Infected *P. monodon*

The present work provides a description of the interaction between two pathogens, *V. harveyi* or *V. parahaemolyticus*, and the inner surface of the GI tract of farmed *P. monodon* following infections via the oral route, with comments on their appearance, their attachment and their colonization sites based on SEM observations. In healthy shrimp, few bacteria were found attached to the inner surface of the stomach or to the midgut, but bacteria could be observed in the posterior midgut and hindgut. Some bacteria were also seen in association with ingested feed. To show that shrimp pathogens like *V. harveyi* and *V. parahaemolyticus* are capable of colonizing the lining of the digestive tract, a simple oral infection model of pathogenic bacteria-induced gut pathology was used in the current study. This approach of bacterial challenge better resembles an actual infection via the digestive tract in aquaculture settings, and helps to gain an understanding of key features of the pathogenesis in shrimp elicited by *V. harveyi* and *V. parahaemolyticus* in the digestive tract.

In *P. monodon* infected with two pathogenic *Vibrio* species, attachment and colonization of bacteria on the stomach and hindgut lining were observed. The higher number of copies of *V. parahaemolyticus* and *V. harveyi* specific genes in the stomach and midgut of challenged shrimp compared to that of the control shrimp (Figure 4.11) suggest that *V. parahaemolyticus* and *V. harveyi* from the challenge became established in the GI tract of shrimp. *Vibrio spp.* are a natural part of the GI microbiota of shrimp, and some species can cause opportunistic infections during adverse culture conditions. In other studies, both *V. harveyi* and *V. parahaemolyticus* have been found in apparently healthy farmed-raised shrimp showing no symptoms [317-322]. Low but detectable levels of *V. harveyi* and *V. parahaemolyticus* were found in the GI tract of control (unchallenged) shrimp in the present experiment, but their concentration was lower than that of the challenged shrimp. In addition to the higher concentration of *V. harveyi* and *V. parahaemolyticus*, the higher virulence of the introduced *V. harveyi* and *V. parahaemolyticus* strains compared to that of the endogenous ones may explain the

observed attachment and colonization in the challenged group. Since the concentration of *V. harveyi* and *V. parahaemolyticus* in this experiment was determined by specific PCR of only one (*V. harveyi)* or two (*V. parahaemolyticus)* genes, other virulent factors associated with either introduced or endogenous *V. harveyi* and *V. parahaemolyticus* were not examined. The difference in virulence with-in a species of clinical *V. parahaemolyticus* have been reported in the literature. Using multilocus sequence analysis, Theethakaew et al [323] reported a distinct cluster of human pathogenic *V. parahaemolyticus* isolates among other environmental *V. parahaemolyticus* isolates in the environment and suggested a high degree of genetic diversity within the species. Other *in situ* techniques such as Fluorescent *in situ* Hybridization (FISH) could provide the most definitive evidence associated *V. harveyi* or *V. parahaemolyticus* at infection sites. At present, FISH analysis of shrimp's stomach and intestinal tissues remains difficult due to auto-fluorescence [324,325].

A few bacterial cells were found to adhere to the peritrophic matrix (PM) or to the gut contents throughout the midgut, except for the posterior end of the midgut where it is connected to the hindgut (Figure 2A, B, E, E, H, I). No bacterial cells were observed between the PM and the epithelium of the midgut or the ectoperitrophic space. The absence of bacterial flora in the ectopertrophic space of the midgut in *P. monodon* in the present study is consistent with observations reported in other marine crustaceans. Martin *et al.* [326] demonstrated that no bacteria were associated with the brush border or were in the ectoperitrophic space of the midgut of ridgeback prawn *Sicyonia ingentis.* Likewise no evidence of bacterial colonization in the midgut of mud shrimps *Calocaris macandreae* was reported [327]. Bacteria capable of attachment to the midgut area could potentially be long-term residents in the midgut due to the fact that this area is not shed during molting. Similar observations were made in an SEM and TEM study of the digestive tract of the hydrothermal vent amphipod *Ventiella sulfuris* [328]. The authors of this study speculated that long rod-shaped bacteria found between the microvillous epithelial cells could be considered as long-term residents within the bacterial community of the midgut due to its locality in the midgut and the healthy appearance of epithelia in contact with the bacteria [328].

In insects and crustaceans, the lining of the GI lumen consists of a thin but tough peritrophic matrix which is quite unlike the thick mucosa seen in mammalian guts. The PM is a semi-permeable, non-cellular structure, which surrounds the food bolus and is composed of chitin, glycoproteins and mucins, providing a chemical and physical barrier against infection by ingested pathogens [326,329,330]. The PM of the *P. monodon* specimens used in the present study are similar to those described in other penaeid shrimp, *e.g. S. ingentis,* which has very small pores that will allow only inert particles less than 20 nm to pass through the PM [326]. Although the PM can provide resistance to pathogenic bacteria, *e.g.* as in *Daphnia magna* [331]; can trap enteropathogenic *Aeromonas caviae* in houseflies *Musca domestica* [332]; and, can limit infection by baculovirus in the moth *Trichoplausia ni* larvae [333], some bacteria can secrete enzymes to degrade the PM resulting in large holes in the membrane allowing bacteria to subsequently colonize the epithelial layer [334]. Moreover, some pathogens such as *V. parahaemolyticus* do not need to penetrate the PM to cause damage because they can produce toxins that are able to pass through the PM of *S. ingentis* [335]. The presence of a PM is one reason why there are no bacteria associated with the brush border of the epithelium; another reason can be that the mucosal immunity within the shrimp's gut may directly and tightly control the number of microbes [336].

Although all *P. monodon* specimens that were used in this study were collected from a commercial farm and were apparently healthy, one specimen was found to have an abundance of a single morphotype rod-shaped bacterium with fimbria-like fibres extensively adhering to the cuticular lining of the stomach. The inner surfaces of the stomachs from the other four specimens of *P. monodon* that were collected at the same time were devoid of microbes. As it is in other animals, an important property of a pathogenic bacterium in shrimp is its ability to gain an appropriate attachment as this is the initial step in the infection process. It is possible that this particular specimen of *P. monodon* may have already been infected by pathogenic bacteria, since it is unusual that ingested microbes can colonize and establish within a harsh environment as the stomach.

All *P. monodon* used in this study were seen to have bacteria attaching to the surface of the hindgut or to the posterior part of the midgut wall where it connects with the start of the hindgut. These findings support those of Harris [337] who reported that the presence of bacteria in the hindguts of Crustacea are widespread, occurring throughout taxa belonging to marine Thalassinidae and Brachyura (9 genera, 16 species). There was, however, a high degree of variability between specimens in both the types and the total numbers of bacteria in the hindguts, indicating that this bacterial population may be regulated by its host. It has been suggested that molting may have a direct influence on the bacterial communities within the hindgut [338,339]. For each molting cycle of the exoskeleton, the chitinous hindgut lining is displaced and replaced with a new lining [340]. While there is no report in the literature on the effect of molting on the hindgut microbiota of shrimp, the newly molted hindgut surface was shown to be devoid of microbes in a study on desert millipedes *Orthoporus ornatus* [341]. It is not currently known how microbes recolonize in the hindgut after molting. From our observations in penaeid shrimp, however, it can be hypothesized that the bacteria attached to the posterior part of the midgut, *i.e.* immediately adjacent to the hindgut, can function as a bacterial inoculum. The presence of bacteria in the posterior midgut in our study supports this hypothesis.

The hindgut environment with its chitinous lining has been shown to be a suitable place for the colonization of bacteria. Not only it is a preference for hindgut attachment in some species of bacteria, but there also appears to be some selective pressure from the host on the types of bacteria present in the hindgut. For example, *V. cholerae* has been reported to preferentially attach to the hindgut of the blue crab *Callinectes sapidus*, but not to the midgut [342]. Selective pressure from bay ghost shrimp *Neotrypaea californiensis* was shown to limit the number of bacterial taxa present in its hindgut [343]. It is likely that hindgut bacterial community in the gut of *P. monodon* is specific for this host and that the majority of bacteria that are attached are *Vibrio* spp. The dominance of *Vibrio* spp. in the GI tract of *P. monodon* has been shown in several studies looking at the bacterial communities in both wild and cultured populations of shrimp [344-347]. Similarly, *Vibrio* spp. were shown to be dominant in the hindgut of white shrimp *L. vannamei* [345].

Adhesion of pathogenic bacteria to the inner surface of the GI tract is crucial to the subsequent establishment of an infection, however, the manner to which *V. harveyi* and *V. parahaemolyticus* attach the epithelial surface of their host is very different from each other. From the results, it is most likely that *V. harveyi* binds to the surface of the stomach and to the epithelial layer of the midgut, while *V. parahaemolyticus* only colonizes the surface of the stomach. In addition, *V. parahaemolyticus* colonizes as a monolayer of cells, while *V. harveyi* colonizes as a multilayered cluster of bacteria. Similar preferences for the site of adhesion have been seen in host-bacteria interactions. The ability of *V. cholerae* to colonize the hindgut surface of the blue crab *Callinectes sapidus,* but not the midgut has been shown, led authors of the study to suggest that chitin was required in the attachment of *V. cholerae* to invertebrate and zooplankton surfaces [342]. In crustaceans and other arthropods, the preferred area for bacterial establishment is the hindgut, which is covered by a chitinous cuticle that provides anchoring surfaces for bacteria and favours symbiotic interactions [343,348]. It has been suggested that in natural marine systems, most bacteria attaching to chitinaceous particles are *Vibrios* [349]. Living crustacean surfaces which possess chitinous components are noted for supporting bacterial attachment and growth [350].

Production of flagella or pili by intestinal bacteria can have an important role in colonization and infection. Induction of peritrichous flagella is associated with conversion of *V. parahaemolyticus* from small (av. 2-3 μm long), polarly flagellated swimmer cells to swarmer cells, which are elongated (av. 5-20 um long) as well as peritrichously flagellated [351,352]. Interestingly, we observed lateral cell appendages were produced by the attached *V. parahaemolyticus* in the present experiment, suggesting that these cells have switched from the swimmer cell to the swarmer cell state. Many pathogenic bacteria such as pathogenic *E. coli* exhibit pili or fimbriae that facilitate their initial attachment to epithelial cells and subsequent successful colonization of their host [353,354]. Pili are virulence factors that mediate interbacterial aggregation and biofilm formation, or mediate the specific recognition of host-cell receptors [355]. It is clear that pili play similar biological roles for commensal bacteria because they also have to colonize specific niches and overcome the host's natural clearing mechanisms. Although *V. parahaemolyticus* is a leading cause of life-threatening gastroenteritis in human, it is most likely that *V. parahaemolyticus* exhibits

lower virulence and has a slower proliferation than *V. harveyi* in *P. monodon*, as indicated by the lack of infection in the midgut at 24 h PI. This might be because the microenvironment in the gut of *P. monodon* is not optimal or suitable for *V. parahaemolyticus*.

Our observations confirm that both *V. parahaemolyticus* and *V. harveyi* in the present study are shrimp pathogens and their attachment properties, that are a prerequisite for the pathogenesis, are similar to those of other pathogens. The typical infectious cycle of these pathogens in *P. monodon* includes: 1) entry of the pathogen through the oral route; 2) bind to chitin on the stomach lining or to the midgut peritrophic matrix, then multiply and cause damage to the host tissues; and, 3) exit from the host. Each step would involve adhesion, chemotaxis, production of various lytic enzymes such as haemolysis, secretion systems of the type II or type III secretion system, biofilm formation, and production of quorum sensing systems [356]. Examination of all the *P. monodon* hindguts in the current study, including the infected specimen, found numerous bacteria attached randomly across the hindgut luminal surface, both singly and in large, biofilm like microcolonies, some of which contained mats of bacterial cells. Since the morphotype of the bacteria attached in the hindgut differed from *V. harveyi* and the *V. parahaemolyticus* morphotype, and that the posterior region adjacent to the upper part of the hindgut was not infected by either of these bacteria, the attached bacteria in the hindgut could be considered to be resident and not pathogenic. All the evidence indicates that these bacteria are not pathogenic and that their presence is not detrimental to the host tissues. If these hindgut bacteria are part of the normal bacterialcommunity in *P. monodon*, then their putative roles or beneficial effects to their host needs to be elucidated.

5.2 Histopathology of Uninfected and Infected *P. monodon* by AHPND/EMS Bacteria (*V. parahaemolyticus* 3HP)

This study investigates the infection of *V. parahaemolyticus* 3HP in stomach and hepatopancreas using oral infection via *Artemia*. Bacteria were seen attaching to stomach cuticle, and a little lesion was formed in hepatopancreas at 3 hours post infection. The necrotic symtoms were first observed at 6-24 hours post infection. The

hepatopancreas tubular epithelial cells were sloughed into the hepatopancreas lumen. The sloughing of hepatopancreatic tubule epithelial cells, non-vacuolated E-cells and a largh number of hemocyte infiltation in the hepatopancreas, it is likely that AHPND infection has been previously observed [16,17,19,21,48]. The results indicated that *Artemia* can be used to successfully induce AHPND infection. Since the first stage of stomach infection was observed at 6 hour post infection; therefore, the differential gene expression profile in stomach between un-infection and infection shrimp was performed at 6 hour post infection.

5.3 Differentially Expressed Genes (DEGs) in the Stomach of Uninfected and Infected *P. monodon* by AHPNS/EMS Bacteria

5.3.1 Suppressive subtractive hyridization (SSH) stomach cDNA libraries

The DEGs profile stomach cDNA libraries at 6 hours post infection was conducted using suppressive subtractive hybridization. The study presented several responses in stomach to *V. parahaemolyticus* 3HP infection including physical barriers (cuticle and chitin), chemical response (salivary alkaline phosphatase, ubiquitin conjugating enzyme), cell proliferation (astakine) and immune defense (pacifastin heavy chain).

The efficiencies of SSH cDNA libraries were basically confirmed by RT-PCR showing the reduced expression level of EF1α in cDNA SSH compared with cDNA without SSH. Preliminary results suggest the success of SSH cDNA libraries construction. However, the SSH analysis has a disadvantage, because this method cannot eliminate all the redundant cDNAs, if the genes are high expression level or that variation is large [357]. Consequently, both forward and reverse libraries were constructed in this study. Additionally, relative qPCR was performed to validate the result from SSH libraries.

For forward library, 48 sequences (42.1%) shared similarity to known sequences in Genbank, and 66 sequences (57.9%) did not share similarity with any sequence in the current database. These 66 sequences were classified as novel genes. High level of non-homologous sequences in forward cDNA library indicated that

several genes involved in the response to stomach infection have not be identified. Moreover, the discovery rate of new transcripts after 306 recombinant clones did not reach a plateau of saturation (30.21%) indicating that new transcripts could be continually identified by further screening. Functional analysis with gene ontology showed that several genes were structural constituents of the cuticle (Table 4.2). This results suggested that the cuticle is important to defend against pathogenic bacteria. The cuticle is the first line of defense as a physical barrier in foregut (stomach) and hindgut of insect [84]. DD9A and DD9B were isolated from the epidermis of the abdominal and tail parts of the kuruma shrimp *P. japonicus* [358]. Kulkarni et al. [27] studied protein profiling in the gut *P. monodon*, and showed that DD9B was over-expressed in gut at 4 hours post infection with WSSV. The results suggest that DD9B might be involved in defense mechanisms in stomach.

In addition, relative qPCR showed that the expression level of salivary alkaline phosphatase and pacifastin heavy chain precursor were significantly up-regulated at 6 hours post infection. The expression level of AMP1B, clottable protein, Ig-like and cathepsin B was slightly up-regulated, and DD9A, C-type lectin and Spz1 were dramatically up-regulated but not significantly. This results suggest that this forward stomach cDNA libraries could be represented by gene up-regulation. This results also indicate that salivary alkaline phosphatase and pacifastin heavy chain precursor might be parts of an important immune response in stomach of *P. monodon*. Beumer et al. [359] showed that the alkaline phosphatase derived from calf intestine (CIAP) was able to reduce *E. coli* in mice and piglet blood [360]. Additionally, they also reported that the intestinal alkaline phosphatase was able to detoxify and prevent bacterial invasion in the gut mucosal barrier [360]. Although the influence of alkaline phosphatase was mostly studied in vertebrates, its activity showed that it could prevent bacterial infection possible also in shrimp. Pacifastin family, proteinase inhibitors, was first characterized in crayfish *Pacifastacus leniusculus* including pacifastin heavy chain (105 kDa) and pacifastin light chain (44 kDa) [184,361]. In shrimp, pacifastin heavy chain was characterized in giant freshwater prawn *M. rosenbergii*. The expression level of *Mr*-PHC was up-regulated in both postlarval stage 45 and adult after challenge with *A. hydrophila* [362].

For reverse library, 57 sequences (57.6%) shared similarity to known sequences in Genbank, and 42 sequences (42.4%) did not share similarity with any sequences in the current database. These 42 sequences was classified as novel genes. High levels of non-homologous sequences in the forward cDNA library indicate that several genes might be involved in stomach shrimp response. Moreover, the discovery rate of new transcripts after 306 recombinant clones still did not reach a plateau of saturation (16.98%) indicating that new transcripts could be continually identified by further screening. Functional analysis with gene ontology showed several genes were related to chitin metabolic processes (Table 4.3). Chitin is a scaffold material to support epidermal cuticle and peritrophic matrix in the gut epithelium of insects and crustaceans [329,363]. Additionally, relative qPCR showed that the expression level of chondroitin proteoglycan 2 was significantly up-regulated at 3 hours post infection and rapidly down-regulated at 6 hours post infection.

In addition, relative qPCR showed that the expression level of 4 genes from the reverse stomach cDNA library was down-regulated (44.4%). The results indicate that only 44.4% of genes could be represented by a down-regulation from the reverse library. It may be from false positives of the SSH method during PCR amplification [357]. However, five genes from the reverse library including ubiquitin-conjugating enzyme H5b, ferritin, astakine variant 1 and dicer 2 showed a significant increase in expression at 6 hours post infection. These results suggest that they might be involved in shrimp immune responses in the stomach. Ubiquitin conjugating enzyme has been shown to respond to both bacterial and viral infection in shrimp. Pongsomboon et al. [364] reported that ubiquitin conjugating enzyme E2-230k and H5b were up-regulated in hemocytes after WSSV, YHV or *V. harveyi* infection at 6, 24 or 48 hour in *P. monodon* using cDNA microarray analysis. A ubiquitin-conjugating enzyme E2 from the Chinese white shrimp *F. chinensis* was significantly down-regulated in hepatopancreas after WSSV infection at 6-24 hours. It was also down-regulated in intestine at 2 hours post infection; however, it was significantly up-regulated at 12 hours post infection [365]. Additionally, the expression profile of ubiquitin conjugating enzyme was up-regulated after challenge with WSSV at 24 hours post infection in *P. monodon* indicating that it might be involved in ubiquitination pathway of *P. monodon* during viral infection [366]. The expression level of ferritin was up-regulated after a

pH change (9.3 and 5.6) in *L. vannamei* [367], and exposed to iron in chinese white shrimp *F. chinensis* [368] and *M. rosenbergii* [369]. The expression of ferritin was changed under stress circumstances, *i.e*. bacterial or viral challenge in many penaeid species. Astakine is directly involved in proliferation, differentiation, and survival of hematopoietic tissue cells in *P. leniusculus* [370] and in *P. monodon* [371]. Additionally, astakine was involved in viral defense in *L. vannamei* [372]. Dicer is a key component in RNA interference (RNAi) pathway. Dicer 1 was involved in viral defense and dicer 2 was involved in viral and bacterial defense in *P. monodon* [373,374].

5.3.2 Transcriptome of DEGs of stomach cDNA libraries by ion torrent sequencing

The present work presents immune response genes in stomach of *P. monodon* after challenge with *V. paraheamolyticus*$_{3HP}$. The immune-related genes were categorized into 11 functions via the manual literature review [375] including antimicrobial peptides, signal transduction pathways, proPO system, oxidative stress, proteinases/proteinase inhibitors, apoptotic tumor-related proteins, pathogen recognition immune regulators, blood clotting system, adhesive protein, heat shock proteins and other immune genes.

From the SSH cDNA libraries, the discovery of new transcripts still did not reach a plateau of saturation. Therefore, the transcriptome of cDNA stomach during EMS/AHPND infection was constructed using Ion torrent PGM sequencing. One thousand five hundred and fourteen unique genes (3.5%) of significantly DEGs between control and challenge group was found, and 141 unique genes (9.3%) are involved in the immune system. From this study, a novel isoform of anti-lipopolysaccharide (ALF) was found in the DEGs of the stomach. The tissue distribution in normal shrimp showed that it is highly expressed in the stomach and lymphoid organ, but low expression was found in hemocytes. The transcript was significantly induced in stomach at 6 and 12 hours post infection. The results suggest that this isoform is possibly involved in defence response in stomach of *P. monodon*. Therefore, the novel isoform was called *Pm*ALF7.

RNA-Seq analysis is useful to exhibit the profile DEGs during the pathogenic infection in shrimp [110,376,377]. Twenty two immune-related genes were randomly selected to confirm the RNA-Seq result. Relative qPCR was performed with two sources of samples including the same sample prepared for RNA-seq (technical validation) and the new samples collected at 6 hours post infection (biological validation). Overall, there were significant correlations between RNA-seq and technical validation or biological validation with coefficients 0.83 and 0.71 (20 from 22), *p*-value <0.001, respectively. This results indicate that RNA-seq presented the level of gene expressed profiles during stomach infection. However, the direction of expression was different in several genes, *i.e.* masq-SP, laminin receptor, crustin 3 and DAAD for technical validation, *i.e.* mitogen and DAAD for biological validation. This dissimilarity might be from the different expression of replicates or the inaccuracy of RNA-seq. In addition, the expression of PPAE2 and SPI6 in technical validation was higher than RNA-seq. Those genes have several isoforms with similar nucleotide sequence; therefore, the qPCR primers of those might be able to bind to more than one isoform [165,188]. Here, the highlights of innate immune system are displayed that might be related to stomach immune response to *V. paraheamolyticus*$_{3HP}$.

5.3.2.1 Antimicrobial peptide

Antibacterial peptides have a broad spectrum in activity towards bacteria. The results show that 2 isoforms of ALF are participating in stomach immune response including *Pm*ALF6 and *Pm*ALF7 (a novel isoform). Ponprateep et al. [109] showed that *Pm*ALF3 is the main, and *Pm*ALF6 is an additionally AMP in hemocytes after challenge with *V. harveyi* and WSSV. From RNA-seq in this study, *Pm*ALF6 and *Pm*ALF7 were shown to have a significant induction at 6 h (3.83 and 3.17 fold, respectively) after challenge with *V. parahaemolyticus* (Table 4.7). The relative qPCR also showed that the transcript of *Pm*ALF7 was highly expression in stomach and lymphoid organ of normal shrimp and significant up-regulated in stomach after challenge with *V. parahaemolyticus* at 6 and 12 h (Figure 4.38 and 4.39). From previous study, *Pm*ALF3 showed no induction in the stomach, but was highly induced in intestine at 3, 6, 12, 24 and 48 h post infection with *V. harveyi* [336]. Therefore,

*Pm*ALF3 is likely the major ALF to protect the microbial invader in hemocytes and intestine, whereas *Pm*ALF6 and *Pm*ALF7 are possibly important ALFs in stomach.

In this study, crustins was down-regulated in expression at 6 h post infection. Crustin is a crustacean anti-bacterial peptide and is mainly expressed in hemocytes. In *P. monodon*, five different isoforms were reported by the group of Tassanakajon [122]. Crustin-like antimicrobial peptides (Crustin-like*Pm*) was down-regulated at the early time points after injection (6 h) and reached a peak of the expression at 24 h post injection in hemocytes. It is likely that the expression profile of crustin was down-regulated before up-regulated after infection, it is similar with our study that crustin was down-regulated at early stage of infection at 6 hours post infection.

5.3.2.2 Signal transduction

The present study shows that the transcripts of IMD was down-regulated, whereas relish was up-regulated during stomach infection indicating that IMD and Relish are possibly involved in regulation of antimicrobial peptides in the basal membrane of stomach. Immune deficiency (IMD) pathway is a main regulation of antimicrobial production in basal membrane of insect intestine [58,84,272]. The components of *Drosophila* IMD pathway consist of PGRP-LC receptor, IMD, the mitogen-activated protein 3 kinase (TAK1), TAB2, DIAP2, IKK signalosome, the dFADD adaptor, the Dredd caspase and the transcription factor Relish [58]. In shrimp, IMD proteins were characterized in *F. chinensis* and *L. vannamei* indicating that IMD likely play an important role in bacterial defense against pathogenic infection [67,378]. Silencing of *Lv*IMD had an influence and a low production of ALF and *Lv*Relish showing that regulation of ALF and *Lv*Relish production may be through IMD pathway [67]. Moreover, silencing of *Pm*Relish had an effect on penaeidin5 mRNA levels, but not on *Pm*ALF3 or *Pm*Crustin1 [379].

In this study, cytokine receptor or Domeless was up-regulated in the stomach after bacterial challenge at 6 hours post infection revealing its likely relation to bacterial defense and regeneration of the epithelial membrane during an infection. The JAK/STAT pathway displays crucial roles in gut homeostasis and tissue regeneration of *Drosophila* [282]. The major components of JAK/STAT pathway in

Drosophila consist of cytokine-like molecules (Upd1, Upd2 and Upd3), cytokine receptor (Dome), the JAK kinase Hopscotch (Hop), and the transcriptional regulator Stat92E [380]. In shrimp, Stat was first characterized in *P. monodon* suggesting that it was possibly activated by WSSV [284]. Stat of *F. chinensis* was also identified and the transcripts of *Fc*Stat were up-regulated in hemocytes, hepatopancreas, and intestine after challenge with *V. anguillarum* [285]. *Mj*Stat was up-regulated in lymphoid organ of *M. japonicus* after induction with peptidoglycan and polycytidylic acid [381]. Recently, *Lv*JAK, and *Lv*Dome were characterized indicating that they were induced by WSSV [382,383].

5.3.2.3 proPO system

In this study, several genes of prophenoloxidase (proPO)-activating system were found, *i.e.* clip domain serine proteinase, masquerade, prophenoloxidase activating factor/enzyme, serine proteinase and serine proteinase inhibitor. The proPO system is a part of innate immune defenses in invertebrates and consists of several proteins involved in this system leading to melanin production, cell adhesion, encapsulation and phagocytosis [152,155,183].

Microbial components are the stimulators of the proPO activating system, which will result in production of several biologically active factors [152,153,155,384]. After stimulation, a serine proteinase cascade triggers activation of the proform of proPPA into PPA which is the active form which cleaves proPO into active PO [156]. Regulators of the proPO system are serine proteinase inhibitor [385]. In *P. monodon*, *Pm*proPOs and PPAEs were suggested to have crucial roles in immune defense during *V. harveyi* injection [25,164]. Serine proteinase inhibitor (SERPIN) is identified as a protease inhibitor. *Pm*SERPIN3, *Pm*SERPIN6 and *Pm*SERPIN8 showed the function in innate immune system of shrimp [186-188]. The proPO system is a crucial system in humoral immunity.

5.3.2.4 Oxidative stress

The results show that thioredoxin was induced, but glutathione was reduced in expression levels during pathogenic infection at 6 h in this study. Similarly, thioredoxin was induced at 6 h after injection with *Listonella anguillarum* in Chinese

mitten crab *E. sinensis* [386]. Reactive oxygen species (ROS) are known for its role in epithelial response to pathogens in the gut of *Drosophila* [58]. Glutathione (GSH) and thioredoxin a buffer systems during cellular thiol/disulfide redox state [387]. In addition, the result also showed that kelch-like protein 26 and kelch-like ECH-associated protein 1 were highly induced to 2.18 and 5.18 fold during infection, respectively. They might able to respond by cell proliferation to pathogens during an infection. Kelch-like ECH-associated protein 1 (keap1) is a crucial protein to control cell proliferation in intestine of *Drosophila* [388]. Keap1 was also induced after lansoprazole stimulation. Lansoprazole stimulation is a drug used to prevent stomach and intestinal damage [389].

5.3.2.5 Proteinases/proteinase inhibitor

This results show that two homologous of alkaline phosphatase were induced. There are 4 functions of alkaline phosphatase in intestine including intestinal absorption of lipid, regulation of duodenal bicarbonate secretion, detoxification of bacterial endotoxin (LPS) and regulation of trans-mucosal passage of bacteria [390]. The intestinal alkaline phosphatase of zebrafish was induced by purified LPS [391]. Moreover, alpha 2 macroglobulin homologues were induced during infection. Alpha 2 macroglobulin is a proteinase inhibitor that is induced by bacterial, viral and fungal infection [392-394]. In addition, alpha 2 macroglobulin prevents the escape of bacteria from blood clotting system in *P. monodon* [395] indicating its possible role in protecting bacterial infection in the stomach epithelia.

5.3.2.6 Apoptotic tumor-related protein

Moreover, two homologues capsizes were highly induced to 2.4 and 3.3 fold. It is similar to results obtained in Chinese mitten crab *E. sinensis* and white shrimp *L. vannamei*, caspase [396,397]. Therefore, alkaline phosphatase and capsizes might be involved in stomach immune response.

5.3.2.7 Pathogen recognition proteins (PRP)

In this study, lectins were found to be pathogen recognition proteins. This study displays that homologous C-type lectins, fibrinogen C domain, galectin and L-type lectin were up-regulated post -infection in stomach. This result suggests that

lectins play a crucial role in immune response in stomach of shrimp. There are 7 types of lectins that are discovered in shrimp including C-type, L-type, M-type, P-type, fibrinogen-like domain lectins, galectins, and calnexin/calreticulin [206]. C-type lectin and fibrinogen domain proteins are abundant as lectins in shrimp and they have a broad spectrum in defending against bacteria and virus [24,207,208,211,217,232,398,399]. L-type lectin was up-regulated in transcript after challenge with *V. anguillarum*, and it was found to agglutinate both Gram-positive and Gram-negative bacteria and promoted phagocytic activity in *M. japonicas* [400].

5.4 The Full Length cDNA of C-type Lectin in Hepatopancreas

C-type lectins are considered crucial pattern recognition proteins in innate immunity and they play significant roles in non self recognition [204] and clearance of invading microorganism [401]. C-type lectins function in a calcium-dependent manner and are involved in immune recognition in invertebrates [204]. This study showed that *Pm*Cr transcript was expressed higher in hepatopancreas than all other tissues. Previous study showed that the transcripts of C-type lectin was reported in various tissues, *i.e.* *Pm*AV and *Pm*LT transcripts were expressed in hepatopancreas, *Pm*Lec transcripts were expressed in hepatopancreas, intestine, hemocytes and stomach as well as *Lv*LT transcripts were also expressed in hepatopancreas. The hepatopancreas is a major tissue for C-type lectin expression [206]. Additionally, the *Pm*Cr protein was found in hepatopancreas, stomach, midgut and hindgut. Therefore, *Pm*Cr protein might be produced in hepatopancreas and then secreted to the stomach, midgut and hindgut. The transcript of *Fc*Lec1 from *F. chinensis* was expressed in hepatopancreas and stomach, while *Fc*Lec1 was expressed in plasma and hepatopancreas. Additionally, the transcript of *Fc*Lec2 was expressed in hepatopancreas and stomach, while *Fc*Lec2 was found in hepatopancreas, stomach and intestine [206].

The transcript pattern of *Pm*Cr was significantly down-regulated at 6 hours post infection with *V. parahaemolyticus* and, the *Pm*Cr binding to *V. parahaemolyticus* was lower than *M. luteus*, *S. aureus*, *V. harveyi*. The results suggest that *Pm*Cr may have a little importance to *V. parahaemolyticus* infection in shrimp. However, more functions of *Pm*Cr have to be studied.

CHAPTER VI

CONCLUSIONS

The attachment and colonization of pathogenic and non-pathogenic bacteria to the gastrointestinal tract of *P. monodon* and the responses of *P. monodon* immunity were examined and compared using scanning electron microscopy (SEM), suppression subtractive hybridization (SSH) and RNA sequencing (RNA-seq).

1. Both pathogenic and non-pathogenic bacteria can pass through the gastrointestinal tract. Pathogenic bacteria, *i.e. V. harveyi* and *V. parahaemolyticus* can establish, proliferate, and cause tissue damage, especially to the epithelial layer of stomach. However, no tissue damage was seen in the posterior midgut or in the hindgut. This result indicated that the tissue most affected by these two pathogens is the stomach.

2. Among 18 genes were randomly selected from SSH and were examined using real-time PCR. Significant up-regulation of 5 genes *i.e.* salivary alkaline phosphatase, pacifastin heavy chain precursor, ubiquitin-conjugating enzyme H5b, ferritin, astakine variant 1 and dicer 2 homologues were found in the stomach at 6 hours post infection. This result indicated that these genes might be involved in the stomach response of *P. monodon*. Other gene responses in stomach of *P. monodon* during infection included physical barriers (cuticle and chitin), chemical response (salivary alkaline phosphatase and ubiquitin conjugating enzyme), cell proliferation (astakine) and immune defense (pacifastin heavy chain).

3. Following RNA-seq result of control and challenged shrimp, a set of 141 immune-related genes classified into 10 functions including antimicrobial peptides, signal transductions, proPO system, oxidative stress, proteinases/proteinase inhibitors, apoptotic tumor-related proteins, pathogen recognition immune regulators, blood clotting system, adhesive proteins and heat shock proteins were reported. This finding indicated that there are many mechanisms involving in stomach response during infection.

4. A novel anti-lipopolysaccharide was discovered in the DEGs called *Pm*ALF7, and the open reading frame is 369 bp encoding 122 amino acids. It has a high expression

in lymphoid organ and stomach. The *Pm*ALF7 transcript is significantly up-regulated in stomach at 6 and 12 hours post infection.

5. C-type lectin (*Pm*Cr) from previous *P. monodon* library was characterized in hepatopancreas. The open reading frame of *Pm*Cr cDNA was 522 bp encoding 173 amino acids. It is dramatically expression in hepatopancreas, and the expression profile of *Pm*Cr showed the significant reduction at 6 hours post infection. The *Pm*Cr protein was detected in hepatopancreas, stomach, midgut and hindgut. Additionally, the recombinant *Pm*Cr protein bound to *M. luteus* the most. These results indicate that *Pm*Cr may be involved in immune response in hepatopancreas of *P. monodon*.

These finding indicated that *P. monodon* responds to the pathogenic infection through the physical barrier and the immune mechanism, while pathogenic bacteria can settle and release the virulent factor to combat to host immunity. These knowledge offers a new insight into the interaction between pathogenic bacteria and the immune response in the gastrointestinal tract of *P. monodon*. It might provide the new strategies for controlling and managing the pathogenic infection in gastrointestinal tract.

REFERENCES

1. Dastidar P, Mallik A, Mandal N (2013) Contribution of shrimp disease research to the development of the shrimp aquaculture industry: an analysis of the research and innovation structure across the countries. Scientometrics 97: 659-674.
2. Austin B (2006) The bacterial microflora of fish, revised. ScientificWorldJournal 6: 931-945.
3. Rawls JF, Samuel BS, Gordon JI (2004) Gnotobiotic zebrafish reveal evolutionarily conserved responses to the gut microbiota. Proc Nat Acad Sci 101: 4596-4601.
4. Harris JM (1993) The presence, nature, and role of gut microflora in aquatic invertebrates: a synthesis. Microb Ecol 25: 195-231.
5. Ringo E, Birkbeck TH (1999) Intestinal microflora of fish larvae and fry. Aquac Res 30: 73-93.
6. Farzanfar A (2006) The use of probiotics in shrimp aquaculture. FEMS Immunol Med Microbiol 48: 149-158.
7. Bassler BL, Gibbons PJ, Yu C, Roseman S (1991) Chitin utilization by marine bacteria: Chemotaxis to chitin oligosaccharides by *Vibrio furnissii*. J Biol Chem 266: 24268-24275.
8. Montgomery MT, Kirchman DL (1993) Role of chitin-binding Pproteins in the specific attachment of the marine bacterium *Vibrio harveyi* to chitin. Appl Environ Microbiol 59: 373-379.
9. Montgomery MT, Kirchman DL (1994) Induction of chitin-binding proteins during the specific attachment of the marine bacterium *Vibrio harveyi* to chitin. Appl Environ Microbiol 60: 4284-4288.
10. Gildemeister OS, Zhu BCR, Laine RA (1994) Chitovibrin: A chitin-binding lectin from *Vibrio parahemolyticus*. Glycoconjugate J 11: 518-526.
11. Brock JA, Lightner DV (1990) Diseases of crustacea diseases caused by microorganisms. Anstalt Helgoland: Hamburg, Germany.
12. Ishimaru K, Akagawa-Matsushita M, Muroga K (1995) *Vibrio penaeicida* sp. nov., a pathogen of kuruma prawns (*Penaeus japonicus*). Int J Syst Bacteriol 45: 134-138.

13. Lightner DV (1983) Diseaese of penaeid shrimp. In: McVey J, editor. Handbook of mariculture vol1 Crustacean Aquaculture. Boca Raton: CRC Press. pp. 289-320.

14. Lavilla-Pitogo CR, Baticados MCL, Cruz-Lacierda ER, de la Pena LD (1990) Occurrence of luminous bacterial disease of *Penaeus monodon* larvae in the Philippines. Aquaculture 91: 1-13.

15. Jiravanichpaisal P, Miyazaki T, Limsuwan C (1994) Histopathology, biochemistry, and pathogenicity of *Vibrio harveyi* infecting black tiger prawn *Penaeus monodon*. J Aquat Anim Health 6: 27-35.

16. Leaño EM, Mohan CV (2012) Early mortality syndrome threatens Asia's shrimp farms. GAA: 38-39.

17. Lightner DV, Redman R, Pantoja C, Noble B, Tran L (2012) Early mortality syndrome affects shrimp in Asia. GAA 15: 40.

18. Flegel TW (2012) Historic emergence, impact and current status of shrimp pathogens in Asia. J Invertebr Pathol 110: 166-173.

19. Joshi J, Srisala J, Truong VH, Chen IT, Nuangsaeng B, et al. (2014) Variation in *Vibrio parahaemolyticus* isolates from a single Thai shrimp farm experiencing an outbreak of acute hepatopancreatic necrosis disease (AHPND). Aquaculture 428-429: 297-302.

20. FAO (2015) Shrimp - March 2015. (Retrieved from: http://www.fao.org/in-action/globefish/market-reports/resource-detail/en/c/338028/, 12 April 2015).

21. Tran L, Nunan L, Redman RM, Mohney LL, Pantoja CR, et al. (2013) Determination of the infectious nature of the agent of acute hepatopancreatic necrosis syndrome affecting penaeid shrimp. Dis Aquat Organ 105: e55.

22. Lemaitre B, Reichhart JM, Hoffmann JA (1997) *Drosophila* host defense: differential induction of antimicrobial peptide genes after infection by various classes of microorganisms. Proc Nat Acad Sci 94: 14614-14619.

23. Tassanakajon A, Klinbunga S, Paunglarp N, Rimphanitchayakit V, Udomkit A, et al. (2006) *Penaeus monodon* gene discovery project: The generation of an EST collection and establishment of a database. Gene 384: 104-112.

24. Ma THT, Benzie JAH, He JG, Chan SM (2008) PmLT, a C-type lectin specific to hepatopancreas is involved in the innate defense of the shrimp *Penaeus monodon*. J Invertebr Pathol 99: 332-341.

25. Amparyup P, Charoensapsri W, Tassanakajon A (2009) Two prophenoloxidases are important for the survival of *Vibrio harveyi* challenged shrimp *Penaeus monodon*. Dev Comp Immunol 33: 247-256.

26. Rungrassamee W, Leelatanawit R, Jiravanichpaisal P, Klinbunga S, Karoonuthaisiri N (2010) Expression and distribution of three heat shock protein genes under heat shock stress and under exposure to *Vibrio harveyi* in *Penaeus monodon*. Dev Comp Immunol 34: 1082-1089.

27. Kulkarni AD, Kiron V, Rombout JHWM, Brinchmann MF, Fernandes JMO, et al. (2014) Protein profiling in the gut of *Penaeus monodon* gavaged with oral WSSV-vaccines and live white spot syndrome virus. Proteomics 14: 1660-1673.

28. Katesombun B (1992) Aquaculture promotion: endangering the mangrove forests. In: The future of people and forests in Thailand after the logging ban. Bangkok, Thailand. pp. 103-122.

29. Sue J, Paul T. S, Siri T, Michael J. P (1999) An assessment of the status of the shrimp farming industry in Thailand

In: Paul T. S, editor. Coastal shrimp aquaculture in Thailand: Key issues for research: ACIAR Technical Reports , Australia. pp. 14-68.

30. Pillay T (1990) Asian aquaculture: an overview. Aquaculture in Asia Asian Fisheries Society, Indian Branch, Department of Aquaculture, College of Fisheries, Mangalore, Karnataka, India: 31-42.

31. Flegel TW, Fegan DF, Kongsom S, Vuthikornudomkit S, Sriurairatana S, et al. (1992) Occurrence, diagnosis and treatment of shrimp diseases in Thailand. Diseases of cultured penaeid shrimp in Asian and the United States. The Oceanic Institute, Honolulu, HI: 57-112.

32. Karunasagar I, Pai R, Malathi GR, Karunasagar I (1994) Mass mortality of *Penaeus monodon* larvae due to antibiotic-resistant *Vibrio harveyi* infection. Aquaculture 128: 203-209.

33. Flegel TW (1997) Major viral diseases of the black tiger prawn (*Penaeus monodon*) in Thailand. World J Microbiol Biotechnol 13: 433-442.

34. Chayaburakul K, Nash G, Pratanpipat P, Sriurairatana S, Withyachumnarnkul B (2004) Multiple pathogens found in growth-retarded black tiger shrimp *Penaeus monodon* cultivated in Thailand. Dis Aquat Organ 60: 89-96.

35. Tanticharoen M, Flegel TW, Meerod W, Grudloyma U, Pisamai N (2008) Aquacultural biotechnology in Thailand: the case of the shrimp industry. Int J Biotechnol 10: 588-603.

36. Nielsen L, Sangoum W, Cheevadhanarak S, Flegel TW (2005) Taura syndrome virus (TSV) in Thailand and its relationship to TSV in China and the Americas. Dis Aquat Organ 63: 101-106.

37. Primavera JH (1990) External and internal anatomy of adult penaeid prawn/shrimps. SEAFDEC. Aquaculture Department, The Philippines, Poster.

38. Arkarajamorn A (1991) Histology of tiger shrimp (*Penaeus monodon* Fabricius). Kasetsart University: Kasetsart University. 168 p.

39. Lavilla-Pitogo CR, Leaño EM, Paner MG (1998) Mortalities of pond-cultured juvenile shrimp, *Penaeus monodon*, associated with dominance of luminescent vibrios in the rearing environment. Aquaculture 164: 337-349.

40. Leaño EM, Lavilla-Pitogo CR, Paner MG (1998) Bacterial flora in the hepatopancreas of pond-reared *Penaeus monodon* juveniles with luminous vibriosis. Aquaculture 164: 367-374.

41. Lightner DV (1993) Diseases of cultured penaeid shrimp. In: McVey JP, editor. CRC handbook of mariculture. Maryland, USA. pp. 393-486.

42. Takahashi Y, Shimoyama Y, Momoyama K (1985) Pathogenicity and characteristics of *Vibrio* sp. isolated from cultured kuruma prawn *Penaeus japonicus* Bate. B Jpn Soc Sci Fish 51: 721-730.

43. Anderson I, Shamsudin MN, Din M, Shariff M, Nash G (1988) Bacterial septicemia in juvenile tiger shrimp, *Penaeus monodon*, cultured in Malaysian brackishwater ponds. Asian Fish Sci 2: 93-108.

44. NACA (2012) Report of the Asia Pacific emergency regional consultation on the emerging shrimp disease: early mortality syndrome (EMS)/ acute hepatopancreatic necrosis syndrome (AHPNS). 9-10 Aug 2012 ed: Network of

Aquaculture Centres in Asia-Pacific, Bangkok, Thailand (Retrieved from: http://library.enaca.org/Health/Publication/ahpns-emergency-consultation-report.pdf).

45. Drake SL, DePaola A, Jaykus L-A (2007) An overview of *Vibrio vulnificus* and *Vibrio parahaemolyticus*. Compr Rev Food Sci F 6: 120-144.
46. Han JE, Tang KFJ, Tran LH, Lightner DV (2015) *Photorhabdus* insect-related (Pir) toxin-like genes in a plasmid of *Vibrio parahaemolyticus*, the causative agent of acute hepatopancreatic necrosis disease (AHPND) of shrimp. Dis Aquat Organ 113: 33-40.
47. Yang YT, Chen IT, Lee CT, Chen CY, Lin SS, et al. (2014) Draft genome sequences of four strains of *Vibrio parahaemolyticus*, three of which cause early mortality syndrome/acute hepatopancreatic necrosis disease in shrimp in China and Thailand. Genome Announc 2.
48. Soto-Rodriguez SA, Gomez-Gil B, Lozano-Olvera R, Betancourt-Lozano M, Morales-Covarrubias MS (2015) Field and experimental evidence of *Vibrio parahaemolyticus* as the causative agent of acute hepatopancreatic necrosis disease of cultured shrimp (*Litopenaeus vannamei*) in Northwestern Mexico. Appl Environ Microbiol 81: 1689-1699.
49. Chiang HC, Lo CF (1995) Pathogenicity of a baculovirus infection causing white spot syndrome in cultured penaeid shrimp in Taiwan. Dis Aquat Organ 23: 165-173.
50. Lotz J (1997) Viruses, biosecurity and specific pathogen-free stocks in shrimp aquaculture. World J Microbiol Biotechnol 13: 405-413.
51. Spann KM, Lester RJG (1997) Viral diseases of penaeid shrimp with particular reference to four viruses recently found in shrimp from Queensland. World J Microbiol Biotechnol 13: 419-426.
52. van Hulten MC, Witteveldt J, Peters S, Kloosterboer N, Tarchini R, et al. (2001) The white spot syndrome virus DNA genome sequence. Virology 286: 7-22.
53. Yang F, He J, Lin X, Li Q, Pan D, et al. (2001) Complete genome sequence of the shrimp white spot bacilliform virus. J Virol 75: 11811-11820.

54. Takahashi Y, Itami T, Kondo M, Maeda M, Fujii R, et al. (1994) Electron microscopic evidence of bacilliform virus infection in kuruma shrimp (*Penaeus japonicus*). Fish Pathol 29: 121-125.

55. Chang P, Lo C, Wang Y, Kou G (1996) Identification of white spot syndrome associated baculovirus (WSBV) target organs in the shrimp *Penaeus monodon* by in situ hybridization. Dis Aquat Organ 27: 131-139.

56. Mohan C, Shankar K, Kulkarni S, Sudha P (1998) Histopathology of cultured shrimp showing gross signs of yellow head syndrome and white spot syndrome during 1994 Indian epizootics. Dis Aquat Organ 34: 9-12.

57. Li F, Xiang J (2013) Signaling pathways regulating innate immune responses in shrimp. Fish Shellfish Immun 34: 973-980.

58. Lemaitre B, Hoffmann J (2007) The host defense of *Drosophila melanogaster*. Annu Rev Immunol 25: 697-743.

59. Imler J-L, Hoffmann JA (2000) Signaling mechanisms in the antimicrobial host defense of *Drosophila*. Curr Opin Microbiol 3: 16-22.

60. Tauszig S, Jouanguy E, Hoffmann JA, Imler J-L (2000) Toll-related receptors and the control of antimicrobial peptide expression in *Drosophila*. Proc Nat Acad Sci 97: 10520-10525.

61. Shi XZ, Zhang RR, Jia YP, Zhao XF, Yu XQ, et al. (2009) Identification and molecular characterization of a Spätzle-like protein from Chinese shrimp (*Fenneropenaeus chinensis*). Fish Shellfish Immun 27: 610-617.

62. Wang P-H, Liang J-P, Gu Z-H, Wan D-H, Weng S-P, et al. (2012) Molecular cloning, characterization and expression analysis of two novel Tolls (LvToll2 and LvToll3) and three putative Spätzle-like Toll ligands (LvSpz1–3) from *Litopenaeus vannamei*. Dev Com Immunol 36: 359-371.

63. Bowie A, O'neill L (2000) The interleukin-1 receptor/Toll-like receptor superfamily: signal generators for pro-inflammatory interleukins and microbial products. J Leukocyte Biol 67: 508-514.

64. Yang LS, Yin ZX, Liao JX, Huang XD, Guo CJ, et al. (2007) A Toll receptor in shrimp. Mol Immunol 44: 1999-2008.

65. Arts JA, Cornelissen FH, Cijsouw T, Hermsen T, Savelkoul HF, et al. (2007) Molecular cloning and expression of a Toll receptor in the giant tiger shrimp, *Penaeus monodon*. Fish Shellfish Immun 23: 504-513.

66. Mekata T, Kono T, Yoshida T, Sakai M, Itami T (2008) Identification of cDNA encoding Toll receptor, MjToll gene from kuruma shrimp, *Marsupenaeus japonicus*. Fish Shellfish Immun 24: 122-133.

67. Hou F, He S, Liu Y, Zhu X, Sun C, et al. (2014) RNAi knock-down of shrimp *Litopenaeus vannamei* Toll gene and immune deficiency gene reveals their difference in regulating antimicrobial peptides transcription. Dev Comp Immunol 44: 255-260.

68. Horng T, Medzhitov R (2001) *Drosophila* MyD88 is an adapter in the Toll signaling pathway. Proc Nat Acad Sci 98: 12654-12658.

69. Letsou A, Alexander S, Orth K, Wasserman SA (1991) Genetic and molecular characterization of tube, a *Drosophila* gene maternally required for embryonic dorsoventral polarity. Proc Nat Acad Sci 88: 810-814.

70. Shelton CA, Wasserman SA (1993) Pelle encodes a protein kinase required to establish dorsoventral polarity in the *Drosophila* embryo. Cell 72: 515-525.

71. Wen R, Li F, Sun Z, Li S, Xiang J (2013) Shrimp MyD88 responsive to bacteria and white spot syndrome virus. Fish Shellfish Immun 34: 574-581.

72. Deepika A, Sreedharan K, Paria A, Makesh M, Rajendran KV (2014) Toll-pathway in tiger shrimp (*Penaeus monodon*) responds to white spot syndrome virus infection: Evidence through molecular characterisation and expression profiles of MyD88, TRAF6 and TLR genes. Fish Shellfish Immun 41: 441-454.

73. Li C, Chen Y, Weng S, Li S, Zuo H, et al. (2014) Presence of Tube isoforms in *Litopenaeus vannamei* suggests various regulatory patterns of signal transduction in invertebrate NF-κB pathway. Dev Com Immunol 42: 174-185.

74. Wang PH, Gu ZH, Wan DH, Zhang MY, Weng SP, et al. (2011) The shrimp NF-κB pathway is activated by White Spot Syndrome Virus (WSSV) 449 to facilitate the expression of *WSSV069 ie1 WSSV303* and *WSSV371*. PLoS ONE 6: e24773.

75. Bradley JR, Pober JS (2001) Tumor necrosis factor receptor-associated factors (TRAFs). Oncogene 20: 6482-6491.

76. Aggarwal K, Silverman N (2008) Positive and negative regulation of the *Drosophila* immune response. BMB Rep 41: 267-277.

77. Shen B, Liu H, Skolnik EY, Manley JL (2001) Physical and functional interactions between *Drosophila* TRAF2 and Pelle kinase contribute to Dorsal activation. Proc Nat Acad Sci 98: 8596-8601.

78. Wang PH, Wan DH, Gu ZH, Deng XX, Weng SP, et al. (2011) *Litopenaeus vannamei* tumor necrosis factor receptor-associated factor 6 (TRAF6) responds to *Vibrio alginolyticus* and white spot syndrome virus (WSSV) infection and activates antimicrobial peptide genes. Dev Comp Immunol 35: 105-114.

79. Anand D, Sreedharan K, Babu PS, Paria A, Makesh M, et al. (2015) Expression profiles of two downstream signalling molecules of Toll-pathway in tiger shrimp (*Penaeus monodon*), Cactus and Dorsal genes in response to infection with white spot syndrome virus and *Vibrio harveyi*. International Conference on Aquaculture and Fisheries (presentation).

80. Wang D, Li F, Li S, Chi Y, Wen R, et al. (2013) An IκB homologue (FcCactus) in Chinese shrimp *Fenneropenaeus chinensis*. Dev Com Immunol 39: 352-362.

81. Li C, Chen YX, Zhang S, Lü L, Chen YH, et al. (2012) Identification, characterization, and function analysis of the Cactus gene from *Litopenaeus vannamei*. PLoS ONE 7: e49711.

82. Huang XD, Yin ZX, Jia X, Liang J, Ai HS, et al. (2010) Identification and functional study of a shrimp Dorsal homologue. Dev Comp Immunol 34: 107-113.

83. Li F, Wang D, Li S, Yan H, Zhang J, et al. (2010) A Dorsal homolog (FcDorsal) in the Chinese shrimp *Fenneropenaeus chinensis* is responsive to both bacteria and WSSV challenge. Dev Comp Immunol 34: 874-883.

84. Vallet-Gely I, Lemaitre B, Boccard F (2008) Bacterial strategies to overcome insect defences. Nat Rev Microbiol 6: 302-313.

85. Kaneko T, Yano T, Aggarwal K, Lim J-H, Ueda K, et al. (2006) PGRP-LC and PGRP-LE have essential yet distinct functions in the drosophila immune response to monomeric DAP-type peptidoglycan. Nat Immunol 7: 715-723.

86. Choe KM, Lee H, Anderson KV (2005) *Drosophila* peptidoglycan recognition protein LC (PGRP-LC) acts as a signal-transducing innate immune receptor. Proc Nat Acad Sci 102: 1122-1126.

87. Hu S, Yang X (2000) dFADD, a novel death domain-containing adapter protein for the *Drosophila* caspase DREDD. J Biol Chem 275: 30761-30764.

88. Stöven S, Ando I, Kadalayil L, Engström Y, Hultmark D (2000) Activation of the *Drosophila* NF-κB factor Relish by rapid endoproteolytic cleavage. EMBO Rep 1: 347-352.

89. Stöven S, Silverman N, Junell A, Hedengren-Olcott M, Erturk D, et al. (2003) Caspase-mediated processing of the *Drosophila* NF-κB factor Relish. Proc Nat Acad Sci 100: 5991-5996.

90. Rutschmann S, Jung AC, Zhou R, Silverman N, Hoffmann JA, et al. (2000) Role of *Drosophila* IKKγ in a Toll-independent antibacterial immune response. Nat Immunol 1: 342-347.

91. Lu Y, Wu LP, Anderson KV (2001) The antibacterial arm of the *Drosophila* innate immune response requires an IκB kinase. Genes Dev 15: 104-110.

92. Silverman N, Zhou R, Stöven S, Pandey N, Hultmark D, et al. (2000) A *Drosophila* IκB kinase complex required for Relish cleavage and antibacterial immunity. Genes Dev 14: 2461-2471.

93. Kleino A, Valanne S, Ulvila J, Kallio J, Myllymäki H, et al. (2005) Inhibitor of apoptosis 2 and TAK1-binding protein are components of the *Drosophila* Imd pathway. EMBO J 24: 3423-3434.

94. Wang PH, Gu ZH, Huang XD, Liu BD, Deng X, et al. (2009) An immune deficiency homolog from the white shrimp, *Litopenaeus vannamei*, activates antimicrobial peptide genes. Mol Immunol 46: 1897-1904.

95. Lan JF, Zhou J, Zhang XW, Wang ZH, Zhao XF, et al. (2013) Characterization of an immune deficiency homolog (IMD) in shrimp (*Fenneropenaeus chinensis*) and crayfish (*Procambarus clarkii*). Dev Comp Immunol 41: 608-617.

96. Wang S, Li H, Qian Z, Song X, Zhang Z, et al. (2015) Identification and functional characterization of the TAB2 gene from *Litopenaeus vannamei*. Fish Shellfish Immun 46: 206-216.

97. Leu JH, Kuo YC, Kou GH, Lo CF (2008) Molecular cloning and characterization of an inhibitor of apoptosis protein (IAP) from the tiger shrimp, *Penaeus monodon*. Dev Comp Immunol 32: 121-133.

98. Wang PH, Wan DH, Gu ZH, Qiu W, Chen YG, et al. (2013) Analysis of expression, cellular localization, and function of three inhibitors of apoptosis (IAPs) from *Litopenaeus vannamei* during WSSV infection and in regulation of antimicrobial peptide genes (AMPs). PLoS ONE 8: e72592.

99. Leu JH, Chen YC, Chen LL, Chen KY, Huang HT, et al. (2012) *Litopenaeus vannamei* inhibitor of apoptosis protein 1 (LvIAP1) is essential for shrimp survival. Dev Comp Immunol 38: 78-87.

100. Wang PH, Gu ZH, Wan DH, Liu BD, Huang XD, et al. (2013) The shrimp IKK-NF-[kgr]B signaling pathway regulates antimicrobial peptide expression and may be subverted by white spot syndrome virus to facilitate viral gene expression. Cell Mol Immunol 10: 423-436.

101. Huang XD, Yin ZX, Liao JX, Wang PH, Yang LS, et al. (2009) Identification and functional study of a shrimp Relish homologue. Fish Shellfish Immun 27: 230-238.

102. Li F, Yan H, Wang D, Priya TAJ, Li S, et al. (2009) Identification of a novel relish homolog in Chinese shrimp *Fenneropenaeus chinensis* and its function in regulating the transcription of antimicrobial peptides. Dev Comp Immunol 33: 1093-1101.

103. Wang D, Li F, Li S, Wen R, Xiang J (2012) Expression profiles of antimicrobial peptides (AMPs) and their regulation by Relish. Chin J Oceanol Limn 30: 611-619.

104. Hancock RE, Diamond G (2000) The role of cationic antimicrobial peptides in innate host defences. Trends Microbiol 8: 402-410.

105. Pan J, Kurosky A, Xu B, Chopra AK, Coppenhaver DH, et al. (2000) Broad antiviral activity in tissues of crustaceans. Antivir Res 48: 39-47.

106. Cruciani RA, Barker JL, Zasloff M, Chen HC, Colamonici O (1991) Antibiotic magainins exert cytolytic activity against transformed cell lines through channel formation. Proc Nat Acad Sci 88: 3792-3796.

107. Tanaka S, Nakamura T, Morita T, Iwanaga S (1982) *Limulus* anti-LPS factor: An anticoagulant which inhibits the endotoxin-mediated activation of *Limulus* coagulation system. Biochem Bioph Res Co 105: 717-723.

108. Supungul P, Klinbunga S, Pichyangkura R, Hirono I, Aoki T, et al. (2004) Antimicrobial peptides discovered in the black tiger shrimp *Penaeus monodon* using the EST approach. Dis Aquat Organ 61: 123-135.

109. Ponprateep S, Tharntada S, Somboonwiwat K, Tassanakajon A (2012) Gene silencing reveals a crucial role for anti-lipopolysaccharide factors from *Penaeus monodon* in the protection against microbial infections. Fish Shellfish Immun 32: 26-34.

110. Li S, Zhang X, Sun Z, Li F, Xiang J (2013) Transcriptome analysis on Chinese shrimp *Fenneropenaeus chinensis* during WSSV acute infection. PLoS ONE 8: e58627.

111. Liu Y, Cui Z, Li X, Song C, Li Q, et al. (2012) A new anti-lipopolysaccharide factor isoform (PtALF4) from the swimming crab *Portunus trituberculatus* exhibited structural and functional diversity of ALFs. Fish Shellfish Immun 32: 724-731.

112. Liu Y, Cui Z, Luan W, Song C, Nie Q, et al. (2011) Three isoforms of anti-lipopolysaccharide factor identified from eyestalk cDNA library of swimming crab *Portunus trituberculatus*. Fish Shellfish Immun 30: 583-591.

113. Liu Y, Cui Z, Li X, Song C, Shi G, et al. (2013) Molecular cloning, genomic structure and antimicrobial activity of PtALF7, a unique isoform of anti-lipopolysaccharide factor from the swimming crab *Portunus trituberculatus*. Fish Shellfish Immun 34: 652-659.

114. Liu Y, Cui Z, Li X, Song C, Shi G (2013) A newly identified anti-lipopolysaccharide factor from the swimming crab *Portunus trituberculatus* with broad spectrum antimicrobial activity. Fish Shellfish Immun 34: 463-470.

115. Jimenez-Vega F, Vargas-Albores F (2007) Isoforms of *Litopenaeus vannamei* anti-lipopolysaccharide and its expression by bacterial challenge. J Shellfish Res 26: 1169-1175.

116. Hoess A, Watson S, Siber G, Liddington R (1993) Crystal structure of an endotoxin-neutralizing protein from the horseshoe crab, Limulus anti-LPS factor, at 1.5 A resolution. EMBO J 12: 3351.

117. Tharntada S, Somboonwiwat K, Rimphanitchayakit V, Tassanakajon A (2008) Anti-lipopolysaccharide factors from the black tiger shrimp, *Penaeus monodon*, are encoded by two genomic loci. Fish Shellfish Immun 24: 46-54.

118. Somboonwiwat K, Bachère E, Rimphanitchayakit V, Tassanakajon A (2008) Localization of anti-lipopolysaccharide factor (ALFPm3) in tissues of the black tiger shrimp, *Penaeus monodon*, and characterization of its binding properties. Dev Com Immunol 32: 1170-1176.

119. Smith VJ, Fernandes JMO, Kemp GD, Hauton C (2008) Crustins: Enigmatic WAP domain-containing antibacterial proteins from crustaceans. Dev Com Immunol 32: 758-772.

120. Relf JM, Chisholm JR, Kemp GD, Smith VJ (1999) Purification and characterization of a cysteine-rich 11.5-kDa antibacterial protein from the granular haemocytes of the shore crab, *Carcinus maenas*. Eur J Biochem 264: 350-357.

121. Vatanavicharn T, Supungul P, Puanglarp N, Yingvilasprasert W, Tassanakajon A (2009) Genomic structure, expression pattern and functional characterization of crustinPm5, a unique isoform of crustin from *Penaeus monodon*. Comp Biochem Phys B 153: 244-252.

122. Tassanakajon A, Vatanavicharn T, Supungul P, Tang S, Amparyup P, et al. (2008) Biotechnology of marine invertebrates-recent advances in shrimp and shellfish. In: Tsukamoto K, Kawamura T, Takeuchi T, Jr TDB, Kaiser MJ, editors. Memorial book of the 5th World Fisheries Congress. Terrapub, Tokyo. pp. 221-239.

123. Chen JY, Pan CY, Kuo CM (2004) cDNA sequence encoding an 11.5-kDa antibacterial peptide of the shrimp *Penaeus monodon*. Fish Shellfish Immunol 16: 659-664.

124. Amparyup P, Kondo H, Hirono I, Aoki T, Tassanakajon A (2008) Molecular cloning, genomic organization and recombinant expression of a crustin-like antimicrobial peptide from black tiger shrimp *Penaeus monodon*. Mol Immunol 45: 1085-1093.

125. Amparyup P, Donpudsa S, Tassanakajon A (2008) Shrimp single WAP domain (SWD)-containing protein exhibits proteinase inhibitory and antimicrobial activities. Dev Comp Immunol 32: 1497-1509.

126. Arayamethakorn S, Krusong K, Tassanakajon A (2013) Cloning, expression and characterization of recombinant Crustin*Pm*7 from black tiger shrimp *Penaeus monodon*. *i*GRC: 231-235.

127. Bartlett TC, Cuthbertson BJ, Shepard EF, Chapman RW, Gross PS, et al. (2002) Crustins, homologues of an 11.5-kDa antibacterial peptide, from two species of penaeid shrimp, *Litopenaeus vannamei* and *Litopenaeus setiferus*. Mar Biotechnol 4: 278-293.

128. Jiménez-Vega F, Yepiz-Plascencia G, Söderhäll K, Vargas-Albores F (2004) A single WAP domain-containing protein from *Litopenaeus vannamei* hemocytes. Biochem Bioph Res Co 314: 681-687.

129. Jia YP, Sun YD, Wang ZH, Wang Q, Wang XW, et al. (2008) A single whey acidic protein domain (SWD)-containing peptide from fleshy prawn with antimicrobial and proteinase inhibitory activities. Aquaculture 284: 246-259.

130. Zhang J, Li F, Wang Z, Xiang J (2007) Cloning and recombinant expression of a crustin-like gene from Chinese shrimp, *Fenneropenaeus chinensis*. J Biol Chem 127: 605-614.

131. Liu F, Li F, Xiang J, Dong B, Liu Y, et al. (2008) Molecular cloning and expression analysis of Crustin-like gene from Chinese shrimp *Fenneropenaeus chinensis*. Acta Oceanol Sin 27: 81-92.

132. Shockey JE, O'Leary NA, de la Vega E, Browdy CL, Baatz JE, et al. (2009) The role of crustins in *Litopenaeus vannamei* in response to infection with shrimp pathogens: An *in vivo* approach. Dev Comp Immunol 33: 668-673.

133. Hipolito SG, Shitara A, Kondo H, Hirono I (2014) Role of *Marsupenaeus japonicus* crustin-like peptide against *Vibrio penaeicida* and white spot syndrome virus infection. Dev Comp Immunol 46: 461-469.

134. Rattanachai A, Hirono I, Ohira T, Takahashi Y, Aoki T (2004) Cloning of kuruma prawn *Marsupenaeus japonicus* crustin-like peptide cDNA and analysis of its expression. Fisheries Sci 70: 765-771.

135. Jiang HS, Sun C, Wang T, Zhao XF, Wang JX (2013) A single whey acidic protein domain containing protein (SWD) inhibits bacteria invasion and dissemination in shrimp *Marsupenaeus japonicus*. Fish Shellfish Immun 35: 310-318.

136. Supungul P, Tang S, Maneeruttanarungroj C, Rimphanitchayakit V, Hirono I, et al. (2008) Cloning, expression and antimicrobial activity of crustinPm1, a major isoform of crustin, from the black tiger shrimp *Penaeus monodon*. Dev Comp Immunol 32: 61-70.

137. Okumura T (2007) Effects of lipopolysaccharide on gene expression of antimicrobial peptides (penaeidins and crustin), serine proteinase and prophenoloxidase in haemocytes of the Pacific white shrimp, *Litopenaeus vannamei*. Fish Shellfish Immun 22: 68-76.

138. Destoumieux D, Munoz M, Cosseau C, Rodriguez J, Bulet P, et al. (2000) Penaeidins, antimicrobial peptides with chitin-binding activity, are produced and stored in shrimp granulocytes and released after microbial challenge. J Cell Sci 113: 461-469.

139. Muñoz M, Vandenbulcke F, Saulnier D, Bachère E (2002) Expression and distribution of penaeidin antimicrobial peptides are regulated by haemocyte reactions in microbial challenged shrimp. Eur J Biochem 269: 2678-2689.

140. Bachère E, Gueguen Y, Gonzalez M, De Lorgeril J, Garnier J, et al. (2004) Insights into the anti-microbial defense of marine invertebrates: the penaeid shrimps and the oyster *Crassostrea gigas*. Immunol Rev 198: 149-168.

141. Cuthbertson B, Shepard E, Chapman R, Gross P (2002) Diversity of the penaeidin antimicrobial peptides in two shrimp species. Immunogenetics 54: 442-445.

142. Li L, Wang JX, Zhao XF, Kang CJ, Liu N, et al. (2005) High level expression, purification, and characterization of the shrimp antimicrobial peptide, Ch-penaeidin, in *Pichia pastoris*. Protein Expres Purif 39: 144-151.

143. Kang CJ, Xue JF, Liu N, Zhao XF, Wang JX (2007) Characterization and expression of a new subfamily member of penaeidin antimicrobial peptides (penaeidin 5) from *Fenneropenaeus chinensis*. Mol Immunol 44: 1535-1543.

144. Destoumieux D, Bulet P, Loew D, Van Dorsselaer A, Rodriguez J, et al. (1997) Penaeidins, a new family of antimicrobial peptides isolated from the shrimp *Penaeus vannamei* (Decapoda). J Biol Chem 272: 28398-28406.

145. Ho SH, Chao YC, Tsao HW, Sakai M, Chou HN, et al. (2004) Molecular cloning and recombinant expression of tiger shrimp *Penaeus monodon* penaeidin. Fish Pathol 39: 15-23.

146. Chen JY, Pan CY, Kuo CM (2004) Molecular cloning and sequencing of shrimp (*Penaeus monodon*) penaeidin-5 cDNA. Fish Shellfish Immunol 16: 665-670.

147. Chiou TT, Wu JL, Chen T, Lu JK (2005) Molecular cloning and characterization of cDNA of penaeidin-like antimicrobial peptide from tiger shrimp (*Penaeus monodon*). Mar Biotechnol 7: 119-127.

148. O'Leary NA, Gross PS (2006) Genomic structure and transcriptional regulation of the penaeidin gene family from *Litopenaeus vannamei*. Gene 371: 75-83.

149. Kang CJ, Wang JX, Zhao X, Yang XM, Shao HL, et al. (2004) Molecular cloning and expression analysis of Ch-penaeidin, an antimicrobial peptide from Chinese shrimp, *Fenneropenaeus chinensis*. Fish Shellfish Immun 16: 513-525.

150. Nappi A, Vass E (1993) Melanogenesis and the generation of cytotoxic molecules during insect cellular immune reactions. Pigm Cell Res 6: 117-126.

151. Ashida M (1990) The prophenoloxidase cascade in insect immunity. Res Immunol 141: 908-910.

152. Söderhäll K, Cerenius L (1998) Role of the prophenoloxidase-activating system in invertebrate immunity. Curr Opin Immunol 10: 23-28.

153. Cerenius L, Lee BL, Söderhäll K (2008) The proPO-system: pros and cons for its role in invertebrate immunity. Trends Immunol 29: 263-271.

154. Jiravanichpaisal P, Lee BL, Söderhäll K (2006) Cell-mediated immunity in arthropods: hematopoiesis, coagulation, melanization and opsonization. Immunobiology 211: 213-236.

155. Sritunyalucksana K, Söderhäll K (2000) The proPO and clotting system in crustaceans. Aquaculture 191: 53-69.

156. Cerenius L, Söderhäll K (2004) The prophenoloxidase-activating system in invertebrates. Immunol Rev 198: 116-126.

157. Cerenius L, Kawabata S, Lee BL, Nonaka M, Söderhäll K (2010) Proteolytic cascades and their involvement in invertebrate immunity. Trends Biochem Sci 35: 575-583.

158. Ashida M, Ishizaki Y, Iwahana H (1983) Activation of pro-phenoloxidase by bacterial cell walls or β-1,3-glucans in plasma of the silkworm, *Bombyx mori*. Biochem and Bioph Res Co 113: 562-568.

159. Yoshida H, Ochiai M, Ashida M (1986) β-1,3-glucan receptor and peptidoglycan receptor are present as separate entities within insect prophenoloxidase activating system. Biochem Bioph Res Co 141: 1177-1184.

160. Aspán A, Söderhäll K (1991) Purification of prophenoloxidase from crayfish blood cells, and its activation by an endogenous serine proteinase. Insect Biochem 21: 363-373.

161. Jiang H, Kanost MR (2000) The clip-domain family of serine proteinases in arthropods. Insect Biochem Molec 30: 95-105.

162. Aspán A, Hall M, Söderhäll K (1990) The effect of endogeneous proteinase inhibitors on the prophenoloxidase activating enzyme, a serine proteinase from crayfish haemocytes. Insect Biochem 20: 485-492.

163. Wang R, Lee SY, Cerenius L, Söderhäll K (2001) Properties of the prophenoloxidase activating enzyme of the freshwater crayfish, *Pacifastacus leniusculus*. Eur J Biochem 268: 895-902.

164. Charoensapsri W, Amparyup P, Hirono I, Aoki T, Tassanakajon A (2009) Gene silencing of a prophenoloxidase activating enzyme in the shrimp, *Penaeus monodon*, increases susceptibility to Vibrio harveyi infection. Dev Comp Immunol 33: 811-820.

165. Charoensapsri W, Amparyup P, Hirono I, Aoki T, Tassanakajon A (2011) PmPPAE2, a new class of crustacean prophenoloxidase (proPO)-activating enzyme and its role in PO activation. Dev Comp Immunol 35: 115-124.

166. Jang IK, Pang Z, Yu J, Kim SK, Seo HC, et al. (2011) Selectively enhanced expression of prophenoloxidase activating enzyme 1 (PPAE1) at a bacteria clearance site in the white shrimp, *Litopenaeus vannamei*. BMC Immunol 12: 70.

167. Pang Z, Kim SK, Yu J, Jang I (2014) Distinct regulation patterns of the two prophenoloxidase activating enzymes corresponding to bacteria challenge and their compensatory over expression feature in white shrimp (*Litopenaeus vannamei*). Fish Shellfish Immun 39: 158-167.

168. Amparyup P, Wiriyaukaradecha K, Charoensapsri W, Tassanakajon A (2010) A clip domain serine proteinase plays a role in antibacterial defense but is not required for prophenoloxidase activation in shrimp. Dev Comp Immunol 34: 168-176.

169. Ren Q, Xu ZL, Wang XW, Zhao XF, Wang JX (2009) Clip domain serine protease and its homolog respond to *Vibrio* challenge in Chinese white shrimp, *Fenneropenaeus chinensis*. Fish Shellfish Immun 26: 787-798.

170. Vaseeharan B, Shanthi S, Prabhu NM (2011) A novel clip domain serine proteinase (SPs) gene from the haemocytes of Indian white shrimp *Fenneropenaeus indicus*: Molecular cloning, characterization and expression analysis. Fish Shellfish Immun 30: 980-985.

171. Aspán A, Huang TS, Cerenius L, Söderhäll K (1995) cDNA cloning of prophenoloxidase from the freshwater crayfish *Pacifastacus leniusculus* and its activation. P Natl Acad Sci USA 92: 939-943.

172. Sritunyalucksana K, Cerenius L, Söderhäll K (1999) Molecular cloning and characterization of prophenoloxidase in the black tiger shrimp, *Penaeus monodon*. Dev Comp Immunol 23: 179-186.

173. Gollas-Galván T, Hernández-López J, Vargas-Albores F (1999) Prophenoloxidase from brown shrimp (*Penaeus californiensis*) hemocytes. Comp Biochem Phys B 122: 77-82.

174. Ai HS, Liao JX, Huang XD, Yin ZX, Weng SP, et al. (2009) A novel prophenoloxidase 2 exists in shrimp hemocytes. Dev Comp Immunol 33: 59-68.

175. Lai CY, Cheng W, Kuo CM (2005) Molecular cloning and characterisation of prophenoloxidase from haemocytes of the white shrimp, *Litopenaeus vannamei*. Fish Shellfish Immun 18: 417-430.

176. Yeh MS, Lai CY, Liu CH, Kuo CM, Cheng W (2009) A second proPO present in white shrimp *Litopenaeus vannamei* and expression of the proPOs during a *Vibrio alginolyticus* injection, molt stage, and oral sodium alginate ingestion. Fish Shellfish Immun 26: 49-55.

177. Liu CH, Tseng DY, Lai CY, Cheng W, Kuo CM (2006) Molecular cloning and characterisation of prophenoloxidase cDNA from haemocytes of the giant freshwater prawn, *Macrobrachium rosenbergii*, and its transcription in relation with the moult stage. Fish Shellfish Immun 21: 60-69.

178. Arockiaraj J, Easwvaran S, Vanaraja P, Singh A, Othman R, et al. (2012) Prophenoloxidase activating enzyme-III from giant freshwater prawn *Macrobrachium rosenbergii*: characterization, expression and specific enzyme activity. Mol Biol Rep 39: 1377-1386.

179. Gao H, Li F, Dong B, Zhang Q, Xiang J (2009) Molecular cloning and characterisation of prophenoloxidase (ProPO) cDNA from *Fenneropenaeus chinensis* and its transcription injected by *Vibrio anguillarum*. Mol Biol Rep 36: 1159-1166.

180. Wang YC, Chang PS, Chen HY (2008) Differential time-series expression of immune-related genes of Pacific white shrimp *Litopenaeus vannamei* in response to dietary inclusion of β-1,3-glucan. Fish Shellfish Immun 24: 113-121.

181. Ai HS, Huang YC, Li SD, Weng SP, Yu XQ, et al. (2008) Characterization of a prophenoloxidase from hemocytes of the shrimp *Litopenaeus vannamei* that is down-regulated by white spot syndrome virus. Fish Shellfish Immun 25: 28-39.

182. Fagutao FF, Koyama T, Kaizu A, Saito-Taki T, Kondo H, et al. (2009) Increased bacterial load in shrimp hemolymph in the absence of prophenoloxidase. FEBS J 276: 5298-5306.

183. Amparyup P, Charoensapsri W, Tassanakajon A (2013) Prophenoloxidase system and its role in shrimp immune responses against major pathogens. Fish Shellfish Immun 34: 990-1001.

184. Liang Z, Sottrup-Jensen L, Aspán A, Hall M, Söderhäll K (1997) Pacifastin, a novel 155-kDa heterodimeric proteinase inhibitor containing a unique transferrin chain. Proc Nat Acad Sci 94: 6682-6687.

185. Angthong P, Watthanasurorot A, Klinbunga S, Ruangdej U, Söderhäll I, et al. (2010) Cloning and characterization of a melanization inhibition protein (PmMIP) of the black tiger shrimp, *Penaeus monodon*. Fish Shellfish Immun 29: 464-468.

186. Wetsaphan N, Rimphanitchayakit V, Tassanakajon A, Somboonwiwat K (2013) PmSERPIN3 from black tiger shrimp *Penaeus monodon* is capable of controlling the proPO system. Dev Comp Immunol 41: 110-119.

187. Homvises T, Tassanakajon A, Somboonwiwat K (2010) *Penaeus monodon* SERPIN, PmSERPIN6, is implicated in the shrimp innate immunity. Fish Shellfish Immun 29: 890-898.

188. Somnuk S, Tassanakajon A, Rimphanitchayakit V (2012) Gene expression and characterization of a serine proteinase inhibitor PmSERPIN8 from the black tiger shrimp *Penaeus monodon*. Fish Shellfish Immun 33: 332-341.

189. Liu Y, Hou F, He S, Qian Z, Wang X, et al. (2014) Identification, characterization and functional analysis of a serine protease inhibitor (*Lv*serpin) from the Pacific white shrimp, *Litopenaeus vannamei*. Dev Comp Immunol 43: 35-46.

190. Liu Y, Liu T, Hou F, Wang X, Liu X (2015) Lvserpin3 is involved in shrimp innate immunity via the inhibition of bacterial proteases and proteases involved in prophenoloxidase system. Fish Shellfish Immun: In Press.

191. Liu Y, Hou F, Wang X, Liu X (2015) Recombinant expression and characterization of a serine protease inhibitor (*Lv*serpin7) from the Pacific white shrimp, *Litopenaeus vannamei*. Fish Shellfish Immun 42: 256-263.

192. Liu Y, Li F, Wang B, Dong B, Zhang X, et al. (2009) A serpin from Chinese shrimp *Fenneropenaeus chinensis* is responsive to bacteria and WSSV challenge. Fish Shellfish Immun 26: 345-351.

193. Zhao YR, Xu YH, Jiang HS, Xu S, Zhao XF, et al. (2014) Antibacterial activity of serine protease inhibitor 1 from kuruma shrimp *Marsupenaeus japonicus*. Dev Comp Immunol 44: 261-269.

194. Hoffmann JA, Kafatos FC, Janeway CA, Ezekowitz R (1999) Phylogenetic perspectives in innate immunity. Science 284: 1313-1318.

195. Vargas-Albores F, Jiménez-Vega F, Söderhäll K (1996) A plasma protein isolated from brown shrimp (*Penaeus californiensis*) which enhances the activation of prophenoloxidase system by β-1, 3-glucan. Dev Comp Immunol 20: 299-306.

196. Christophides GK, Vlachou D, Kafatos FC (2004) Comparative and functional genomics of the innate immune system in the malaria vector *Anopheles gambiae*. Immunol Rev 198: 127-148.

197. Watson FL, Püttmann-Holgado R, Thomas F, Lamar DL, Hughes M, et al. (2005) Extensive diversity of Ig-superfamily proteins in the immune system of insects. Science 309: 1874-1878.

198. Nakamoto M, Moy RH, Xu J, Bambina S, Yasunaga A, et al. (2012) Virus recognition by Toll-7 activates antiviral autophagy in *Drosophila*. Immunity 36: 658-667.

199. Vargas-Albores F, Jiménez-Vega F, Yepiz-Plascencia GM (1997) Purification and comparison of β-1, 3-glucan binding protein from white shrimp (*Penaeus vannamei*). Comp Biochem Phys B 116: 453-458.

200. Duvic B, Söderhäll K (1990) Purification and characterization of a beta-1, 3-glucan binding protein from plasma of the crayfish *Pacifastacus leniusculus*. J Biol Chem 265: 9327-9332.

201. Romo-Figueroa MG, Vargas-Requena C, Sotelo-Mundo RR, Vargas-Albores F, Higuera-Ciapara I, et al. (2004) Molecular cloning of a β-glucan pattern-recognition lipoprotein from the white shrimp *Penaeus* (*Litopenaeus*) vannamei: Correlations between the deduced amino acid sequence and the native protein structure. Dev Comp Immunol 28: 713-726.

202. Pan D, He N, Yang Z, Liu H, Xu X (2005) Differential gene expression profile in hepatopancreas of WSSV-resistant shrimp (*Penaeus japonicus*) by suppression subtractive hybridization. Dev Comp Immunol 29: 103-112.

203. Lai X, Kong J, Wang Q, Wang W, Meng X (2011) Cloning and characterization of a β-1,3-glucan-binding protein from shrimp *Fenneropenaeus chinensis*. Mol Biol Rep 38: 4527-4535.

204. Marques MRF, Barracco MA (2000) Lectins, as non-self-recognition factors, in crustaceans. Aquaculture 191: 23-44.

205. Robinson MJ, Sancho D, Slack EC, LeibundGut-Landmann S, Sousa CR (2006) Myeloid C-type lectins in innate immunity. Nat Immunol 7: 1258-1265.

206. Wang XW, Wang JX (2013) Diversity and multiple functions of lectins in shrimp immunity. Dev Comp Immunol 39: 27-38.

207. Luo T, Zhang X, Shao Z, Xu X (2003) PmAV, a novel gene involved in virus resistance of shrimp *Penaeus monodon*. FEBS Lett 551: 53-57.

208. Luo T, Yang H, Li F, Zhang X, Xu X (2006) Purification, characterization and cDNA cloning of a novel lipopolysaccharide-binding lectin from the shrimp *Penaeus monodon*. Dev Comp Immunol 30: 607-617.

209. Ma TH-T, Benzie JA, He J-G, Chan S-M (2008) PmLT, a C-type lectin specific to hepatopancreas is involved in the innate defense of the shrimp *Penaeus monodon*. J Invertebr Pathol 99: 332-341.

210. Liu YC, Li FH, Dong B, Wang B, Luan W, et al. (2007) Molecular cloning, characterization and expression analysis of a putative C-type lectin (Fclectin) gene in Chinese shrimp *Fenneropenaeus chinensis*. Mol Immunol 44: 598-607.

211. Sun YD, Fu LD, Jia YP, Du XJ, Wang Q, et al. (2008) A hepatopancreas-specific C-type lectin from the Chinese shrimp *Fenneropenaeus chinensis* exhibits antimicrobial activity. Mol Immunol 45: 348-361.

212. Zhang XW, Xu WT, Wang XW, Mu Y, Zhao XF, et al. (2009) A novel C-type lectin with two CRD domains from Chinese shrimp *Fenneropenaeus chinensis* functions as a pattern recognition protein. Mol Immunol 46: 1626-1637.

213. Wang XW, Zhang XW, Xu WT, Zhao XF, Wang JX (2009) A novel C-type lectin (FcLec4) facilitates the clearance of *Vibrio anguillarum* in vivo in Chinese white shrimp. Dev Comp Immunol 33: 1039-1047.

214. Wang XW, Xu WT, Zhang XW, Zhao XF, Yu XQ, et al. (2009) A C-type lectin is involved in the innate immune response of Chinese white shrimp. Fish Shellfish Immun 27: 556-562.

215. Xu WT, Wang XW, Zhang XW, Zhao XF, Yu XQ, et al. (2010) A new C-type lectin (FcLec5) from the Chinese white shrimp *Fenneropenaeus chinensis*. Amino Acids 39: 1227-1239.

216. Ma THT, Tiu SHK, He JG, Chan SM (2007) Molecular cloning of a C-type lectin (LvLT) from the shrimp *Litopenaeus vannamei*: Early gene down-regulation after WSSV infection. Fish Shellfish Immun 23: 430-437.

217. Zhao ZY, Yin ZX, Xu XP, Weng SP, Rao XY, et al. (2009) A novel C-type lectin from the shrimp *Litopenaeus vannamei* possesses anti-white spot syndrome virus activity. J Virol 83: 347-356.

218. Zhang Y, Qiu L, Song L, Zhang H, Zhao J, et al. (2009) Cloning and characterization of a novel C-type lectin gene from shrimp *Litopenaeus vannamei*. Fish Shellfish Immun 26: 183-192.

219. Wei X, Liu X, Yang J, Fang J, Qiao H, et al. (2012) Two C-type lectins from shrimp *Litopenaeus vannamei* that might be involved in immune response against bacteria and virus. Fish Shellfish Immun 32: 132-140.

220. Barondes SH, Cooper DN, Gitt MA, Leffler H (1994) Galectins. Structure and function of a large family of animal lectins. J Biol Chem 269: 20807-20807.

221. Vasta GR (2012) Galectins as pattern recognition receptors: structure, function, and evolution. In: John DL, George H, editors. Current Topics in Innate Immunity II: Springer. pp. 21-36.

222. Hirabayashi J, Kasai K (1993) The family of metazoan metal-independent β-galactoside-binding lectins: structure, function and molecular evolution. Glycobiology 3: 297-304.

223. Shi XZ, Wang L, Xu S, Zhang XW, Zhao XF, et al. (2014) A galectin from the kuruma shrimp *Marsupenaeus japonicus* functions as an opsonin and promotes bacterial clearance from hemolymph. PLoS ONE 9: e91794.

224. Hou F, Liu Y, He S, Wang X, Mao A, et al. (2015) A galectin from shrimp *Litopenaeus vannamei* is involved in immune recognition and bacteria phagocytosis. Fish Shellfish Immun 44: 584-591.

225. Cha GH, Liu Y, Peng T, Huang MZ, Xie CY, et al. (2015) Molecular cloning, expression of a galectin gene in Pacific white shrimp *Litopenaeus vannamei* and the antibacterial activity of its recombinant protein. Mol Immunol 67: 325-340.

226. Blandin S, Levashina EA (2004) Thioester-containing proteins and insect immunity. Mol Immunol 40: 903-908.

227. Blandin S, Shiao SH, Moita LF, Janse CJ, Waters AP, et al. (2004) Complement-like protein TEP1 is a determinant of vectorial capacity in the malaria vector *Anopheles gambiae*. Cell 116: 661-670.

228. Bou Aoun R, Hetru C, Troxler L, Doucet D, Ferrandon D, et al. (2011) Analysis of thioester-containing proteins during the innate immune response of *Drosophila melanogaster*. J Innate Immun 3: 52-64.

229. Wu C, Noonin C, Jiravanichpaisal P, Söderhäll I, Söderhäll K (2012) An insect TEP in a crustacean is specific for cuticular tissues and involved in intestinal defense. Insect Biochem Molec 42: 71-80.

230. Dong Y, Dimopoulos G (2009) Anopheles fibrinogen-related proteins provide expanded pattern recognition capacity against bacteria and malaria parasites. J Biol Chem 284: 9835-9844.

231. Kawabata S, Iwanaga S (1999) Role of lectins in the innate immunity of horseshoe crab. Dev Comp Immunol 23: 391-400.

232. Chai YM, Zhu Q, Yu SS, Zhao XF, Wang JX (2012) A novel protein with a fibrinogen-like domain involved in the innate immune response of *Marsupenaeus japonicus*. Fish Shellfish Immunol 32: 307-315.

233. Yamakawa K, Huo YK, Haendel MA, Hubert R, Chen XN, et al. (1998) DSCAM: a novel member of the immunoglobulin superfamily maps in a Down syndrome region and is involved in the development of the nervous system. Hum Mol Genet 7: 227-237.

234. Hattori D, Millard SS, Wojtowicz WM, Zipursky SL (2008) Dscam-mediated cell recognition regulates neural circuit formation. Annu Rev Cell Dev Biol 24: 597-620.

235. Chou PH, Chang HS, Chen IT, Lin HY, Chen YM, et al. (2009) The putative invertebrate adaptive immune protein *Litopenaeus vannamei* Dscam

(LvDscam) is the first reported Dscam to lack a transmembrane domain and cytoplasmic tail. Dev Comp Immunol 33: 1258-1267.

236. Chou PH, Chang HS, Chen IT, Lee CW, Hung HY, et al. (2011) *Penaeus monodon* Dscam (PmDscam) has a highly diverse cytoplasmic tail and is the first membrane-bound shrimp Dscam to be reported. Fish Shellfish Immun 30: 1109-1123.

237. Kopáček p, Hall M, Söderhäll K (1993) Characterization of a clotting protein, isolated from plasma of the freshwater crayfish *Pacifastacus leniusculus*. Eur J Biochem 213: 591-597.

238. Hall M, Wang R, van Antwerpen R, Sottrup-Jensen L, Söderhäll K (1999) The crayfish plasma clotting protein: a vitellogenin-related protein responsible for clot formation in crustacean blood. Proc Nat Acad Sci 96: 1965-1970.

239. Iwanaga S (2002) The molecular basis of innate immunity in the horseshoe crab. Curr Opin Immunol 14: 87-95.

240. Iwanaga S, Lee BL (2005) Recent advances in the innate immunity of invertebrate animals. BMB Rep 38: 128-150.

241. Hall M, Vanheusden M, Soderhall K (1995) Identification of the major lipoproteins in crayfish hemolymph as proteins involved in immune recognition and clotting. Biochem Bioph Res Commun 216: 939-946.

242. Yeh MS, Kao LR, Huang CJ, Tsai IH (2006) Biochemical characterization and cloning of transglutaminases responsible for hemolymph clotting in *Penaeus monodon* and *Marsupenaeus japonicus*. Biochim Biophys Acta 1764: 1167-1178.

243. Komatsu M, Ando S (1998) A very-high-density lipoprotein with clotting ability from hemolymph of sand crayfish, *Ibacus ciliatus*. Biosci Biotechnol Biochem 62: 459-463.

244. Yeh MS, Huang CJ, Leu JH, Lee YC, Tsai IH (1999) Molecular cloning and characterization of a hemolymph clottable protein from tiger shrimp (*Penaeus monodon*). Eur J Biochem 266: 624-633.

245. Montaño-Pérez K, Yepiz-Plascencia G, Higuera-Ciapara I, Vargas-Albores F (1999) Purification and characterization of the clotting protein from the white shrimp *Penaeus vannamei*. Comp Biochem Phys B 122: 381-387.

246. Perazzolo LM, Lorenzini DM, Daffre S, Barracco MA (2005) Purification and partial characterization of the plasma clotting protein from the pink shrimp *Farfantepenaeus paulensis*. Comp Biochem Phys B 142: 302-307.

247. Wang R, Liang Z, Hall M, Söderhäll K (2001) A transglutaminase involved in the coagulation system of the freshwater crayfish, *Pacifastacus leniusculus*. Tissue localisation and cDNA cloning. Fish Shellfish Immun 11: 623-637.

248. Huang CC, Sritunyalucksana K, Söderhäll K, Song YL (2004) Molecular cloning and characterization of tiger shrimp (*Penaeus monodon*) transglutaminase. Dev Comp Immunol 28: 279-294.

249. Chen MY, Hu KY, Huang CC, Song YL (2005) More than one type of transglutaminase in invertebrates? A second type of transglutaminase is involved in shrimp coagulation. Dev Comp Immunol 29: 1003-1016.

250. Fagutao FF, Maningas MBB, Kondo H, Aoki T, Hirono I (2012) Transglutaminase regulates immune-related genes in shrimp. Fish Shellfish Immun 32: 711-715.

251. Maningas MBB, Kondo H, Hirono I, Saito-Taki T, Aoki T (2008) Essential function of transglutaminase and clotting protein in shrimp immunity. Mol Immunol 45: 1269-1275.

252. Song YL, Yu CI, Lien TW, Huang CC, Lin MN (2003) Haemolymph parameters of Pacific white shrimp (*Litopenaeus vannamei*) infected with Taura syndrome virus. Fish Shellfish Immun 14: 317-331.

253. Wang KCHC, Tseng CW, Lin HY, Chen IT, Chen YH, et al. (2010) RNAi knock-down of the *Litopenaeus vannamei* Toll gene (LvToll) significantly increases mortality and reduces bacterial clearance after challenge with *Vibrio harveyi*. Dev Comp Immunol 34: 49-58.

254. Daffre S, Kylsten P, Samakovlis C, Hultmark D (1994) The lysozyme locus in *Drosophila melanogaster*: an expanded gene family adapted for expression in the digestive tract. Mol Gen Genet 242: 152-162.

255. Jollès P (1996) Lysozymes: model enzymes in biochemistry and biology. 498 p.

256. Dimarcq JL, Hoffmann D, Meister M, Bulet P, Lanot R, et al. (1994) Characterization and transcriptional profiles of a *Drosophila* gene encoding an insect defensin. Eur J Biochem 221: 201-209.

257. Ritsick DR, Edens WA, McCoy JW, Lambeth JD (2004) The use of model systems to study biological functions of Nox/Duox enzymes. Biochem Soc Symp 71: 85-96.

258. Ha EM, Oh CT, Ryu JH, Bae YS, Kang SW, et al. (2005) An antioxidant system required for host protection against gut infection in *Drosophila*. Dev Cell 8: 125-132.

259. Ryu JH, Ha EM, Oh CT, Seol JH, Brey PT, et al. (2006) An essential complementary role of NF-κB pathway to microbicidal oxidants in *Drosophila* gut immunity. EMBO J 25: 3693-3701.

260. Tzou P, Ohresser S, Ferrandon D, Capovilla M, Reichhart J-M, et al. (2000) Tissue-specific inducible expression of antimicrobial peptide genes in *Drosophila* surface epithelia. Immunity 13: 737-748.

261. Ryu JH, Nam KB, Oh CT, Nam HJ, Kim SH, et al. (2004) The homeobox gene Caudal regulates constitutive local expression of antimicrobial peptide genes in *Drosophila* epithelia. Mol Cell Biol 24: 172-185.

262. Han SH, Ryu JH, Oh CT, Nam KB, Nam HJ, et al. (2004) The moleskin gene product is essential for Caudal-mediated constitutive antifungal Drosomycin gene expression in *Drosophila* epithelia. Insect Mol Biol 13: 323-327.

263. Tingvall TÖ, Roos E, Engström Y (2001) The *imd* gene is required for local *Cecropin* expression in *Drosophila* barrier epithelia. EMBO Rep 2: 239-243.

264. Basset A, Khush RS, Braun A, Gardan L, Boccard F, et al. (2000) The phytopathogenic bacteria *Erwinia carotovora* infects *Drosophila* and activates an immune response. P Natl Acad Sci USA 97: 3376-3381.

265. Muñoz M, Cedeño R, Rodríguez J, van der Knaap WPW, Mialhe E, et al. (2000) Measurement of reactive oxygen intermediate production in haemocytes of the penaeid shrimp, *Penaeus vannamei*. Aquaculture 191: 89-107.

266. Gómez-Anduro GA, Barillas-Mury CV, Peregrino-Uriarte AB, Gupta L, Gollas-Galván T, et al. (2006) The cytosolic manganese superoxide dismutase from the shrimp *Litopenaeus vannamei*: Molecular cloning and expression. Dev Comp Immunol 30: 893-900.

267. Vidya N, Thiagarajan R, Arumugam M (2007) *In vitro* generation of superoxide anion by the hemocytes of *Macrobrachium rosenbergii*: possible mechanism and pathways. J Exp Zool A 307A: 383-396.

268. Itami T, Ohno Y, Suzuki N, Doi K, Kondo M, et al. (2002) Superoxide and nitric oxide production of kuruma prawn (*Marsupenaeus japonicus*) hemocytes. Fisheries Sci 68: 1119-1122.

269. Inada M, Mekata T, Sudhakaran R, Okugawa S, Kono T, et al. (2010) Molecular cloning and characterization of the nitric oxide synthase gene from kuruma shrimp, *Marsupenaeus japonicus*. Fish Shellfish Immun 28: 701-711.

270. Inada M, Sudhakaran R, Kihara K, Nishi J, Yoshimine M, et al. (2012) Molecular cloning and characterization of the NADPH oxidase from the kuruma shrimp, *Marsupenaeus japonicus*: Early gene up-regulation after *Vibrio penaeicida* and poly(I:C) stimulations *in vitro*. Mol Cell Probe 26: 29-41.

271. Inada M, Kihara K, Kono T, Sudhakaran R, Mekata T, et al. (2013) Deciphering of the Dual oxidase (Nox family) gene from kuruma shrimp, *Marsupenaeus japonicus*: Full-length cDNA cloning and characterization. Fish Shellfish Immun 34: 471-485.

272. Engel P, Moran NA (2013) The gut microbiota of insects-diversity in structure and function. FEMS Microbiol Rev 37: 699-735.

273. Kim SH, Lee WJ (2013) Role of DUOX in gut inflammation: lessons from *Drosophila* model of gut-microbiota interactions. Front Cell Infect Microbiol 3: 1-11.

274. Buchon N, Broderick NA, Poidevin M, Pradervand S, Lemaitre B (2009) *Drosophila* intestinal response to bacterial infection: activation of host defense and stem cell proliferation. Cell Host Microbe 5: 200-211.

275. Chatterjee M, Ip YT (2009) Pathogenic stimulation of intestinal stem cell response in *Drosophila*. J Cell Physiol 220: 664-671.

276. Buchon N, Broderick NA, Chakrabarti S, Lemaitre B (2009) Invasive and indigenous microbiota impact intestinal stem cell activity through multiple pathways in *Drosophila*. Genes Dev 23: 2333-2344.

277. Buchon N, Broderick NA, Kuraishi T, Lemaitre B (2010) *Drosophila* EGFR pathway coordinates stem cell proliferation and gut remodeling following infection. BMC Biol 8: 152.

278. Jiang H, Patel PH, Kohlmaier A, Grenley MO, McEwen DG, et al. (2009) Cytokine/Jak/Stat signaling mediates regeneration and homeostasis in the *Drosophila* midgut. Cell 137: 1343-1355.

279. Jiang H, Grenley MO, Bravo MJ, Blumhagen RZ, Edgar BA (2011) EGFR/Ras/MAPK signaling mediates adult midgut epithelial homeostasis and regeneration in *Drosophila*. Cell Stem Cell 8: 84-95.

280. Zhou F, Rasmussen A, Lee S, Agaisse H (2013) The UPD3 cytokine couples environmental challenge and intestinal stem cell division through modulation of JAK/STAT signaling in the stem cell microenvironment. Dev Biol 373: 383-393.

281. Cordero JB, Stefanatos RK, Scopelliti A, Vidal M, Sansom OJ (2012) Inducible progenitor-derived Wingless regulates adult midgut regeneration in *Drosophila*. EMBO J 31: 3901-3917.

282. Buchon N, Broderick NA, Lemaitre B (2013) Gut homeostasis in a microbial world: insights from *Drosophila melanogaster*. Nat Rev Microbiol 11: 615-626.

283. Agaisse H, Perrimon N (2004) The roles of JAK/STAT signaling in *Drosophila* immune responses. Immunol Rev 198: 72-82.

284. Chen WY, Ho KC, Leu JH, Liu KF, Wang HC, et al. (2008) WSSV infection activates STAT in shrimp. Dev Comp Immunol 32: 1142-1150.

285. Sun C, Shao HL, Zhang XW, Zhao XF, Wang JX (2011) Molecular cloning and expression analysis of signal transducer and activator of transcription (STAT) from the Chinese white shrimp *Fenneropenaeus chinensis*. Mol Biol Rep 38: 5313-5319.

286. Rengpipat S, Tunyanun A, Fast AW, Piyatiratitivorakul S, Menasveta P (2003) Enhanced growth and resistance to *Vibrio* challenge in pond-reared black tiger shrimp *Penaeus monodon* fed a *Bacillus* probiotic. Dis Aquat Organ 55: 169-173.

287. Lee SY, Söderhäll K (2001) Characterization of a pattern recognition protein, a masquerade-like protein, in the freshwater crayfish *Pacifastacus leniusculus*. J Immunol 166: 7319-7326.

288. Seidman JG (2003) *In Situ* Hybridization and Immunohistochemistry. Current Protocols in Molecular Biology: John Wiley & Sons, Inc. pp. 14.10.11-14.16.13.

289. Zheng D, Alm EW, Stahl DA, Raskin L (1996) Characterization of universal small-subunit rRNA hybridization probes for quantitative molecular microbial ecology studies. Appl Environ Microbiol 62: 4504-4513.

290. Huggett MJ, Crocetti GR, Kjelleberg S, Steinberg PD (2008) Recruitment of the sea urchin Heliocidaris erythrogramma and the distribution and abundance of inducing bacteria in the field. Aquat Microb Ecol 53: 161-171.

291. Meier H, Amann R, Ludwig W, Schleifer KH (1999) Specific oligonucleotide probes for in situ detection of a major group of Gram-positive bacteria with low DNA G+C content. Syst Appl Microbiol 22: 186-196.

292. Sawabe T, Yoshizawa A, Kawanishi Y, Komatsu-Takeda E, Nakagawa S, et al. (2009) Multi-probe-fluorescence *in situ* hybridization for the rapid enumeration of viable *Vibrio parahaemolyticus*. Microb Ecol 24: 259-264.

293. Fukui Y, Sawabe T (2008) Rapid detection of *Vibrio harveyi* in seawater by real-time PCR. Microb Ecol 23: 172-176.

294. Zhou J, Bruns MA, Tiedje JM (1996) DNA recovery from soils of diverse composition. Appl Environ Microb 62: 316-322.

295. Lane DJ (1991) 16S/23S rRNA sequencing. In: Stackebrandt E, Goodfellow M, editors. Nucleic acid techniques in bacterial systematics. Academic: Chichester. pp. 115-175.

296. Muyzer G, de Waal EC, Uitterlinden AG (1993) Profiling of complex microbial populations by denaturing gradient gel electrophoresis analysis of polymerase chain reaction-amplified genes coding for 16S rRNA. Appl Environ Microbiol 59: 695-700.

297. Tourlomousis P, Kemsley EK, Ridgway K, Toscano M, Humphrey T, et al. (2010) PCR-denaturing gradient gel electrophoresis of complex microbial

communities: A two-step approach to address the effect of gel-to-gel variation and allow valid comparisons across a large dataset. Microb Ecol 59: 776-786.

298. Thaithongnum S, Ratanama P, Weeradechapol K, Sukhoom A, Vuddhakul V (2006) Detection of *V. harveyi* in shrimp postlarvae and hatchery tank water by the most probable number technique with PCR. Aquaculture 261: 1-9.

299. Venkateswaran K, Dohmoto N, Harayama S (1998) Cloning and nucleotide sequence of the *gyrB* gene of *Vibrio parahaemolyticus* and its application in detection of this pathogen in shrimp. Appl Environ Microbiol 64: 681-687.

300. Nordstrom JL, Vickery MCL, Blackstone GM, Murray SL, DePaola A (2007) Development of a multiplex real-time PCR assay with an internal amplification control for the detection of total and pathogenic *Vibrio parahaemolyticus* bacteria in oysters. Appl Environ Microbiol 73: 5840-5847.

301. Fierer N, Jackson JA, Vilgalys R, Jackson RB (2005) Assessment of soil microbial community structure by use of taxon-specific quantitative PCR assays. Appl Environ Microbiol 71: 4117-4120.

302. Whelan JA, Russell NB, Whelan MA (2003) A method for the absolute quantification of cDNA using real-time PCR. J Immunol Methods 278: 261-269.

303. Fogel GB, Collins CR, Li J, Brunk CF (1999) Prokaryotic genome size and ssu rdna copy number: estimation of microbial relative abundance from a mixed population. Microb Ecol 38: 93-113.

304. Fegatella F, Lim J, Kjelleberg S, Cavicchioli R (1998) Implications of rRNA operon copy number and ribosome content in the marine oligotrophic ultramicrobacterium *Sphingomonas* sp. Strain RB2256. Appl Environ Microbiol 64: 4433-4438.

305. Coenye T, Vandamme P (2003) Intragenomic heterogeneity between multiple 16S ribosomal RNA operons in sequenced bacterial genomes. FEMS Microbiol Lett 228: 45-49.

306. Bell TA, Lightner DV (1988) A Handbook of Normal Penaeid Shrimp Histology: World Aquaculture Society, USA. 114 p.

307. Humason GL (1979) Animal tissue techniques: 4th ed., W H Freeman & Co., San Francisco. 496 p.

308. Huang X, Madan A (1999) CAP3: A DNA Sequence Assembly Program. Genome Res 9: 868-877.

309. Koressaar T, Remm M (2007) Enhancements and modifications of primer design program Primer3. Bioinformatics 23: 1289-1291.

310. Untergasser A, Cutcutache I, Koressaar T, Ye J, Faircloth BC, et al. (2012) Primer3—new capabilities and interfaces. Nucleic Acids Res 40: e115.

311. Preechaphol R, Klinbunga S, Ponza P, Menasveta P (2010) Isolation and characterization of progesterone receptor-related protein p23 (Pm-p23) differentially expressed during ovarian development of the giant tiger shrimp *Penaeus monodon*. Aquaculture 308: S75-S82.

312. Livak KJ, Schmittgen TD (2001) Analysis of relative gene expression data using real-time quantitative PCR and the $2^{-\Delta\Delta CT}$ method. Methods 25: 402-408.

313. Tamura K, Stecher G, Peterson D, Filipski A, Kumar S (2013) MEGA6: Molecular evolutionary genetics analysis version 6.0. Mol Biol Evol 30: 2725-2729.

314. Saitou N, Nei M (1987) The neighbor-joining method: a new method for reconstructing phylogenetic trees. Mol Biol Evol 4: 406-425.

315. Felsenstein J (1985) Confidence limits on phylogenies: An approach using the bootstrap. Evolution 39: 783-791.

316. Zuckercandl E, Pauling L (1965) Evolutionary divergence and convergence in proteins. In: Bryson V, Vogel HJ, editors. Evolving Genes and Proteins. Academic Press: California, USA. pp. 97-165.

317. Rungrassamee W, Klanchui A, Maibunkaew S, Chaiyapechara S, Jiravanichpaisal P, et al. (2014) Characterization of intestinal bacteria in wild and domesticated adult black tiger shrimp (*Penaeus monodon*). PLoS ONE 9: e91853.

318. Kraxberger-Beatty T, McGarey DJ, Grier HJ, Lim DV (1990) *Vibrio harveyi*, an opportunistic pathogen of common snook, *Centropomus undecimalis* (Bloch), held in captivity. J Fish Dis 13: 557-560.

319. Vaseeharan B, Ramasamy P (2003) Abundance of potentially pathogenic micro-organisms in *Penaeus monodon* larvae rearing systems in India. Microbiol Res 158: 299-308.

320. Sung HH, Li HC, Tsai FM, Ting YY, Chao WL (1999) Changes in the composition of *Vibrio communities* in pond water during tiger shrimp (*Penaeus monodon*) cultivation and in the hepatopancreas of healthy and diseased shrimp. J Exp Mar Biol Ecol 236: 261-271.

321. Moss SM, LeaMaster BR, Sweeney JN (2000) Relative abundance and species composition of gram-negative, aerobic bacteria associated with the gut of juvenile white shrimp *Litopenaeus vannamei* reared in oligotrophic well water and eutrophic pond water. J World Aquacult Soc 31: 255-263.

322. Oxley APA, Shipton W, Owens L, McKay D (2002) Bacterial flora from the gut of the wild and cultured banana prawn, *Penaeus merguiensis*. J Appl Microbiol 93: 214-223.

323. Theethakaew C, Feil EJ, Castillo-Ramírez S, Aanensen DM, Suthienkul O, et al. (2013) Genetic relationships of *Vibrio parahaemolyticus* isolates from clinical, human carrier and environmental sources in Thailand determined by multilocus sequence analysis. Appl Environ Microbiol 79(7): 2358-2370.

324. Koga R, Tsuchida T, Fukatsu T (2009) Quenching autofluorescence of insect tissues for *in situ* detection of endosymbionts. Appl Entomol Zool 44: 281-291.

325. Epis S, Mandrioli M, Genchi M, Montagna M, Sacchi L, et al. (2013) Localization of the bacterial symbiont *Candidatus* Midichloria mitochondrii within the hard tick Ixodes ricinus by whole-mount FISH staining. Ticks Tick Borne Dis 4: 39-45.

326. Martin GG, Simcox R, Nguyen A, Chilingaryan A (2006) Peritrophic membrane of the penaeid shrimp *Sicyonia ingentis*: structure, formation, and permeability. Biol Bull 211: 275-285.

327. Pinn EH, Nickell LA, Rogerson A, Atkinson RJA (1999) Comparison of gut morphology and gut microflora of seven species of mud shrimp (Crustacea: Decapoda: Thalassinidea). Mar Biol 133: 103-114.

328. Corbari L, Durand L, Cambon-Bonavita MA, Gaill F, Compère P (2012) New digestive symbiosis in the hydrothermal vent amphipoda *Ventiella sulfuris*. C R Biol 335: 142-154.

329. Merzendorfer H, Zimoch L (2003) Chitin metabolism in insects: Structure, function and regulation of chitin synthases and chitinases. J Exp Biol 206: 4393-4412.

330. Kuraishi T, Binggeli O, Opota O, Buchon N, Lemaitre B (2011) Genetic evidence for a protective role of the peritrophic matrix against intestinal bacterial infection in *Drosophila melanogaster*. Proc Nat Acad Sci 108: 15966-15971.

331. Avtsyn AP, Petrova TP (1986) Resistance of the alimentary canal of *Daphnia magna* Straus to the effect of enteropathogenic NAG-vibrios. Biul Eksp Biol Med 102: 342-345.

332. Nayduch D, Pittman NG, Stutzenberger FJ (2005) Fate of bacteria, *Aeromonas caviae*, in the midgut of the housefly, *Musca domestica*. Invertebr Biol 124: 74-78.

333. Wang P, Granados RR (1998) Observations on the presence of the peritrophic membrane in larval *Trichoplusia ni* and its role in limiting baculovirus infection. J Invertebr Pathol 72: 57-62.

334. Peters W (1992) Peritrophic membranes. Springer-Verlag: Berlin, Germany. 238 p.

335. Martin GG, Rubin N, Swanson E (2004) *Vibrio parahaemolyticus* and *V. harveyi* cause detachment of the epithelium from the midgut trunk of the penaeid shrimp *Sicyonia ingentis*. Dis Aquat Organ 60: 21-29.

336. Soonthornchai W, Rungrassamee W, Karoonuthaisiri N, Jarayabhand P, Klinbunga S, et al. (2010) Expression of immune-related genes in the digestive organ of shrimp, *Penaeus monodon*, after an oral infection by *Vibrio harveyi*. Dev Com Immunol 34: 19-28.

337. Austin B (2006) The bacterial microflora of fish, revised. Sci World J 6: 931-945.

338. Dempsey AC, Kitting CL, Rosson RA (1989) Bacterial variability among individual penaeid shrimp digestive tracts. Crustaceana 56: 266-278.

339. Lau WWY, Jumars PA, Armbrust EV (2002) Genetic diversity of attached bacteria in the hindgut of the deposit-feeding shrimp *Neotrypaea* (formerly

Callianassa) *californiensis* (Decapoda: Thalassinidae). Microb Ecol 43: 455-466.

340. Ceccaldi HJ (1998) A synopsis of the morphology and physiology of the digestive system of some crustacean species studied in France. Rev Fish Sci 6: 13-39.

341. Crawford CS, Minion GP, Boyers MD (1983) Intima morphology, bacterial morphotypes, and effects of annual molt on microflora in the hindgut of the desert millipede, *Orthoporus ornatus* (Girard) (Diplopoda : Spirostreptidae). Int J Insect Morphol Embryol 12: 301-312.

342. Huq A, Huq SA, Grimes DJ, O'Brien M, Chu KH, et al. (1986) Colonization of the gut of the blue crab (*Callinectes sapidus*) by *Vibrio cholerae*. Appl Environ Microb 52: 586-588.

343. Bignell DE (1989) The arthropod gut as an environment for microorganisms. In: Anderson JM, Rayner ADM, Walton DWH, editors. Invertebrate-microbial interactions. Cambridge University Press: Cambridge. pp. 205-228.

344. Shakibazadeh S, Saad C, Christianus A, Kamarudin M, Sijam K, et al. (2009) Bacteria flora associated with different body parts of hatchery reared juvenile *Penaeus monodon*, tanks water and sediment. Ann Microbiol 59: 425-430.

345. Johnson CN, Barnes S, Ogle J, Grimes DJ, Chang Y-J, et al. (2008) Microbial community analysis of water, foregut, and hindgut during growth of pacific white shrimp, *Litopenaeus vannamei*, in closed-system aquaculture. J World Aquacult Soc 39: 251-258.

346. Chaiyapechara S, Rungrassamee W, Suriyachay I, Kuncharin Y, Klanchui A, et al. (2012) Bacterial community associated with the intestinal tract of *P. monodon* in commercial farms. Microb Ecol 63: 938-953.

347. Li P, Burr GS, Gatlin DM, Hume ME, Patnaik S, et al. (2007) Dietary supplementation of short-chain fructooligosaccharides influences gastrointestinal microbiota composition and immunity characteristics of pacific white shrimp, *Litopenaeus vannamei*, cultured in a recirculating system. J Nutr 137: 2763-2768.

348. Drobne D (1995) Bacteria adherent to the hindgut of terrestrial isopods. Acta Microbiol Immunol Hung 42: 45-52.

349. Nagasawa S, Terazaki M, Nemoto T (1987) Bacterial attachment to the epipelagic copepod *Acartia* and the bathypelagic copepod *Calanus*. Proc Jpn Acad Ser B 63: 33-35.

350. Keyhani NO, Roseman S (1999) Physiological aspects of chitin catabolism in marine bacteria. Biochim Biophys Acta 1473: 108-122.

351. Gode-Potratz CJ, Kustusch RJ, Breheny PJ, Weiss DS, McCarter LL (2011) Surface sensing in *Vibrio parahaemolyticus* triggers a programme of gene expression that promotes colonization and virulence. Mol Microbiol 79: 240-263.

352. McCarter LL (1999) The multiple identities of *Vibrio parahaemolyticus*. J Mol Microbiol Biotechnol 1: 51-57.

353. Ofek I, Hasty DL, Doyle RJ (2003) Bacterial adhesion to animal cells and tissues. ASM Press: Washington, USA. 416 p.

354. Rendón MA, Saldaña Z, Erdem AL, Monteiro-Neto V, Vázquez A, et al. (2007) Commensal and pathogenic *Escherichia coli* use a common pilus adherence factor for epithelial cell colonization. Proc Nat Acad Sci 104: 10637-10642.

355. Jonson A, Normark S, Rhen M (2005) Fimbriae, pili, flagella and bacterial virulence. In: Russell W, Herwald H, editors. Concepts in bacterial virulence vol 12. Basel: Karger. pp. 67-89.

356. Defoirdt T (2013) Antivirulence therapy for animal production: Filling an arsenal with novel weapons for sustainable disease control. PLoS Pathog 9: e1003603.

357. Diatchenko L, Lau YF, Campbell AP, Chenchik A, Moqadam F, et al. (1996) Suppression subtractive hybridization: A method for generating differentially regulated or tissue-specific cDNA probes and libraries. Proc Nat Acad Sci 93: 6025-6030.

358. Watanabe T, Persson P, Endo H, Kono M (2000) Molecular analysis of two genes, DD9A and B, which are expressed during the postmolt stage in the decapod crustacean *Penaeus japonicus*. Comp Biochem Phys B 125: 127-136.

359. Beumer C, Wulferink M, Raaben W, Fiechter D, Brands R, et al. (2003) Calf intestinal alkaline phosphatase, a novel therapeutic drug for lipopolysaccharide (LPS)-mediated diseases, attenuates LPS toxicity in mice and piglets. J Pharmacol Exp Ther 307: 737-744.

360. Goldberg RF, Austen WG, Zhang X, Munene G, Mostafa G, et al. (2008) Intestinal alkaline phosphatase is a gut mucosal defense factor maintained by enteral nutrition. Proc Nat Acad Sci 105: 3551-3556.

361. Hergenhahn HG, Aspan A, Soderhall K (1987) Purification and characterization of a high-Mr proteinase inhibitor of pro-phenol oxidase activation from crayfish plasma. Biochem J 248: 223-228.

362. Toe A, Areechon N, Srisapoome P (2012) Molecular characterization and immunological response analysis of a novel transferrin-like, pacifastin heavy chain protein in giant freshwater prawn, *Macrobrachium rosenbergii* (De Man, 1879). Fish Shellfish Immun 33: 801-812.

363. Kelkenberg M, Odman-Naresh J, Muthukrishnan S, Merzendorfer H (2015) Chitin is a necessary component to maintain the barrier function of the peritrophic matrix in the insect midgut. Insect Biochem Molec 56: 21-28.

364. Pongsomboon S, Tang S, Boonda S, Aoki T, Hirono I, et al. (2011) A cDNA microarray approach for analyzing transcriptional changes in *Penaeus monodon* after infection by pathogens. Fish Shellfish Immun 30: 439-446.

365. Chen AJ, Wang S, Zhao XF, Yu XQ, Wang JX (2011) Enzyme E2 from Chinese white shrimp inhibits replication of white spot syndrome virus and ubiquitinates its ring domain proteins. J Virol 85: 8069-8079.

366. Jeena K, Prasad KP, Pathan MK, Babu PG (2012) Expression profiling of WSSV ORF 199 and shrimp ubiquitin conjugating enzyme in WSSV infected *Penaeus monodon*. Asian Austral J Anim 25: 1184.

367. Hsieh SL, Chiu YC, Kuo CM (2006) Molecular cloning and tissue distribution of ferritin in Pacific white shrimp (*Litopenaeus vannamei*). Fish Shellfish Immun 21: 279-283.

368. Zhang J, Li F, Wang Z, Zhang X, Zhou Q, et al. (2006) Cloning, expression and identification of ferritin from Chinese shrimp, *Fenneropenaeus chinensis*. J Biol Chem 125: 173-184.

369. Qiu GF, Zheng L, Liu P (2008) Transcriptional regulation of ferritin mRNA levels by iron in the freshwater giant prawn, *Macrobrachium rosenbergii*. Comp Biochem Phys B 150: 320-325.

370. Lin X, Söderhäll I (2011) Crustacean hematopoiesis and the astakine cytokines. Blood 117: 6417-6424.

371. Hsiao CY, Song YL (2010) A long form of shrimp astakine transcript: Molecular cloning, characterization and functional elucidation in promoting hematopoiesis. Fish Shellfish Immun 28: 77-86.

372. Liang GF, Liang Y, Xue Q, Lu JF, Cheng JJ, et al. (2015) Astakine LvAST binds to the β subunit of F1-ATP synthase and likely plays a role in white shrimp *Litopeneaus vannamei* defense against white spot syndrome virus. Fish Shellfish Immun 43: 75-81.

373. Su J, Oanh DTH, Lyons RE, Leeton L, van Hulten MCW, et al. (2008) A key gene of the RNA interference pathway in the black tiger shrimp, *Penaeus monodon*: Identification and functional characterisation of Dicer-1. Fish Shellfish Immun 24: 223-233.

374. Li X, Yang L, Jiang S, Fu M, Huang J, et al. (2013) Identification and expression analysis of Dicer2 in black tiger shrimp (*Penaeus monodon*) responses to immune challenges. Fish Shellfish Immun 35: 1-8.

375. Tassanakajon A, Somboonwiwat K, Supungul P, Tang S (2013) Discovery of immune molecules and their crucial functions in shrimp immunity. Fish Shellfish Immun 34: 954-967.

376. Sookruksawong S, Sun F, Liu Z, Tassanakajon A (2013) RNA-Seq analysis reveals genes associated with resistance to Taura syndrome virus (TSV) in the Pacific white shrimp *Litopenaeus vannamei*. Dev Comp Immunol 41: 523-533.

377. Rao R, Zhu YB, Alinejad T, Tiruvayipati S, Thong KL, et al. (2015) RNA-seq analysis of *Macrobrachium rosenbergii* hepatopancreas in response to *Vibrio parahaemolyticus* infection. Gut Pathog 7: 6.

378. Feng N, Wang D, Wen R, Li F (2014) Functional analysis on immune deficiency (IMD) homolog gene in Chinese shrimp *Fenneropenaeus chinensis*. Mol Biol Rep 41: 1437-1444.

379. Visetnan S, Supungul P, Hirono I, Tassanakajon A, Rimphanitchayakit V (2015) Activation of PmRelish from *Penaeus monodon* by yellow head virus. Fish Shellfish Immun 42: 335-344.

380. Zhou F, Agaisse H (2012) JAK/STAT signaling and invertebrate immune responses. In: Decker T, Müller M, editors. Jak-Stat signaling : From basics to disease. Springer Vienna: Vienna, Austria. pp. 133-151.

381. Okugawa S, Mekata T, Inada M, Kihara K, Shiki A, et al. (2013) The SOCS and STAT from JAK/STAT signaling pathway of kuruma shrimp *Marsupenaeus japonicus*: Molecular cloning, characterization and expression analysis. Mol Cell Probe 27: 6-14.

382. Yan M, Li C, Su Z, Liang Q, Li H, et al. (2015) Identification of a JAK/STAT pathway receptor domeless from Pacific white shrimp *Litopenaeus vannamei*. Fish Shellfish Immun 44: 26-32.

383. Song X, Zhang Z, Wang S, Li H, Zuo H, et al. (2015) A Janus Kinase in the JAK/STAT signaling pathway from *Litopenaeus vannamei* is involved in antiviral immune response. Fish Shellfish Immun 44: 662-673.

384. Li F, Xiang J (2013) Recent advances in researches on the innate immunity of shrimp in China. Dev Comp Immunol 39: 11-26.

385. Kanost MR, Jiang H, Yu XQ (2004) Innate immune responses of a lepidopteran insect, *Manduca sexta*. Immunol Rev 198: 97-105.

386. Mu C, Zhao J, Wang L, Song L, Song X, et al. (2009) A thioredoxin with antioxidant activity identified from *Eriocheir sinensis*. Fish Shellfish Immun 26: 716-723.

387. McEligot AJ, Yang S, Frank L. Meyskens J (2005) Redox regulation by intrinsic species and extrinsic nutrients in normal and cancer cells. Annu Rev Nutr 25: 261-295.

388. Hochmuth CE, Biteau B, Bohmann D, Jasper H (2011) Redox regulation by Keap1 and Nrf2 controls intestinal stem cell proliferation in *Drosophila*. Cell Stem Cell 8: 188-199.

389. Takagi T, Naito Y, Okada H, Ishii T, Mizushima K, et al. (2009) Lansoprazole, a proton pump inhibitor, mediates anti-inflammatory effect in gastric mucosal cells through the induction of heme oxygenase-1 via activation of NF-E2-related factor 2 and oxidation of kelch-like ech-associating protein 1. J Pharmacol Exp Ther 331: 255-264.

390. Lallès JP (2010) Intestinal alkaline phosphatase: multiple biological roles in maintenance of intestinal homeostasis and modulation by diet. Nutr Rev 68: 323-332.

391. Bates JM, Akerlund J, Mittge E, Guillemin K (2007) Intestinal alkaline phosphatase detoxifies lipopolysaccharide and prevents inflammation in zebrafish in response to the gut microbiota. Cell Host Microbe 2: 371-382.

392. Lin YC, Vaseeharan B, Ko CF, Chiou TT, Chen JC (2007) Molecular cloning and characterisation of a proteinase inhibitor, alpha 2-macroglobulin (α2-M) from the haemocytes of tiger shrimp *Penaeus monodon*. Mol Immunol 44: 1065-1074.

393. Ma H, Wang B, Zhang J, Li F, Xiang J (2010) Multiple forms of alpha-2 macroglobulin in shrimp *Fenneropenaeus chinesis* and their transcriptional response to WSSV or *Vibrio* pathogen infection. Dev Comp Immunol 34: 677-684.

394. Shanthi S, Vaseeharan B (2014) Alpha 2 macroglobulin gene and their expression in response to GFP tagged *Vibrio parahaemolyticus* and WSSV pathogens in Indian white shrimp *Fenneropenaeus indicus*. Aquaculture 418–419: 48-54.

395. Chaikeeratisak V, Somboonwiwat K, Tassanakajon A (2012) Shrimp alpha-2-macroglobulin prevents the bacterial escape by inhibiting fibrinolysis of blood clots. PLoS ONE 7: e47384.

396. Jin XK, Li WW, He L, Lu W, Chen LL, et al. (2011) Molecular cloning, characterization and expression analysis of two apoptosis genes, caspase and nm23, involved in the antibacterial response in Chinese mitten crab, *Eriocheir sinensis*. Fish Shellfish Immun 30: 263-272.

397. Wang PH, Wan DH, Chen YG, Weng SP, Yu XQ, et al. (2013) Characterization of four novel caspases from *Litopenaeus vannamei* (Lvcaspase2-5) and their role in wssv infection through dsRNA-mediated gene silencing. PLoS ONE 8: e80418.

398. Yang C, Wang L, Zhang H, Wang L, Huang M, et al. (2014) A new fibrinogen-related protein from *Argopecten irradians* (AiFREP-2) with broad recognition

spectrum and bacteria agglutination activity. Fish Shellfish Immun 38: 221-229.

399. Chai Y, Yu S, Zhu Q (2012) The molecular cloning and characteristics of a fibrinogen-related protein (TfFREP1) gene from roughskin sculpin (*Trachidermus fasciatus*). Fish Shellfish Immunol 33: 614-618.

400. Xu S, Wang L, Wang XW, Zhao YR, Bi WJ, et al. (2014) l-Type lectin from the kuruma shrimp *Marsupenaeus japonicus* promotes hemocyte phagocytosis. Dev Comp Immunol 44: 397-405.

401. Yu XQ, Kanost MR (2000) Immulectin-2, a lipopolysaccharide-specific lectin from an insect, *Manduca sexta*, is induced in response to gram-negative bacteria. J Biol Chem 275: 37373-37381.

VITA

Miss Wipasiri Soonthornchai was born on May 28, 1983 in Nongkhai province. She graduated with the degree of Bachelor of Science from Department of Biology, Faculty of Science at Khon Kaen University in 2006 and the degree of Master of Science from Department of Marine Science (Marine Biology), Faculty of Science at Chulalongkorn University in 2009. She has studied for the Degree of Doctor of Philosophy in Biotechnology, Chulalongkorn University since 2010.

She had published her works in the research journal, Development and Comparative Immunology, on the topic of "Expression of immune-related genes in the digestive organ of shrimp, Penaeus monodon, after an oral infection by Vibrio harveyi" and the research journal, PLoS ONE, no the topic of "Interaction of Vibrio spp. with the inner surface of the digestive tract of Penaeus monodon". In addition, the topic of "Differentially expressed genes in stomach of Penaeus monodon in response to EMS/AHPND pathogen using Ion torrent sequencing" is in the published process.